

10-23-2019 1:30 PM

Hydrodynamics of Liquid-Solid and Three-Phase Inverse Circulating Fluidized Beds

Tian Nan, *The University of Western Ontario*

Supervisor: Zhu, Jesse, *The University of Western Ontario*

A thesis submitted in partial fulfillment of the requirements for the Doctor of Philosophy degree
in Chemical and Biochemical Engineering

© Tian Nan 2019

Follow this and additional works at: <https://ir.lib.uwo.ca/etd>

 Part of the [Catalysis and Reaction Engineering Commons](#)

Recommended Citation

Nan, Tian, "Hydrodynamics of Liquid-Solid and Three-Phase Inverse Circulating Fluidized Beds" (2019).
Electronic Thesis and Dissertation Repository. 6663.
<https://ir.lib.uwo.ca/etd/6663>

This Dissertation/Thesis is brought to you for free and open access by Scholarship@Western. It has been accepted for inclusion in Electronic Thesis and Dissertation Repository by an authorized administrator of Scholarship@Western. For more information, please contact wlsadmin@uwo.ca.

Abstract

The hydrodynamics of inverse liquid-solid circulating fluidized bed (ILSCFB) is experimentally studied in a 5.4 m tall and 0.076 m ID column. 5 types of low density particles are investigated with different particle terminal velocities.

Solids holdup distribution is found to be uniform in a wide range of superficial liquid velocities and over 10 solid circulation rates. Average solids hold is not sensitive to particle properties. Clustering phenomenon is found to be significant affecting the slip velocity in the ILSCFB. And the cluster phenomenon is directly related to particle Reynolds number (Re_t). Particles with little Re_t tends to have higher slip velocity which is believed as an indicator of clustering phenomenon. A modified Richardson-Zaki equation is proposed for the prediction of solids holdup in ILSCFB

Comparative study between upward and inverse liquid-solid CFBs is conducted. General hydrodynamics is found to be similar. Axial solids holdup is uniform in both systems. Radial flow structure is also uniform although some decreasing trend from center to the wall is observed in inverse liquid-solid circulating fluidized bed due to the effect of lifting force. Residence time per unit height is used as a tool to compare different reactor performance, and also compare particle properties. Particles with little Re_t will lead to less homogeneous behavior in the circulating fluidized bed for both heavy and low density particles.

A new type of circulating fluidized bed, conventional circulating fluidized bed, operating below particle terminal velocity, is proposed and experimentally investigated. Solids holdup is found to be significantly increased compared with both conventional fluidization and regular circulating fluidization. And better solids holdup control is achieved with the help of solids circulation.

Preliminary study on the counter-current flow of liquid and solids is carried out with both heavy and density particles. Inverse gas-liquid-solid circulating fluidized bed is proposed, and its hydrodynamics is experimentally investigated.

A detail flow regimes map is presented and discussed based on flow directions of liquid and solids. The studied configurations of liquid-solid fluidization systems in this research are highlighted in the flow regimes map, which greatly enriches the operating modes of liquid-solid fluidization.

.

Keywords

Inverse Fluidization, Circulating Fluidized Bed, Fluidization Regime, Gas-Liquid-Solid Fluidization, Conventional-Circulating Fluidization

Summary for Lay Audience

In chemical and biochemical processes, multiphase contact is of great importance for mass transfer, heat transfer and reaction performance. And fluidized bed is an approved candidate due to its intensified solids movement within the fluid. This study focuses on the hydrodynamics of multiple liquid fluidization systems which covers both co-current and counter-current flow of liquid and solid with both light and heavy density particles in relative to liquid.

In Inverse Liquid-Solid Circulating Fluidized Bed, solids holdup distribution is found to be uniform both axially and radially. And solids holdup is increasing solid circulating rate and decreasing with superficial liquid velocity. The effects of particle properties are not significant in determining solids holdup, but quite notable in affecting the slip velocity between liquid and solid. A model is presented for the prediction of solids holdup.

A new type of Liquid-Solid Circulating Fluidized Bed is proposed that can operate below particle terminal is proposed that can increase solids holdup significantly.

Preliminary study on the counter-current flow of liquid and solids were studied with both heavy and density particles. Inverse gas-liquid-solid circulating fluidized bed is proposed and experimentally investigated the hydrodynamics.

Comparative study on the flow of heavy and low density particles were conducted and some clustering phenomenon were believed to exist in particles with low terminal velocity. And a discussion on liquid fluidization based on Four-Quadrant Fluidization Regime Map is conducted at the end that summarized the studied systems and may also lead to findings in new liquid fluidization regimes.

Co-Authorship Statement

Title: Hydrodynamics in Inverse Liquid-Solid Circulating Fluidized Bed

Author: Tian Nan, Jesse Zhu, Dominic Pjontek

Tian Nan designed and performed the major part of the experiment and carried out data analysis under the guidance of advisor Dr. Jesse Zhu and Dr. Dominic Pjontek. All drafts of this manuscript were written by Tian Nan. Modifications were carried out under close supervision of advisor Dr. J. Zhu. The final version of this article is ready for submission.

Title: Comparative study of inverse and upward Liquid-Solid Circulating Beds

Author: Tian Nan, Jesse Zhu

Tian Nan designed and performed the major part of the experiment and carried out data analysis under the guidance of advisor Dr. Jesse Zhu. All drafts of this manuscript were written by Tian Nan. Modifications were carried out under close supervision of advisor Dr. J. Zhu. The final version of this article is to be submitted.

Title: Hydrodynamics study on a Conventional Circulating Fluidized Bed

Author: Tian Nan, Jesse Zhu

Tian Nan designed and performed the major part of the experiment and carried out data analysis under the guidance of advisor Dr. Jesse Zhu. All the experimental work was undertaken by Tian Nan. All drafts of this manuscript were written by Tian Nan. Modifications were carried out under close supervision of advisor Dr. Jesse. Zhu. The final version of this article is to be submitted.

Title: Counter-Current flow of liquid and solid in circulating fluidized beds

Author: Tian Nan, Jesse Zhu

Tian Nan designed and performed the major part of the experiment and carried out data analysis under the guidance of advisor Dr. Jesse Zhu. All the experimental work was

undertaken by Tian Nan. All drafts of this manuscript were written by Tian Nan. Modifications were carried out under close supervision of advisor Dr. Jesse. Zhu. The final version of this article is to be submitted.

Title: On the basic hydrodynamics of Inverse Gas-Liquid-Solid Circulating Fluidized bed

Author: Tian Nan, Jesse Zhu, Dominic Pjontek

The experimental setup of Inverse Gas-Liquid-Solid Circulating Fluidized Bed was designed and modified by Tian Nan together with Jianzhang Wen under the guidance of advisor Dr. Jesse. Zhu. All the experimental work was undertaken by Tian Nan. All drafts of this manuscript were written by Tian Nan. Modifications were carried out under close supervision of advisor Dr. Jesse. Zhu and Dr. Dominic Pjontek. The final version of this article is ready for submission.

Acknowledgments

First and foremost, I would like to thank my supervisor Dr. Jesse Zhu for the generously financial support. Nothing can be achieved without his expertise and mentorship in research and life.

I would like to express my sincerest gratitude and thanks to Dr. Dominic Pjontek for his guidance and extensive support through many aspects of my life at Western University. I am inspired by his attitudes towards academia and teaching.

I would like to acknowledge Saleh Ahmed Srabet for his help with experiment design and data analysis. And also, the technical staff in our research group, Jianzhang Wen, Danni Bao and George Zhang for their assistance and service.

Thanks to Gong Zhang, Jiaqi Huang, Haohao Zhou, Sylena Song, Lukang Sun, Jing Wang for their efforts in helping with experiment measurement and operation.

Many thanks go to Dr. Xiaoyang Wei and Dr. Zhijie Fu for the many late-night heated discussions we had ever since the starting of our Ph.D. life

I'd like to express my gratitude to Mengze Zhang, Wenhao Lian and Hanlin Wang for their patience and understanding to help me struggling through the final period on my Ph.D.

Last but not the least, I'd like to thank my parents for their unconditional love. They support me all the way through whenever I am in doubt or regret.

Table of Contents

Abstract	ii
Summary for Lay Audience	iv
Co-Authorship Statement.....	v
Acknowledgments.....	vii
Table of Contents	viii
List of Tables	xiv
List of Figures	xv
List of Appendices	xx
Chapter 1	1
1 General Introduction	1
1.1 Introduction.....	1
1.2 Research objective	4
1.3 Thesis Structure	5
Reference.....	6
Chapter 2.....	10
2 Literature Review.....	10
2.1 Fundamental.....	10
2.1.1 Superficial liquid velocity	10
2.1.2 Interstitial liquid velocity.....	10
2.1.3 Particle terminal velocity	11
2.1.4 Solid circulation rate	12
2.2 Fluidization regimes.....	13
2.3 Hydrodynamics of LSCFB	13
2.3.1 Solids holdup distribution	13

2.3.2	Onset velocity	15
2.3.3	Pressure balance in LSCFB	16
2.3.4	Transition Regime.....	16
2.3.5	Cluster in liquid-solid circulating fluidized bed	17
2.4	Hydrodynamics of Inverse Conventional fluidization.....	18
2.4.1	Behavior of low density particles in liquid.....	19
2.4.2	Richardson-Zaki equation.....	20
2.4.3	Hydrodynamics of inverse three-phase fluidization	21
	Nomenclature	23
	Reference.....	25
Chapter 3	28
3	Hydrodynamics of Inverse Liquid-Solid Circulating Fluidized Bed	28
	Abstract	28
3.1	Introduction.....	28
3.2	Experiment.....	30
3.2.1	Apparatus	30
3.2.2	Particle properties	32
3.3	Results and Discussion	32
3.3.1	Particle terminal velocity	32
3.3.2	Axial flow structure	34
3.3.3	Radial flow structure.....	45
3.3.4	Average solids holdup and particle property effects.....	54
3.3.5	Slip velocity	57
3.4	Prediction of solids holdup	59
3.5	Conclusions and recommendations.....	63
	Nomenclature	65

Reference.....	67
Chapter 4.....	70
4 Comparative Study of Inverse and Upward Liquid-Solid Circulating Fluidized Bed .	70
Abstract	70
4.1 Introduction.....	70
4.2 Experiment setup	74
4.2.1 Operation of LSCFB and ILSCFB.....	74
4.2.2 Residence time per unit height.....	75
4.3 Results and discussion	76
4.3.1 Change of T_s , T_1 with U_s and U_1	76
4.3.2 Particle property effects T_s	79
4.3.3 Comparison between CCFB and LSCFB	81
4.3.4 Change of T_s/T_1 with U_1 in LSCFB and ILSCFB	81
4.3.5 Significance of T_s , T_1 and T_s/T_1	85
4.3.6 Failure of Richardson-Zaki equation in (I)-LSCFB.....	85
4.3.7 Comparison of T_s/T_1 in Gas-Solid CFB	87
4.4 Conclusions and recommendations.....	87
Nomenclature	89
Reference.....	91
Chapter 5.....	93
5 Hydrodynamics of inverse liquid-solid circulating fluidized bed below particle terminal velocity	93
Abstract	93
5.1 Introduction.....	93
5.1.1 Conventional fluidization.....	94
5.1.2 LSCFB	94

5.1.3	Concept of CCFB.....	95
5.2	Experiment procedures	97
5.3	Results and discussion	99
5.3.1	Axial Solids holdup distribution	101
5.3.2	Apparent slip velocity	103
5.3.3	Bed Intensification factor.....	105
5.3.4	The connection between conventional fluidization and circulating fluidization - CCFB.....	107
5.3.5	Solids circulation rate (Us)	109
5.3.6	Richardson-Zaki equation in CCFB.....	110
5.4	Conclusion and recommendation.....	112
	Nomenclature	113
	Reference.....	115
Chapter 6	119
6	Counter-Current flow in (I)-LSCFB systems.....	119
	Abstract	119
6.1	Introduction.....	119
6.2	Experiment setup	122
6.2.1	Operation of solids down, liquid up.....	122
6.2.2	Operation of solids up and liquid down.....	123
6.3	Results and discussion	125
6.3.1	Force balance of particles falling.....	126
6.3.2	Effects of U_1	126
6.3.3	Effects of U_s	129
6.4	Comparison between light and density particle	131
6.5	Conclusions and Recommendations	133

Nomenclature	134
Reference.....	136
Chapter 7	138
7 Preliminary study of an inverse gas-liquid-solid circulating fluidized bed	138
Abstract	138
7.1 Introduction.....	138
7.2 Experiment setup	141
7.2.1 Operation of IGLSCFB.....	142
7.2.2 Measurement of phase holdups.....	143
7.3 Gas-Liquid experiment and observation.....	144
7.3.1 Phase holdup distributions and mixture density	147
7.3.2 Average solids holdup at different operation conditions	148
7.4 Comparison between the behavior of gas and solid in IGLSCFB	150
7.5 Comparison between IGLSCFB and ILSCFB	151
7.6 Conclusions and recommendations.....	152
Nomenclature	154
Reference.....	156
Chapter 8.....	159
8 General Discussion.....	159
8.1 Development of Four-Quadrant Fluidization Regime map	159
8.2 Description of each Quadrant	162
8.3 Projection of solids holdup in different modes of operation.....	165
8.4 Critical solids flowrates and liquid velocities	172
8.4.1 Stagnant liquid flow	174
8.4.2 Assisting flow	174
8.4.3 Hindering flow	174

8.4.4	Supporting flow	174
8.5	Transition between regimes	175
8.5.1	Connection between CCFB and LSCFB.....	175
8.5.2	Connection between counter-current flow and circulating fluidized bed	176
8.6	Feasible operating conditions of heavy density particles	177
8.7	Feasible operating conditions of low density particles	178
	Nomenclature	179
Chapter 9	181
9	Conclusions and Recommendations	181
9.1	Conclusions.....	181
9.2	Recommendations.....	182
Appendices	185
A.	Materials and Method	185
B.	Average solids holdup of each particle	196
C.	Published article.....	201
Curriculum Vitae	202

List of Tables

Table 3.2-1 Particle properties	32
Table 3.4-1 Fitted n and k in modified Richardson-Zaki equation	62
Table 4.1-1 Comparison of T_s , T_l and T_s/T_l at constant solids holdup	73
Table 5.2-1 Particle properties	97
Table 8.2-1 Flow directions of solids and liquid in four-quadrant flow regimes map	164
Table 8.4-1 Summary on different types of flow	175
Table A-1 Particle properties	187

List of Figures

Figure 1.1.1 Modes of Gas-Liquid-Solid Fluidization (Muroyama and Fan 1985).....	1
Figure 1.1.2 Four-Quadrant flow regimes map based on flow directions of liquid and solids	3
Figure 2.2.1 Liquid-solid fluidization regime map based on dimensionless particle diameter and dimensionless superficial liquid velocity (J. Wang et al. 2019)	13
Figure 2.3.1 Axial solids holdup distribution in LSCFB at constant solid circulation rate for different particles (Sang and Zhu 2012)	14
Figure 2.3.2 Solids holdup radial distribution in LSCFB riser (Sang and Zhu 2012)	15
Figure 2.3.3 Typical Cluster in liquid-solid transport bed obtained from PIV with time interval of 0.6s (Chen et al. 1991).....	18
Figure 2.4.1 Flow regime map for the inverse three-phase fluidized bed based on U_l and U_g . (A) fixed or partially fluidized bed; (B) fluidized bed with dispersed bubbles; (C) fluidized bed with transition to coalescing bubble flow. (Buffière and Moletta 1999)	22
Figure 3.2.1 Schematic diagram of inverse liquid-solid circulating fluidized bed	31
Figure 3.3.1 The relationship between $\ln(U_l)$ and $\ln(\epsilon_l)$ of studied particles,	33
Figure 3.3.2 Axial solids holdup distribution of EPS28	36
Figure 3.3.3 Axial solids holdup distribution of EPS122	37
Figure 3.3.4 Axial solids holdup distribution of EPS303	38
Figure 3.3.5 Axial solids holdup distribution of EPS638	39
Figure 3.3.6 Effects of U_l on axial solids holdup distribution of EPS28.	40
Figure 3.3.7 Effects of U_l on axial solids holdup distribution of EPS303	41

Figure 3.3.8 Axial solids holdup distribution of different particles under different constant U_1 and U_s	42
Figure 3.3.9 Axial solids holdup distribution under different U_1 - U_t and	44
Figure 3.3.10 Solids holdup radial distribution of five types of particles.....	45
Figure 3.3.11 Radial solids holdup distribution of EPS28.....	47
Figure 3.3.12 Local particle velocity of EPS28	48
Figure 3.3.13 Radial flow structure of EPS 122	49
Figure 3.3.14 Radial flow structure of EPS 303	50
Figure 3.3.15 Radial flow structure of EPS636	51
Figure 3.3.16 Change of average particle velocity with U_s	52
Figure 3.3.17 Change of average particle velocity with U_s under difference U_1	53
Figure 3.3.18 Effects of particle properties on average solids holdup in the ILSCFB at constant superficial liquid velocity	54
Figure 3.3.19 Effects of particle properties on average solids holdup in the ILSCFB at constant solids circulation rate	55
Figure 3.3.20 3D map of the relationship between solids holdup and U_1 , U_s	56
Figure 3.3.21 Effects of particle property on U_{slip}/U_t under different solids holdup	58
Figure 3.3.22 Clustering phenomenon observed in ILSCFB.....	59
Figure 3.4.1 Predicted solids holdup vs experiment solids holdup with original Richardson-Zaki equation, U_t and n were obtained from conventional bed expansion experiment	61
Figure 3.4.2 Prediction of solids holdup vs experimented solids holdup with modified Richardson-Zaki equation.	63

Figure 4.1.1 The change of average solids holdup with U_1 when $U_s = 1\text{ cm/s}$ in LSCFB	72
Figure 4.2.1 Schematic diagram of ILSCFB	74
Figure 4.2.2 Schematic diagram of LSCFB	75
Figure 4.3.1 Change of T_s with U_s under different U_1 in ILSCFB	76
Figure 4.3.2 Change of T_s with U_s under different U_1 in LSCFB	77
Figure 4.3.3 Change of T_1 with U_s under different U_1 in ILSCFB	78
Figure 4.3.4 Change of T_s of different particles	79
Figure 4.3.5 Comparison between LSCFB and ILSCFB	80
Figure 4.3.6 Change of T_s/T_1 with U_1 in ILSCFB	82
Figure 4.3.7 Change of T_s/T_1 with U_1 in LSCFB	83
Figure 4.3.8 Change of T_s/T_1 in gas-solid CFB riser(Wang et al. 2014).....	87
Figure 5.3.1 Schematic diagram of inverse CCFB	99
Figure 5.3.2 Solids holdup vs superficial liquid velocity at different flow regimes.....	100
Figure 5.3.3 Axial solids holdup distribution in inverse CCFB of two types of low density particles.	102
Figure 5.3.4 Axial distribution of solids holdup, $\rho = 122\text{ kg/m}^3$	103
Figure 5.3.5 The change of slip velocity with U_s of EPS122.....	104
Figure 5.3.6 The change of slip velocity with U_s of EPS122.....	104
Figure 5.3.7 The change of Bed Intensification Factor with U_s	106
Figure 5.3.8 The change of average solids holdup with U_1 in inverse conventional fluidized bed, CCFB and LSCFB.....	108

Figure 5.3.9 The change of average solids holdup with U_s in inverse CCFB and LSCFB ..	108
Figure 5.3.10 Relationship between $\ln(U_{slip}/U_t)$ with $\ln(\epsilon_l)$ in inverse CCFB	111
Figure 6.1.1 Schematic diagram of liquid-solid circulating fluidized bed	121
Figure 6.2.1 Schematic diagram of solids falling down in upflow liquid.....	123
Figure 6.2.2 Schematic diagram of solids rising in downflow liquid in ILSCFB	124
Figure 6.3.1 Force balance on heavy particles falling in upflow liquid	126
Figure 6.3.2 Axial solids holdup in counter-current flow of heavy solids at different upflow liquid and constant superficial solid velocity. (a), $U_s = 1.89$ cm/s, (b) $U_s = 5.29$ cm/s, (c) $U_s = 8.57$ cm/s	128
Figure 6.3.3 The change of average solids holdup with U_l at constant U_s of heavy particles	130
Figure 6.3.4 The change of average solids holdup with U_s at constant U_s of low density particles	130
Figure 6.4.1 Axial solids holdup distribution of light particles rising	132
Figure 7.2.1 Schematic diagram of inverse gas-liquid-solid circulating fluidized bed	141
Figure 7.3.1 Gas holdup vs downflow liquid velocity at different superficial gas velocity .	144
Figure 7.3.2 Gas holdup axial distribution at different downflow liquid velocity when $U_g = 4.3$ mm/s.....	146
Figure 7.3.3 Mixture density of IGLSCFB	148
Figure 7.3.4 Solids holdup (ϵ_s) versus solids circulation (U_s) rate at constant superficial liquid velocity (U_l) and superficial gas velocity (U_g).....	149
Figure 7.5.1 Comparison between ILSCFB and IGLSCFB	151

Figure 8.1.1 Four-Quadrant Fluidization Regimes Map with operating liquid velocity beyond particle terminal velocity.	160
Figure 8.1.2 Four-Quadrant Fluidization Regimes Map with conventional circulating fluidized bed.....	161
Figure 8.1.3 Four-Quadrant Fluidization Regimes Map.....	162
Figure 8.3.1 Projection of ϵ_s versus U_s based on Richardson-Zaki equation ($n = 4$)	167
Figure 8.3.2 Projection of ϵ_s versus U_l/U_t based on Richardson-Zaki equation ($n = 4$)	168
Figure 8.3.3 Effects of n on the change of ϵ_s with U_s in circulating fluidized bed below U_t	170
Figure 8.3.4 Effects of n on the change of ϵ_s with U_s in LSCFB.....	171
Figure 8.6.1 Feasible operating condition of heavy density particles.....	177
Figure 8.7.1 Feasible operating condition of low density particles	178
Figure A.1 Schematic diagram of inverse liquid-solid circulating fluidized bed	188
Figure A.2 Schematic diagram of CCFB	191
Figure A.3 Measurement of local particle velocity with OFP	195

List of Appendices

Appendix B-1 Average solids holdup data of EPS122	196
Appendix B-2 Average solids holdup data of EPS638	197
Appendix B-3 Average solids holdup data of EPS303	198
Appendix B-4 Average solids holdup data of EPS28	199
Appendix B-5 Average solids holdup data of PS1020	200
Appendix B-1 Published article in ILSCFB with previous student	201

Chapter 1

1 General Introduction

1.1 Introduction

Liquid fluidization has becoming increasingly important in human history since 19th century in mineral dressing industry to today's environment and energy industry, due to its versatility and applicability for phase contact (Epstein 2002). With the development over the years, gas phase is also introduced as the third phase. Liquid-Solid fluidization and Gas-Liquid-Solid fluidization can be used for physical processes exemplified by particle classification, crystallization (van Dijk and Braakensiek 1985) and leaching (Kwauk 1991) etc., and chemical processes such as fluidized bed electrodes (Goff et al. 1969) and fluidized bed bioreactors (Nelson, Nakhla, and Zhu 2017; Chavarie and Karamanev 1986).

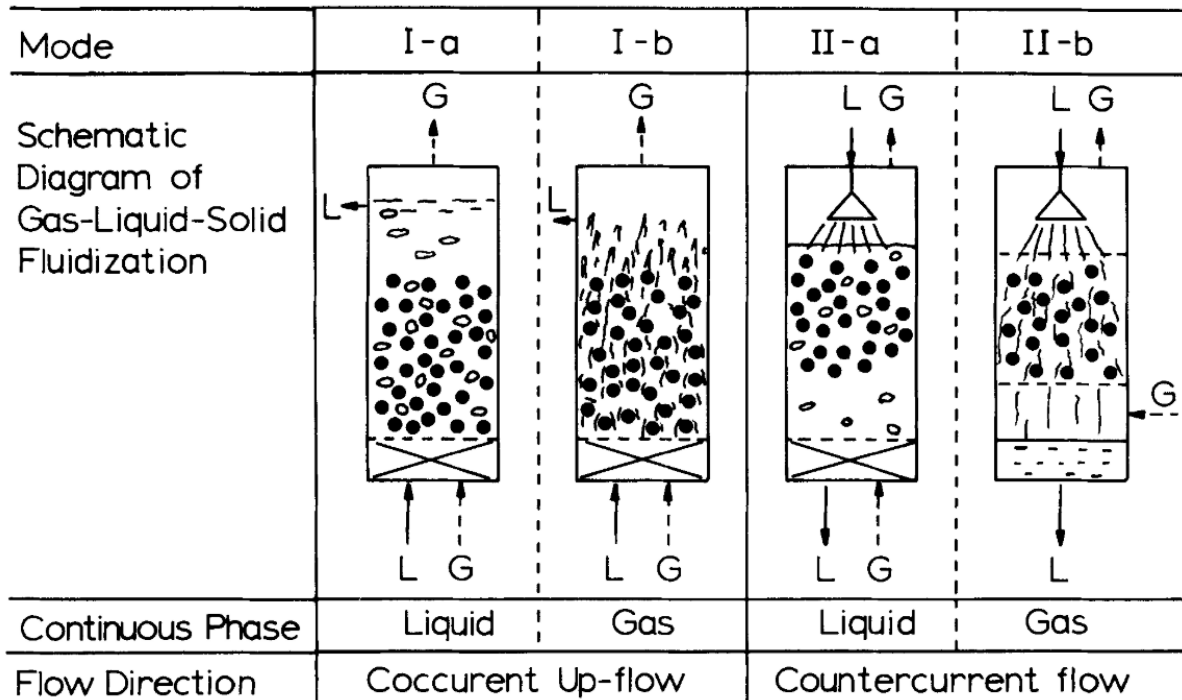


Figure 1.1.1 Modes of Gas-Liquid-Solid Fluidization (Muroyama and Fan 1985)

The demand is rising for the proper design and operation of different types of liquid fluidized bed to satisfy the booming environmental and energy industries (Zhu et al. 2000). Fan has summarized different types of two-phase and three-phase fluidized bed based on categorization of continuous phase and flow direction of gas phase and liquid phase as shown in Figure 1.1.1. And in the age of 80s, many studies were focusing on the bubble behavior in three-phase fluidized bed ;Tzeng, Chen, and Fan 1993; Tsuchiya et al. 1997; Yang, Du, and Fan 2007; Chen, Reese, and Fan 1994), while the study on particles are not well addressed. In recent years, more applications have been developed that require intensive solid-liquid contact. The flow of solids phase has start to draw more attention. Based on that, liquid-solid circulating fluidized bed (LSCFB) (Zheng et al. 1999; Zheng and Zhu 2001; Lan et al. 2000; Zheng and Zhu 2000a, 2000b; Sang and Zhu 2012; Trivedi, Bassi, and Zhu 2006) and gas-liquid-solid circulating fluidized bed (GLSCFB) have been developed (Razzak, Zhu, and Barghi 2010, 2009; Zhu et al. 2000), where solids phase is continuously flowing through the fluidized bed. The uniform distribution of solids and high contact efficiency between solid and liquid have justified their potential applications for ion exchange process (Lan et al. 2002; M. Patel et al. 2008), waste water treatment (Eldyasti et al. 2010; A. Patel, Zhu, and Nakhla 2006; Nelson, Nakhla, and Zhu 2017) and polymerization reaction (Trivedi, Bassi, and Zhu 2006). Many studies have been carried out to investigate the hydrodynamics of LSCFB and GLSCFB which are crucial in fluidized bed design and operation. The development of LSCFB and GLSCFB opens new spectrum in the perspective of liquid based fluidized beds. Thus, the modes of fluidization could be extended based on the flow directions of solid and liquid and it is summarized in Figure 1.1.2, which has been proposed by Prof. Jesse Zhu in many conferences over the years.(Jesse Zhu 2014)

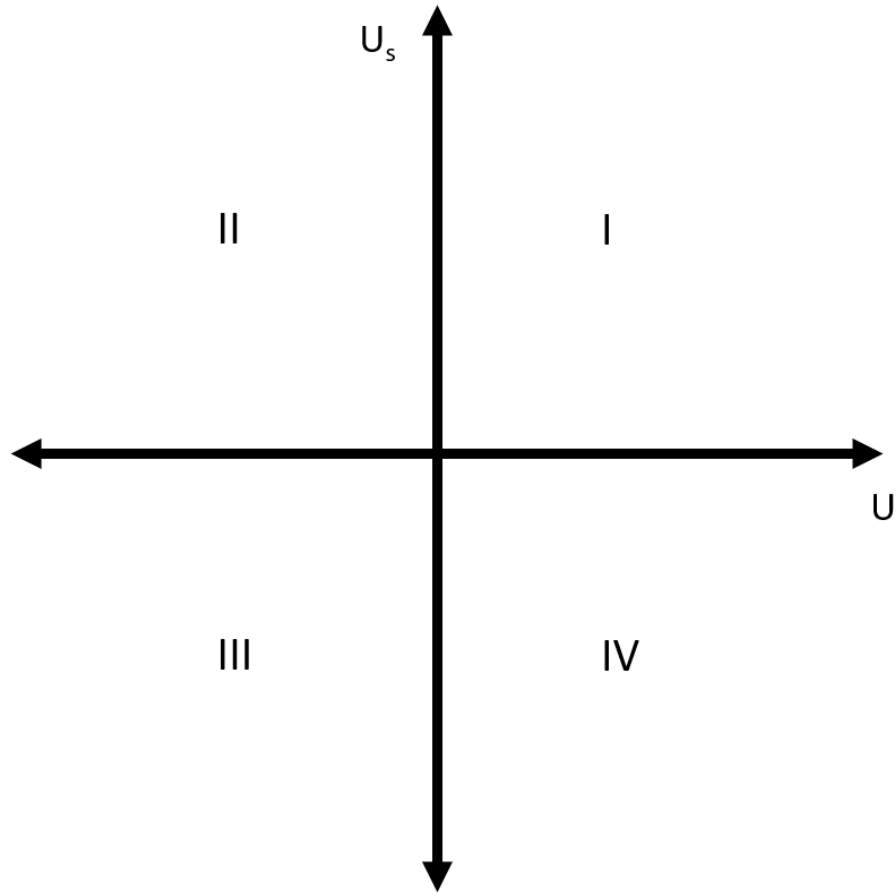


Figure 1.1.2 Four-Quadrant flow regimes map based on flow directions of liquid and solids

The horizontal axis represents liquid flow, and the vertical axis represent solids flow. And in Quadrant-I both liquid and solids are flowing upwards, while in Quadrant-III both are flowing downwards.

Conventional fluidization occupies the horizontal axis where there is no solid circulation. LSCFB take place in Quadrant-I by adding superficial solid velocity to the system. Based on extensive literature review, 90% study on liquid fluidized lies in Quadrant-I (including the positive horizontal axis).

With two continuous flow of solids and liquid, multiple combinations of flow directions could exist in each quadrant of the four-quadrant flow regimes map. Counter-current flow of liquid and solid will take place in the second and fourth quadrant, and the first and third quadrant will be occupied by co-current flow. To fulfill and enrich this four-quadrant fluidization map for liquid

fluidization, the change of fluid/particle density ratio is necessary. As recent years, the study of inverse (downward) fluidization with low density particles have already drawn some attention that is placed on the left side of the horizontal axis and further extended to Quadrant-III by adding downward solid circulation

The flow behavior of low density particles has been studied long before in many areas, such as crystallization and wastewater treatment (Matas, Morris, and Guazzelli 2004; GOTOH 1970; Saffman 1965; Han and Hunt 1995). Most studies focused on neutrally-buoyant particles, whose density are slightly smaller than liquid and have small particle diameter. It wasn't until late 20th century that inverse fluidization was first extensively studied by Fan and Karamanev etc (Fan, Muroyama, and Chern 1982; Nikolov and Karamanev 1991; Dimitar G. Karamanev and Nikolov 1992; D. G. Karamanev and Nikolov 1992). Most common fluidized beds, the particles are heavier than the fluid, thus the gas or liquid always has to flow upward to support the weight of particles. When particle density is lighter than the fluid, the direction of fluid flow has to be inversed to fluidize the floating particles, so-called inverse fluidization.

More regimes can be discovered based on this extensive Four-Quadrant Fluidization Regime Map. The hydrodynamics of each regime, especially of which with low density particles are not well studied. This study will focus on the hydrodynamics of inverse liquid-solid circulating fluidized bed in Quadrant-III and fill some blank areas in the Four-Quadrant Fluidization Regime Map.

1.2 Research objective

The main objective of this study is to systematically investigate the hydrodynamics of multiple circulating liquid-solid fluidized bed systems

The secondary objectives are:

- Study the hydrodynamics of inverse liquid-solid circulating fluidized bed experimentally
- Study the hydrodynamics of liquid-solid circulating fluidized bed below particle terminal velocity
- Investigate the characteristics of the first proposed inverse gas-liquid-solid circulating fluidized bed

- Fulfill the four-quadrant flow regimes map

1.3 Thesis Structure

Chapter 2 gives a literature review on conventional liquid-solid fluidization, liquid-solid circulating fluidization and inverse fluidization, which covers multiple flow conditions in the area liquid fluidization

Chapter 3 studies hydrodynamics of an inverse liquid-solid circulating fluidized bed with five types of low density particles. The study on of axial and radial flow structure, average solids holdup, and particle property effects is covered.

Chapter 4 compares its hydrodynamics of liquid-solid circulating fluidized bed with heavy density particles based on solids holdup distribution, particle property effects and solids residence time per unit height.

Chapter 5 proposes the idea of low velocity circulating fluidized bed, called conventional circulating fluidized bed (CCFB), where solids circulation take place while the system is operating under particle terminal velocity. And studied the hydrodynamics of inverse CCFB.

Chapter 6 shows some preliminary results of counter-current flow of free-falling and free-rising particles

Chapter 7 describes some preliminary results in the hydrodynamics of inverse gas-liquid-solid circulating fluidized bed (IGLSCFB). And compared its hydrodynamics with ILSCFB.

Chapter 8 provide a general discussion on the Four-Quadrant Fluidization Regime map.

Chapter 9 concludes the finding of this research and lists many recommendations in the area of fluidization.

Reference

- Buffière, Pierre, and René Moletta. 1999. "Some Hydrodynamics Characteristics of Inverse Three Phase Fluidized-Bed Reactors." *Chemical Engineering Science* 54 (9): 1233–42. [https://doi.org/10.1016/S0009-2509\(98\)00436-9](https://doi.org/10.1016/S0009-2509(98)00436-9).
- Chavarie, C, and D Karamanev. 1986. "Use of Inverse Fluidization in Biofilm Reactors." In *Proc. Int. Conf. on Bioreactor Fluid Dynamics, Cambridge* (15-17 April), 181–90.
- Chen, R. C., J. Reese, and L.-S. Fan. 1994. "Flow Structure in a Three-Dimensional Bubble Column and Three-Phase Fluidized Bed." *AIChE Journal* 40 (7): 1093–1104. <https://doi.org/10.1002/aic.690400702>.
- Dijk, J. C. van, and H. Braakensiek. 1985. "Phosphate Removal by Crystallization in a Fluidized Bed." *Water Science and Technology* 17 (2–3): 133–42. <https://doi.org/10.2166/wst.1985.0125>.
- Eldyasti, Ahmed, Nabin Chowdhury, George Nakhla, and Jesse Zhu. 2010. "Biological Nutrient Removal from Leachate Using a Pilot Liquid–Solid Circulating Fluidized Bed Bioreactor (LSCFB)." *Journal of Hazardous Materials* 181 (1–3): 289–97. <https://doi.org/10.1016/J.JHAZMAT.2010.05.010>.
- Epstein, Norman. 2002. "Applications of Liquid-Solid Fluidization." *International Journal of Chemical Reactor Engineering* 1 (1). <https://doi.org/10.2202/1542-6580.1010>.
- Fan, Liang Shih, Katsuhiko Muroyama, and Song Hsing Chern. 1982. "Hydrodynamics Characteristics of Inverse Fluidization in Liquid-Solid and Gas-Liquid-Solid Systems." *The Chemical Engineering Journal* 24 (2): 143–50. [https://doi.org/10.1016/0300-9467\(82\)80029-4](https://doi.org/10.1016/0300-9467(82)80029-4).
- Goff, P. Le., F. Vergnes, F. Coeuret, and J. Bordet. 1969. "APPLICATIONS OF FLUIDIZED BEDS IN ELECTROCHEMISTRY." *Industrial & Engineering Chemistry* 61 (10): 8–17. <https://doi.org/10.1021/ie50718a004>.
- GOTOH, KEISHI. 1970. "Migration of a Neutrally Buoyant Particle in Poiseuille Flow: A Possible Explanation." *Nature* 225 (5235): 848–50. <https://doi.org/10.1038/225848a0>.

Han, Q., and J.D. Hunt. 1995. "Particle Pushing: Critical Flow Rate Required to Put Particles into Motion." *Journal of Crystal Growth* 152 (3): 221–27. [https://doi.org/10.1016/0022-0248\(95\)00085-2](https://doi.org/10.1016/0022-0248(95)00085-2).

Jesse Zhu. 2014. "The Four Quadrant Fluidization Regime Map, a Reflection on Prof. Kwauk's Generalized Fluidization." In *World Congress of Particle Technology-7*. Beijing, China.

Karamanev, D. G., and L. N. Nikolov. 1992. "Bed Expansion of Liquid-Solid Inverse Fluidization." *AIChE Journal* 38 (12): 1916–22. <https://doi.org/10.1002/aic.690381208>.

Karamanev, Dimitar G., and Ludmil N. Nikolov. 1992. "Free Rising Spheres Do Not Obey Newton's Law for Free Settling." *AIChE Journal* 38 (11): 1843–46. <https://doi.org/10.1002/aic.690381116>.

Kwauk, Mooson. 1991. "Particulate Fluidization: An Overview." *Advances in Chemical Engineering* 17 (January): 207–360. [https://doi.org/10.1016/S0065-2377\(08\)60116-7](https://doi.org/10.1016/S0065-2377(08)60116-7).

Lan, Qingdao, Amarjeet Bassi, Jing-Xu (Jesse) Zhu, and Argyrios Margaritis. 2002. "Continuous Protein Recovery from Whey Using Liquid-Solid Circulating Fluidized Bed Ion-Exchange Extraction." *Biotechnology and Bioengineering* 78 (2): 157–63. <https://doi.org/10.1002/bit.10171>.

Lan, Qingdao, Jing-Xu Jesse Zhu, Amarjeet S. Bassi, Argyrios Margaritis, Ying Zheng, and Gerald E. Rowe. 2000. "Continuous Protein Recovery Using a Liquid-Solid Circulating Fluidized Bed Ion Exchange System: Modelling and Experimental Studies." *The Canadian Journal of Chemical Engineering* 78 (5): 858–66. <https://doi.org/10.1002/cjce.5450780502>.

Matas, J P, J F Morris, and E Guazzelli. 2004. "Lateral Forces on a Sphere." *Oil & Gas Science and Technology – Rev. IFP* 59 (1): 59–70. http://ogst.ifpenergiesnouvelles.fr/articles/ogst/pdf/2004/01/matas_vol59n1.pdf.

Muroyama, Katsuhiko, and Liang-shih (Ohio State University) Fan. 1985. "Fundamentals of Gas- Liquid -Solid Fluidization." *AIChE Journal* 31 (1): 1–34. <https://doi.org/10.1002/aic.690310102>.

- Nelson, Michael J., George Nakhla, and Jesse Zhu. 2017. "Fluidized-Bed Bioreactor Applications for Biological Wastewater Treatment: A Review of Research and Developments." *Engineering* 3 (3): 330–42. <https://doi.org/10.1016/J.ENG.2017.03.021>.
- Nikolov, L., and D. Karamanev. 1991. "The Inverse Fluidization - A New Approach to Biofilm Reactor Design, to Aerobic Wastewater Treatment." In , 177–82. [https://doi.org/10.1016/S0166-1116\(08\)70325-X](https://doi.org/10.1016/S0166-1116(08)70325-X).
- Patel, Ajay, Jesse Zhu, and George Nakhla. 2006. "Simultaneous Carbon, Nitrogen and Phosphorous Removal from Municipal Wastewater in a Circulating Fluidized Bed Bioreactor." *Chemosphere* 65 (7): 1103–12. <https://doi.org/10.1016/J.CHEMOSPHERE.2006.04.047>.
- Patel, Manoj, Amarjeet S. Bassi, Jesse J.-X. Zhu, and Hassan Gomaa. 2008. "Investigation of a Dual-Particle Liquid-Solid Circulating Fluidized Bed Bioreactor for Extractive Fermentation of Lactic Acid." *Biotechnology Progress* 24 (4): 821–31. <https://doi.org/10.1002/btpr.6>.
- Razzak, S. A., J.-X. Zhu, and S. Barghi. 2009. "Particle Shape, Density, and Size Effects on the Distribution of Phase Holdups in an LSCFB Riser." *Chemical Engineering & Technology* 32 (8): 1236–44. <https://doi.org/10.1002/ceat.200900075>.
- Razzak, S. A., J. X. Zhu, and S. Barghi. 2010. "Effects of Particle Shape, Density, and Size on a Distribution of Phase Holdups in a Gas-Liquid-Solid Circulating Fluidized Bed Riser." *Industrial and Engineering Chemistry Research* 49 (15): 6998–7007. <https://doi.org/10.1021/ie901704d>.
- Saffman, P. G. 1965. "The Lift on a Small Sphere in a Slow Shear Flow." *Journal of Fluid Mechanics* 22 (02): 385. <https://doi.org/10.1017/S0022112065000824>.
- Sang, Long, and Jesse Zhu. 2012. "Experimental Investigation of the Effects of Particle Properties on Solids Holdup in an LSCFB Riser." *Chemical Engineering Journal* 197: 322–29.
- Trivedi, Umang, Amarjeet Bassi, and Jing-Xu (Jesse) Zhu. 2006. "Continuous Enzymatic Polymerization of Phenol in a Liquid–Solid Circulating Fluidized Bed." *Powder Technology* 169 (2): 61–70. <https://doi.org/10.1016/J.POWTEC.2006.08.001>.
- Tsuchiya, Katsumi, Akihiko Furumoto, Liang-Shih Fan, and Jianping Zhang. 1997. "Suspension

Viscosity and Bubble Rise Velocity in Liquid-Solid Fluidized Beds.” *Chemical Engineering Science* 52 (18): 3053–66. [https://doi.org/10.1016/S0009-2509\(97\)00127-9](https://doi.org/10.1016/S0009-2509(97)00127-9).

Tzeng, J.-W., R. C. Chen, and L.-S. Fan. 1993. “Visualization of Flow Characteristics in a 2-D Bubble Column and Three-Phase Fluidized Bed.” *AIChE Journal* 39 (5): 733–44. <https://doi.org/10.1002/aic.690390502>.

Yang, G.Q., Bing Du, and L.S. Fan. 2007. “Bubble Formation and Dynamics in Gas–Liquid–Solid Fluidization—A Review.” *Chemical Engineering Science* 62 (1–2): 2–27. <https://doi.org/10.1016/J.CES.2006.08.021>.

Zheng, Ying, and Jing-Xu (Jesse) Zhu. 2000a. “Microstructural Aspects of the Flow Behaviour in a Liquid-Solids Circulating Fluidized Bed.” *The Canadian Journal of Chemical Engineering* 78 (1): 75–81. <https://doi.org/10.1002/cjce.5450780112>.

Zheng, Ying, and Jing-Xu (Jesse) Zhu. 2000b. “Overall Pressure Balance and System Stability in a Liquid–Solid Circulating Fluidized Bed.” *Chemical Engineering Journal* 79 (2): 145–53. [https://doi.org/10.1016/S1385-8947\(00\)00168-6](https://doi.org/10.1016/S1385-8947(00)00168-6).

Zheng, Ying, and Jing-Xu (Jesse) Zhu. 2001. “The Onset Velocity of a Liquid–Solid Circulating Fluidized Bed.” *Powder Technology* 114 (1–3): 244–51. [https://doi.org/10.1016/S0032-5910\(00\)00318-1](https://doi.org/10.1016/S0032-5910(00)00318-1).

Zheng, Ying, Jing-Xu Zhu, Jianzhang Wen, Steve A Martin, Amarjeet S Bassi, and Argyrios Margaritis. 1999. “The Axial Hydrodynamics Behavior in a Liquid-solid Circulating Fluidized Bed.” *The Canadian Journal of Chemical Engineering* 77 (2): 284–90.

Zhu, Jing-Xu (Jesse), Dimitre G. Karamanev, Amarjeet S. Bassi, and Ying Zheng. 2000. “(Gas-)Liquid-Solid Circulating Fluidized Beds and Their Potential Applications to Bioreactor Engineering.” *The Canadian Journal of Chemical Engineering* 78 (1): 82–94. <https://doi.org/10.1002/cjce.5450780113>.

Chapter 2

2 Literature Review

Extensive researches have been carried out on the hydrodynamics of liquid-solid fluidized bed. Due to its homogeneous characteristics, many similarities can be found between different modes and regimes of liquid-solid fluidized beds. Since this study aims to explore on different modes of liquid-solid circulating fluidized beds from on the Four-Quadrant Fluidization Regime Map, mainly with low density particles, this review will try to summarize some key features of the studied upward liquid-solid circulating fluidized bed and inverse fluidization.

2.1 Fundamental

In liquid solid fluidized bed, liquid velocity provides the drag force for fluidization. The velocity profile of liquid flow that pass around each particle will determine the drag force. However, the actual velocity profile is hard to determine due to turbulence of liquid flow, fluctuation of solids holdup, liquid-solid and solid-solid interaction etc.

So different expressions of liquid velocities have been adopted to describe the liquid flow at different conditions. Comparing with the liquid flowrate, proper definition of liquid velocity is important when comparing results from reactors in different dimensions, which is also crucial in the scaling up process.

2.1.1 Superficial liquid velocity

Superficial liquid velocity is defined as the liquid velocity is the absence of particles, which can be expressed as the liquid flowrate over the cross-section area of the fluidized bed $U_l = \frac{Q}{A}$. The term ‘superficial’ is used because the true liquid velocity is never U_l since the cross-section area for liquid flow is partially occupied by particles in the fluidized bed.

2.1.2 Interstitial liquid velocity

Apparent liquid velocity is defined as the superficial liquid velocity over voidage, $\frac{U_l}{\epsilon_l}$, which can also be viewed as liquid flowrate over the cross-section area that's been occupied by liquid, $\frac{Q}{A\epsilon_l}$.

Apparent liquid velocity can be used to represent the spatial average of actual liquid velocity. Because both liquid velocity and local voidage in the fluidized bed is not uniform both spatially and timely, same as liquid velocity. However, apparent liquid velocity can help us get a closer estimate of true liquid velocity that pass

2.1.3 Particle terminal velocity

Particle terminal velocity is the settling velocity of particle in stagnant liquid at steady state. When the particle density is lighter than the density of liquid, particle terminal velocity is defined as the free rising velocity of particle at steady state. On the other hand, when particle is settled, particle terminal velocity is also the transient liquid velocity to move the particles. When liquid and particle are in motion, it is believed the particle terminal velocity is the velocity difference between particle and liquid, which is also defined as slip velocity. However, in fluidized bed systems, where particle-particle interaction and liquid turbulence are involved, slip velocity could deviate from single particle terminal velocity. Particle terminal velocity can be calculated in stokes region, where liquid flow is at laminar region. When a uniform liquid flow is passing by a single particle

Slip velocity is the difference of liquid velocity and particle velocity.

In very dilute condition, the relationship of particle velocity, superficial liquid velocity and solids holdup can be expressed by $U_p = \frac{U_s}{\varepsilon_s} = \frac{U_l}{1-\varepsilon_s} - U_t$. Where particle velocity can be expressed by solids circulation rate over solids holdup, or transient liquid velocity minus particle terminal velocity. The equation is based on a few assumptions:

- 1) Dilute condition where solids behave as one particle in the fluid. No particle-particle interaction is considered. Thus, solids holdup distribution is uniform axially and radially, no cluster and back-mixing existed
- 2) Uniform liquid velocity distribution so that interstitial velocity can be expressed by $U_l/(1-\varepsilon_s)$
- 3) Particles size distribution is narrow.
- 4) Slip velocity equals particle terminal velocity.

From experiments of fluidized bed, it is hard to satisfy the above assumptions. But liquid-solid circulating fluidized bed is the most promising candidate to satisfy the above ideal conditions. Particulate fluidized behavior allows us to use equation with little modification. Since a wide range of solids holdup is aimed to be covered for the functionality of the model, the dilution condition cannot be satisfied. Thus, slip velocity cannot be estimated using particle terminal velocity. Apparent slip velocity can be applied for the model. $U_{slip} = \frac{U_l}{1-\varepsilon_s} - \bar{U}_p$ Average particle velocity is obtained by averaging radial particle velocity based on volume.

2.1.4 Solid circulation rate

Solids circulation rate is used to characterize the flowrate of solids in the circulating fluidized bed. In gas-solid systems, the mass flowrate of solids (G_s , kg/m²s)(Bi and Zhu 1993) is commonly used while in liquid-solid systems the superficial solid velocity (U_s , m/s)(W. Liang et al. 1997) is adopted. The relationship between G_s and U_s is $G_s = \rho \cdot U_s$. Both variables could be used to represent the amounts of solids that are being transported in the circulating fluidized bed. In this study, solids holdup, volume fraction of the solids phase, is the main hydrodynamics characteristics of interest in inverse liquid-solid circulating fluidized bed. So, the superficial solid velocity U_s is used as it reflects the volume flowrate of solids.

2.2 Fluidization regimes

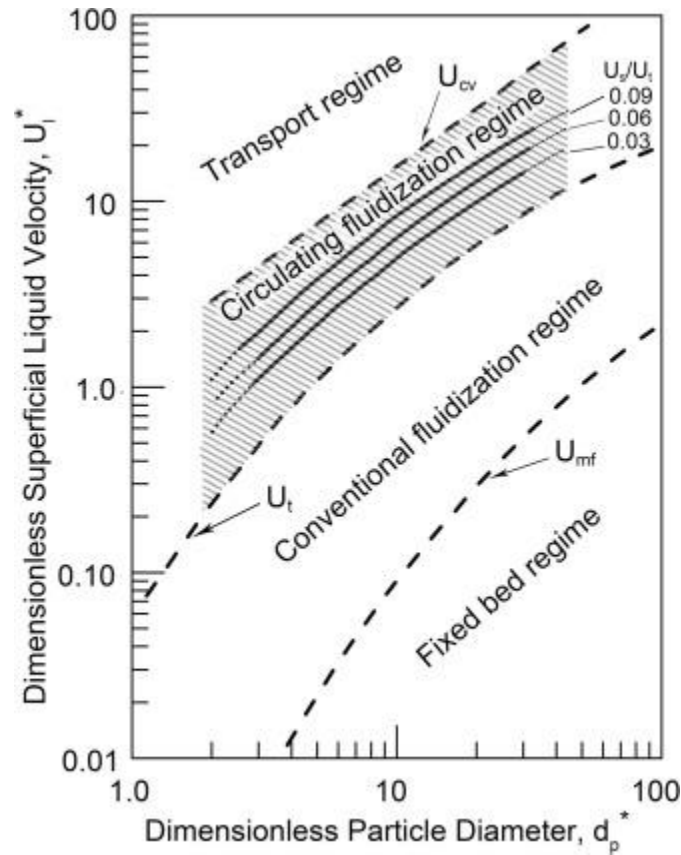


Figure 2.2.1 Liquid-solid fluidization regime map based on dimensionless particle diameter and dimensionless superficial liquid velocity (J. Wang et al. 2019)

Many studies have focused on the flow regimes map of liquid-solid fluidized bed (Sang and Zhu 2012). With the development of liquid-solid circulating fluidized bed, the circulating fluidization regime has been added and studied extensively. Long and Zhu have modified the calculation of U_{cv} which is also extended to inverse liquid-solid circulating fluidization with low density particles.

2.3 Hydrodynamics of LSCFB

2.3.1 Solids holdup distribution

Axial solids holdup in LSCFB has been reported by many researchers under a wide range of superficial liquid velocities and solid circulation rates (Zheng et al. 1999; Sang and Zhu 2012). Some key results are shown in Figure 2.3.1. Solids holdup is uniform in the LSCFB riser, and non-

uniformity has only been observed in steel shots particles with high particle terminal velocity under relatively low superficial liquid velocity. The slow acceleration of the heavy particle accounts for the non-uniform axial profile.

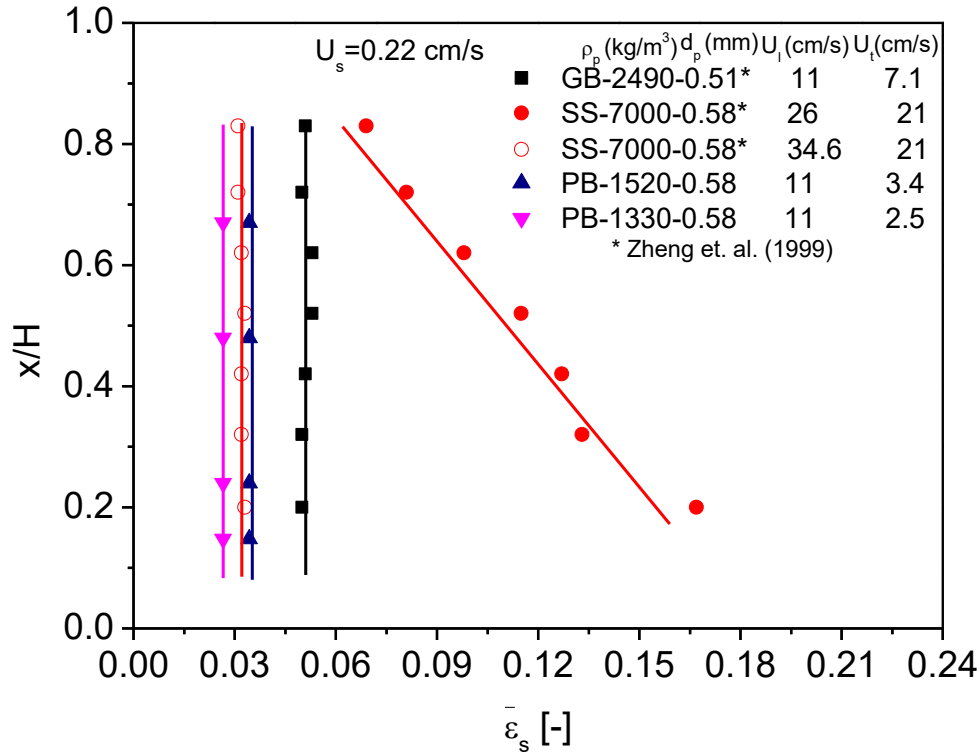


Figure 2.3.1 Axial solids holdup distribution in LSCFB at constant solid circulation rate for different particles (Sang and Zhu 2012)

Radial solids holdup has also been studied by Liang, Sang and Zheng (Zheng et al. 2002; W.-G. Liang et al. 1996; Sang and Zhu 2012). They have found that an increasing trend of solids holdup from center to the wall measured by optical fiber probe. And the degree of non-uniformity is increasing with solids circulation rates and decreasing with superficial liquid velocity. And the particle properties will also affect the radial distribution.

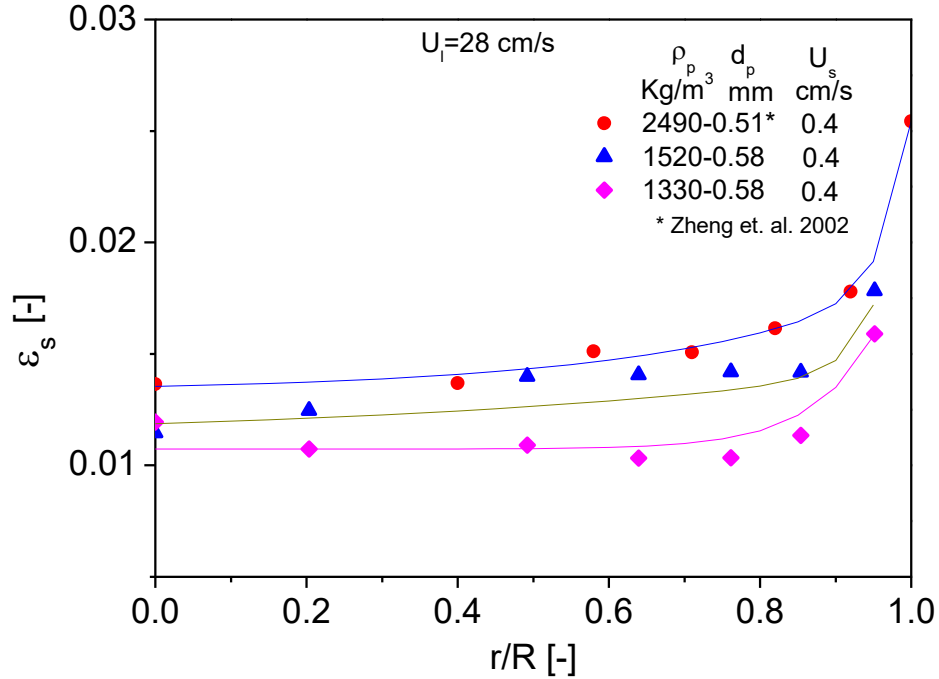


Figure 2.3.2 Solids holdup radial distribution in LSCFB riser (Sang and Zhu 2012)

2.3.2 Onset velocity

Bed empty experiments were carried out in downer of inverse liquid-solid circulating fluidized bed. The circulating fluidized bed is operating at steady state as solids are flowing downwards in the downer, collected in the upcomer and been returned to the downer. The bed empty experiment starts when solids feed was shut down while liquid flow was unchanged. The time was measured for liquid flow to carry away all the particles in the solids till the fluidized bed is empty. For each superficial liquid velocity, there is a corresponding bed empty time. Apparently, the bed empty time is decreasing with superficial liquid velocity because solids travel faster under higher superficial liquid velocities. And the change is more abrupt when the liquid velocity is relatively low, and slope becomes less steep with the increase of liquid velocity.

The onset velocity of liquid-solid circulating fluidized bed is defined as the critical superficial liquid velocity where a sudden change of bed empty time occurred. Below onset velocity, it takes incredibly long time to empty the fluidized bed as the system is not in complete circulating regime.

And beyond onset velocity, the system is under fully developed circulating regime where all particles can be transported easily out of the column. (Zheng and Zhu 2001)

2.3.3 Pressure balance in LSCFB

Pressure balance in LSCFB is crucial in the design and operation of the circulating fluidized bed. Particles in LSCFB are circulating between the two columns. Starting from the distributor, particles are transported to the top by high velocity liquid and fall down to the downcomer by the force of gravity. A packed bed or semi-fluidized bed is formed at the bottom of the downcomer, and solids are gradually fed to the distributor in the riser through the feeding pipe with the help of gravity. A steady and controllable circulation of solids is achieved by adjusting the pressure difference between the bottom of the riser and the downcomer. The riser and the downcomer work as a U-tube. The downcomer that contains more heavy solids will have higher pressure that constantly push particles to the riser that has less pressure due to its less holding of solids. Solids are packed from the bottom section of the downcomer to the feeding pipe before entering the riser. When solids are packed, their weight are supported by the wall of the column, which inhibit the pressure to be transferred, thus some liquid are injected to semi fluidized the particles in the downcomer, so particles are loosened and the pressure from the particles are easier to be transferred to the distributor region in the riser. The auxiliary flow distributor works as a non-mechanical valve that controls the pressure drop from the packed solids to the riser which is used to adjust the solid circulation rate. (Zheng and Zhu 2000)

2.3.4 Transition Regime

In Zheng's study, the transition regime is mentioned when describing the operating window of LSCFB. For a constant auxiliary flow rate, solids circulation rate is increasing with superficial liquid velocity. Beyond a critical liquid velocity (turning point), solid circulation rate will reach constant. Beyond the turning point, solids circulation rate is limited by the pressure drop between the storage column and liquid flow distributor dictated by auxiliary flowrate. In other words, solid circulation rate reaches maximum. Prior to reach the turning point, the pressure drop from the storage column is not the limiting factor for solid circulation rate, which explains the increasing trend of solids circulation rate with liquid velocity. (Zheng et al. 1999)

2.3.5 Cluster in liquid-solid circulating fluidized bed

Liquid fluidization is often regarded as homogeneous fluidization. Very rare literature has mentioned clusters in liquid-solid circulation fluidized bed operating under high superficial liquid velocity. Chen and Fan have studied clusters in liquid-solid transport bed. The formation and disintegration of clusters were captured in the 2D liquid-solid transport bed by PIV, where the range of solids holdup is 0.056 to 0.028. Some captured cluster photos are presented in Figure 2.3.3. It is found that clusters formed in the vertical direction and will be rotated to a horizontal alignment to gradually disperse. The studied cluster size was ranging from 2 to 7 particle diameters. It is found that the degree of clustering is increasing with solids holdup and is also dependent on Re . The probability of clusters and cluster characteristics were investigated followed by the slip velocity of clusters which is found to be dependent on cluster size and cluster arrangement. (Chen et al. 1991)

Clusters have also been studied in non-circulating liquid-solid fluidized bed where solids holdup is ranging from 0.07 to 0.114. The cluster size and cluster number were found to be increasing with solids holdup due to increased particle collision in dense condition as explained by the author. And the overall clustering effects were quantified by box fractal dimension, a measure of complexity of cluster images, which is believed to be a reflection of cluster coalescences and large-scale clusters. (An, Liu, and Fu 2007)

Up to date, no researchers have given quantitative and systematic results on clusters in liquid fluidized bed. Most results remain in qualitative description. And the cluster size, frequency of cluster formation and disintegration, cluster arrangement and volume fraction of cluster etc. are crucial effects of cluster on the flow behavior of solids. It is still unclear the impact of instantaneous clustering phenomenon on the general hydrodynamics of liquid fluidized bed.

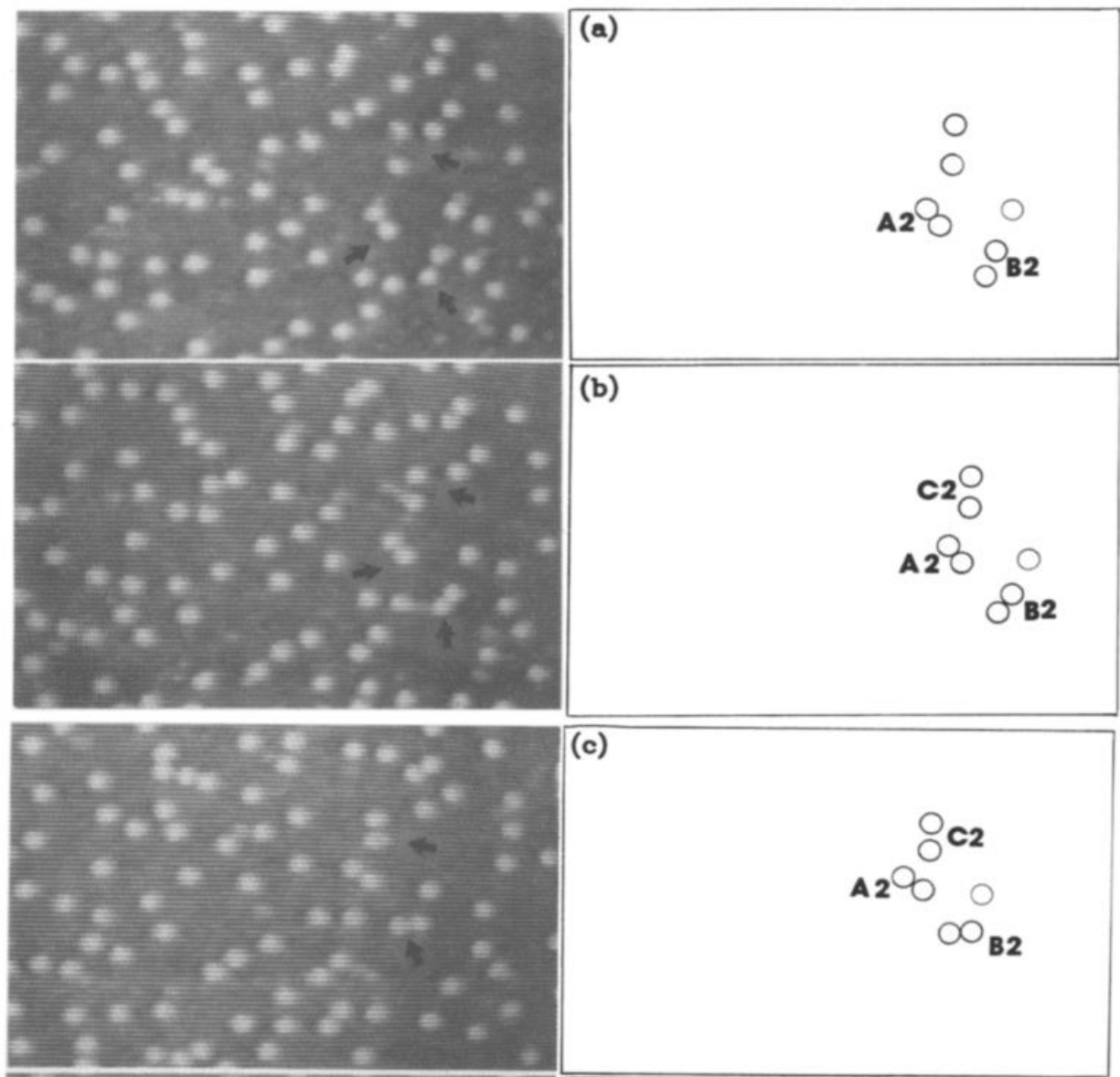


Figure 2.3.3 Typical Cluster in liquid-solid transport bed obtained from PIV with time interval of 0.6s (Chen et al. 1991)

2.4 Hydrodynamics of Inverse Conventional fluidization

In most fluidization systems, heavy solids are fluidized by an upflow of liquid or gas. Whereas, when the solids density is lower than the fluid, a downflow of liquid is required as particles are floating at the top at its starting position, so called inverse fluidization. Due to the small inertia of low density particles, the hydrodynamics of inverse fluidization is different from upward

fluidization. Fan (Fan, Muroyama, and Chern 1982) is the first to report that bed expansion of inverse fluidization didn't follow the well-known Richard-Zaki equation, and the exponent n is modified to better fit in prediction of voidage of inverse fluidization. Continuing Fan's work, Karamanev (Nikov and Karamanev 1991; Dewsbury, Karamanev, and Margaritis 2000; Dimitar G. Karamanev and Nikolov 1992; D. G. Karamanev and Nikolov 1992) has found out the free rising of low density particle doesn't obey newton's law. And the updated drag coefficient is measured for many types of particle in a wide range of density and diameter, all in newton regime. Based on the modified drag coefficient, revised particle terminal velocity can be calculated. And the Richard-Zaki equation for upflow fluidization is found to be valid without changing exponent n . Other hydrodynamics characteristics, such as minimum fluidization has been investigated as well in the last few decades.

Inverse fluidized bed has been adopted as bioreactor for wastewater treatment (Buffière 2000)(D. Wang et al. 2010; Nikolov and Karamanev 1987; Buffière and Moletta 1999). And the mass transfer in inverse fluidization has been studied experimentally as well.

2.4.1 Behavior of low density particles in liquid

In circulating fluidized bed risers, the radial flow structure of solids has been studied extensively. A core-annulus flow structure has been found, as dilute particles are carried by fast flowing fluid, and a dense region near the wall is observed. In many cases, the flowing direction of wall region is opposite to the direction of fluid flow in the core region due to insufficient drag force from the hindered fluid velocity near the wall. Thus, the radial flow structure is governed by the drag force in the streamline direction.

In liquid solid systems, lateral forces play significant roles in the migration of particles, which result in a different radial flow structure. Since the net weight of particles is drastically reduced due to the existence of liquid, the drag force required to fluidize the particles is lowered. The hindered liquid velocity near the wall is more likely to provide sufficient drag force. (Carlo et al. 2009; Matas, Morris, and Guazzelli 2004)

Figure showing the radial solids holdup distribution of low density particles in the downer. We can see a slightly dense region near the wall when the liquid velocity is relatively low. And the

dense region gradually disappears with increasing liquid velocity. And at high liquid velocity, solids holdup is found to be lower in the wall region. This is because of lifting force push particles against the wall. Lifting force can be expressed in the following equation.

At high liquid velocity, the velocity gradient near the wall region is high, which intensifies the lateral movement of particle from the wall to the center.

The lifting force is a function of velocity gradient. A large velocity gradient will lead to a higher lifting force. Based on the velocity profile of both laminar and turbulent flow, velocity gradient increases from center to the wall in pressure induced pipe flow. In the center region, velocity gradient diminished with increasing liquid velocity, when the flow is approaching turbulent flow regime. In the wall region, the velocity gradient becomes more significant as the velocity change from the center to the wall become abrupt. The features contribute to the particle radial flow structure as well.(Han and Hunt 1995, 1994; Saffman 1965; GOTOH 1970)

2.4.2 Richardson-Zaki equation

JF Richardson etc. have done many studies on the sedimentation and fluidization of liquid-solid system in the last century. The most notable results is Richardson and Zaki equation which dictate the relationship of slip velocity and voidage in both sedimentation and fluidization processes. The beauty of Richardson-Zaki equation is the simplicity of calculating voidage in the form of $\frac{U_l}{U_t} = \varepsilon^n$ with n being a semi empirical value. Over the years, many studies have been focused on improving the correlation of exponent n to provide a better prediction of voidage with different particle properties and operating conditions. Khan and JF Richardson have demonstrated that n is ranging from 2.4 and 4.8. Karamanev has proven that the same correlation from Khan can be applied to inverse fluidization with low density particles that have to be fluidized downwardly. Many correlations have been proposed for exponent n as a function of Re, Ar, d/D etc., and n is being treated as an empirical parameter that can be helpful in providing a better fit. Countless data have been fitted under various conditions and particle properties, which leave many the impression that n is an empirical number. However, n is actually a theoretical parameter that can be derived from Navi-Stokes equation.

In 1954, Richardson and Zaki have walked through the derivation process of drag force exerted on the particle considering the effects of particle-particle interaction. Particles don't interact with each other directly, but the existence of other particles will shape the velocity profile/gradient around each particle. Since the drag force is directly related to velocity gradient, effects of surround particles can't be ignored when studying the drag force on a single particle. Richardson and Zaki derived the drag force equation assuming particle arrangement pattern under certain solids holdup conditions, in order to solve the equation analytically. They were able to derive the drag force equation for different solids holdup and two configurations of particle arrangements. First configuration gives the most space for liquid flow, while the second configuration offers the minimum space for liquid, under the same solids holdup condition.

From the derivation process, we can conclude what variables are included in exponent n : particle and fluid properties such as densities, viscosities and particle diameter, particle-particle interaction such as particle position arrangement.

Traditional method estimating exponent n using particle Reynolds number or Archimedes number fail to consider particle arrangement. It is commonly believed, that particle arrangement is consistent within one type of particle, so it can be a manifestation of particle properties.

2.4.3 Hydrodynamics of inverse three-phase fluidization

The hydrodynamics of inverse three-phase fluidized bed have also been studied before with the application of low density particles. A typical flow regime map is shown in Figure 2.4.1 from Buffière (Buffière and Moletta 1999). It has shown that the hydrodynamics is greatly affected by the gas flow and liquid flow. The liquid flow is providing the drag force to fluidize the particles, and the gas bubbles are going to change the liquid-solid mixture which helps to the floating solids to move down. And many studies have reported on the study of relationship between gas holdups and operating conditions. The behavior of solids has not been well studied.

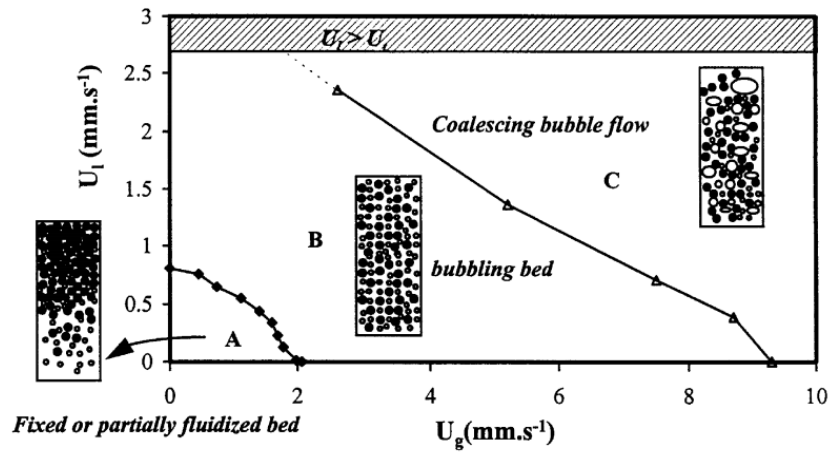


Figure 2.4.1 Flow regime map for the inverse three-phase fluidized bed based on U_l and U_g . (A) fixed or partially fluidized bed; (B) fluidized bed with dispersed bubbles; (C) fluidized bed with transition to coalescing bubble flow. (Buffière and Moletta 1999)

Nomenclature

Ar	Archimedes number defined by $d_p^3 g (\rho_p - \rho_l) \rho_l / \mu_l^2$
C_D	Particle drag coefficient
d_p	Particle diameter (mm)
D	Column diameter (m)
F_b, F_d, F_g	Buoyancy, drag force and gravity
G_s	Solids circulation rate (kg/ (m ² s))
g	Gravity acceleration
Re	Reynolds number defined by $U_l d_p \rho_l / \mu_l$
Re_t	Particle terminal Reynolds number defined by $U_t d_p \rho_l / \mu_l$
U_a	Auxiliary liquid velocity (cm/s)
U_l	Superficial liquid velocity (cm/s)
U_s	Superficial solids velocity (cm/s)
U_{slip}	Slip velocity (cm/s)
U_t	Particle terminal velocity (cm/s)
U_{tr}	Transition velocity demarcate the conventional particulate regime and circulating fluidization regime (cm/s)
V_l, V_p	Local liquid velocity and local particle velocity (cm/s)
\bar{V}_p	Average particle velocity (cm/s)

Greek letters

$\bar{\varepsilon}$	Average bed voidage
$\bar{\varepsilon}_s$	Average solids holdup
μ_l	Liquid viscosity (mPa·s)
ρ_p	Particle density (kg/m ³)

Subscripts

l	Liquid
p	Particle
s	Solids

Reference

- An, Xiaodong, Mingyan Liu, and Yunguan Fu. 2007. "Clustering Behavior of Solid Particles in Two-Dimensional Liquid-Solid Fluidized-Beds." *China Particuology*.
<https://doi.org/10.1016/j.cpart.2007.07.001>.
- Bi, Hsiaotao, and Jingxu Zhu. 1993. "Static Instability Analysis of Circulating Fluidized Beds and Concept of High-Density Risers." *AIChE Journal* 39 (8): 1272–80.
<https://doi.org/10.1002/aic.690390803>.
- Buffière, P. 2000. "The Inverse Turbulent Bed: A Novel Bioreactor for Anaerobic Treatment." *Water Research* 34 (2): 673–77. [https://doi.org/10.1016/S0043-1354\(99\)00166-9](https://doi.org/10.1016/S0043-1354(99)00166-9).
- Buffière, Pierre, and René Moletta. 1999. "Some Hydrodynamics Characteristics of Inverse Three Phase Fluidized-Bed Reactors." *Chemical Engineering Science* 54 (9): 1233–42.
[https://doi.org/10.1016/S0009-2509\(98\)00436-9](https://doi.org/10.1016/S0009-2509(98)00436-9).
- Carlo, Dino Di, Jon F Edd, Katherine J Humphry, Howard A Stone, and Mehmet Toner. 2009. "Particle Segregation and Dynamics in Confined Flows."
<https://doi.org/10.1103/PhysRevLett.102.094503>.
- Chen, Ye Mon, Chien Sheng Jang, Ping Cai, and Liang Shih Fan. 1991. "On the Formation and Disintegration of Particle Clusters in a Liquid-Solid Transport Bed." *Chemical Engineering Science* 46 (9): 2253–68. [https://doi.org/10.1016/0009-2509\(91\)85124-G](https://doi.org/10.1016/0009-2509(91)85124-G).
- Dewsbury, K H, D G Karamanov, and A Margaritis. 2000. "Dynamic Behavior of Freely Rising Buoyant Solid Spheres in Non-Newtonian Liquids." *AIChE Journal* 46 (1): 46–51.
- Fan, Liang Shih, Katsuhiko Muroyama, and Song Hsing Chern. 1982. "Hydrodynamics Characteristics of Inverse Fluidization in Liquid-Solid and Gas-Liquid-Solid Systems." *The Chemical Engineering Journal* 24 (2): 143–50. [https://doi.org/10.1016/0300-9467\(82\)80029-4](https://doi.org/10.1016/0300-9467(82)80029-4).
- GOTOH, KEISHI. 1970. "Migration of a Neutrally Buoyant Particle in Poiseuille Flow: A Possible Explanation." *Nature* 225 (5235): 848–50. <https://doi.org/10.1038/225848a0>.

Han, Q., and J.D. Hunt. 1994. "Particle Pushing: The Attachment of Particles on the Solid-Liquid Interface during Fluid Flow." *Journal of Crystal Growth* 140 (3–4): 406–13. [https://doi.org/10.1016/0022-0248\(94\)90317-4](https://doi.org/10.1016/0022-0248(94)90317-4).

Han, Q., and J.D. Hunt. 1995. "Particle Pushing: Critical Flow Rate Required to Put Particles into Motion." *Journal of Crystal Growth* 152 (3): 221–27. [https://doi.org/10.1016/0022-0248\(95\)00085-2](https://doi.org/10.1016/0022-0248(95)00085-2).

Karamanev, D. G., and L. N. Nikolov. 1992. "Bed Expansion of Liquid-Solid Inverse Fluidization." *AIChE Journal* 38 (12): 1916–22. <https://doi.org/10.1002/aic.690381208>.

Karamanev, Dimitar G., and Ludmil N. Nikolov. 1992. "Free Rising Spheres Do Not Obey Newton's Law for Free Settling." *AIChE Journal* 38 (11): 1843–46. <https://doi.org/10.1002/aic.690381116>.

Liang, W.-G., J.-X. Zhu, Y. Jin, Z.-Q. Yu, Z.-W. Wang, and J. Zhou. 1996. "Radial Nonuniformity of Flow Structure in a Liquid-Solid Circulating Fluidized Bed." *Chemical Engineering Science* 51 (10): 2001–10. [https://doi.org/10.1016/0009-2509\(96\)00057-7](https://doi.org/10.1016/0009-2509(96)00057-7).

Liang, Wugeng, Shuliang Zhang, Jing-Xu Zhu, Yong Jin, Zhiqing Yu, and Zhanwen Wang. 1997. "Flow Characteristics of the Liquid-Solid Circulating Fluidized Bed." *Powder Technology* 90 (2): 95–102. [https://doi.org/10.1016/S0032-5910\(96\)03198-1](https://doi.org/10.1016/S0032-5910(96)03198-1).

Matas, J P, J F Morris, and E Guazzelli. 2004. "Lateral Forces on a Sphere." *Oil & Gas Science and Technology – Rev. IFP* 59 (1): 59–70. http://ogst.ifpenergiesnouvelles.fr/articles/ogst/pdf/2004/01/matas_vol59n1.pdf.

Nikolov, L., and D. Karamanev. 1987. "Experimental Study of the Inverse Fluidized Bed Biofilm Reactor." *The Canadian Journal of Chemical Engineering* 65 (2): 214–17. <https://doi.org/10.1002/cjce.5450650204>.

Nikov, I., and D. Karamanev. 1991. "Liquid-solid Mass Transfer in Inverse Fluidized Bed." *AIChE Journal* 37 (5): 781–84. <https://doi.org/10.1002/aic.690370515>.

Saffman, P G. 1965. "The Lift on a Small Sphere in a Slow Shear Flow." *J. Fluid Mech* 22 (2):

385–400. <https://doi.org/10.1017/S0022112065000824>.

Sang, Long, and Jesse Zhu. 2012. “Experimental Investigation of the Effects of Particle Properties on Solids Holdup in an LSCFB Riser.” *Chemical Engineering Journal* 197 (July): 322–29. <https://doi.org/10.1016/J.CEJ.2012.05.048>.

Wang, Ding, Trent Silbaugh, Robert Pfeffer, and Y.S. Lin. 2010. “Removal of Emulsified Oil from Water by Inverse Fluidization of Hydrophobic Aerogels.” *Powder Technology* 203 (2): 298–309. <https://doi.org/10.1016/J.POWTEC.2010.05.021>.

Wang, Jiaying, Yuanyuan Shao, Xilong Yan, and Jesse Zhu. 2019. “Review of (Gas)-Liquid-Solid Circulating Fluidized Beds as Biochemical and Environmental Reactors.” *Chemical Engineering Journal*, June, 121951. <https://doi.org/10.1016/J.CEJ.2019.121951>.

Zheng, Ying, and Jing-Xu (Jesse) Zhu. 2000. “Overall Pressure Balance and System Stability in a Liquid–Solid Circulating Fluidized Bed.” *Chemical Engineering Journal* 79 (2): 145–53. [https://doi.org/10.1016/S1385-8947\(00\)00168-6](https://doi.org/10.1016/S1385-8947(00)00168-6).

Zheng, Ying, and Jing-Xu (Jesse) Zhu. 2001. “The Onset Velocity of a Liquid–Solid Circulating Fluidized Bed.” *Powder Technology* 114 (1–3): 244–51. [https://doi.org/10.1016/S0032-5910\(00\)00318-1](https://doi.org/10.1016/S0032-5910(00)00318-1).

Zheng, Ying, Jing-Xu Zhu, Narenderpal S Marwaha, and Amarjeet S Bassi. 2002. “Radial Solids Flow Structure in a Liquid–Solids Circulating Fluidized Bed.” *Chemical Engineering Journal* 88 (1–3): 141–50. [https://doi.org/10.1016/S1385-8947\(01\)00294-7](https://doi.org/10.1016/S1385-8947(01)00294-7).

Zheng, Ying, Jing-Xu Zhu, Jianzhang Wen, Steve A. Martin, Amarjeet S. Bassi, and Argyrios Margaritis. 1999. “The Axial Hydrodynamics Behavior in a Liquid-Solid Circulating Fluidized Bed.” *The Canadian Journal of Chemical Engineering* 77 (2): 284–90. <https://doi.org/10.1002/cjce.5450770213>.

Chapter 3

3 Hydrodynamics of Inverse Liquid-Solid Circulating Fluidized Bed

Abstract

Hydrodynamics of inverse liquid-solid circulating fluidized bed is experimentally studied with five types of low density particles under a wide range of operating conditions. Solids holdup axial distribution is found to be uniform. And radial solids holdup is found to be generally uniform with occasional dilute region exist near the wall. The general trend of average solids holdup with superficial liquid velocity and solids circulation rate is examined, and the effects of particle properties are found to be not significant. The slip velocity calculated using measured solids holdup is found to be uncommonly higher than particle terminal velocity using particles with small particle Reynolds number. Modification is applied to Richardson-Zaki equation to account for clustering effects in liquid-solid circulating fluidized bed.

Key words: liquid-solid fluidization, solids holdup, circulating fluidized bed, inverse fluidization, slip velocity, Richardson-Zaki equation

3.1 Introduction

A typical upward circulating fluidized bed has two columns, a riser fluidized bed and a downer fluidized bed. The riser operates at high liquid velocity to transport particles upwards and can provide high contact efficiency and high mass and heat transfer rate (Zhu et al. 2000). The downer, usually in large diameter, operates in less liquid velocity that offers longer residence time compared with the riser. The two distinct operating zones allows continuous operation of solids and large throughput of liquid. Because of the above advantages, liquid-solid circulating fluidized bed has drawn many attentions in chemical, biochemical, food and pharmaceutical industries. It has demonstrated promising potential in wastewater treatment (Nelson, Nakhla, and Zhu 2017; A. Patel, Zhu, and Nakhla 2006; Eldyasti et al. 2010), iron-exchange and lactic acid production processes (M. Patel et al. 2008) The riser usually take advantage of the short residence time of liquid and solid for better contact. For example, in iron-exchange process (M. Patel et al. 2008; Lan et al. 2002), the desorption, a fast process, takes place in the riser with high liquid velocity

and the adsorption happens in the downcomer since it requires long residence time which can be achieved with low liquid velocity

Inverse fluidized bed uses low density particles which are suspended by downward liquid flow (Fan, Muroyama, and Chern 1982). It is believed to be suitable as bioreactor due to the application of small inertia particles and the unique downflow liquid for fluidization. (Chavarie and Karamanev 1986; Nelson, Nakhla, and Zhu 2017). Inverse liquid-solid circulating fluidized bed (ILSCFB) was first proposed by Long and Zhu to combine the characteristics of liquid-solid circulating fluidized bed and inverse fluidization (Sang et al. 2019), where low density particles are fluidized with high downward liquid velocity in a downer and being recycled in a riser connected by a liquid-solid separator. Preliminary experiments on the hydrodynamics in the downer have been carried out using only two types of particles under a limited range of operating conditions.

Understanding the hydrodynamics is crucial in the design and operation of fluidized bed systems (Sang and Zhu 2012). Reaction rate, mass transfer and heat transfer etc. in inverse liquid-solid circulating fluidized bed will be affected by solids holdup, solids holdup distribution and particle properties under various operating conditions. Solids holdup is the volume fraction of solids in a given volume, which has shown to be very important. The distribution of solids holdup distribution is also an important parameter to evaluate the performance of the fluidized bed. Solids holdup and solids holdup distribution can be affected by particle properties and operating conditions, such as superficial liquid velocity and solids circulation rate. In this study, the solids holdup distribution in inverse liquid-solid circulating fluidized bed has been studied experimentally with five types of particles.

Particle property affects the hydrodynamics of fluidized bed. Particles in different densities and diameters will have different slip velocities and behave differently under the same operating conditions. In addition, the small inertia of low density particles has been reported to behave distinctly different from heavy particles when fluidized by liquid, which makes the study of particle property effects in more important. This study focuses on the particle property effects on hydrodynamics in ILSCFB covering a wide range of particle density from 28 kg/m^3 to 1020 kg/m^3 .

And a modified Richardson-Zaki equation is used for the prediction of average solids holdup in ILSCFB downer based on particle property effects.

3.2 Experiment

3.2.1 Apparatus

The schematic diagram of ILSCFB is shown in Figure 3.2.1 The inverse liquid-solid circulating fluidized bed consists of a 5.4-meter downer (0.076m ID) and a 4-meter upcomer (0.203m ID), connected by two connecting pipes at the top and the bottom. Liquid flow enters from the top of the downer, through main flow distributor and auxiliary flow distributor, and exit from the liquid-solid separator at the bottom. In the downer, downward liquid carries solids to the bottom liquid-solids separator, and then solids flow upwards in the riser. For simplicity, the upcomer is used. Optional flow in the upcomer may be used to aid the transportation of particles to the top of the downer by loosening the packing of solids. Average solids holdup is measured by manometers and local solids holdup and particle velocity are measured by optical fiber probe.

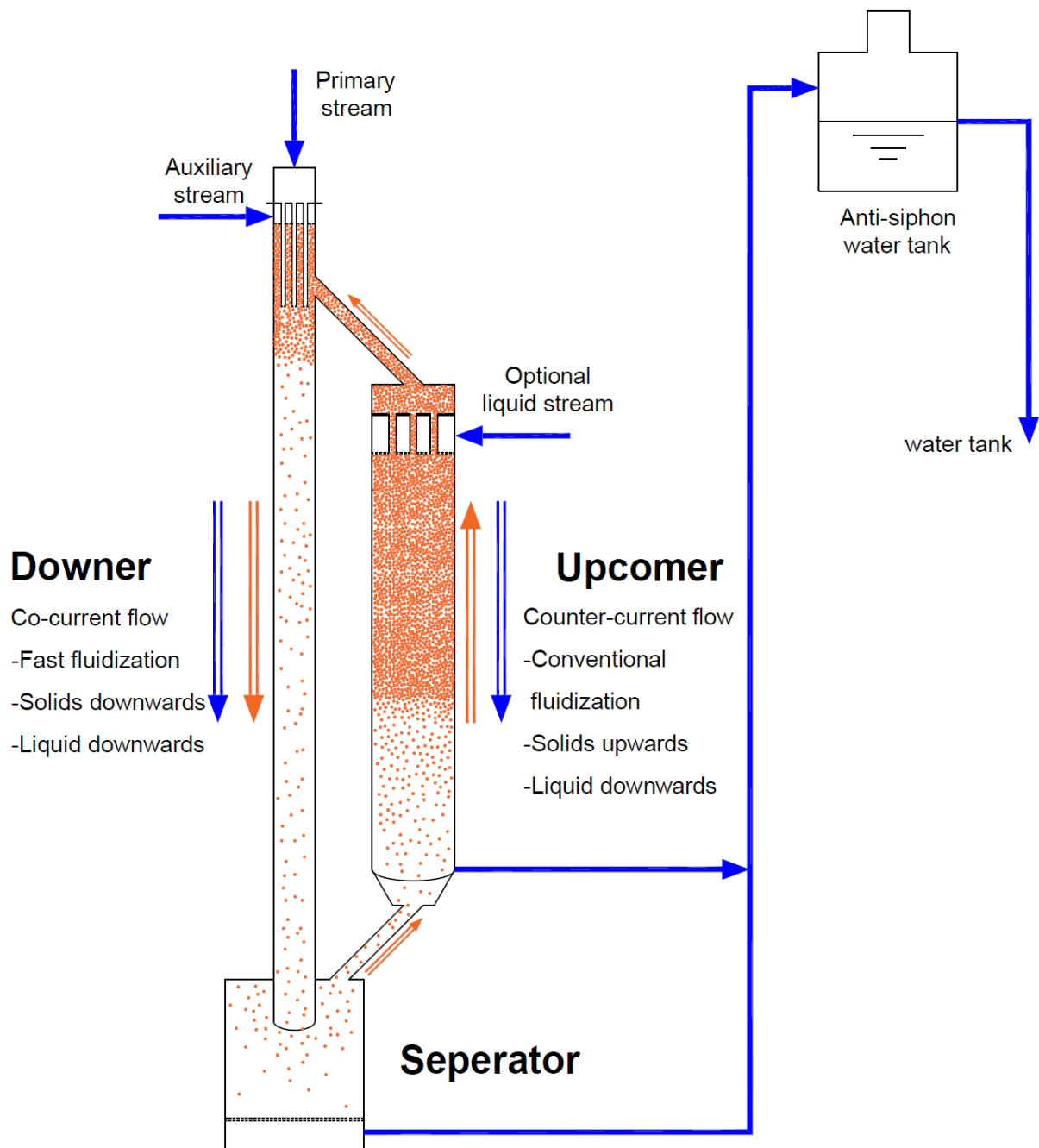


Figure 3.2.1 Schematic diagram of inverse liquid-solid circulating fluidized bed

A series of manometers have been installed on the downer to measure the pressure drop along the downer, which is used to calculate the axial solids holdup. Local solids holdup was measured using optical fiber probe.

3.2.2 Particle properties

The studied particle properties is listed in Table 3.2-1. Four particles are expanded polystyrene (EPS) with closed pores structure and the one particle is polystyrene. All particles are in spherical shape.

Table 3.2-1 Particle properties

Particles	Density (kg/m ³)	Diameter (mm)
EPS28	28	0.8
EPS122	122	1.1
EPS303	303	1.2
EPS638	638	1.1
PS1020*	1020	0.9

*Experiment carried out in salt water with 1080 kg/m³ density

3.3 Results and Discussion

3.3.1 Particle terminal velocity

Particle terminal velocity is an important parameter as it is directly related to slip velocity between liquid and solids in fluidized bed. And many models have been investigated to predict the particle terminal velocity covering a wide range of particle properties. However, for a particular particle, it is better to obtain the particle terminal velocity by experiment since the models aims to satisfy as much particle properties as possible, and errors could exist for a single type of particle. Thus, the bed expansion experiment in a fluidized bed is carried out for the measurement of particle terminal velocity. Since many particles are used in fluidized bed, the obtained particle terminal velocity accounts for particle size and density distribution, which might exist in expanded polystyrene particles. The terminal velocity can be measured through bed expansion experiment

with a series of superficial liquid velocities(KHAN and RICHARDSON 1989). The intercept is $\ln(U_t)$ as shown in Figure 3.3.1.

The results are shown in Table 3.2-1 Particle properties. PS1020 has the lowest particle terminal velocity, due to its little density difference with the fluid. EPS28 and EPS122 have the higher terminal velocity for their low density. And EPS122 has even higher terminal velocity due to the effect of particle diameter. Exponent n in Equation can also be obtained to account for particle-particle interaction. And constant n is usually believed to be a function of particle properties and fluid properties.

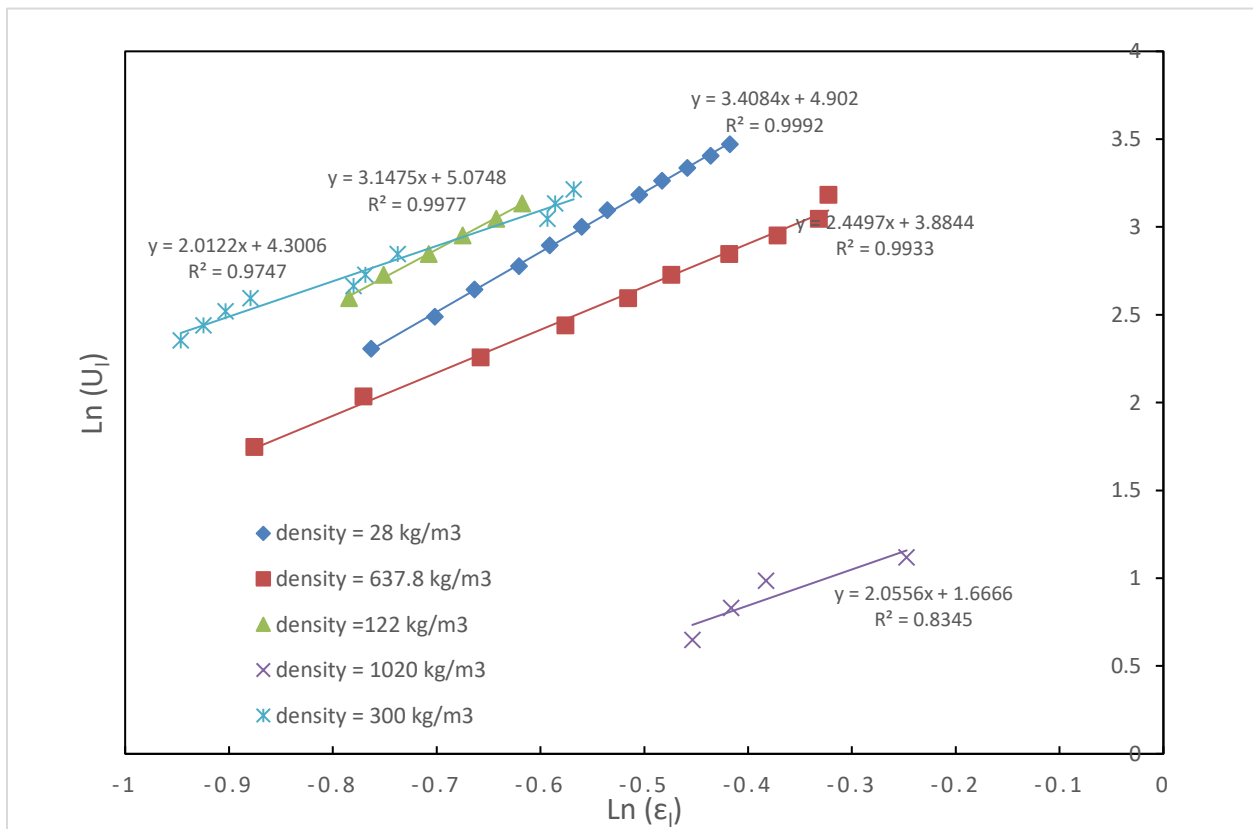


Figure 3.3.1 The relationship between $\ln(U_t)$ and $\ln(\epsilon_l)$ of studied particles, $\ln(U_t) = n \cdot \ln(\epsilon_l) + \ln(U_t)$ (KHAN and RICHARDSON 1989)

Particles	Terminal Velocity (cm/s)	Ret
-----------	--------------------------	-----

EPS28	13.4	176
EPS122	16.0	107
EPS303	7.37	74
EPS638	4.86	53
PS1020	0.53	5.3

3.3.2 Axial flow structure

Detail study of axial solids holdup distribution is shown in Figure 3.3.2 to Figure 3.3.5. The axial position is labelled as distance from the distributor, so in each graph, the vertical direction is aligned with the vertical direction in ILSCFB downer as shown in Figure 3.2.1.

The effects of U_s of each particle can be found in each graph (Figure 3.3.2 to Figure 3.3.5). It is shown that with increasing U_s , solids holdup increased significantly under a constant U_l . And solids holdup is uniform at all solid circulation rates (U_s). And The effects of U_l on axial solids holdup distribution can also be found in Figure 3.3.6 and Figure 3.3.7 under constant U_l represented by EPS28 and EPS 303. Solids holdup is uniform at all superficial liquid velocities. And solids holdup is decreasing with superficial liquid velocity, as more space is needed between particles to accommodate the increment of liquid flowrate. And the decreasing trend with superficial liquid velocity is sharper when liquid velocity is low and more gradual when liquid velocity is high. This is because solids holdup is a dimensionless parameter that represent the volume fraction of solids in the mixture. The absolution change at low solids holdup condition is not very significant. In term of axial solids holdup distribution, a dilute region can be found near the distributor region (Figure 3.3.3 and Figure 3.3.4) when superficial liquid velocity is operating at extreme high conditions. More representative results is shown in Figure 3.3.6 and Figure 3.3.7. The non-uniformity is believed to be caused by the distributor. In the distributor zone, solids undo an acceleration period, and large vortex is created due to the design of the distributor. As a result,

the measured solids holdup from manometer is not uniform in the distributor region. And the effect from distributor is not significant when the location is 1m after the entrance.

Particle density is an important parameter determining the hydrodynamics behavior in the downer. By comparing the uniform axial solids holdup distribution of different types of particles, we can conclude that particle density has no significant effect on solids holdup axial distribution.

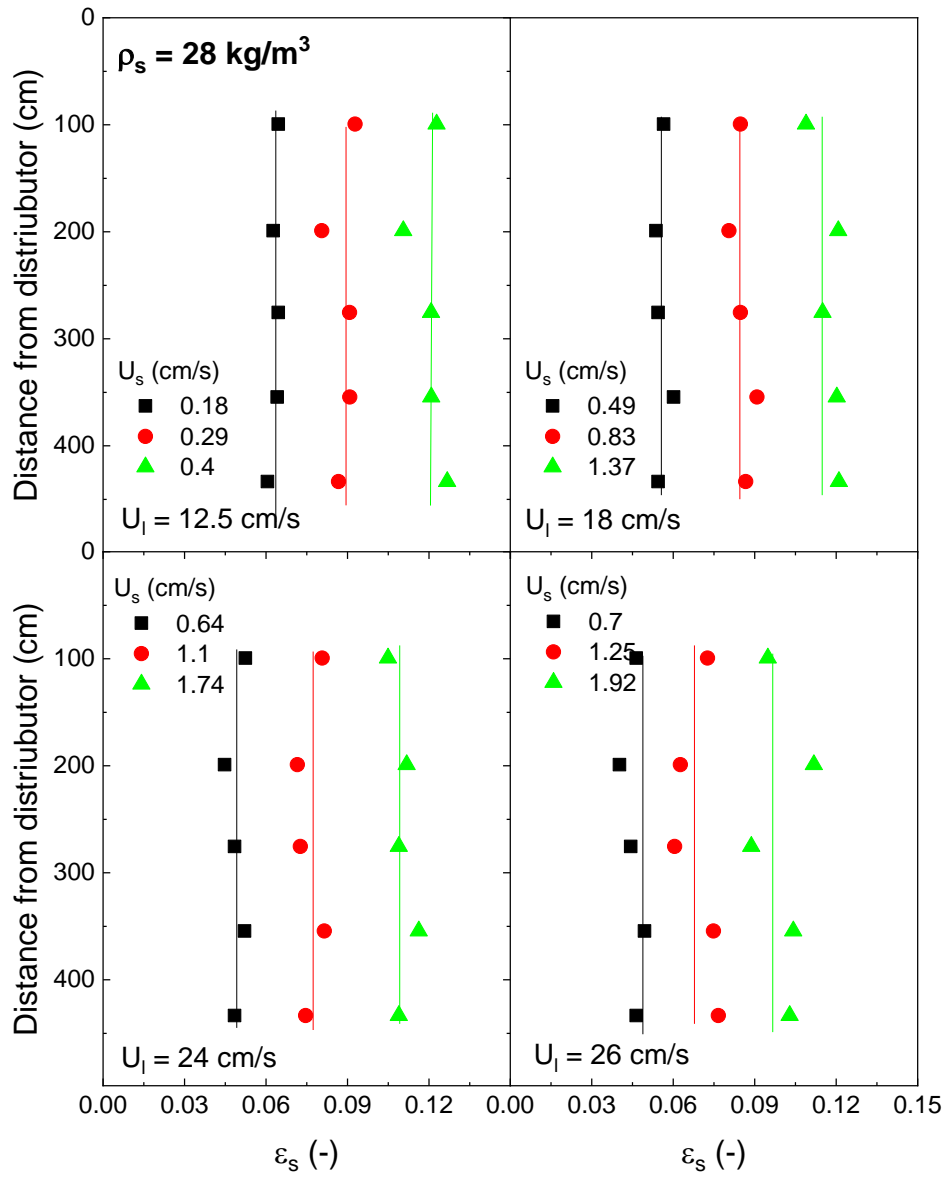


Figure 3.3.2 Axial solids holdup distribution of EPS28

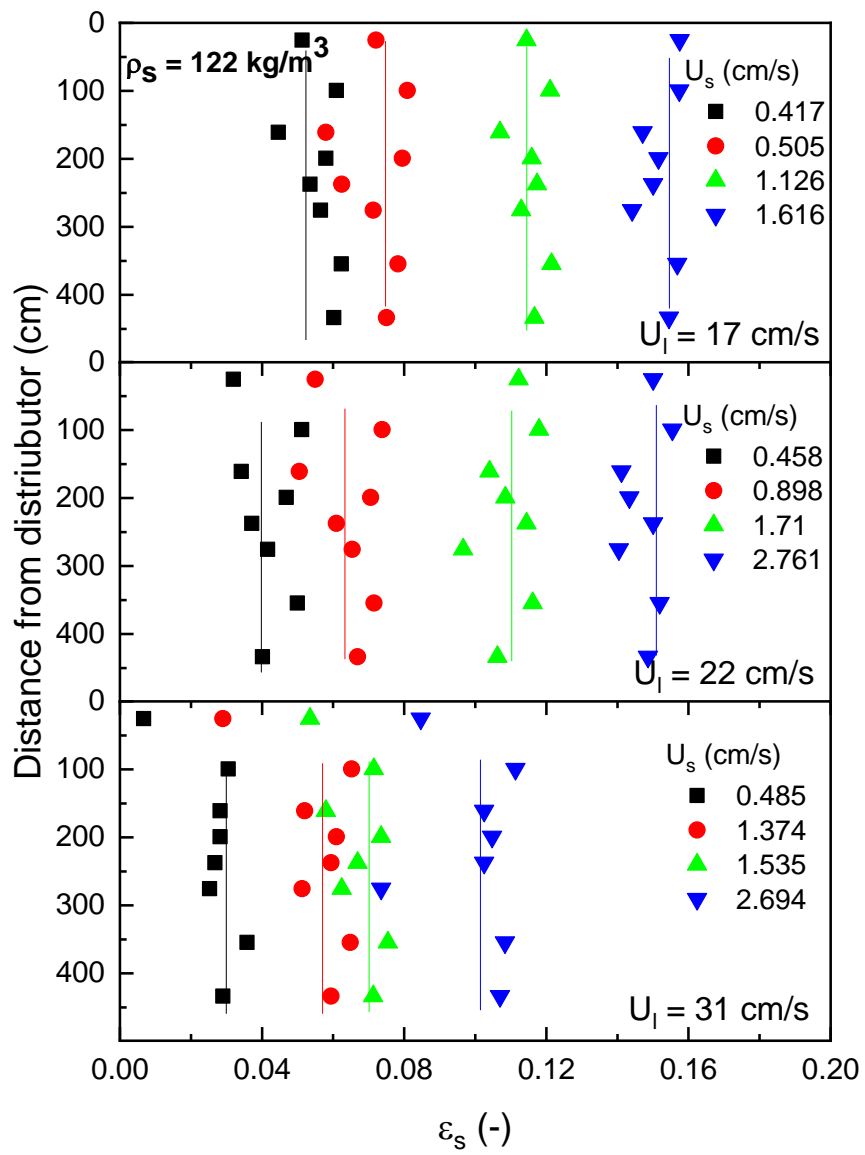


Figure 3.3.3 Axial solids holdup distribution of EPS122

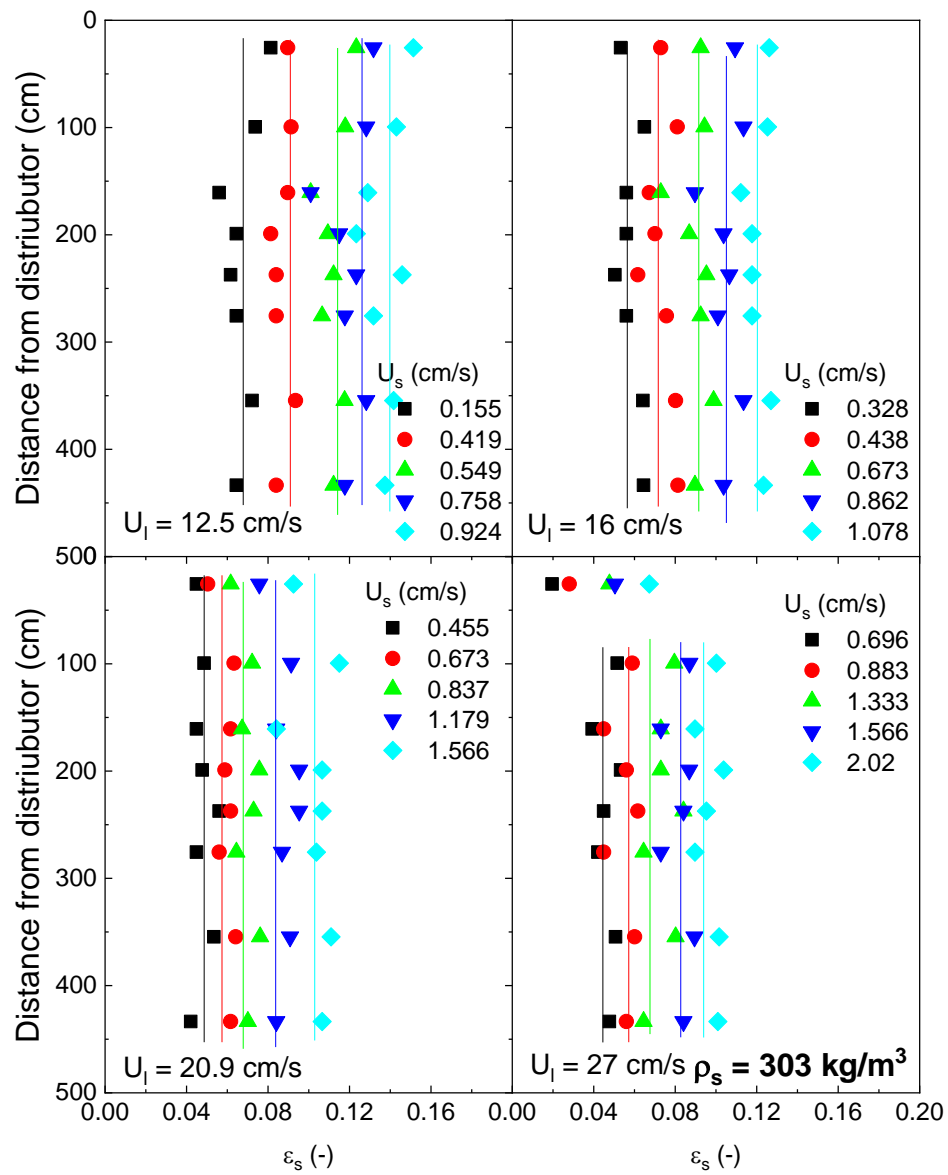


Figure 3.3.4 Axial solids holdup distribution of EPS303

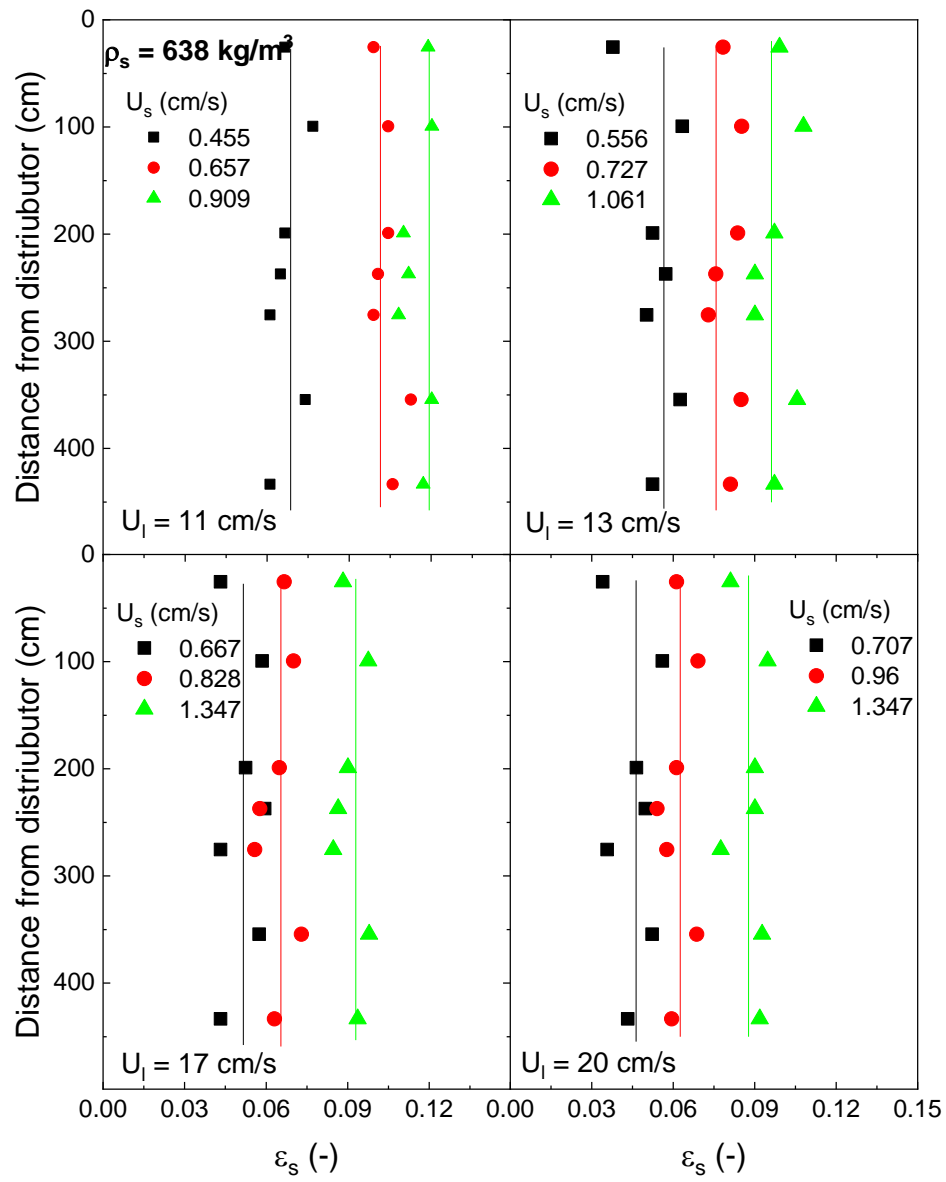


Figure 3.3.5 Axial solids holdup distribution of EPS638

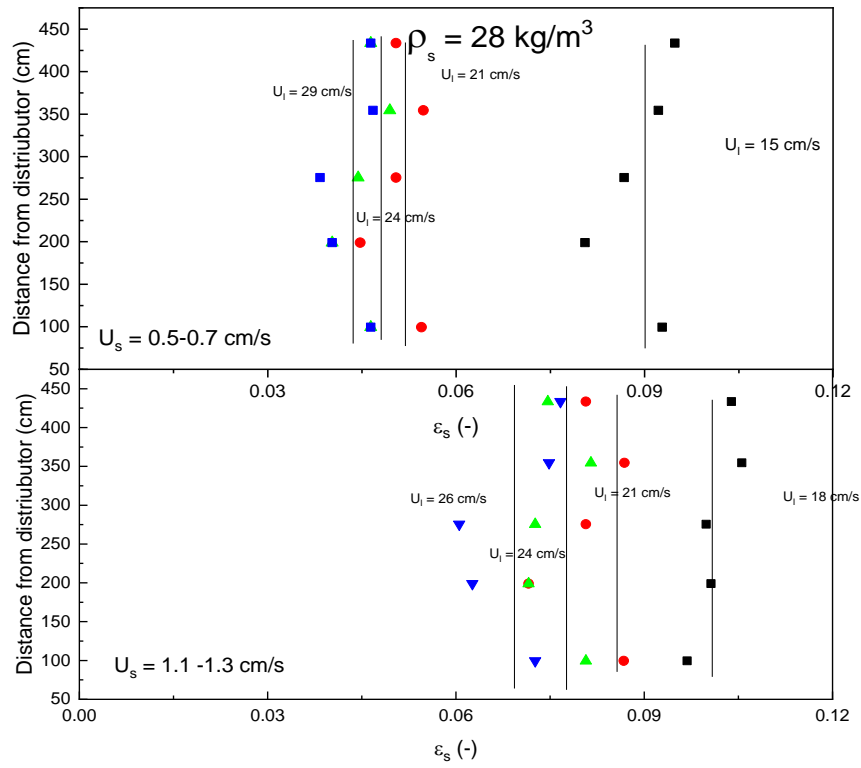


Figure 3.3.6 Effects of U_l on axial solids holdup distribution of EPS28.

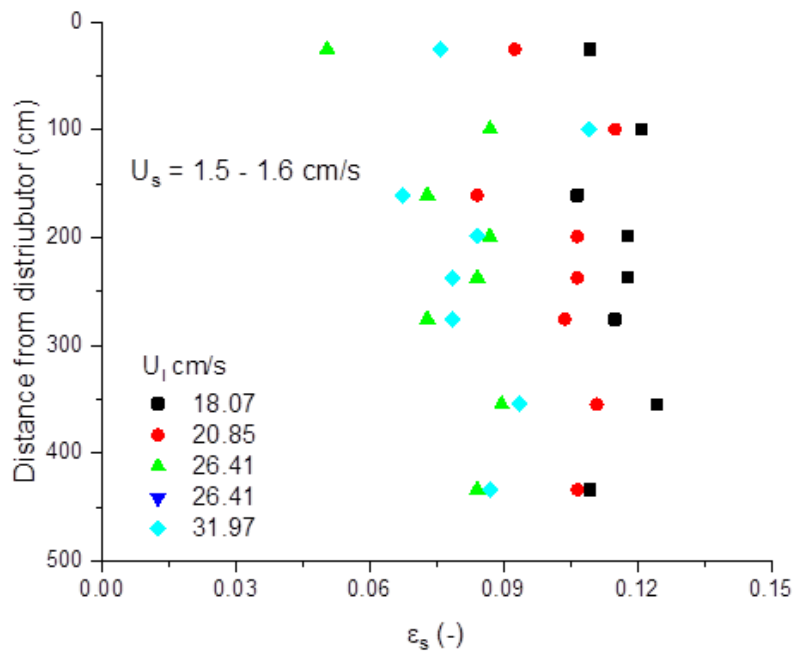
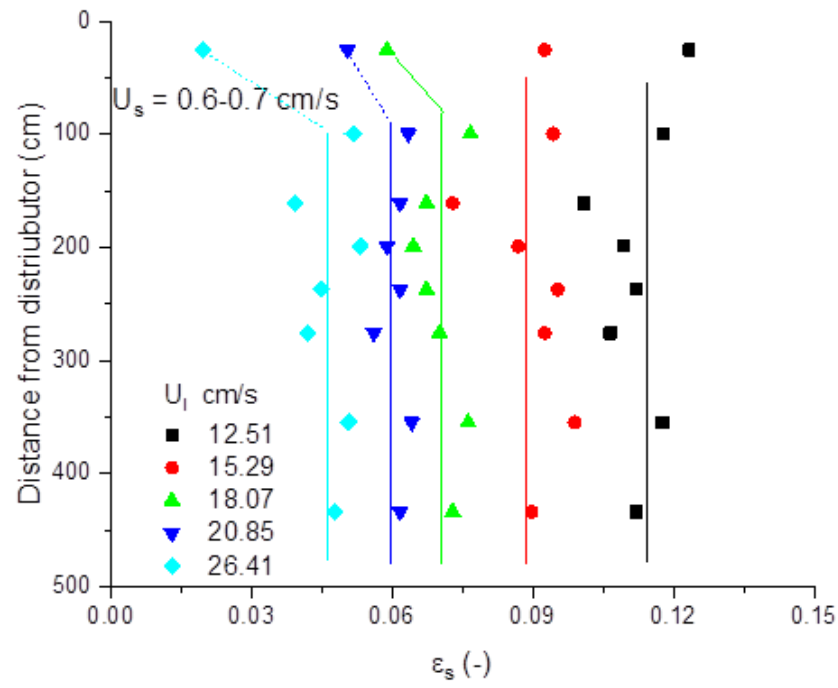


Figure 3.3.7 Effects of U_1 on axial solids holdup distribution of EPS303

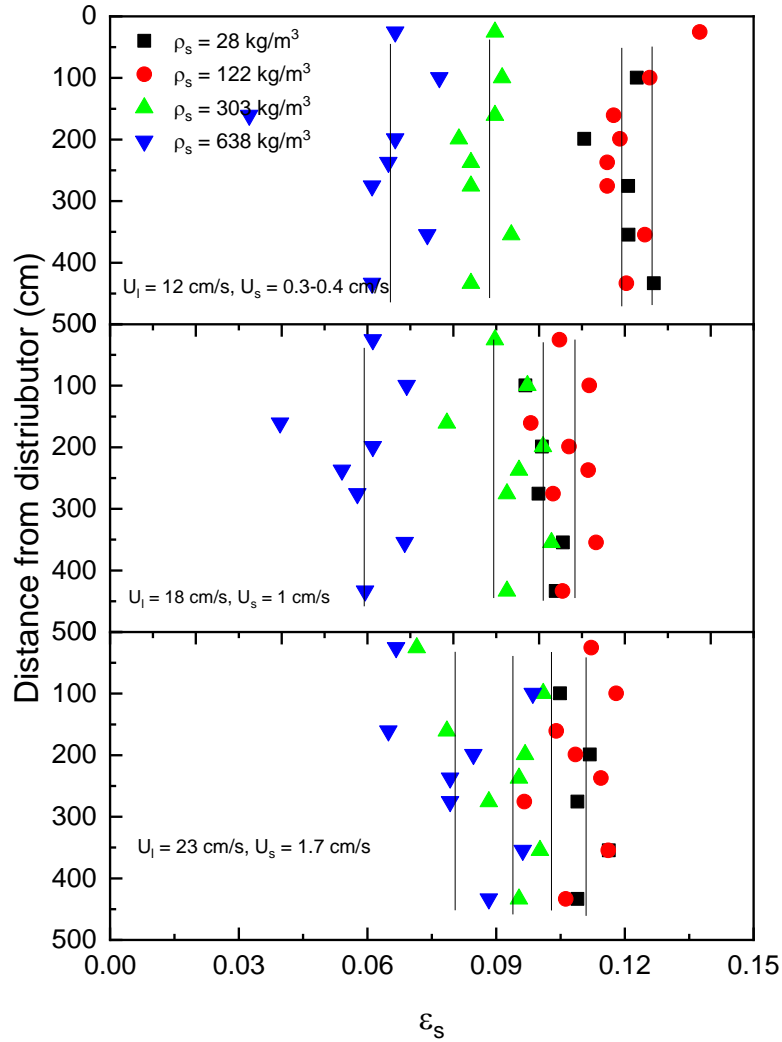


Figure 3.3.8 Axial solids holdup distribution of different particles under different constant U_1 and U_s

The effects of particle properties on axial solids holdup distribution can be found in Figure 3.3.8. Axial solids holdup distributions of different particles are plotted under different U_1 and U_s . EPS28 and EPS122 have the highest solids holdup while EPS 638 have the least solids holdup under the selected conditions. The difference is believed to be caused by the different in particle terminal

velocity. For a better understanding of the particle property effects on axial solids holdup distribution, the results are shown at constant $U_l - U_t$ in Figure 3.3.9. No significant trend have been found between different particles. EPS122 has the highest solids holdup when $U_l - U_t = 5$ cm/s, while it has the lowest solids holdup when $U_l - U_t = 10$ cm/s, both under constant U_s . The same inconsistency has been found with other particles.

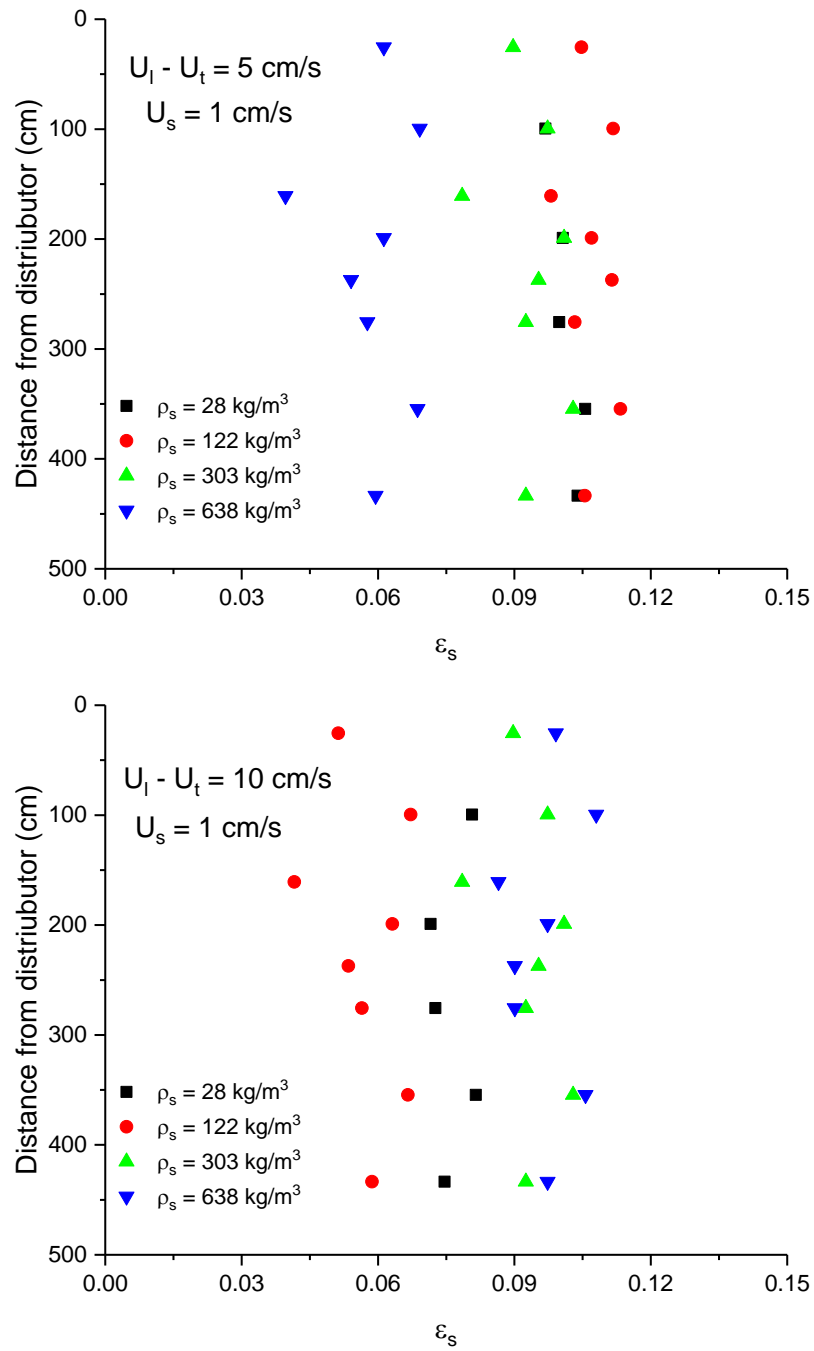


Figure 3.3.9 Axial solids holdup distribution under different $U_l - U_t$ and

3.3.3 Radial flow structure

Radial solids holdup distribution is important evaluating the performance of the fluidized bed reactor. A uniform distribution is often desired for better control of mass and heat transfer and reaction efficiency. The solids holdup radial distribution is shown in Figure 3.3.10. Similar decreasing trend was found from center to the wall for all five types of particles. Detail radial flow structure represent by local solids holdup and particle velocity is shown in Figure 3.3.11 and Figure 3.3.12 for EPS28, in Figure 3.3.13 for EPS 122 and Figure 3.3.14 for EPS 303.

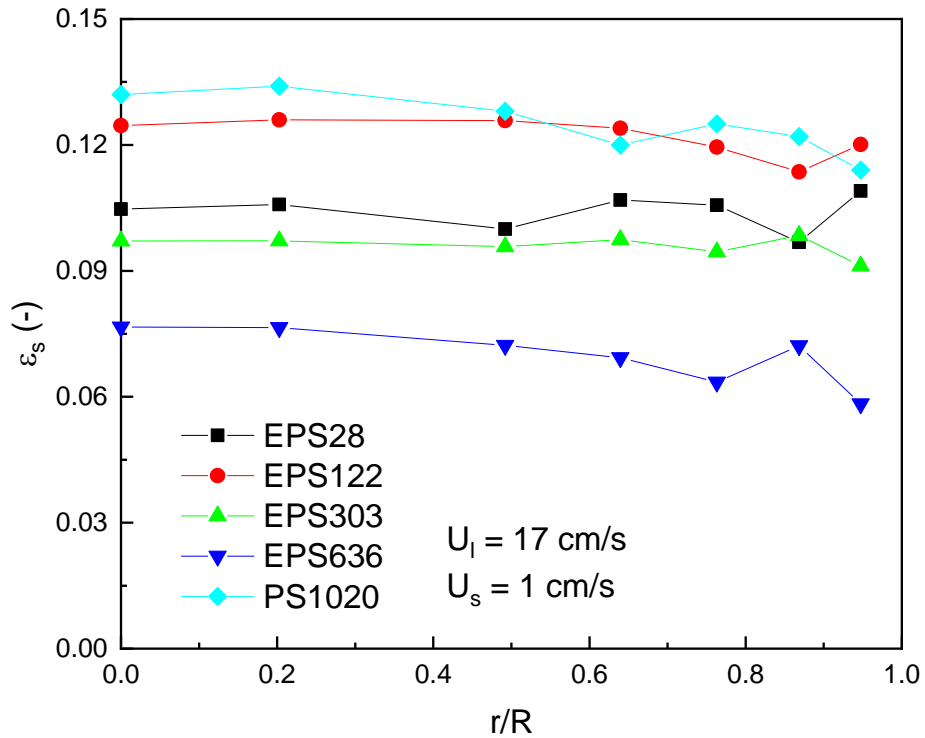


Figure 3.3.10 Solids holdup radial distribution of five types of particles

Non-uniformity of radial solids holdup distribution in the riser of liquid-solid circulating fluidized bed has been investigated by many researchers (Liang et al. 1996; Zheng et al. 2002). A slight increase of solids holdup near the wall region has been found which agrees with the phenomena in gas solid circulating fluidized bed. The explanation is believed that the solids are easy to accumulate close to the wall due to the slower fluid velocity near the wall. The friction between

liquid and the wall will hinder the liquid velocity in the wall region, which leads to the reduction of solids velocity. The same phenomenon has been found in ILSCFB as well as shown in Figure 3.3.12. However, no accumulation of solids holdup in the wall have been found. Only a slight increase of solids holdup in the wall region can be found when superficial liquid velocity is relatively low at 18.07 cm/s. And beyond that superficial liquid velocity, a decreasing trend of solids holdup from center to the wall has been discovered. The difference of solids holdup from center to the wall is not severe, but the trend is consistent. For each radial position, 30 seconds (370000 data points) of voltage data is obtained to ensure the solids holdup measurement is reliable.

Previous study on local solids holdup distribution in the downer of ILSCFB found a flat distribution from center to the wall using optical fiber probe based on the calibration method in gas-solid systems(Sang et al. 2019). In this study, the new calibration method is adopted for a higher resolution of solids holdup measurement, and different radial solids holdup profile has been discovered. The radial solids holdup profile of multiple particles under various conditions are shown in Fig 5. It is interesting to find a dilute region near the wall, which is opposite to the behavior of all circulating fluidized bed. The decreasing trend of solids holdup from center to the wall has been found with all experimented particles, as shown in Figure 3.3.11. Radial distribution of light particles in downflow liquid is rarely investigated in the field of fluidization but has drawn a lot of attention in physics in the 1960s leading by Saffman (Saffman 1965). In addition, Han (Han and Hunt 1993) has observed the same dilute region near the wall in crystallization process, where casting cannot be formed near the wall because of the use of small diameter low density particles. Several experiment studies have been carried out to model solids holdup radial distribution with consideration of the particle radial movement (Han and Hunt 1995). Drag force and net gravity dominant particle motion in the axial direction. In radial direction, when particles are placed near the wall, the force pushing particles to move against the wall is defined as lifting force, which can be generated due to velocity gradient of liquid flow and rotation of individual particle. Lifting force is independent of particle density and is usually too small comparing net gravity and drag force. However, in the case of low density particles, lifting force becomes significant to provide particle radial movement due to the decreased inertia

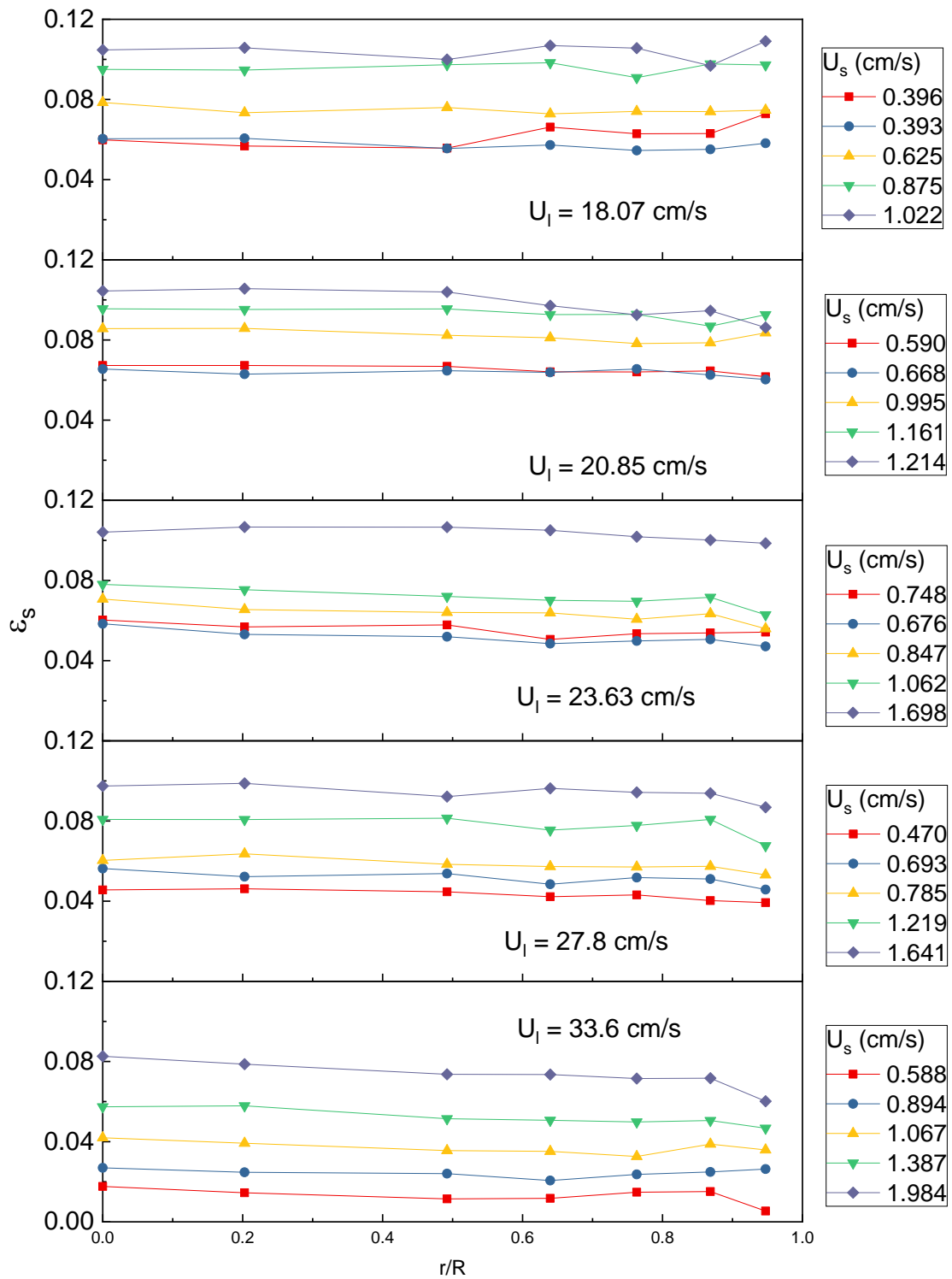


Figure 3.3.11 Radial solids holdup distribution of EPS28

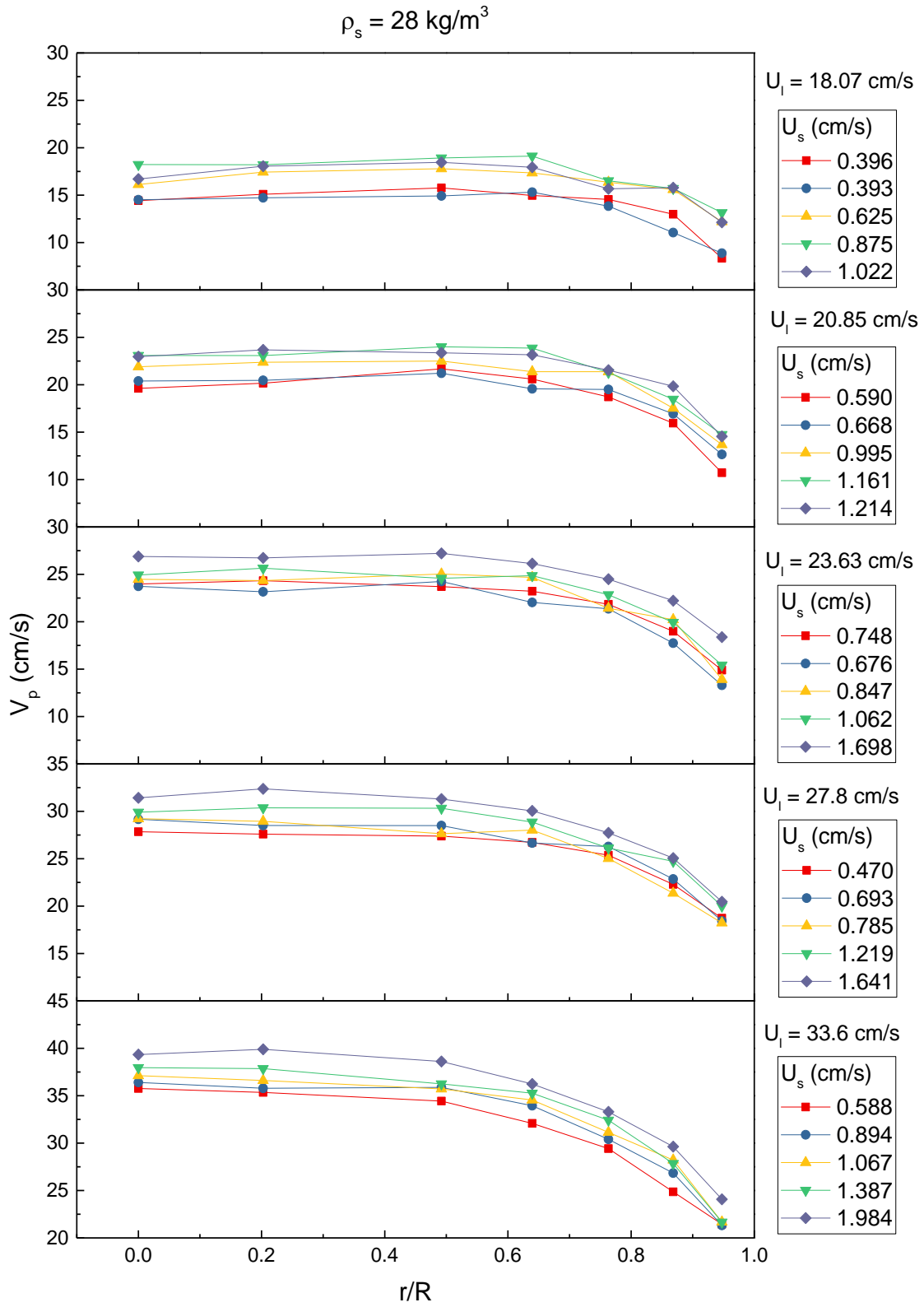


Figure 3.3.12 Local particle velocity of EPS28

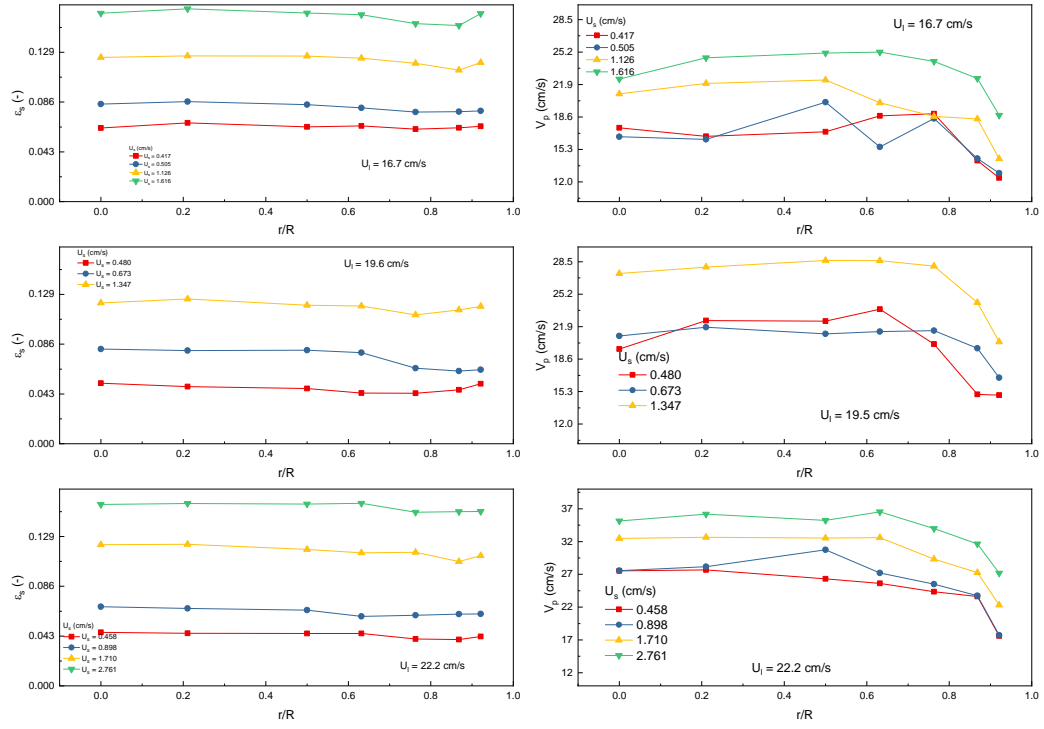


Figure 3.3.13 Radial flow structure of EPS 122

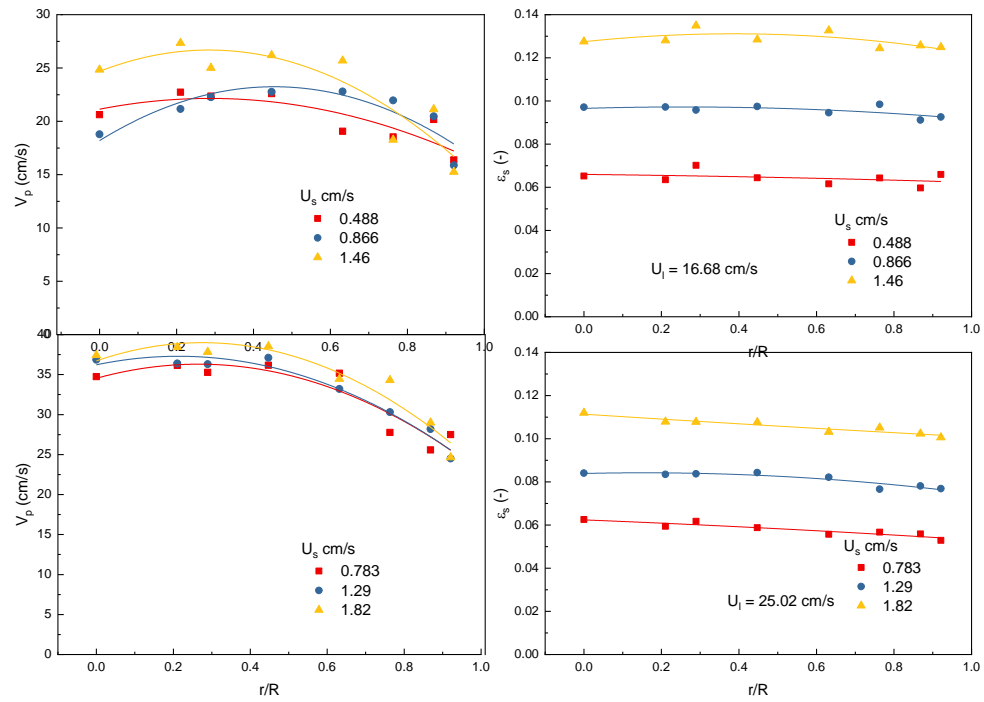


Figure 3.3.14 Radial flow structure of EPS 303

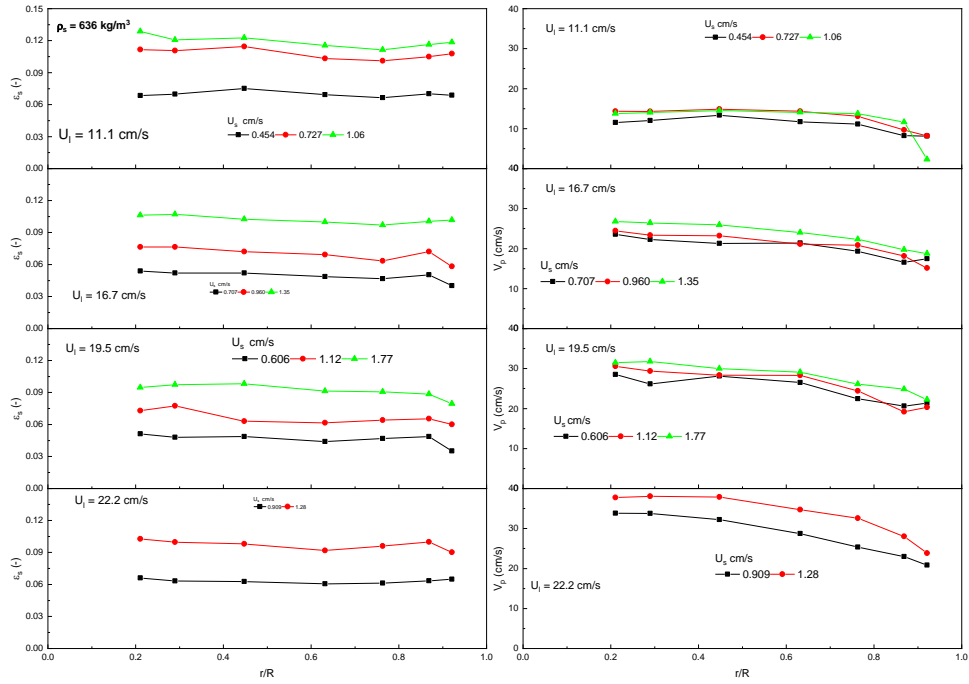


Figure 3.3.15 Radial flow structure of EPS636

Particle migration

In circulating fluidized bed risers, the radial flow structure of solids has been studied extensively. A core-annulus flow structure has been found, as dilute particles are carried by fast flowing fluid, and a dense region near the wall is observed. In many cases, the flowing direction of wall region is opposite to the direction of fluid flow in the core region due to insufficient drag force from the hindered fluid velocity near the wall. Thus, the radial flow structure is governed by the drag force in the streamline direction.

In liquid solid systems, lateral forces play significant roles in the migration of particles, which result in a different radial flow structure. Since the net weight of particles is drastically reduced due to the existence of liquid, the drag force required to fluidize the particles is lowered. The hindered liquid velocity near the wall is more likely to provide sufficient drag force.

Figure 3.3.11 showing the radial solids holdup distribution of low density particles in the downer. We can see a slightly dense region near the wall when the liquid velocity is relatively low. And the dense region gradually disappears with increasing liquid velocity. And at high liquid velocity, solids holdup is found to be lower in the wall region. This is because of lifting force push particles against the wall. Lifting force can be expressed in the following equation. At high liquid velocity, the velocity gradient near the wall region is high, which intensifies the lateral movement of particle from the wall to the center.

Average particle velocity

The change of average particle velocity with operating conditions is shown in Figure 3.3.17 with EPS28 and EPS122. Obviously, particle velocity is increasing with superficial liquid velocity, as particles have to travel faster to catch up with the increased liquid velocity to maintain force balance. And particle velocity is also increasing with solid circulation rate as shown in Figure 3.3.16. for four types of particles under the same superficial liquid velocity. Because extra solids flow will take the space of liquid, leading to an increase of intestinal liquid velocity.

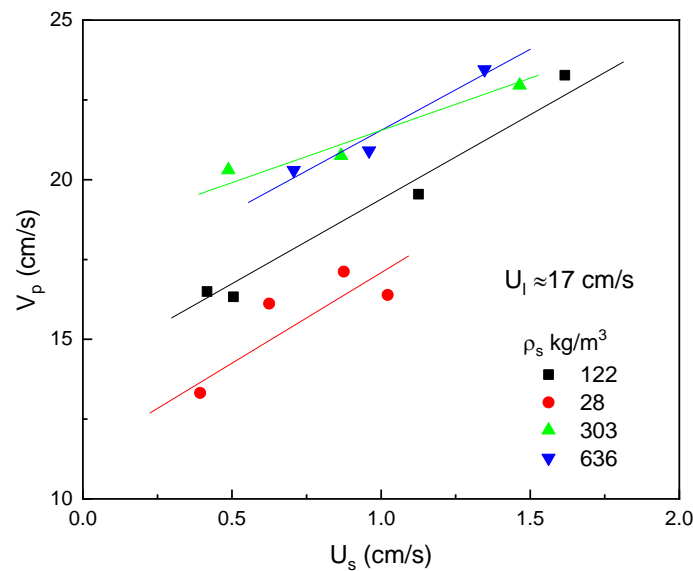


Figure 3.3.16 Change of average particle velocity with U_s

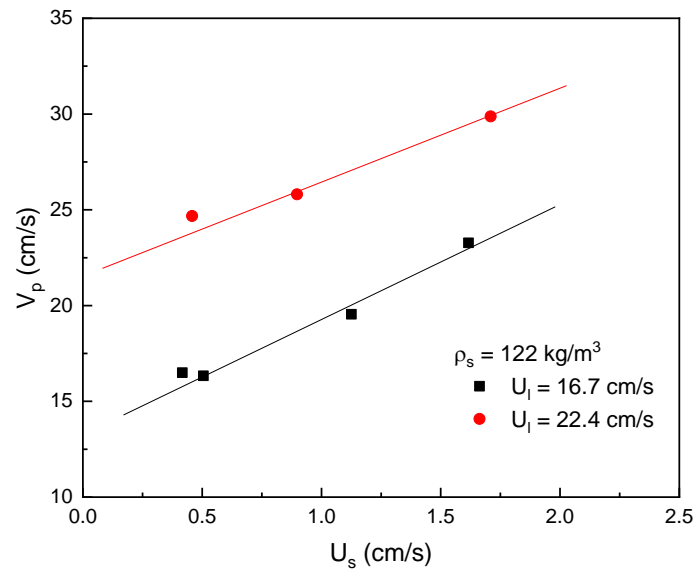
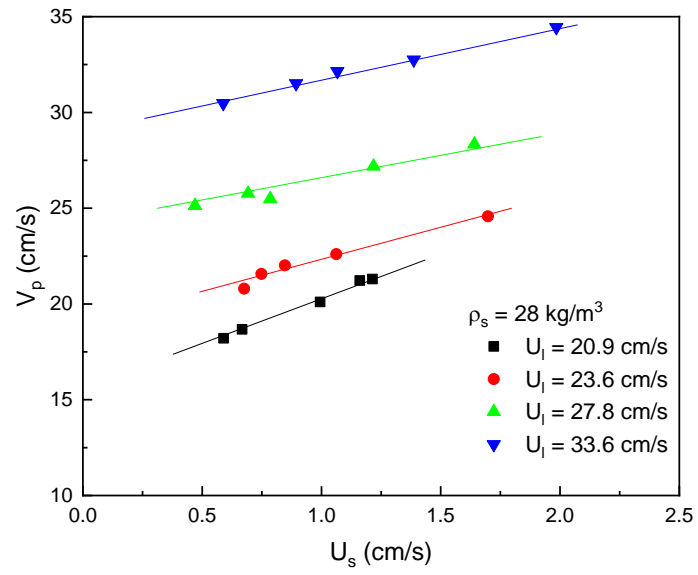


Figure 3.3.17 Change of average particle velocity with U_s under difference U_l

3.3.4 Average solids holdup and particle property effects

The average solids holdup in ILSCFB is affected by superficial liquid velocity and solid circulation rates. And the results are shown in Figure 3.3.18 and Figure 3.3.19. Solids holdup is decreasing with superficial liquid velocity and increase with solid circulation rate. The effects of particle properties are shown in Figure 3.3.19, at constant solid circulation rate $U_s = 0.9\text{--}1.1$ cm/s. No obvious trend is observed between different particles. Close solids holdup was obtained under the same operation conditions, even with different particle terminal velocities. Only feature is that EPS122 has shown to have significant less solids holdup at low liquid velocity. The results are not shown for PS1020 as there is not superficial liquid velocity to allow solids circulation rate to be controlled around 1 cm/s. The behavior of PS1020 will be discussed in the next chapter.

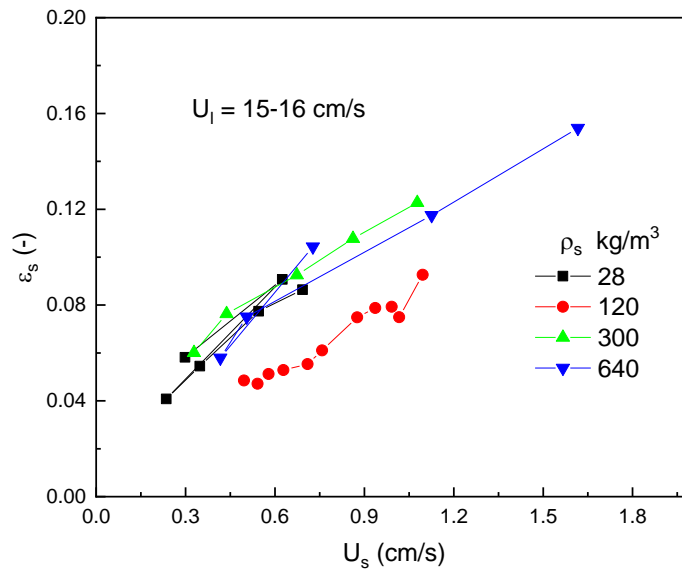


Figure 3.3.18 Effects of particle properties on average solids holdup in the ILSCFB at constant superficial liquid velocity

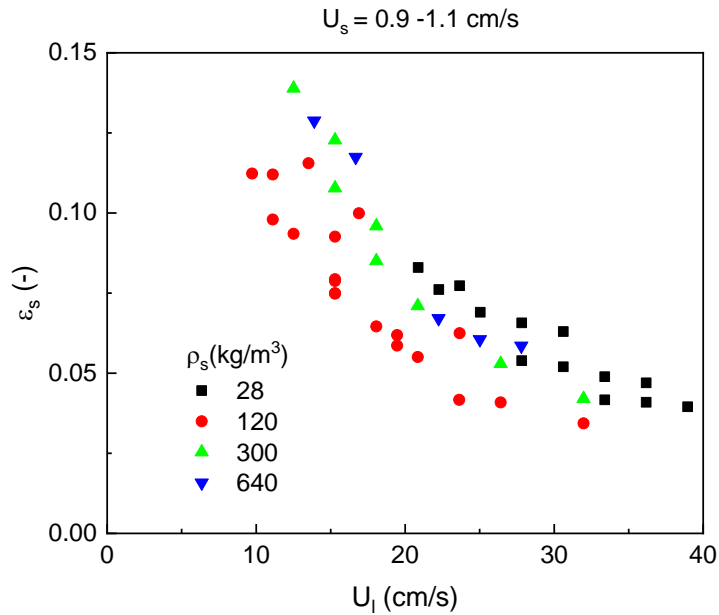


Figure 3.3.19 Effects of particle properties on average solids holdup in the ILSCFB at constant solids circulation rate

Particle properties such as density and diameter play an important role affecting the hydrodynamics behavior of fluidized bed. Long have studied the particle property effects on liquid-solid circulating fluidized bed, and a model is proposed to predict the solids holdup in the riser based on particle terminal velocity which reflects particle density and diameter (Sang and Zhu 2012). The particle terminal velocity at quiescent liquid dictates the slip velocity between particle and liquid in a circulating fluidized bed.

Previous researchers have examined the particle terminal velocity of low density particle in a free rising condition. A zig-zag movement have been observed of free rising particle due to the small particle inertia that can be easily affected by the liquid wave, which indicate the standard curve cannot be directly applied to calculate the drag coefficient of low density particles (Karamanev and Nikolov 1992). As a result, drag coefficient have been modified for low density particle based on particle Reynolds number to account for the different particle moving behavior comparing to heavy density particle. It is noteworthy to investigate the behavior of low density particles in circulating regime. As summarized in Table 3.2-1 Particle properties the particle density ranges from 28 kg/m^3 to 1080 kg/m^3 . All particles are polystyrene with closed porous structure to reduce to density.

For a better understanding of particle properties' effects, especially on average solids holdup, the 3D map of solids holdup against U_l and U_s is used. Solids holdup in the circulating fluidized bed is determined by particle properties and operating conditions. Superficial liquid velocity and solid circulation rate are the two varying operating variables that are used to control solids holdup. Previous studies have focused on the effects of U_l and U_s individually by plotting the relationship between solids holdup and U_l or U_s while keeping the other operating variable constant. For which, only limited amount of operating conditions can be demonstrated in the plot. In this study, 3D surface plot is applied to capture ϵ_s under various combinations of U_l and U_s . The surface is created by fitting the three-dimension data with poly2D ($Z = Z_0 + ax + by + cx^2 + dy^2 + fxy$) method. The 3d surface plot is able to present the full picture of the relationship between ϵ_s and U_l and U_s . For all types of particles solids holdup is decreasing with U_l while increasing with U_s . It can be found that the effect of U_s is always more profound than the effect of U_l , as shown in Figure 3.3.20.

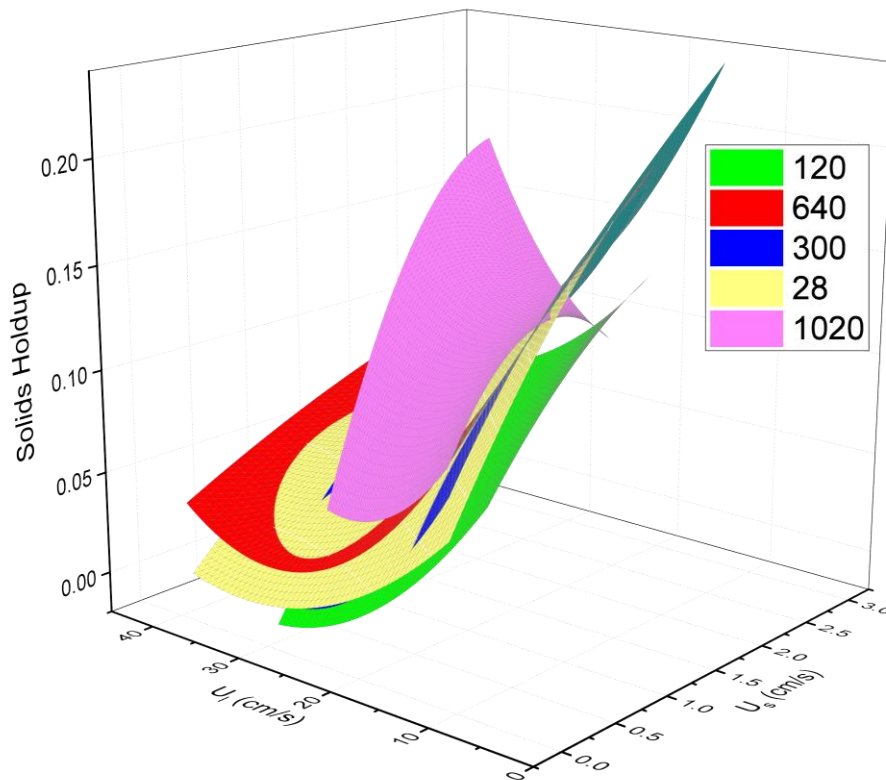


Figure 3.3.20 3D map of the relationship between solids holdup and U_l , U_s

It is interesting to see that the surface represent solids holdup of PS1020 is above all other types of particles, which means PS1020 achieved highest solids holdup under the same conditions. And the rest surfaces of other types of particles are indistinguishable. It is not common to find out that particle property effects have little impact in average solids holdup in ILSCFB downer. Different particle terminal velocities should travel in different velocity under the same operating condition, which lead to difference in solids holdup. Furthermore, PS1020 has the least particle terminal velocity, which should have the least solids holdup as they are regarded to be the easiest to be fluidized. On the contrary, EPS122 which has the highest particle terminal velocity is has the least solids holdup.

3.3.5 Slip velocity

To explain the not-common particle property effects, the slip velocity of each particle at different solids holdup conditions is investigated. The average slip velocity is calculated from equation (3.3-1) as the solids holdup distribution is uniform in general.

$$U_{slip} = \frac{U_l}{\varepsilon_l} - \frac{U_s}{\varepsilon_s} \quad \mathbf{3.3-1}$$

And for each particle, U_{slip} is directly related to its particle terminal velocity, so the ratio of U_{slip}/U_t vs solids holdup for different particles are presented for a fair comparison in Figure 3.3.21. A slight decrease of U_{slip}/U_t with solids holdup can be observed in PS1020, EPS638, EPS303 and EPS 28 particles. While EPS 122, which has the higher Re_t , its U_{slip}/U_t are fluctuating below one. What is striking from the figure is that PS1020, EPS638, EPS303 all have high U_{slip}/U_t , which were also above than 1 as the projected maximum under all solids holdup conditions. For EPS 28, U_{slip}/U_t is above 1 at low solids holdup condition, and dropped to below than 1 with increasing solids holdup.

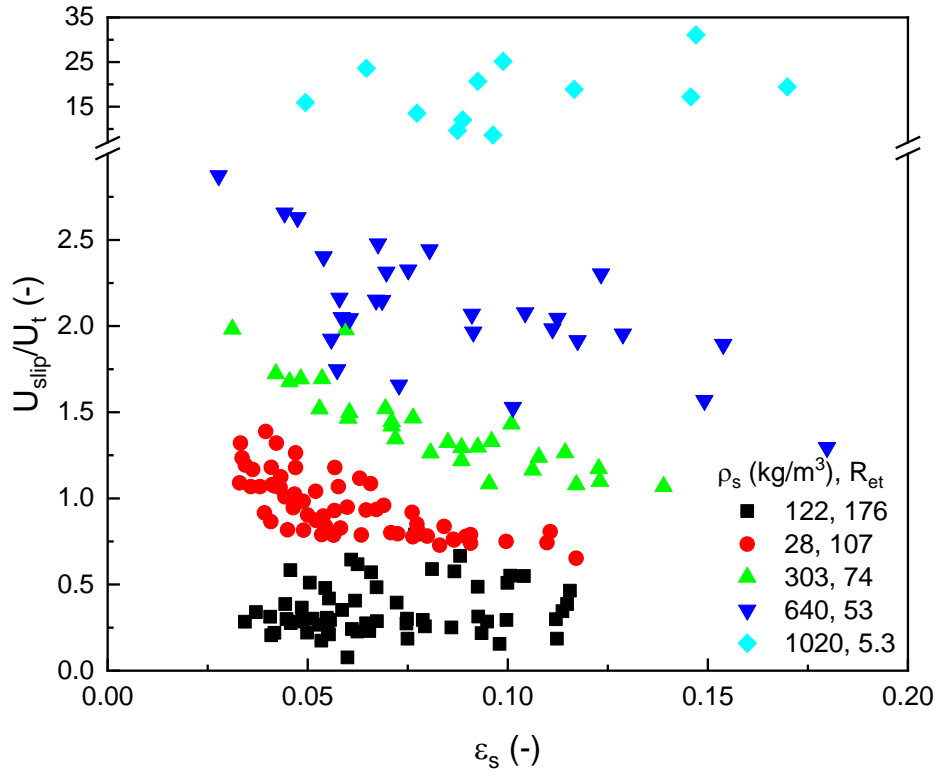


Figure 3.3.21 Effects of particle property on U_{slip}/U_t under different solids holdup

As discussed in previous section, particle properties are not significant in affecting solids holdup. But U_{slip}/U_t is sensitive to particle Reynolds number. Higher R_{et} will lead to less U_{slip}/U_t , which means the fluidization is more homogeneous. And it is striking to find out that particle with least R_{et} and U_t has the highest U_{slip}/U_t , which is believed to have the most severe clustering phenomenon. Particle that has high R_{et} and U_t tends to act on its own due to its larger inertia, and particle-particle interaction is not significant. On the other hand, particle-particle interaction could be significant enough to generate cluster with small R_{et} and U_t particles.

The higher than one U_{slip}/U_t as shown in Figure is an indication that solid fluidization may not be homogeneous in inverse liquid-solid circulating fluidized bed. And since solids holdup radial profile is uniform under a wide range of conditions, the non-homogeneous behavior is not caused by core-annulus flow structure as gas-solid circulating fluidized beds. Clustering of particles in a

large scale could be a possible explanation for the excessively high U_{slip}/U_t as illustrated in Figure 3.3.22, which has been observed in experiment.

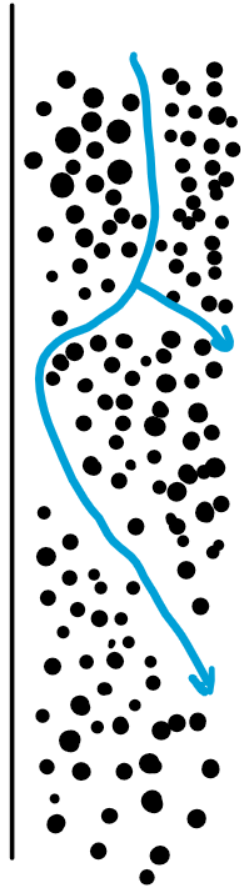


Figure 3.3.22 Clustering phenomenon observed in ILSCFB

Similar to the definition of Reynolds number in pipe flow, particle Reynolds number at particle terminal velocity is the ratio of inertia force to viscous force. Inertia force is the force caused by impact between liquid and solid, while viscous force is caused by shear stress along the surface of solids. Particle with high Reynolds number is not likely to be affected by the change of velocity field caused by other particles.

3.4 Prediction of solids holdup

Homogeneous fluidization can be described using Richardson-Zaki equation, where high bed expansion can be achieved under conventional fluidization. By pivoting the equation, we can see

that Richardson-Zaki equation also suggests that the slip velocity is a function of voidage or solids holdup. Slip velocity is decreasing with solids holdup, in other words, increasing with voidage, and the maximum slip velocity is particle terminal velocity where voidage is one

The relationship between U_{slip} and ε_s is found observed which resembles the Richardson-Zaki equation, 3.4-1 in the form of U_{slip} in conventional fluidization:

$$\frac{U_l}{U_t} = \varepsilon_l^n \quad \mathbf{3.4-1}$$

$$U_{slip} = \frac{U_l}{\varepsilon_l} = U_t \varepsilon_l^{n-1} \quad \mathbf{3.4-2}$$

In circulating fluidization with the existence of solid circulation rate the equation can be expressed in equation 3.4-3

$$U_{slip} = \frac{U_l}{\varepsilon_l} - \frac{U_s}{\varepsilon_s} = U_t \varepsilon_l^{n-1} \quad \mathbf{3.4-3}$$

The predicted solids holdup based on Richardson-Zaki equation versus experiment results are shown in Figure 3.4.1. The constant parameters U_t and exponent n were obtained by fitting with bed expansion results in conventional fluidization to avoid introducing errors if using empirical models. Excel solver was set up to solve solids holdup from equation (3.4-3). U_{slip} is calculated from equation (3.3-1), because solids holdup radial and axial distribution are found to be uniform for most studied conditions. A significant deviation is found between experiment results and prediction. Furthermore, for particles EPS300, EPS640 and PS1020, no feasible solution for solids

holdup can be found from equation (3.4-3). Because the calculated U_{slip} is greater than U_t of corresponding particle.

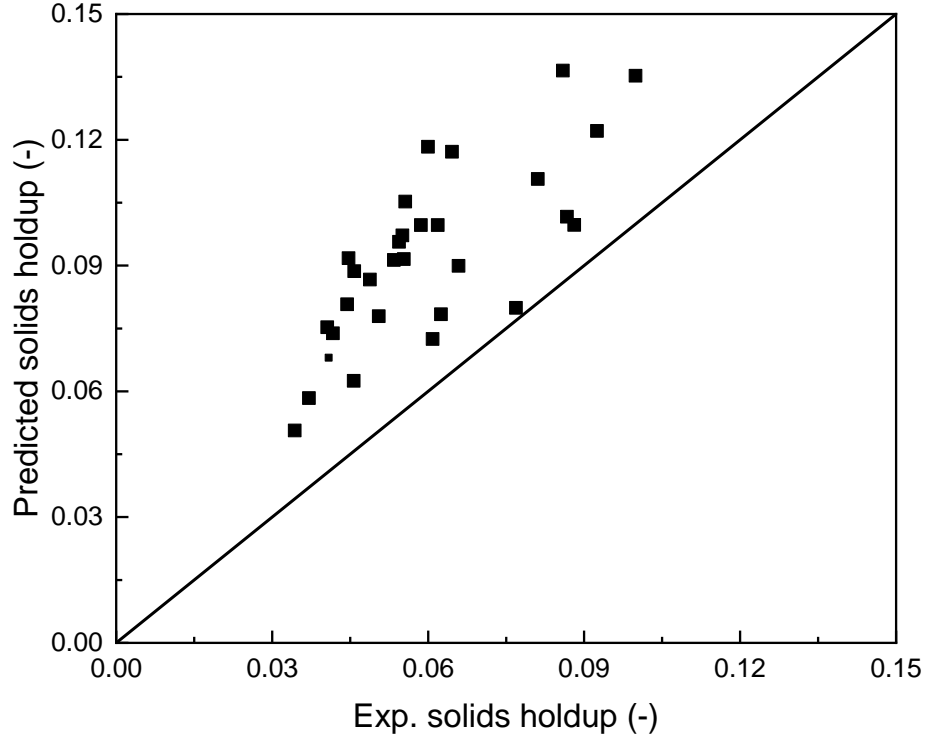


Figure 3.4.1 Predicted solids holdup vs experiment solids holdup with original Richardson-Zaki equation, U_t and n were obtained from conventional bed expansion experiment

In hydraulic transportation, some researchers have found similar phenomenon. And the problem can be resolved by fitting exponent n and adding a new parameter in the Richardson-Zaki equation as shown in equation (3.4-4) (Kopko, Barton, and McCormick n.d.)

$$U_{slip} = \frac{U_t}{\epsilon_l} - \frac{U_s}{\epsilon_s} = k U_t \epsilon_l^{n-1} \quad 3.4-4$$

The modified Richardson – Zaki equation is widely applied in hydraulic transportation and some homogeneous gas-solid fluidization systems (Avidan and Yerushalmi 1982). The parameter k is usually greater than 1, and kU_t accounts for the clustering particle terminal velocity. The common explanation is that occasional clustering exists in the fluidized bed, increasing the aerodynamic

diameter of shear stress, which lead to the increasing slip velocity to be greater than particle terminal velocity.

Table 3.4-1 shows the modified Richardson – Zaki equation for EPS 28, and EPS303 and EPS638. And a good agreement can be found between predicted solids holdup and measured solids holdup as shown in Figure 3.4.2. PS1020 is not included in the model, because its large deviation from homogeneous fluidization as dictated by the large U_{slip}/U_t .

Table 3.4-1 Fitted n and k in modified Richardson-Zaki equation

Particle Density	Re_t	n from ILSCFB	k
28	107	6.93	1.35
303	74	5.77	2.07
638	53	3.8	2.71

In comparison with the original Richardson-Zaki for conventional fluidization as shown in Table 3.4-1. The apparent terminal velocity (kU_t) is increased due to clustering phenomenon and exponent n is increased as well. Exponent n is an indication of particle-particle interaction which can be solved under Stoke's Law with some assumptions when first proposed by Richardson and Zaki(Richardson and Zaki 1997; 1954). If particles are aligned in hexagon style, lowest $n \approx 2.4$ can be reached. And if particles are stacked in a plane, highest $n \approx 4.8$ is reached. The increased exponent n also suggests that particle arrangement is changed to horizontal alignment compared with conventional fluidization, which is another indication of the existence of clustering in ILSCFB.

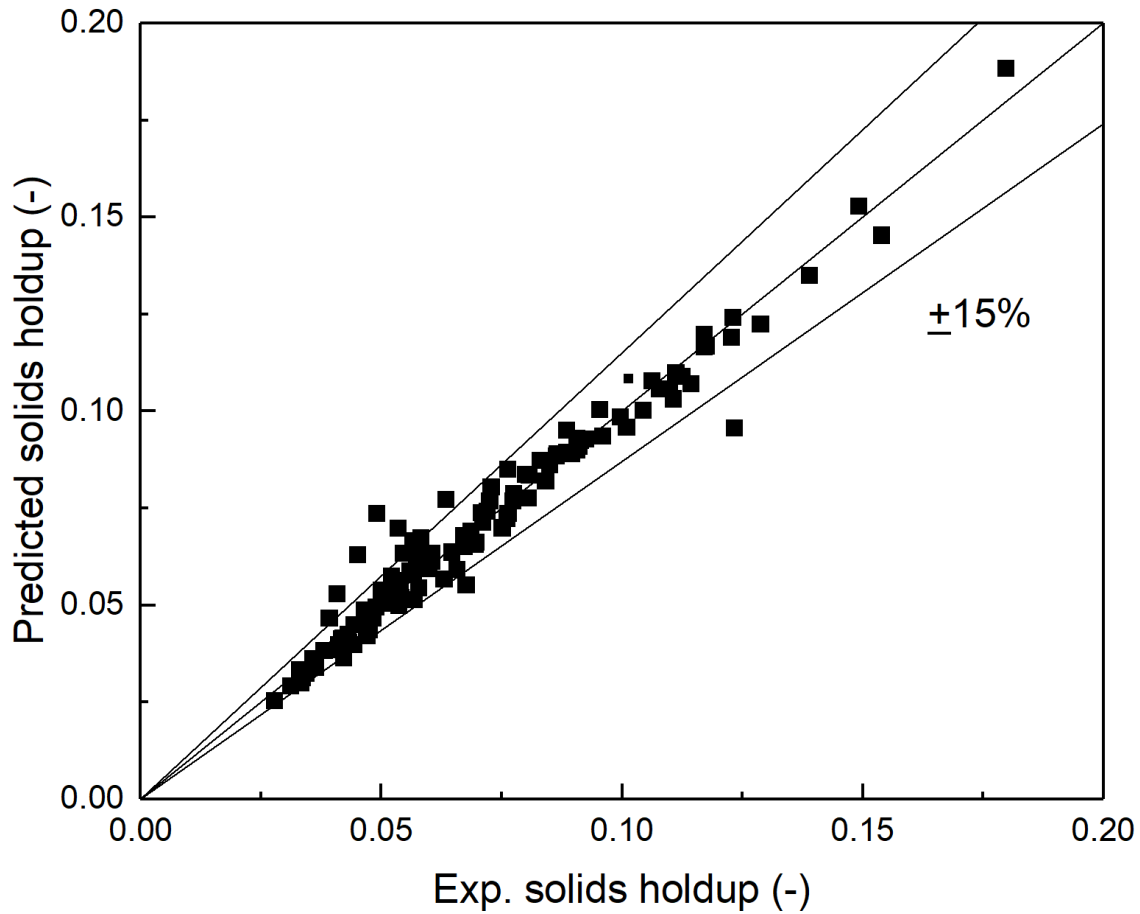


Figure 3.4.2 Prediction of solids holdup vs experimented solids holdup with modified Richardson-Zaki equation.

3.5 Conclusions and recommendations

Hydrodynamics of inverse liquid-solid circulating fluidized bed is experimentally investigated with five types of particles. Axial solids holdup in the downer is found to be uniform. Radial solids holdup distribution is generally uniform with occasion dilute region to be found in the wall region due to the effect of lifting force acting on small inertia particles. The change of average solids holdup with superficial liquid velocity and solid circulation rate is plotted in a 3D surface plot. Average solids holdup is increasing with solid circulation rate and decreasing with superficial liquid velocity. The effect of solid circulation rate is more significant than superficial liquid velocity on average solids holdup in the downer. Experiments also suggest particle property effects

is not noteworthy in determining average solids holdup in the downer. By analyzing the slip velocities of particles in different Reynolds number under different operating conditions, it is believed clustering phenomenon exists in ILSCFB downer. And it is related to particle Reynolds number at particle terminal velocity. Experiments have shown that particles with low Re_t are more likely to generate cluster. Also, clustering phenomenon is significant at low solids holdup or high superficial liquid velocity condition. A modified Richardson-Zaki equation is proposed to account for the clustering effects.

Future work can be done to study particles in different shapes and in a wider size range, which is kind of limited in this study. In addition, the clustering effects in liquid-solid circulating fluidized bed deserve some attention. Effective optical methods can be used to capture and study the clustering phenomenon. It is believed that cluster, if ever exists, will behave very differently from gas-solid clusters due to the vast difference between gas and liquid. Since no obvious observation is found in experiment, it is recommended to investigate in large scale liquid fluidized bed system, as cluster size in diameter may beyond the diameter of the studied ILSCFB downer.

Nomenclature

Ar	Archimedes number defined by $d_p^3 g (\rho_p - \rho_l) \rho_l / \mu_l^2$
C_D	Particle drag coefficient
d_p	Particle diameter (mm)
D	Column diameter (m)
F_b, F_d, F_g	Buoyancy, drag force and gravity
G_s	Solids circulation rate (kg/ (m ² s))
g	Gravity acceleration
Re	Reynolds number defined by $U_l d_p \rho_l / \mu_l$
Re_t	Particle terminal Reynolds number defined by $U_t d_p \rho_l / \mu_l$
U_a	Auxiliary liquid velocity (cm/s)
U_l	Superficial liquid velocity (cm/s)
U_s	Superficial solids velocity (cm/s)
U_{slip}	Slip velocity (cm/s)
U_t	Particle terminal velocity (cm/s)
U_{tr}	Transition velocity demarcate the conventional particulate regime and circulating fluidization regime (cm/s)
V_l, V_p	Local liquid velocity and local particle velocity (cm/s)
\bar{V}_p	Average particle velocity (cm/s)

Greek letters

$\bar{\varepsilon}$	Average bed voidage
$\bar{\varepsilon}_s$	Average solids holdup
μ_l	Liquid viscosity (mPa·s)
ρ_p	Particle density (kg/m ³)

Subscripts

l	Liquid
p	Particle
s	Solids

Abbreviation

LSCFB	Liquid-Solid Circulating Fluidized Bed
ILSCFB	Inverse Liquid-Solid Circulaing fluidized Bed
IGLSCFB	Inverse Gas-Liquid-Solid Circulaing fluidized Bed
CCFB	Conventional Circulating Fluidized Bed

Reference

- Avidan, A. A., and J. Yerushalmi. 1982. "Bed Expansion in High Velocity Fluidization." *Powder Technology* 32 (2): 223–32. [https://doi.org/10.1016/0032-5910\(82\)85024-9](https://doi.org/10.1016/0032-5910(82)85024-9).
- Chavarie, C, and D Karamanev. 1986. "Use of Inverse Fluidization in Biofilm Reactors." In *Proc. Int. Conf. on Bioreactor Fluid Dynamics, Cambridge (15-17 April)*, 181–90.
- Eldyasti, Ahmed, Nabin Chowdhury, George Nakhla, and Jesse Zhu. 2010. "Biological Nutrient Removal from Leachate Using a Pilot Liquid–Solid Circulating Fluidized Bed Bioreactor (LSCFB)." *Journal of Hazardous Materials* 181 (1–3): 289–97. <https://doi.org/10.1016/J.JHAZMAT.2010.05.010>.
- Fan, Liang-Shih, Katsuhiko Muroyama, and Song-Hsing Chern. 1982. "Hydrodynamics Characteristics of Inverse Fluidization in Liquid—Solid and Gas—Liquid—Solid Systems." *The Chemical Engineering Journal* 24 (2): 143–50. [https://doi.org/10.1016/0300-9467\(82\)80029-4](https://doi.org/10.1016/0300-9467(82)80029-4).
- Han, Q., and J.D. Hunt. 1993. "Particle Pushing: The Distribution of Particles in Liquid near a Solid Surface." *Materials Science and Engineering: A* 173 (1–2): 221–25. [https://doi.org/10.1016/0921-5093\(93\)90219-5](https://doi.org/10.1016/0921-5093(93)90219-5).
- Han, Q., and J.D. Hunt 1995. "Particle Pushing: Critical Flow Rate Required to Put Particles into Motion." *Journal of Crystal Growth* 152 (3): 221–27. [https://doi.org/10.1016/0022-0248\(95\)00085-2](https://doi.org/10.1016/0022-0248(95)00085-2).
- Karamanev, Dimitar G., and Ludmil N. Nikolov. 1992. "Free Rising Spheres Do Not Obey Newton's Law for Free Settling." *AIChE Journal* 38 (11): 1843–46. <https://doi.org/10.1002/aic.690381116>.
- KHAN, A.R., and J.F. RICHARDSON. 1989. "FLUID-PARTICLE INTERACTIONS AND FLOW CHARACTERISTICS OF FLUIDIZED BEDS AND SETTLING SUSPENSIONS OF SPHERICAL PARTICLES." *Chemical Engineering Communications* 78 (1): 111–30. <https://doi.org/10.1080/00986448908940189>.
- Kopko, Ronald J, Paul Barton, and Robert H McCormick. n.d. "Hydrodynamics of Vertical

Liquid-Solids Transport.” Accessed March 28, 2018.
<https://pubs.acs.org/doi/pdf/10.1021/i260055a012>.

Lan, Qingdao, Amarjeet Bassi, Jing-Xu (Jesse) Zhu, and Argyrios Margaritis. 2002. “Continuous Protein Recovery from Whey Using Liquid-Solid Circulating Fluidized Bed Ion-Exchange Extraction.” *Biotechnology and Bioengineering* 78 (2): 157–63.
<https://doi.org/10.1002/bit.10171>.

Liang, W. G., J. X. Zhu, Y. Jin, Z. Q. Yu, Z. W. Wang, and J. Zhou. 1996. “Radial Nonuniformity of Flow Structure in a Liquid-Solid Circulating Fluidized Bed.” *Chemical Engineering Science* 51 (10): 2001–10. [https://doi.org/10.1016/0009-2509\(96\)00057-7](https://doi.org/10.1016/0009-2509(96)00057-7).

Nelson, Michael J., George Nakhla, and Jesse Zhu. 2017. “Fluidized-Bed Bioreactor Applications for Biological Wastewater Treatment: A Review of Research and Developments.” *Engineering* 3 (3): 330–42. <https://doi.org/10.1016/J.ENG.2017.03.021>.

Patel, Ajay, Jesse Zhu, and George Nakhla. 2006. “Simultaneous Carbon, Nitrogen and Phosphorous Removal from Municipal Wastewater in a Circulating Fluidized Bed Bioreactor.” *Chemosphere* 65 (7): 1103–12. <https://doi.org/10.1016/J.CHEMOSPHERE.2006.04.047>.

Patel, Manoj, Amarjeet S. Bassi, Jesse J.-X. Zhu, and Hassan Gomaa. 2008. “Investigation of a Dual-Particle Liquid-Solid Circulating Fluidized Bed Bioreactor for Extractive Fermentation of Lactic Acid.” *Biotechnology Progress* 24 (4): 821–31. <https://doi.org/10.1002/btpr.6>.

Richardson, J.F., and W.N. Zaki. 1954. “The Sedimentation of a Suspension of Uniform Spheres under Conditions of Viscous Flow.” *Chemical Engineering Science* 3 (2): 65–73.
[https://doi.org/10.1016/0009-2509\(54\)85015-9](https://doi.org/10.1016/0009-2509(54)85015-9).

Richardson, J.F., and W.N. Zaki. 1997. “Sedimentation and Fluidisation: Part I.” *Chemical Engineering Research and Design* 75 (December): S82–100. [https://doi.org/10.1016/S0263-8762\(97\)80006-8](https://doi.org/10.1016/S0263-8762(97)80006-8).

Saffman, P. G. 1965. “The Lift on a Small Sphere in a Slow Shear Flow.” *Journal of Fluid Mechanics* 22 (02): 385. <https://doi.org/10.1017/S0022112065000824>.

Sang, Long, Tian Nan, Amin Jaber, and Jesse Zhu. 2019. "On the Basic Hydrodynamics of Inverse Liquid-Solid Circulating Fluidized Bed Downer." *Powder Technology*, April. <https://doi.org/10.1016/j.powtec.2019.04.021>.

Sang, Long, and Jesse Zhu. 2012. "Experimental Investigation of the Effects of Particle Properties on Solids Holdup in an LSCFB Riser." *Chemical Engineering Journal* 197: 322–29.

Zheng, Ying, Jing-Xu Zhu, Narendra S Marwaha, and Amarjeet S Bassi. 2002. "Radial Solids Flow Structure in a Liquid–Solids Circulating Fluidized Bed." *Chemical Engineering Journal* 88 (1–3): 141–50. [https://doi.org/10.1016/S1385-8947\(01\)00294-7](https://doi.org/10.1016/S1385-8947(01)00294-7).

Zhu, Jing-Xu (Jesse), Dimitre G. Karamanev, Amarjeet S. Bassi, and Ying Zheng. 2000. "(Gas-)Liquid-Solid Circulating Fluidized Beds and Their Potential Applications to Bioreactor Engineering." *The Canadian Journal of Chemical Engineering* 78 (1): 82–94. <https://doi.org/10.1002/cjce.5450780113>.

Chapter 4

4 Comparative Study of Inverse and Upward Liquid-Solid Circulating Fluidized Bed

Abstract

Upward and inverse liquid-solid circulating fluidized beds had drawn many attentions in environmental and chemical industries. The two continues phases, solids and liquid, This study compared the performance of inverse and upwards liquid-solids circulating fluidized beds based on residence times of solids (T_s) and liquid (T_l), Both solids and liquid residence times are decreasing with superficial liquid velocity and solids circulation rate. The ratio of solids and liquid residence time is used to characterize the hydrodynamics of different circulating fluidized beds and operating conditions. Similar trends of residence times were observed from upward and inverse liquid-solid circulating fluidized bed under close operating conditions with particles in similar terminal velocities. Particles that have smaller terminal velocities were found to have uncommon high T_s/T_l , which is an implication of clustering in liquid-solid circulating fluidized bed.

Key words: liquid-solid fluidization, solids holdup, circulating fluidized bed, inverse fluidization, residence time

4.1 Introduction

Circulating fluidized bed has been widely used in chemical industries exemplified by riser reactors for fluid catalytic cracking process, where the fast cracking reaction take place in the circulating fluidized bed riser and catalyst are regenerated in the downcomer (Bi and Zhu 1993). The concept of circulating fluidized bed with two columns was adopted in liquid systems, liquid-solid circulating fluidized bed (LSCFB), to meet the need for intensified interaction between liquid and solid, and also for continuous operation of solids if ever regeneration of solids is required.

Following LSCFB, inverse liquid-solid circulating fluidized bed (I-LSCFB)(Sang et al. 2019) has also drawn some interest due to its potential application as bioreactor for biological wastewater

treatment (Nelson, Nakhla, and Zhu 2017; BuffiÃ`re 2000) with low density particles that have to be fluidized downward.

Many researches have been carried out to investigate the hydrodynamics of LSCFB (Zheng et al. 1999; Zhu et al. 2000) and I-LSCFB which is crucial to the performance of (I)-LSCFB reactors. In (I)-LSCFBs(Sang et al. 2019), global solids holdup, local solids holdup axial and radial distribution, particle velocity, local liquid velocity, slip velocity, etc. are all interested hydrodynamics parameters, and they are determined by particle properties, operating conditions such as superficial liquid velocity and solid circulating rate, and fluidized bed geometry, etc. collectively. The hydrodynamics parameters are all correlated. Global solids holdup is affected by solids holdup distribution; slip velocity is determined by particle velocity and liquid velocity, which is also an effect of local solids holdup; local solids holdup distribution is also a result of local liquid velocity distribution. The complexity relationship between these variables makes it difficult and not reasonable to study them individually.

Average solids holdup in (I)-LSCFB is determined by particle properties such as particle diameter, density and particle shape and also operating conditions such as superficial liquid velocity and solid circulation rate.

Many qualitative results and trend were already known. Particles with different properties were studied under different range of operating conditions. Some studies have tried to unify the operating conditions with U_l/U_t , U_l/U_{mf} , U_l-U_{mf} or U_l-U_t (Zheng et al. 1999; Sang and Zhu 2012). Each method has its own physical meaning, which are all applicable for comparative study, but the results lost their identity. Furthermore, even the range of investigated solids holdup might be different for different particle properties and achievable operating conditions. It is difficult, almost not feasible, to do a fare comparative study on solids holdup considering all types of particles, operating conditions. And from a reactor point of view, the same average solids holdups are not likely to perform the same. Same solids holdup can be achieved with a different combination of U_s and U_l , but will lead to different heat transfer, mass transfer and reaction performance.

When comparing the hydrodynamics behavior of different types of fluidized bed with different particle properties, similar operation conditions and particles properties were selected for

comparison. Only a small portion of studied result of each type of fluidized bed can be selected. A much wider range of data are abandoned, making the selected data are not representative.

The idea of residence time per unit height T_s , T_l and their ratio, T_s/T_l are applied to analyze different types of liquid-solid circulating fluidized bed. And some similarities are also found in gas-solid circulating fluidized bed.

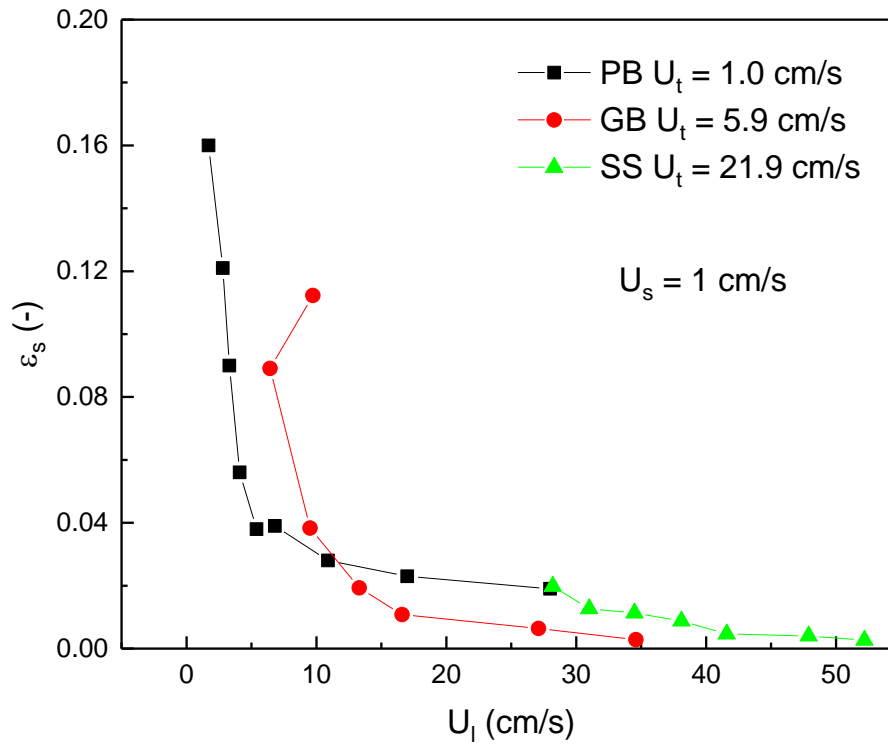


Figure 4.1.1 The change of average solids holdup with U_l when $U_s = 1$ cm/s in LSCFB

Table 4.1-1 Comparison of T_s , T_l and T_s/T_l at constant solids holdup

Solids holdup	U_l (cm/s)	U_s (cm/s)	T_s (s/m)	T_l (s/m)	T_s/T_l
0.053	26.41	0.88	6.00	3.59	1.67
	18.07	0.35	15.15	5.24	2.89
0.60	15.29	0.33	18.31	6.15	2.98
	20.85	0.67	8.97	4.51	1.99
0.089	12.51	0.42	21.14	7.29	2.90
	20.85	1.18	7.51	4.37	1.72
0.11	12.51	0.55	20.83	7.08	2.94
	18.07	1.46	8.00	4.89	1.64

4.2 Experiment setup

4.2.1 Operation of LSCFB and ILSCFB

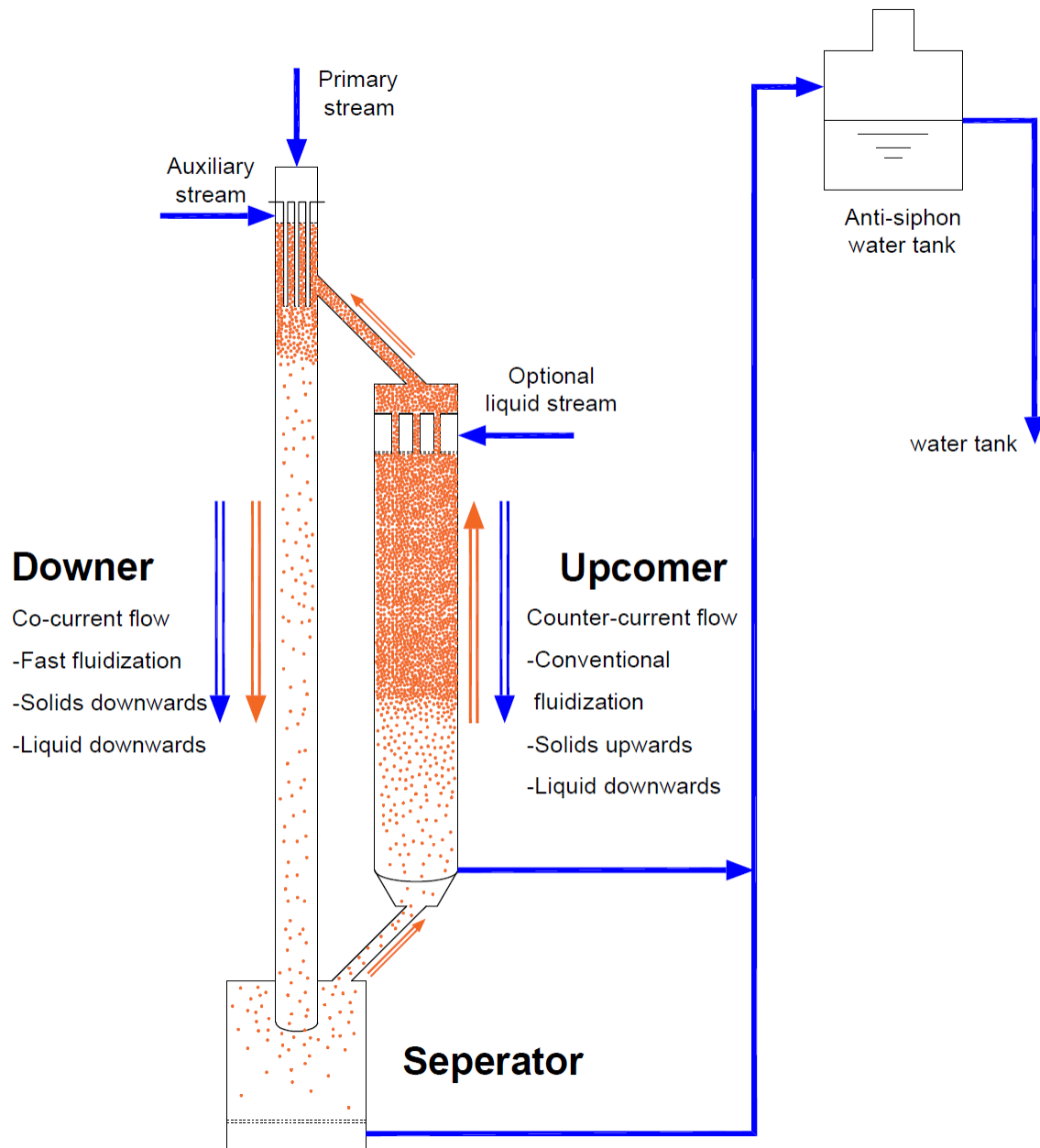


Figure 4.2.1 Schematic diagram of ILSCFB

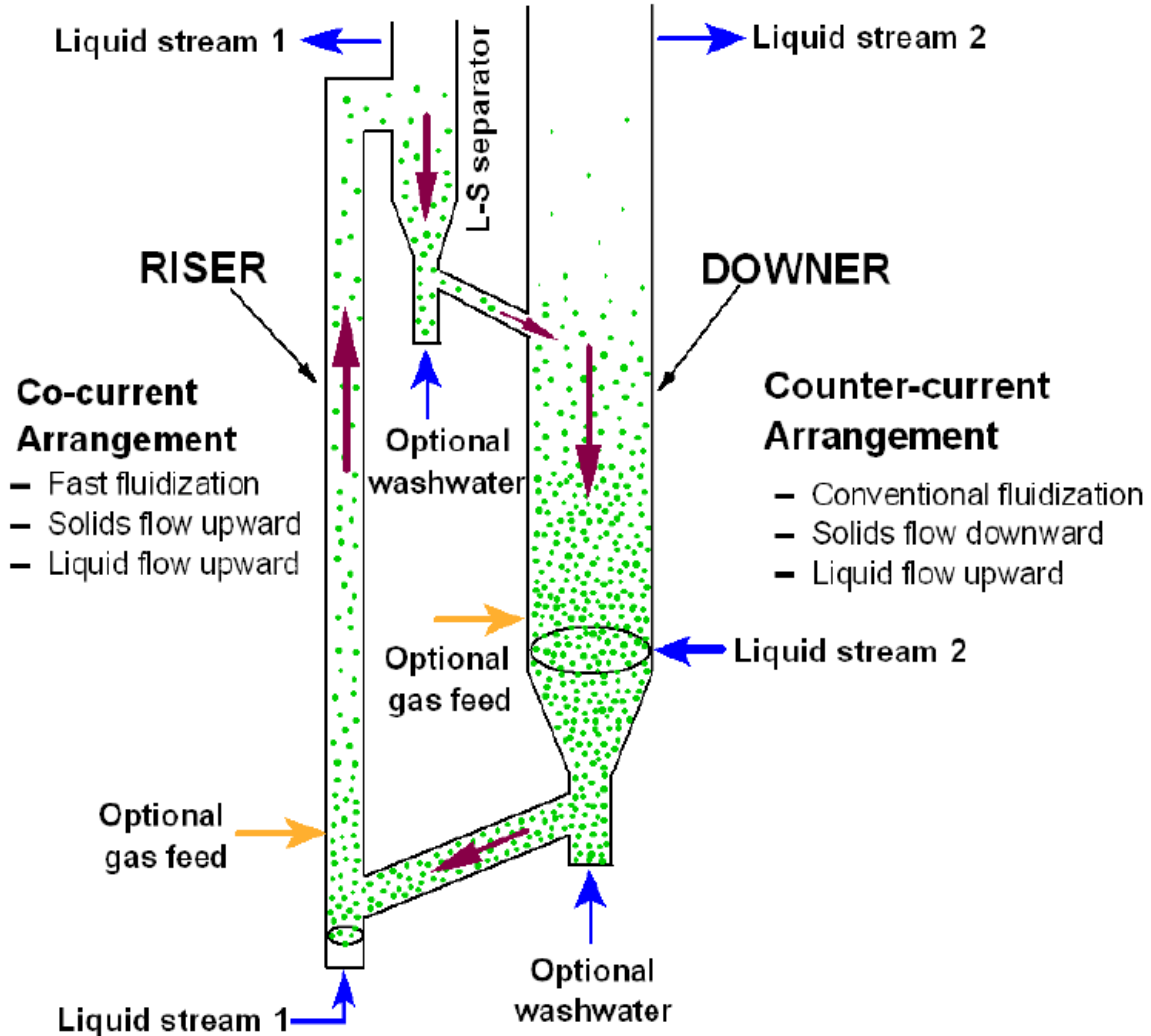


Figure 4.2.2 Schematic diagram of LSCFB

4.2.2 Residence time per unit height

Unified solids residence (t_s) is the retention time of solids to pass through a unit of reactor volume. T_s is a geometry independent variable that can represent the solids residence time of a typical reactor. In a circulating fluidized bed system, $T_s = \epsilon_s/U_s$ based on conservation of solids volume. Similarly, unified liquid residence can be obtained from $T_l = \epsilon_l/U_l$.

Unified solids residence time is an important hydrodynamics parameter in LSCFB. Understanding of unified solids residence time can lead to direct prediction of solids holdup in the fluidized bed by $\varepsilon_s = t_s * U_s$. In addition, unified solids residence is a crucial variable for fluidized bed reactors since it can affect the reactor performance such as conversion and selectivity. In this study, the unified solids residence time is investigated in both inverse liquid-solid circulating fluidized bed and liquid-solid circulating fluidized. In conventional liquid fluidized bed, t_s is infinite as all solids are retained in the confined volume with U_s equals zero. In fast or circulating fluidized beds, t_s is

4.3 Results and discussion

4.3.1 Change of T_s , T_l with U_s and U_l

Unified solids residence time under different operating conditions, U_l and U_s , are plotted in Figure 4.3.1 and Figure 4.3.2. T_s is decreasing with increasing solid circulation rate and the slope of change get steadier with increasing superficial liquid velocity. In addition, a higher U_l will lead to a less T_s .

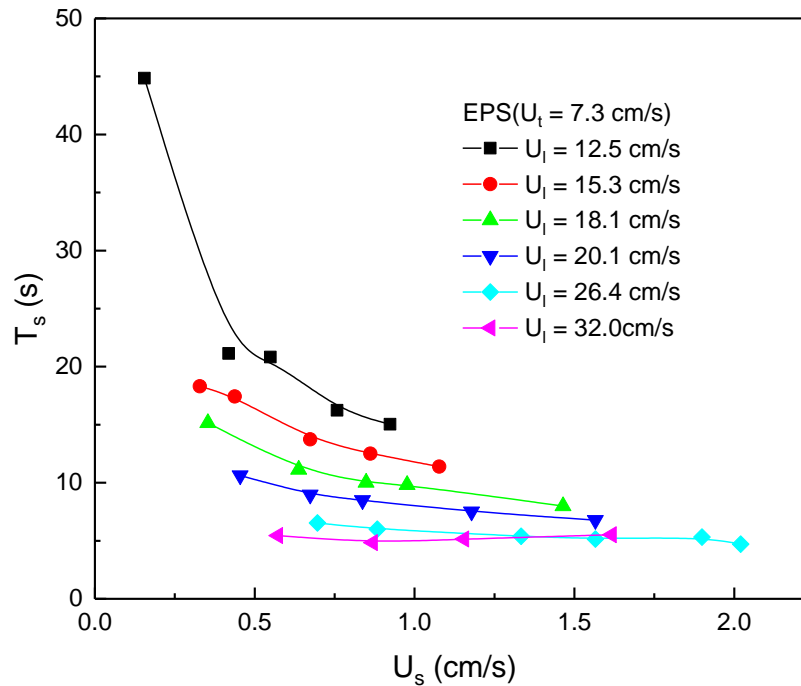


Figure 4.3.1 Change of T_s with U_s under different U_l in ILSCFB

When U_1 is relatively low, a sharp decrease of T_s is observed with increasing U_s . This is because at low U_1 , particle-particle interaction is more severe. Thus, particle velocity is sensitive to the addition U_s . And when U_s is further increased, solids holdup is increased significantly as shown in Figure 3.3.18. As a result, particle velocity is not increased that much which leads to a gradual decrease of T_s . On the other hand, when U_1 is high, the effect particle-particle interaction is greatly reduced by the high interstitial velocity. As a result, T_s is decreasing with U_s in a much lower rate and will reach plateau eventually. And the trend is consistent in LSCFB with high density particles as shown in Figure 4.3.2.

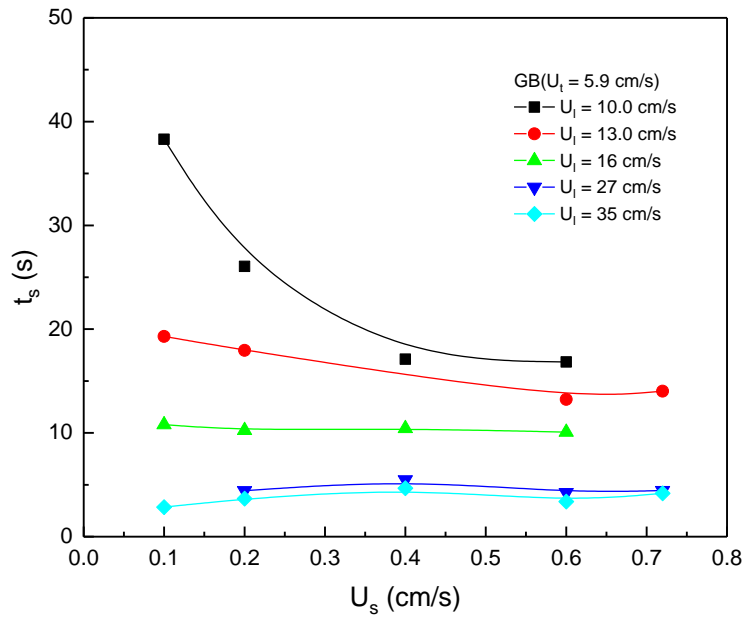


Figure 4.3.2 Change of T_s with U_s under different U_1 in LSCFB

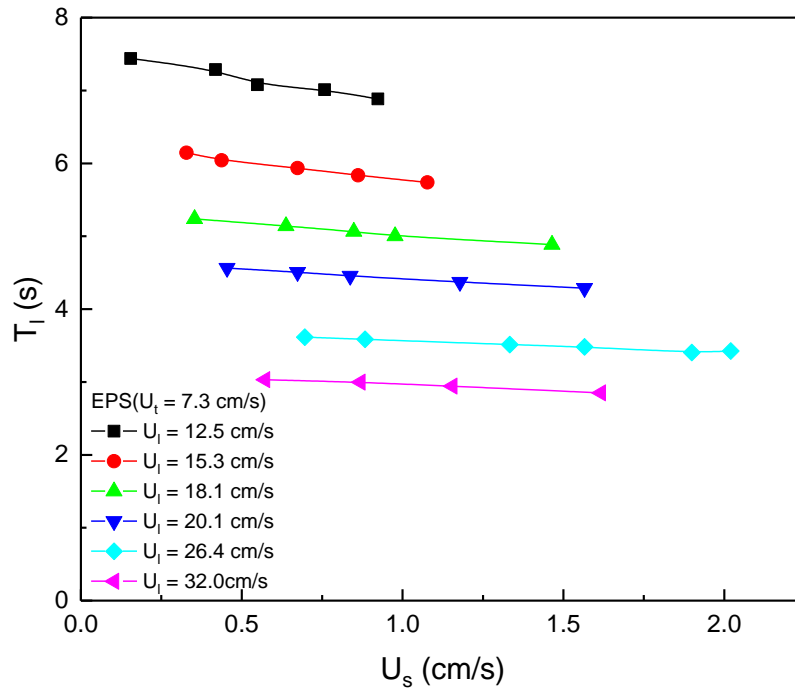


Figure 4.3.3 Change of T_1 with U_s under different U_1 in ILSCFB

Unified liquid residence time is calculated from $T_1 = \varepsilon_l/U_1$ which represent the time required for liquid to travel unit reactor volume. Figure 4.3.3. shows the relationship between T_1 and U_s at different U_1 . A high superficial liquid velocity always leads to low liquid residence time, as more volume of liquid is fed to the same reactor volume. T_1 is also decreasing with U_s under all superficial liquid velocities, and the slope get flatter with increasing superficial liquid velocity. This is due to the volume of liquid is reduced with more solids fed to the system, as shown in Figure 4.3.3. And the change of T_1 with U_s is in a linear fashion, while the change of T_s with U_s is much abrupt.

4.3.2 Particle property effects T_s

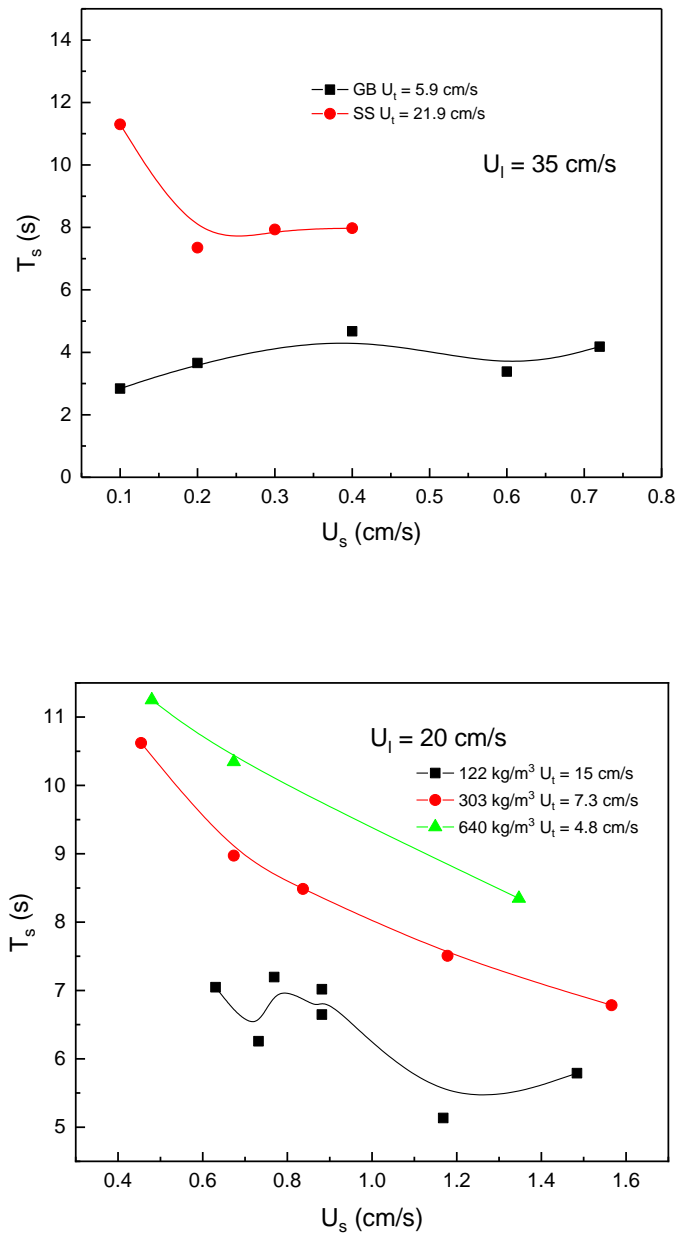


Figure 4.3.4 Change of T_s of different particles

The relationship between solids residence time T_s and solid circulation rate U_s are plotted in Figure 4.3.4 at constant superficial liquid velocity with particles of different terminal velocities. Under the same operating condition, particles with higher U_t always have less residence time. This is due

to the large terminal velocity, which often means large slip velocity, hindered the particle velocity in the fluidized bed, but the trend is not consistent with ILSCFB.

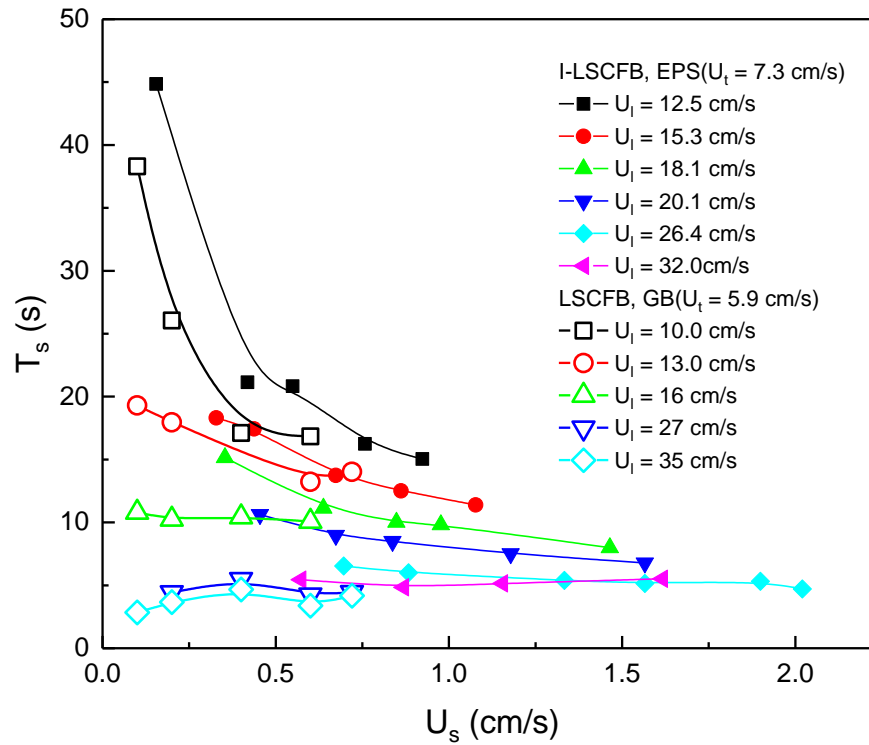
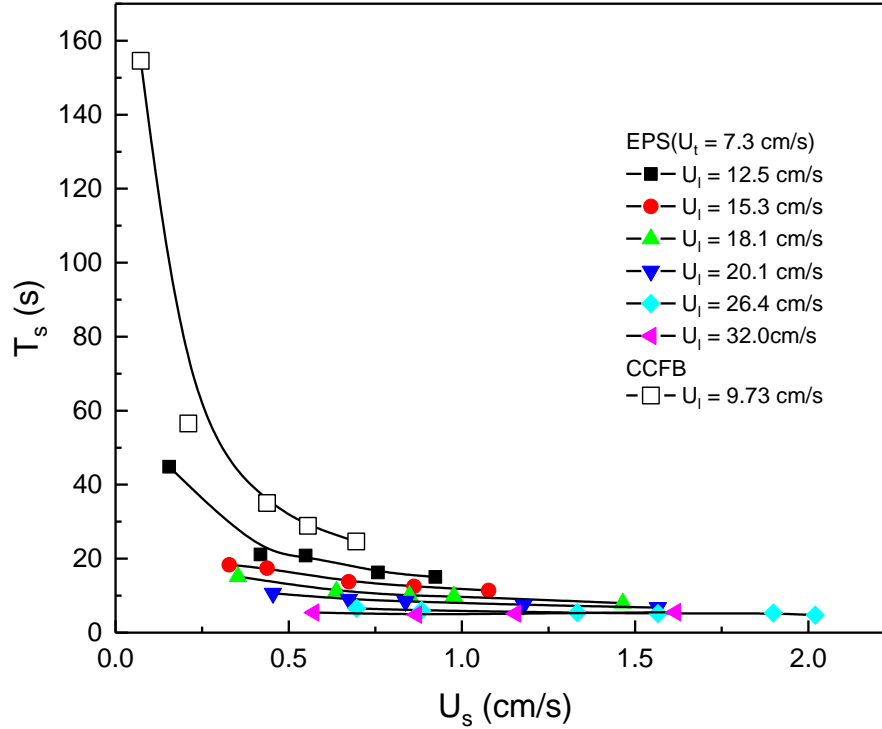


Figure 4.3.5 Comparison between LSCFB and ILSCFB

Under similar operating conditions and particle terminal velocities, ILSCFB always have less residence time compared with LSCFB. In the figure above, low density EPS have slightly higher U_t than Glass beads in LSCFB, which is supposed to travel slower in the same condition. But the results suggest, low density particles tend to travel slower than projected which lead to higher solid residence time.

4.3.3 Comparison between CCFB and LSCFB



Based on the results in chapter 6, Inverse Conventional Circulating Fluidized Bed has a much high solids retention time than Inverse LSCFB, and its T_s is decreasing very sharply with U_s .

4.3.4 Change of T_s/T_l with U_l in LSCFB and ILSCFB

T_s/T_l represents the ratio of solids residence time to liquid residence time in the circulating fluidized bed. The residence time ratio is shown in Figure 4.3.6 and Figure 4.3.7 of three types of particle in LSCFB and 5 types of particles in ILSCFB. The ratio is descending with superficial liquid velocity, and the residence time ratio is approaching to 1 at high superficial liquid velocity. This phenomenon can be explained by slip velocity between liquid and solids. The solids in circulating fluidized bed are transported by drag force provided by liquid. Thus, a slip velocity between liquid and solids always exists, and liquid always travels faster than solids. So, the residence time of solids is always higher than liquid in (I)-LSCFB, which lead to T_s/T_l always higher than 1. With increasing superficial liquid velocity, both solids and liquid will obtain a higher

speed, but the slip velocity doesn't change much. Therefore, the residence time of solids and liquid are both reduced and their difference is less. At extreme high superficial liquid velocity, the slip velocity is negligible compared with the solids or liquid velocity, which lead to $T_s \approx T_l$, and the minimum of T_s/T_l is reached.

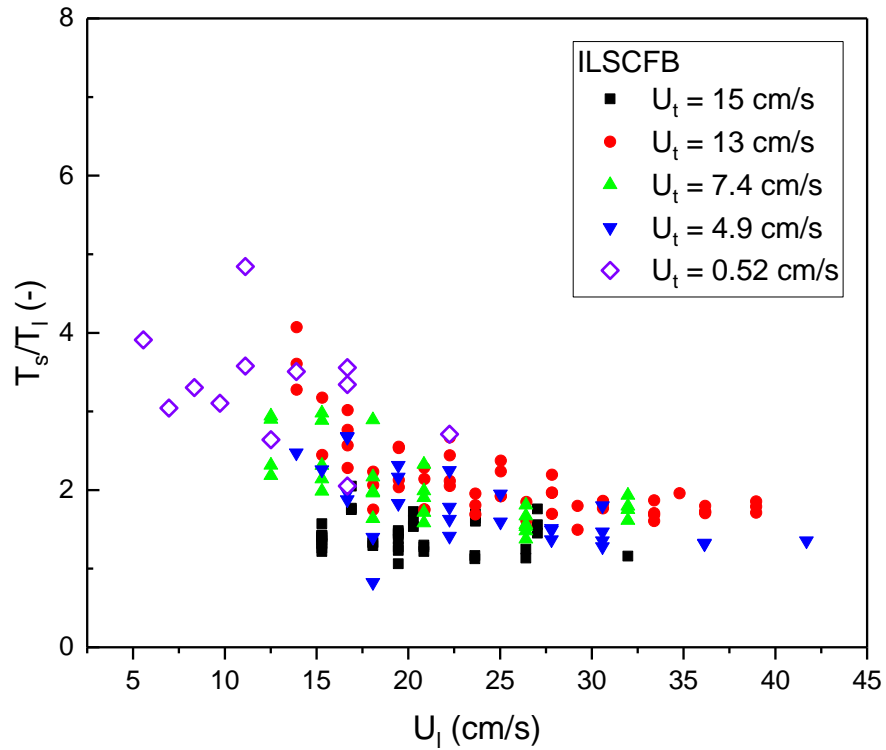


Figure 4.3.6 Change of T_s/T_l with U_l in ILSCFB

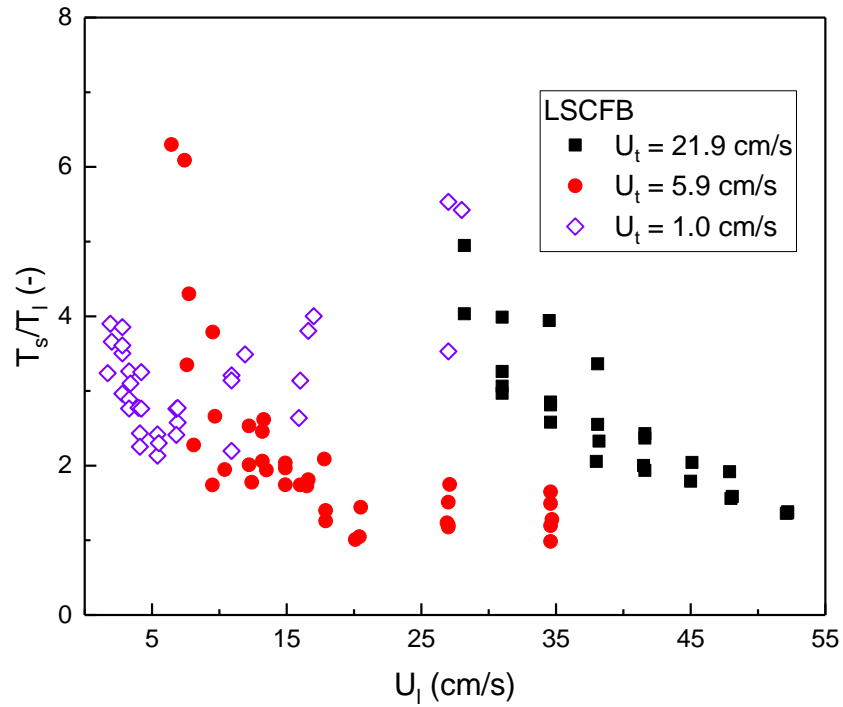


Figure 4.3.7 Change of T_s/T_1 with U_l in LSCFB

It can also be found in the Figure 4.3.7 that particles with higher terminal velocity tends to have higher T_s/T_1 ratio. This is also aligned with the explanation using the slip velocity. Particle terminal velocity can also be regarded as the slip velocity of solids in stagnant liquid, and the slip velocity in circulating fluidized bed is directly related with particle terminal velocity. Particle with higher terminal velocity will have higher slip velocity between solid and liquid, thus a larger difference in travelling velocity in the fluidized bed, which lead to a higher T_s/T_1 ratio.

However, the decreasing trend of T_s/T_1 with superficial liquid velocity doesn't apply to PB($U_t = 1$ cm/s) in LSCFB and PS ($U_t = 0.52$ cm/s) in ILSCFB. It is interesting to see that those particles with very low terminal velocity still have high T_s/T_1 ratio even at high superficial liquid velocity. From the results shown in Figure 4.3.7, the T_s/T_1 ratio are sticking at 3 while other particles are approaching 1-1.5 under similar U_l/U_t conditions.

It is commonly believed that those particles that will lose their identity and just follow the liquid flow because of their little inertia indicated by their particle terminal velocity. A potential explanation can be used for this phenomenon:

Particle clustering may exist among small inertial particles. There is no universal explanation for the formation of cluster in circulating fluidized bed due to the complexity of solids behavior and the turbulence of fluid. One popular reason which can be adopted from gas-solid circulating fluidized bed is that the fluctuation of fluid flow will cause and shape the solids to move in a clustering pattern, and the dynamic movement of fluid flow will cause the formation and breakage of clusters along the circulating fluidized bed. Particles with small inertia are more likely to be bonded together and form big cluster, while particles with significant particle terminal velocities tends to stay in its own path. To validate this explanation, particle Reynolds number at particle terminal velocity is calculated. Particle Reynolds number ($Re_t = dU_t\rho_l/\mu$) can also back up the explanation. Particle Reynolds number of investigated particles are listed in Table 2. It is showing particle with less terminal velocities in (I)-LSCFB have less than 10 Re_t , and the widely studied gas-solid circulating fluidized bed FCC particles have similar small Re_t . EPS 1020 and PB have the least Re_t because their terminal velocity is small, while the small diameter of FCC particle contribute to its small Re_t . The little difference between their Re_t indicates they might share similar flowing pattern in the circulating fluidized bed.

In addition, there is a slightly increase of T_s/T_l with superficial liquid velocity of small inertial particles, and this trend is aligned with Gas-Solid CFB as shown in Figure 4.3.8, which is believed to be caused by cluster as well. in As a Conclusions, the clustering of small inertial particles will cause particles to stay longer in the fluidized bed relatively, causing a higher T_s/T_l ratio compared with large inertia particles.

Particle Reynolds number ($Re_t = dU_t\rho_l/\mu$) can also back up the explanation. Particle Reynolds number of investigated particles are listed in Table 2. It is showing particle with less terminal velocities in (I)-LSCFB have less than 10 Re_t , and the widely studied gas-solid circulating fluidized bed FCC particles have similar small Re_t . EPS 1020 and PB have the least Re_t because their terminal velocity is small, while the small diameter of FCC particle contribute to its small

R_{et} . The little difference between their R_{et} indicates they might share similar flowing pattern in the circulating fluidized bed.

Particle Reynolds number can be originated from Navi-Stokes equation, when calculating drag force along a sphere in creeping flow. And that concept has been adopted widely to represent the effect of inertia over viscous force on the particle in fluidized bed. Low Reynolds number means the flow pattern of solids are more likely to be governed by inertia or momentum of the fluid. In the presence of turbulence in the fluid such as vortex, those low R_{et} particles will be affected, while high R_{et} particles won't be affected that much. This explains why T_s/T_l increase with fluid velocity for EPS1020, PB and FCC particles, since the degree of turbulence got intensified.

4.3.5 Significance of T_s , T_l and T_s/T_l

T_s can reflect backmixing and T_s/T_l is the inverse of interstitial particle velocity (U_s/ϵ_s). As discussed above, solids residence time T_s and liquid residence time T_l are reflections of particle properties, solid circulation rate, superficial liquid velocity and phase holdups in (I)-LSCFB.

The residence time ratio T_s/T_l can be used to represent the degree of backmixing in (I)-LSCFB. In conventional fluidized bed, where backmixing or contact efficiency of solids is at its extreme, solids are in contact with fresh liquid all the time, and T_s/T_l is infinite since T_s is infinite. In circulating fluidized bed with high superficial liquid velocity, T_s/T_l is approaching 1, which indicate solids and liquid are travelling under similar speed and pattern through the reactor. It is very likely the solids and liquid met at the entrance of the reactor, and travels together to the exit. And in the middle, LSCFB with moderate superficial liquid velocity, the T_s/T_l ratio often lies between 3-10. For example, if $T_s/T_l = 3$, the chance of solids to contact with fresh liquid almost tripled compared with condition where $T_s/T_l = 1$. Thus, T_s/T_l ratio can be used as a parameter to evaluate the solids/liquid contact, which can't be analyzed by solids holdup individually. T_s/T_l is not a directly representation of backmixing, but its trend with U_s and U_l can represent its degree of backmixing.

4.3.6 Failure of Richardson-Zaki equation in (I)-LSCFB

Richardson-Zaki equation is widely in liquid solid fluidized beds. We have attempted to adopt the same method for solids holdup prediction. The particles were first studied in conventional

fluidization regime to obtain the exponent n and particle terminal velocity as variable constants for Richardson-Zaki equation. And the obtained constants were used in derived Richardson-Zaki equation for circulating fluidized bed as shown in chapter 4.(Liang et al. 1997)

A large discrepancy between experiment and estimated results have been found. Some studies have addressed this issue and attempted to solve it by modifying exponent n or adding extra variables with data fitting, which were all empirical methods.

Richard-Zaki equation describes the direct relationship between slip velocity and solids holdup, which can be applied to solids holdup prediction. However, the results from T_s/T_1 is suggesting that slip velocity is not always in effect when determining the solids and liquid behavior in the fluidized bed, such as particles with low terminal velocity. In addition, at high superficial liquid velocity, T_s/T_1 is close to 1, the effects of slip velocity are not significant. As a result, the Richard-Zaki equation oriented from slip velocity may not be suitable for the modelling solids holdup in (I)-LSCFB.

4.3.7 Comparison of T_s/T_l in Gas-Solid CFB

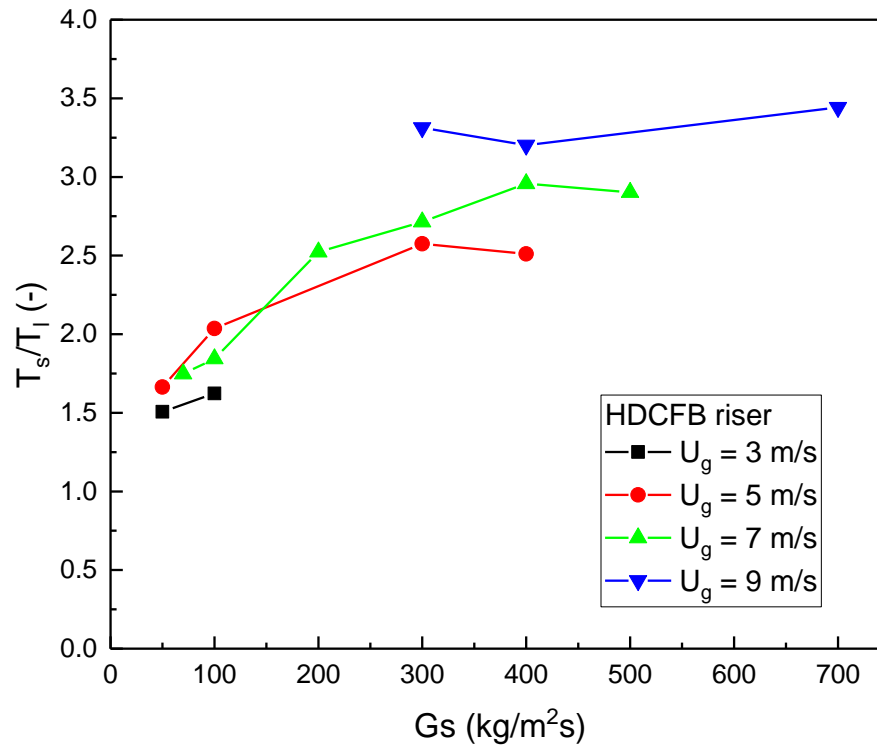


Figure 4.3.8 Change of T_s/T_l in gas-solid CFB riser(Wang et al. 2014)

For comparison, T_s/T_f are also calculated in gas-solid circulating fluidized bed. T_s/T_f with the change of solid circulation rate and superficial gas velocity in HDCFB are shown in the Figure 4.3.8. T_s/T_f is found to increase with solid circulating rate. And high superficial gas velocity will lead to a high T_s/T_f ratio. The trend is very different (I)-LSCFB. T_s/T_l is increasing with solid circulation rate G_s , which is opposite in liquid systems.

4.4 Conclusions and recommendations

The hydrodynamics behavior in LSCFB and ILSCFB is systematically studied based on residence time of solid and liquid.

- T_s , T_l , T_s/T_l are more effective tools for analysis and comparison for (I) – LSCFBs for a wide range of solid circulation rates and superficial liquid velocities

- The overall hydrodynamics in LSCFB and I-LSCFB are very similar, Inverse liquid-solid circulating fluidized bed has less back mixing than upwards LSCFB
- Hydrodynamics in (I)-LSCFBs is quite different from gas-solid circulating fluidized bed mainly due to the clustering phenomenon
- Particles with small terminal velocity or small inertia has severe back mixing in (I)-LSCFBs, which also resembles the behavior of FCC particles in Gas-Solid CFB risers

In the future, more effort could be devoted to study the cluster phenomenon which is the cause to the increasing T_s/T_l . Microscopic flow structure of particles with little Re_t should be investigated to study the mechanism of particle clustering phenomenon. Based on resemblance of liquid-solid and gas-solid circulating fluidized bed with particles at low Re_t , more detail comparative study could be made to study the underlying difference or similarities caused by fluidization medium.

Nomenclature

Ar	Archimedes number defined by $d_p^3 g (\rho_p - \rho_l) \rho_l / \mu_l^2$
C_D	Particle drag coefficient
d_p	Particle diameter (mm)
D	Column diameter (m)
F_b, F_d, F_g	Buoyancy, drag force and gravity
G_s	Solids circulation rate (kg/ (m ² s))
g	Gravity acceleration
Re	Reynolds number defined by $U_l d_p \rho_l / \mu_l$
Re_t	Particle terminal Reynolds number defined by $U_t d_p \rho_l / \mu_l$
U_a	Auxiliary liquid velocity (cm/s)
U_l	Superficial liquid velocity (cm/s)
U_s	Superficial solids velocity (cm/s)
U_{slip}	Slip velocity (cm/s)
U_t	Particle terminal velocity (cm/s)
U_{tr}	Transition velocity demarcate the conventional particulate regime and circulating fluidization regime (cm/s)
V_l, V_p	Local liquid velocity and local particle velocity (cm/s)
\bar{V}_p	Average particle velocity (cm/s)

Greek letters

$\bar{\varepsilon}$	Average bed voidage
$\bar{\varepsilon}_s$	Average solids holdup
μ_l	Liquid viscosity (mPa·s)
ρ_p	Particle density (kg/m ³)

Subscripts

l	Liquid
p	Particle
s	Solids

Abbreviation

LSCFB	Liquid-Solid Circulating Fluidized Bed
ILSCFB	Inverse Liquid-Solid Circulaing fluidized Bed
IGLSCFB	Inverse Gas-Liquid-Solid Circulaing fluidized Bed
CCFB	Conventional Circulating Fluidized Bed

Reference

- Avidan, A. A., and J. Yerushalmi. 1982. "Bed Expansion in High Velocity Fluidization." *Powder Technology* 32 (2): 223–32. [https://doi.org/10.1016/0032-5910\(82\)85024-9](https://doi.org/10.1016/0032-5910(82)85024-9).
- Bi, Hsiaotao, and Jingxu Zhu. 1993. "Static Instability Analysis of Circulating Fluidized Beds and Concept of High-Density Risers." *AIChE Journal* 39 (8): 1272–80. <https://doi.org/10.1002/aic.690390803>.
- BuffiÃ”re, P. 2000. "The Inverse Turbulent Bed: A Novel Bioreactor for Anaerobic Treatment." *Water Research* 34 (2): 673–77. [https://doi.org/10.1016/S0043-1354\(99\)00166-9](https://doi.org/10.1016/S0043-1354(99)00166-9).
- Liang, Wugeng, Shuliang Zhang, Jing-Xu Zhu, Yong Jin, Zhiqing Yu, and Zhanwen Wang. 1997. "Flow Characteristics of the Liquid–Solid Circulating Fluidized Bed." *Powder Technology* 90 (2): 95–102.
- Nelson, Michael J., George Nakhla, and Jesse Zhu. 2017. "Fluidized-Bed Bioreactor Applications for Biological Wastewater Treatment: A Review of Research and Developments." *Engineering* 3 (3): 330–42. <https://doi.org/10.1016/J.ENG.2017.03.021>.
- Sang, Long, Tian Nan, Amin Jaber, and Jesse Zhu. 2019. "On the Basic Hydrodynamics of Inverse Liquid-Solid Circulating Fluidized Bed Downer." *Powder Technology*, April. <https://doi.org/10.1016/j.powtec.2019.04.021>.
- Sang, Long, and Jesse Zhu. 2012. "Experimental Investigation of the Effects of Particle Properties on Solids Holdup in an LSCFB Riser." *Chemical Engineering Journal* 197 (July): 322–29. <https://doi.org/10.1016/J.CEJ.2012.05.048>.
- Wang, Chengxiu, Jesse Zhu, Chunyi Li, and Shahzad Barghi. 2014. "Detailed Measurements of Particle Velocity and Solids Flux in a High Density Circulating Fluidized Bed Riser." *Chemical*

Engineering Science 114 (July): 9–20. <https://doi.org/10.1016/J.CES.2014.04.004>.

Zheng, Ying, Jing-Xu Zhu, Jianzhang Wen, Steve A. Martin, Amarjeet S. Bassi, and Argyrios Margaritis. 1999. “The Axial Hydrodynamics Behavior in a Liquid-Solid Circulating Fluidized Bed.” *The Canadian Journal of Chemical Engineering* 77 (2): 284–90.
<https://doi.org/10.1002/cjce.5450770213>.

Zhu, Jing-Xu Jesse, Dimitre G Karamanev, Amarjeet S Bassi, and Ying Zheng. 2000. “(Gas-) Liquid-solid Circulating Fluidized Beds and Their Potential Applications to Bioreactor Engineering.” *The Canadian Journal of Chemical Engineering* 78 (1): 82–94.

Chapter 5

5 Hydrodynamics of inverse liquid-solid circulating fluidized bed below particle terminal velocity

Abstract

The concept of liquid-solid circulating fluidized bed operating below particle terminal velocity is proposed by applying solid circulation under conventional fluidization regime, which is called conventional circulating fluidized bed (CCFB). The objective is to develop a new flow regime to combine the advantages of circulating fluidized bed and conventional fluidized bed. The study is carried under an inverse liquid-solid circulating fluidized bed downer (0.076 m ID and 5.4 m in height). The operation of CCFB is similar to inverse liquid-solid circulating fluidized bed. Solids holdup at various solids circulation rates and superficial liquid velocities are measured to demonstrate the hydrodynamics in an inverse CCFB downer with two types low density expanded polystyrene particles. CCFB is able achieve higher solids holdup comparing to conventional fluidization and liquid-solid circulating fluidized bed downer. Axial solids holdup distribution is uniform in CCFB downer. A new parameter is defined to present the degree of unsteady state in CCFB and apparent slip velocity was calculated and to understand the circulating solids behavior under low liquid velocity.

Key words: liquid-solid fluidization, solids holdup, circulating fluidized bed, inverse fluidization, slip velocity

5.1 Introduction

Liquid-solid fluidized beds have a long history in environmental, chemical, mining industries (Epstein 2002). Many industrial applications of liquid fluidization have been focused on batch or semi-batch conventional liquid fluidization. In the last decade, liquid-solid circulating fluidized bed, inherited from gas-solid fast fluidization, has drawn much attention in iron-exchange and waste water treatment process, due to its high contact efficiency between solids and liquid.(Lan et

al. 2000)(Nelson, Nakhla, and Zhu 2017)(Eldyasti et al. 2010)(Trivedi, Bassi, and Zhu 2006) Thus many hydrodynamics study concentrated on conventional liquid fluidization and circulating liquid fluidization both experimentally and numerically, which is crucial in designing fluidized unit(Cheng and Zhu 2008)(Sang 2013)(Fan, Muroyama, and Chern 1982). Comparing to gas-solid fluidization, the simplicity of flow regimes and the particulate fluidization behavior in liquid systems is more predictable. Many models, mostly semi-empirical or empirical, have be proposed to predict the behavior in liquid fluidization, which is helpful determining the operating window, fluidization condition and performance of the fluidized bed unit.(Ulaganathan and Krishnaiah 1996; Thiruvengadam Renganathan and Krishnaiah 2008; T Renganathan and Krishnaiah 2005; D. G. Karamanev and Nikolov 1992)

5.1.1 Conventional fluidization

For a single particle, when net gravity is countered by drag force, the particle is suspended in the liquid. And the drag force is determined by the slip velocity between particles and liquid(Haider and Levenspiel 1989). For a mixture of particles, the actual slip velocity is hard to determine due to flow turbulence and solids packing. Superficial liquid velocity is used in prediction solids fluidization properties. After minimum fluidization, when the weight of all the particles is carried over by the flow of liquid, voidage increases with increasing superficial liquid velocity, so as bed expansion ratio, since more distance between particles is required to compensate the increasing liquid flow to maintain a suspension(Kopko, Barton, and McCormick n.d.)(D. G. Karamanev and Nikolov 1992). When the superficial liquid velocity is approaching particle terminal velocity, solids holdup is close to zero, and distance between particles have reached its maximum. The solids holdup is determined by the superficial liquid velocity and particle terminal velocity, which is a function of particle properties. The relationship can be described by the well-known Richard-Zaki equation(D. G. Karamanev and Nikolov 1992). For a conventional fluidized bed, solids holdup can only be controlled by superficial liquid velocity. And solids holdup become very sensitive to superficial liquid velocity when it is operating close to particle terminal velocity.

5.1.2 LSCFB

If the superficial liquid velocity is beyond particle terminal velocity, particles will be carried away since there is not enough space for particle expansion to maintain the surrounding liquid velocity

at particle terminal velocity. Because of the high liquid velocity, particles will follow the liquid flow, thus a net solids flux exist, which is represented by solids circulation rate (U_s). Solids must be fed continuously to form a circulating fluidized bed, otherwise the column will be empty as all solids are carried by the fluid in one direction. Many studies have been carried out to investigate the hydrodynamics of liquid-solid circulating fluidized bed. In liquid-solid circulating fluidized bed, solids holdup is determined by superficial liquid velocity and solids circulation rate (Razzak, Barghi, and Zhu 2009; Sang and Zhu 2012; Zheng et al. 1999; Liang et al. 1996; Zheng and Zhu 2000; Zheng et al. 2002). Comparing to conventional fluidization, LSCFB has higher solids contact efficiency due to its high slip velocity, but solids holdup is much lower ($<15\%$) (Zheng et al. 1999; Sang and Zhu 2012).

5.1.3 Concept of CCFB

For a liquid-solid fluidized bed, voidage or solids holdup is always the most essential parameter when studying the hydrodynamics, as it is closely related to estimating reaction performance, heat and mass transfer efficiency, and energy consumption of the fluidized bed. Low solids holdup usually indicates good mixing due to the sufficient contact area per particle volume between solids and liquid exemplified by liquid-solid circulating fluidized bed (LSCFB). High solids holdup provides more total surface area of particles, although contact efficiency of individual particle is compromised due to solids interaction (Eldyasti et al. 2010; Lan et al. 2000).

In this study, the concept of circulating fluidized bed operating below particle terminal velocity is proposed. The expected operation regime is illustrated in **Figure 5.3.2**. High expansion conventional fluidization in conjunction with solids circulation is believed to have the following advantages over existing liquid-solid fluidized beds.

- (1) Solids circulation is introduced to a conventional fluidized bed, allowing continuous operation if particles need regeneration
- (2) Achievable higher solids holdup comparing to conventional liquid-solid fluidization and LSCFB at similar conditions
- (3) Better control of solids holdup with U_s and U_L

The concept of unsteady state suspension is applied to explain the phenomenon of conventional fluidization with solids circulation.

5.2 Experiment procedures

Unlike gas-solid fluidized bed, extreme high expansion can be reached in liquid-solid fluidized bed. The voidage can be maintained up to 0.95, when liquid velocity is below particle terminal velocity. And the bed expansion ratio could be 10 ~ 12 (D. G. Karamanev and Nikolov 1992). If the bed height exceeds the height of the column, depending on the initial bed height, extra particles will be lost from the exit of the column until the suspension bed height equals the height of the column. At this condition, if particles can be fed to the fluidized bed without changing the superficial liquid velocity, a higher bed height is achievable. Since the suspension height is at its maximum, extra particles will be carried away through the end of the column. Then, a circulating fluidized bed is formed operating below particle terminal velocity by recycling the extra particles from the outlet back to the conventional fluidized bed.

In this work, an inverse circulating fluidized bed is applied to study the hydrodynamics of CCFB. Custom made Styrofoam powders are used as fluidization particles, and the properties are summarized in Table 1. The circulating fluidized is comprised of a 5.4 m downer (0.076 m ID) and a 4 m upcomer (0.20 m ID). Primary and auxiliary flow distributors are located at the top of the downer; additional distributor is at the top of the upcomer (Sang and Zhu 2012).

Table 5.2-1 Particle properties

	D_p	ρ	U_t
1	1.1mm	122 kg/m³	15.9 cm/s
2	1.2 mm	300 kg/m³	9.9 cm/s

Starting with an initial height of solids in the downer, the system is operated under conventional regime, where there is clear boundary between the suspension and the freeboard. And the bed height is sensitive to superficial liquid velocity. The bed expansion is controlled by superficial liquid velocity reaching a dilute suspension. Based on experiment operation, when the superficial liquid velocity has reached 80% of particle terminal velocity, the solids holdup will be around 10% and the suspension can easily be higher than the column height. For difference types of particles,

the suspension can be estimated by Richard-Zaki equation. At steady state, the height of high expansion conventional fluidized bed will match the height of downer, as extra particles are transported to the upcomer when the downer is reaching steady state. With conventional fluidization as the initial stage, transferring to conventional circulating regime by opening auxiliary flow but maintain total flowrate in the downer at constant allows particles fed from the top of the downer.

Main flow distributor is located below the particle feeding pipe, thus cannot control solids feed. However, auxiliary flow distributor is located above the feeding pipe, which can push particles downward to converge with main flow, as seen in Figure 5.3.1. Although mainflow distributor is where fluidization started, it is auxiliary flow that serve as non-mechanical valve to travel the particles to the fluidized bed (Zheng and Zhu 2000). In addition to auxiliary flow, additional stream is introduced from the top of the upcomer to fluidize the inventory particles so that light particles have more pressure to travel to the downer. Solids feed rate, so called solids circulating rate can be controlled by adjusting the auxiliary flow and the additional flow stream in the upcomer. Increasing auxiliary flow or addition flow in the upcomer and improve solids circulating rate. Solids circulation rate is monitored using two butterfly valves located at the bottom of the upcomer, which collects the of solids leaving the downer. As at steady state, the volume flowrate of solids leaving the downer equals solids circulation rate.

Solids holdup at different axial positions is the most important parameter to study the hydrodynamics of CCFB. Nine manometers are connected to the downer for solids holdup measurement.

5.3 Results and discussion

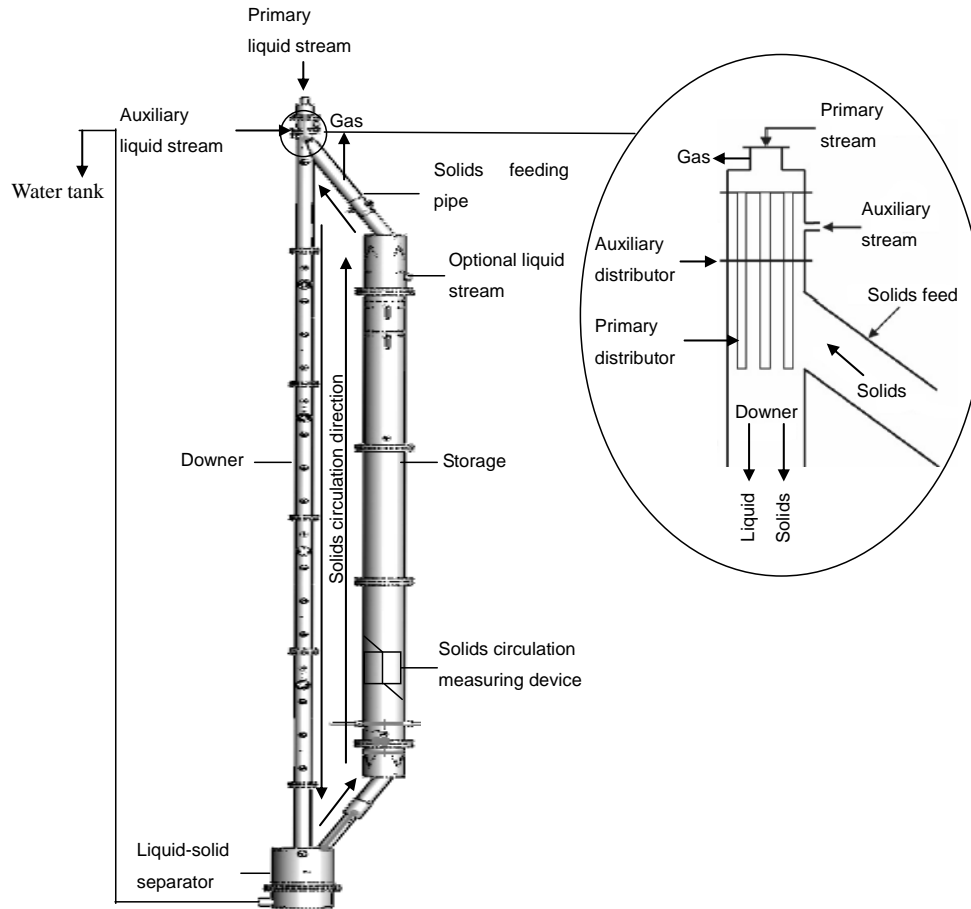


Figure 5.3.1 Schematic diagram of inverse CCFB

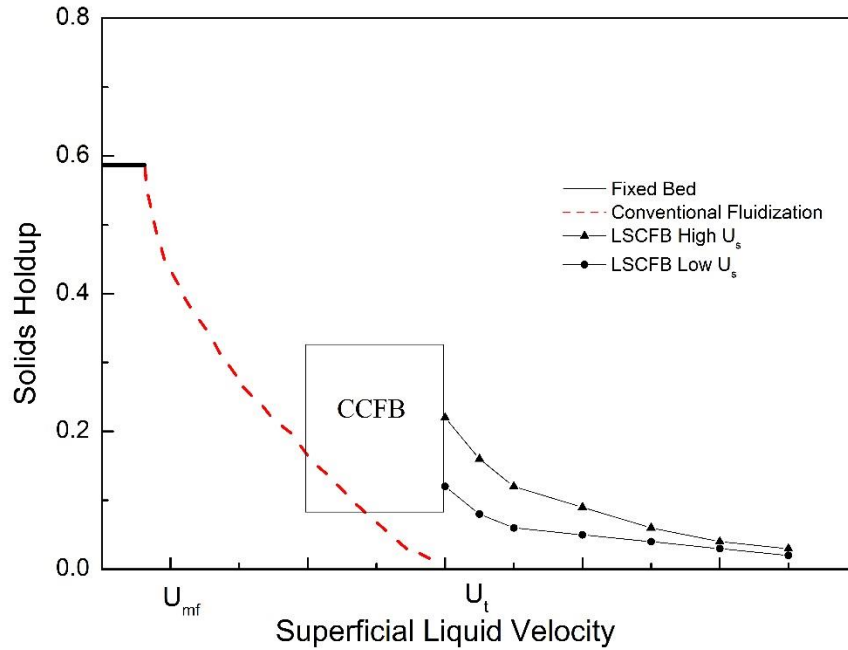


Figure 5.3.2 Solids holdup vs superficial liquid velocity at different flow regimes

For a liquid velocity, there is a corresponding solids holdup to balance drag and net gravity forces exerted on the particles. If extra solids are fed to an existing suspension, a transient higher solids holdup condition is created, thus actual liquid velocity around particles increase, which lead to a higher drag force than net gravity. The higher solids holdup condition cannot be maintained, as the forces are no longer balanced making solids to be further suspended giving more room to liquid, thus drag force is reduced adapting net gravity. Eventually, some solids are transported to a higher position due to the extra particles feed while maintain constant liquid velocity. The motion of particle transportation is determined by solids compression, whereas slip velocity in LSCFB.

Average solids holdup is the most important parameter, which reflects the amount of solids contacting with liquid in the fluidized bed. It plays an important role determine the overall pressure drop, mass and heat transfer, reactor performance of a fluidized bed unit. The average solids holdup in the downer is measured by the top and bottom two manometers in the downer. Fig. 3 shows the relationship between average solids holdup and solids circulation rate at constant liquid velocities. Solids holdup is increasing with solids circulation rate, since more solids is fed in the downer. In other words, the fluidized bed is compressed with solids feed, creating a denser suspension. It is interesting to see that the average solids holdup can be significantly increased by 50-200% with solids circulation. An obvious increase can be observed even with solids circulation rate as low as 0.1 cm/s. In addition, solids holdup is increasing with decreasing liquid velocity. This can be easily explained that higher liquid velocity would generate higher voidage allowing liquid to flow through.

5.3.1 Axial Solids holdup distribution

The performance of a fluidized bed unit is directly associated with solids holdup, which is an indication of solid and liquid contact intensity and efficiency. In physical process, such as particle classification, separation performance is closely associated with axial density distribution, so as axial solids holdup distribution. Knowing solids holdup distribution is crucial in designing a fluidized bed reactor, as the same average solids holdup but different axial solids holdup distribution may result in different performance.

Axial solids holdup distribution of CCFB at constant liquid velocities and varying solids circulation rate are presented in Figure 5.3.3 with two types of low density particles. Under similar operating conditions, EPS303 has less solids holdup than EPS122. Because EPS303 has less particle terminal velocity, that requires less energy to fluidize. And with increasing U_s axial solids holdup become more uniform for both types of particles. More operating conditions were examined with EPS122 as shown in Figure 5.3.4. Axial solids holdup is not uniform when no particle is circulating. It can be found that a dense region exists near the distributor, due to undeveloped liquid flow at the inlet region. The dense region is affecting the onwards solids, thus a solids holdup gradient is observed from the distributor to the exist. Solids holdup distribution

becomes more uniform with the help of solids circulation. It is almost uniform through the downer at highest operating solids circulation rate for each corresponding velocity. A raise of solids holdup at all heights were observed with increasing solids circulation rate. Due to the redundant solids near the distributor, the undeveloped region will have high solids holdup. With increasing solids circulation rate, the redundancy condition is severed due to constant liquid velocity. Therefore, the undeveloped region extended to onward position which leads to an increase of solids holdup at successive height.

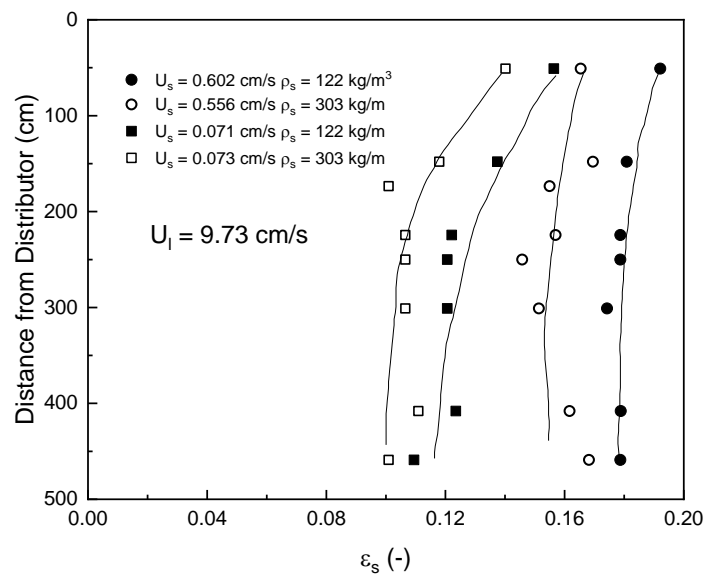


Figure 5.3.3 Axial solids holdup distribution in inverse CCFB of two types of low density particles.

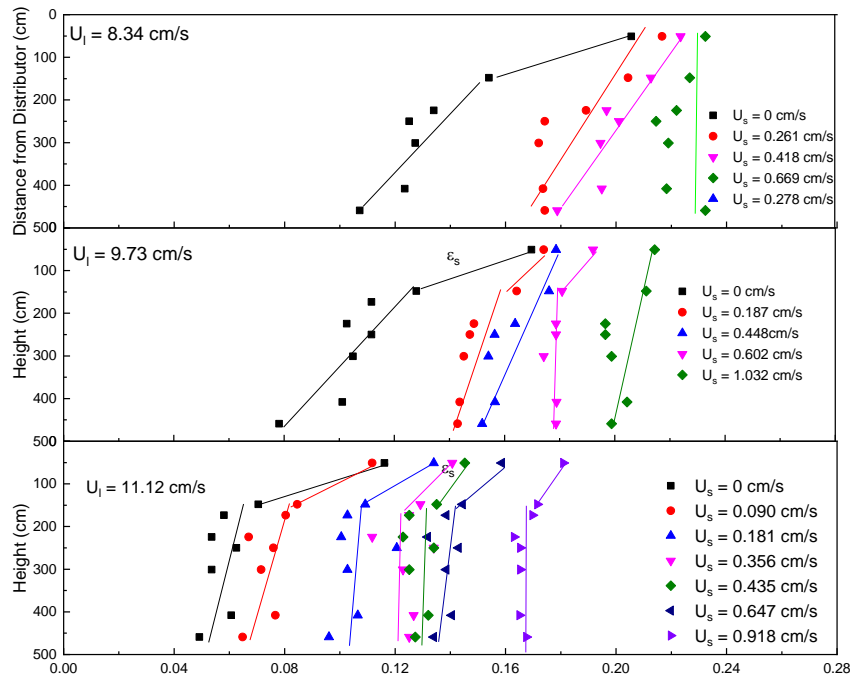


Figure 5.3.4 Axial distribution of solids holdup, $\rho = 122 \text{ kg/m}^3$

5.3.2 Apparent slip velocity

Apparent slip velocity can be used to estimate contact efficiency between solids and liquid qualitatively. As shown in Figure 5.3.5 and Figure 5.3.6, apparent slip velocity is decreasing with the addition of solid circulation rate. The apparent slip velocity is calculated by $U_{slip} = \frac{U_L}{\epsilon_L} - \frac{U_s}{\epsilon_s}$. LSCFB is believed to have high contact efficiency, since high slip velocity is achieved with high velocity liquid passing by the solids. At steady state, for each individual particle, the slip velocity should equal particle terminal velocity. In CCFB, the slip velocity might be different from LSCFB. In conventional fluidization, a balance is formed between drag force and net gravity. When extra solids are fed to the suspension, the balance is broken since a portion of the space for liquid flow is occupied by solids, thus generating higher transient liquid velocity, which is believed to lead to a higher slip velocity. However, the apparent slip velocity is found to be decreasing with increasing solids circulating rate, and significant lower than particle terminal velocity. The

transient liquid velocity around the particles cannot surpass particle terminal velocity, therefore the slip velocity is always below particle terminal velocity. Based on the force balance of particles, particles should be in deceleration due to the shortage of slip velocity, thus a dense region occurred.

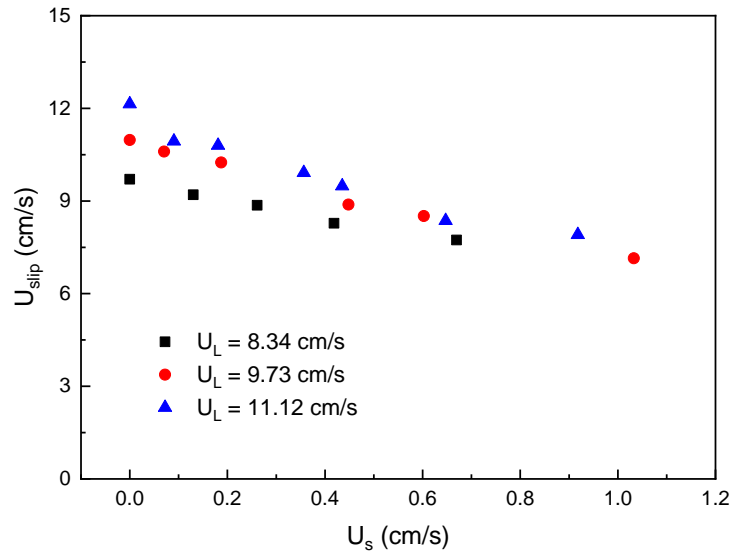


Figure 5.3.5 The change of slip velocity with U_s of EPS122

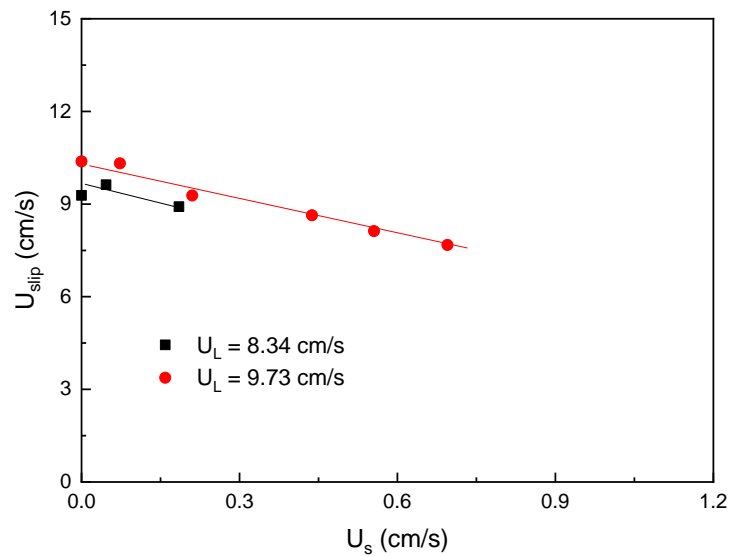


Figure 5.3.6 The change of slip velocity with U_s of EPS122

Since solids circulation rate is constant, solids holdup has to increase to serve the purpose for lowering particle velocity, as a result of solids feed. Which is also the reason behind higher solids holdup in CCFB comparing to conventional liquid fluidization and LSCFB. Starting from the distributor region, where particles are fed, and the deceleration initiate. The dense suspension will generate further increase of solids holdup on its path to reach steady state gradually with increasing bed height. In other words, particles are pushed by the extra feed of particles through the downer, and it remains at unsteady state spatially. Which can explain the low slip velocity profile in downer as presented in Figure 5.3.5 and Figure 5.3.6 in CCFB comparing to conventional fluidization and LSCFB. It is also an indication of good mixing as solids are in unsteady state, random movement might enhance the contact between solids and liquid.

Although there is net flux of particle not all solids are moving in one direction. Solid retention time in the downer is much longer than the liquid retention time. Solids retention time is around 5 to 20 minutes, and it is taking a long path for particles to travel through the fluidized bed and leave the system, which provide a good mixing between solid and liquid.

5.3.3 Bed Intensification factor

Experiments have found out that the addition of solids circulation can cause the increase of solids holdup comparing with conventional fluidization. As a result, the amount of solids been contained in the fluidized is increased at the same superficial liquid velocity, which is believed to intensify the performance of the fluidized bed. Thus, the Bed Intensified Factor is proposed to describe the increase of solids holdup. And the Bed Intensified Factor is defined as the ratio of the operating solids holdup with solids circulation over the solids holdup at conventional fluidization under a constant superficial liquid velocity. Conventional fluidization is used as a bench mark as its Bed Intensified Factor = 1.

The results have shown that Bed Intensification Factor is increasing with U_s . And for each type of particle, the change of Bed Intensification Factor is independent of U_l . So solids circulation rate will bring the same degree of deviation from conventional fluidization for different superficial liquid velocity. In addition, the effects of U_s on Bed Intensification Factor differs between types of particles. EPS303 has shown to be more sensitive to the addition of U_s as Bed Intensification Factor

increased sharply with U_s comparing with the trend observed from EPS122. The difference between particles can be explained by difference in particle terminal velocities. EPS303 has smaller particle terminal velocity. The fluidized bed can be viewed as a compressible fluid with liquid-solid mixture (Foscolo and Gibilaro 1984; Gibilaro 2001). EPS122 has higher particle terminal velocity and inertia, which makes the ‘compressible fluid’ more rigid. On the contrary, EPS303 with less inertia will make the fluidized bed easier to be compressed. The fluidized bed would have more ability to contain more solids under the same solid circulation rate with EPS303 than EPS122.

Bed Intensification Factor also shows the deviation from conventional fluidized caused by solids circulation. Circulating Conventional Fluidized Bed share the same superficial liquid velocity as Conventional Fluidized bed. And the addition of solids circulation changes the axial hydrodynamics and average solids holdup as shown in Figure 5.3.7 and previous shown in Figure 5.3.4.

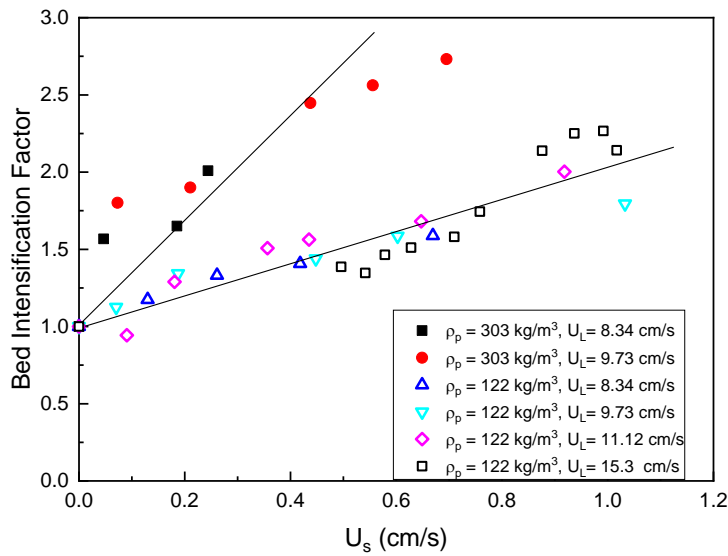


Figure 5.3.7 The change of Bed Intensification Factor with U_s

5.3.4 The connection between conventional fluidization and circulating fluidization - CCFB

The change of average solids holdup with superficial liquid velocity is plotted in full range of operating conditions, and EPS122 is chosen as a typical particle. In conventional fluidization, solids holdup is decreasing sharply with U_1 until U_t when solids holdup reaches zero. And CCFB find its place above conventional fluidization, since solids holdup is increased under each U_1 by adding U_s . And each point from region CCFB in Figure 5.3.8 have different U_s . Further increasing U_1 , it is in LSCFB regime, where a gradual decreasing trend of solids holdup with U_1 is found. And apparently solids circulation will also enhance solids holdup in the circulating fluidized bed dictated by the several lines when U_1 is greater than U_t . By connecting data points in similar U_s , the trend of CCFB and LSCFB joins together, which suggests that CCFB can be viewed as an extension of liquid-solid circulating fluidized by operating at low U_1 in the conventional fluidization region. The change of solids holdup with U_s under different U_1 is also studied in Figure 5.3.9. The relationship between solids holdup and superficial liquid velocity is consistent whether the superficial liquid velocity is beyond or below particle terminal velocity. Solids holdup is increasing with U_s in similar rate under all U_1 conditions. Thus, it also suggests the continuity of CCFB and LSCFB. One noteworthy difference other than the operating U_1 between CCFB and LSCFB is that the solids circulation could start when $\varepsilon_s = 0$ in LSCFB, while a certain solids volume fraction has to be reached to initiate solids circulation in CCFB.

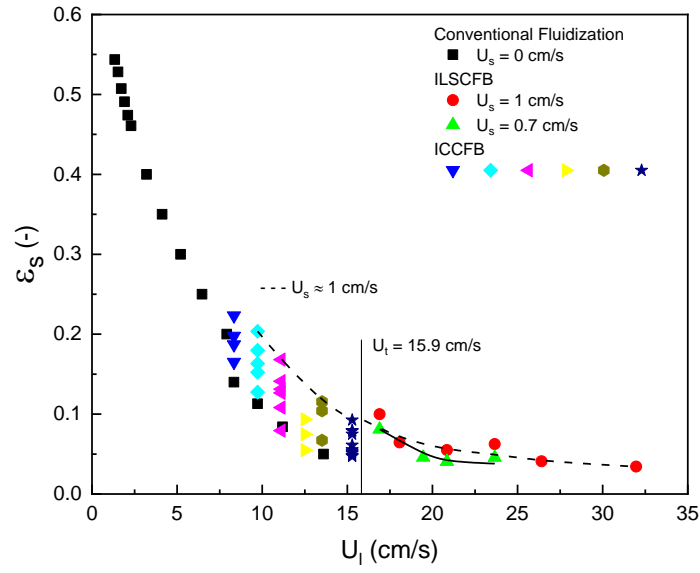


Figure 5.3.8 The change of average solids holdup with U_l in inverse conventional fluidized bed, CCFB and LSCFB

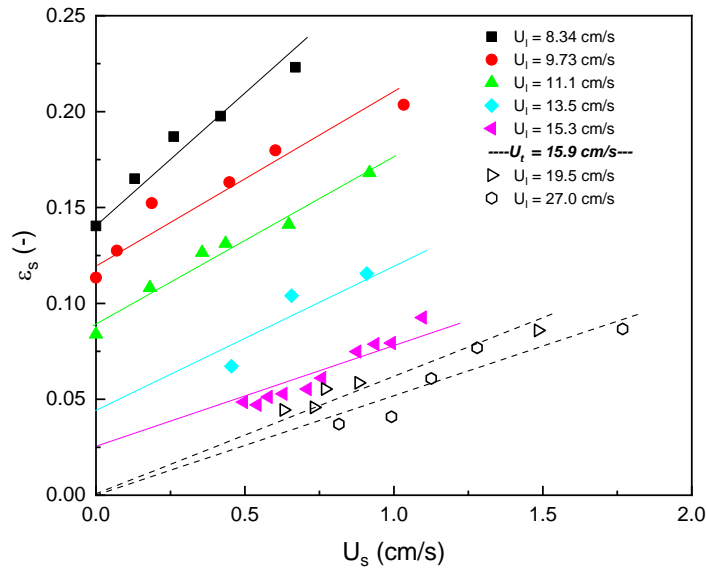


Figure 5.3.9 The change of average solids holdup with U_s in inverse CCFB and LSCFB

In comparison, many similarities and difference can be found between difference modes of liquid fluidization. CCFB is operating between conventional and circulating fluidization regimes. The superficial velocity is below the operating velocity in circulating regimes. However, solids circulation rate inherited from circulating fluidization is been applied in CCFB. Comparing to conventional fluidization, CCFB can achieve higher solids holdup, and the axial solids holdup is more uniform. The addition of solids circulation allows conventional fluidization to be operated with continuous solids flow. The many applications of liquid-solid circulating fluidized bed are no long limited to be operated at high superficial liquid velocity. CCFB shares the same uniform axial solids holdup distribution with circulating fluidized bed, but with higher solids concentration. Therefore, liquid-solid contact is enhanced due to high solid to liquid volume ratio. However, due to the natural of CCFB, solids circulation rate is limited to a small range comparing to high velocity LSCFB.

The energy consumption of CCFB is yet to be studied. Although is it operating at a relatively low velocity, additional flow in the upcomer is necessary to be included in the analysis as it is still required to provide the pressure for solids circulation which should be taken into consideration in further evaluation.

5.3.5 Solids circulation rate (U_s)

The main difference between CCFB and conventional fluidization is the existence of solids circulation. As discussed above, solids circulation rate plays an important role determine solids holdup in the downer. And solids circulation rate is controlled by the pressure difference between the upcomer and downer near the main flow distributor (Zheng and Zhu 2000; H. Zhu and Zhu 2008; Wee and Lim 2007). The top section of the upcomer where low density particles floating and packed at the top surface of the upcomer distributor, which can be considered as a packed bed. Additional flow to the top packed bed will generate pressure towards the top. The pressure is determined by the flowrate and the inventory of solids. The higher the flowrate to the upcomer the higher pressure is generated which will provide higher solids circulation rate. Although the two light particles used in this study have close particle terminal velocities, the difference of density shows a significant effect on solids circulation rate control. Particles with larger density difference

from water could generate higher pressure at the same liquid velocity based on Ergun equation, which result in higher solid circulation rate. This explains the achievable high solids circulation rate with light particles ($\rho = 122 \text{ kg/m}^3$) comparing to heavier particles ($\rho = 303 \text{ kg/m}^3$). In addition, auxiliary flow also plays an important role affecting solid circulation. It works as a non-mechanical valve controlling the pressure drop between the upcomer and the downer.

Due to size and density distribution of solids, a distribution of particle terminal velocity exists. In CCFB, liquid velocity is operated close to particle terminal velocity, which is predicted knowing average particle diameter and density and validated in circulating regime. However, some particles' terminal velocities are very likely to fall above operating liquid velocity. And these particles have less chance to be carried to the upcomer, comparing to small terminal velocity particles which have a higher tendency to be washed away. If the system is operated for a long time, segregation could appear by accumulating large and light particles in the downer who have high particle terminal velocity. Segregation is not observed with 120 kg/m^3 particles, because the particle terminal velocity is not sensitive to size or density distribution considering its large density difference with water. Whereas, for 300 kg/m^3 particles, measurements have to be taken after circulating all particles at high velocity to avoid accumulation of high terminal velocity particles. A narrow size and density distribution of particles is preferred when designing a CCFB.

Although there is net flux of particles, not all solids are moving in one direction. Solid retention time in the downer is much longer than the liquid retention time. Solids retention time is around 5 to 20 minutes, and it is taking a long path for particles to travel through the fluidized bed and leave the system, which provide a good mixing between solid and liquid.

5.3.6 Richardson-Zaki equation in CCFB

Richard-Zaki equation is commonly used to predict voidage or solids holdup for particulate fluidization (Richardson and Zaki 1954). It has been justified to be applicable with low density particles in inverse liquid fluidization (D. G. Karamanev and Nikolov 1992), with modification of estimating particle terminal velocity, as light particle free rising trajectory is different from heaving particle direct free-falling behavior (Dimitar G. Karamanev and Nikolov 1992). Richard-Zaki equation to predict voidage is originated from hindered setting (KHAN and RICHARDSON 1989a), as denser suspension settled slower than dilute suspension as a result of the effects of

solids holdup on slip velocity. In an effort to use Richard-Zaki to predict solids holdup in CCFB, solids circulation rate has to be involved as shown by Equation 5.3-1. Solids holdup can be estimated knowing the relationship between slip velocity and voidage. Exponent n can be found from semi-empirical correlations or bed expansion experiment. Figure 5.3.10 shows the relationship between U_{slip}/U_t and ϵ_l of EPS303 and EPS 122 in the inverse conventional circulating fluidized bed. The linear relationship between $\ln(U_{slip}/U_t)$ and $\ln(\epsilon_l)$ have been found, which validate the application of Richardson-Zaki equation.

$$\frac{U_L}{(1 - \epsilon_s)} - \frac{U_s}{\epsilon_s} = U_t(1 - \epsilon_s)^{n-1} \quad \text{Equation 5.3-1}$$

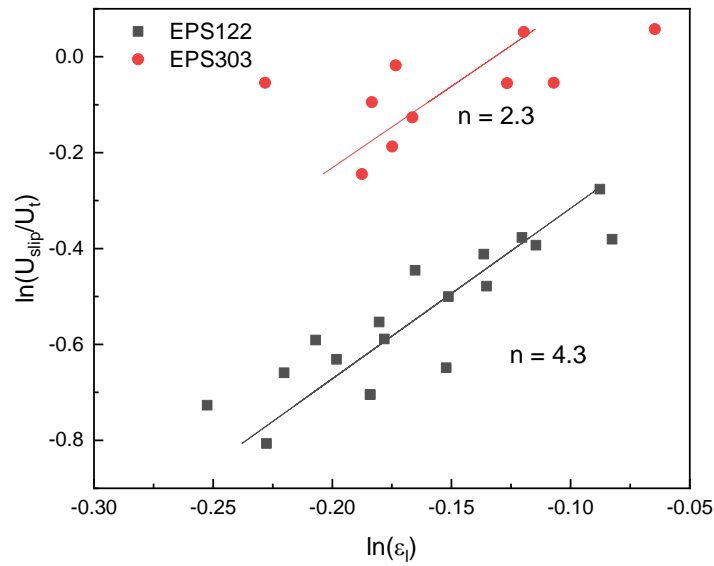


Figure 5.3.10 Relationship between $\ln(U_{slip}/U_t)$ with $\ln(\epsilon_l)$ in inverse CCFB

By comparing conventional fluidization and circulating conventional fluidization, it is worth noticing that circulating conventional fluidization has a significant higher exponent n in Richardson-Zaki equation. Exponent n of EPS122 has increased from 3.1 to 4.3, and for EPS303 it has increased from 2.0 to 2.3. Exponent n is an indication of particle-particle interaction as can be solved under Stoke's Law with some assumptions as first proposed by Richardson and Zaki (Richardson and Zaki 1954). If particles are aligned in hexagon style, lowest $n \approx 2.4$ can be

reached. And if particles are stacked in a plane, highest $n \approx 4.8$ is reached.(Richardson and Zaki 1954)(KHAN and RICHARDSON 1989b) Therefore, in CCFB, the same type of particle has a higher exponent n compared to conventional fluidization demonstrates particles are stacked in a more closed fashion in CCFB, which also explains the enhanced solids holdup in CCFB. It is believed that particle-particle interaction is intensified in CCFB.

5.4 Conclusion and recommendation

The concept of conventional circulating fluidized bed is proposed, by combining the characteristics of LSCFB and conventional liquid fluidization. The hydrodynamics of CCFB is investigated, with respect to solid holdup at different operating conditions, with two types of particles. The effect of particle density, superficial liquid velocity, and solids circulation rate is experimentally studied. Solids holdup is found to be increasing with solids circulation rate and decreasing with superficial liquid velocity. And particles with higher density will have less solids holdup due to its less particle terminal velocity, when the effects of particle diameter is negligible. The axial solids holdup distribution is studied under a wide range of solids circulation rates. And it has found that solids holdup axial distribution is becoming more uniform with increasing solids circulation rate. The apparent slip velocity is also studied and is found to be decreasing with solids circulation rate.

In comparison with conventional liquid-solid fluidization, CCFB can reach higher solids holdup at the same superficial liquid velocity. Bed Intensification Factor is defined to quantify the effects of U_s on the increased solids holdup from conventional fluidization. And particle-particle interaction is found to be increased in CCFB due to the enhanced exponent n in Richardson-Zaki equation.

In the future, particles in different sizes and densities are waited to be investigated in conventional circulating regime. Furthermore, the micro structure of particle movement could be further examined. And the dynamic behavior of particle movement caused by forcing solids flow under moderate liquid flow should be studied.

Nomenclature

Ar	Archimedes number defined by $d_p^3 g (\rho_p - \rho_l) \rho_l / \mu_l^2$
C_D	Particle drag coefficient
d_p	Particle diameter (mm)
D	Column diameter (m)
F_b, F_d, F_g	Buoyancy, drag force and gravity
G_s	Solids circulation rate (kg/ (m ² s))
g	Gravity acceleration
Re	Reynolds number defined by $U_l d_p \rho_l / \mu_l$
Re_t	Particle terminal Reynolds number defined by $U_t d_p \rho_l / \mu_l$
U_a	Auxiliary liquid velocity (cm/s)
U_l	Superficial liquid velocity (cm/s)
U_s	Superficial solids velocity (cm/s)
U_{slip}	Slip velocity (cm/s)
U_t	Particle terminal velocity (cm/s)
U_{tr}	Transition velocity demarcate the conventional particulate regime and circulating fluidization regime (cm/s)
V_l, V_p	Local liquid velocity and local particle velocity (cm/s)
\bar{V}_p	Average particle velocity (cm/s)

Greek letters

$\bar{\varepsilon}$	Average bed voidage
$\bar{\varepsilon}_s$	Average solids holdup
μ_l	Liquid viscosity (mPa·s)
ρ_p	Particle density (kg/m ³)

Subscripts

l	Liquid
p	Particle
s	Solids
b	Bubble
g	gas

Abbreviation

LSCFB	Liquid-Solid Circulating Fluidized Bed
ILSCFB	Inverse Liquid-Solid Circulaing fluidized Bed
IGLSCFB	Inverse Gas-Liquid-Solid Circulaing fluidized Bed
CCFB	Conventional Circulating Fluidized Bed

Reference

- Cheng, Yi, and Jesse Zhu. 2008. "Hydrodynamics and Scale-up of Liquid–Solid Circulating Fluidized Beds: Similitude Method vs. CFD." *Chemical Engineering Science* 63 (12): 3201–11. <https://doi.org/10.1016/J.CES.2008.03.036>.
- Eldyasti, Ahmed, Nabin Chowdhury, George Nakhla, and Jesse Zhu. 2010. "Biological Nutrient Removal from Leachate Using a Pilot Liquid–Solid Circulating Fluidized Bed Bioreactor (LSCFB)." *Journal of Hazardous Materials* 181 (1–3): 289–97. <https://doi.org/10.1016/J.JHAZMAT.2010.05.010>.
- Epstein, Norman. 2002. "Applications of Liquid-Solid Fluidization." *International Journal of Chemical Reactor Engineering* 1 (1). <https://doi.org/10.2202/1542-6580.1010>.
- Fan, Liang-Shih, Katsuhiko Muroyama, and Song-Hsing Chern. 1982. "Hydrodynamics Characteristics of Inverse Fluidization in Liquid—Solid and Gas—Liquid—Solid Systems." *The Chemical Engineering Journal* 24 (2): 143–50.
- Foscolo, P.U., and L.G. Gibilaro. 1984. "A Fully Predictive Criterion for the Transition between Particulate and Aggregate Fluidization." *Chemical Engineering Science* 39 (12): 1667–75. [https://doi.org/10.1016/0009-2509\(84\)80100-1](https://doi.org/10.1016/0009-2509(84)80100-1).
- Gibilaro, L. G. 2001. *Fluidization-Dynamics : The Formulation and Applications of a Predictive Theory for the Fluidized State*. Butterworth-Heinemann.
- Haider, A., and O. Levenspiel. 1989. "Drag Coefficient and Terminal Velocity of Spherical and Nonspherical Particles." *Powder Technology* 58 (1): 63–70. [https://doi.org/10.1016/0032-5910\(89\)80008-7](https://doi.org/10.1016/0032-5910(89)80008-7).
- Karamanev, D. G., and L. N. Nikolov. 1992. "Bed Expansion of Liquid-Solid Inverse Fluidization." *AIChE Journal* 38 (12): 1916–22. <https://doi.org/10.1002/aic.690381208>.
- Karamanev, Dimitar G., and Ludmil N. Nikolov. 1992. "Free Rising Spheres Do Not Obey Newton's Law for Free Settling." *AIChE Journal* 38 (11): 1843–46. <https://doi.org/10.1002/aic.690381116>.

KHAN, A.R., and J.F. RICHARDSON. 1989a. "FLUID-PARTICLE INTERACTIONS AND FLOW CHARACTERISTICS OF FLUIDIZED BEDS AND SETTLING SUSPENSIONS OF SPHERICAL PARTICLES." *Chemical Engineering Communications* 78 (1): 111–30. <https://doi.org/10.1080/00986448908940189>.

Kopko, Ronald J, Paul Barton, and Robert H McCormick. n.d. "Hydrodynamics of Vertical Liquid-Solids Transport." Accessed March 28, 2018. <https://pubs.acs.org/doi/pdf/10.1021/i260055a012>.

Lan, Qingdao, Jing-Xu Jesse Zhu, Amarjeet S. Bassi, Argyrios Margaritis, Ying Zheng, and Gerald E. Rowe. 2000. "Continuous Protein Recovery Using a Liquid-Solid Circulating Fluidized Bed Ion Exchange System: Modelling and Experimental Studies." *The Canadian Journal of Chemical Engineering* 78 (5): 858–66. <https://doi.org/10.1002/cjce.5450780502>.

Liang, W.-G., J.-X. Zhu, Y. Jin, Z.-Q. Yu, Z.-W. Wang, and J. Zhou. 1996. "Radial Nonuniformity of Flow Structure in a Liquid-Solid Circulating Fluidized Bed." *Chemical Engineering Science* 51 (10): 2001–10. [https://doi.org/10.1016/0009-2509\(96\)00057-7](https://doi.org/10.1016/0009-2509(96)00057-7).

Nelson, Michael J., George Nakhla, and Jesse Zhu. 2017. "Fluidized-Bed Bioreactor Applications for Biological Wastewater Treatment: A Review of Research and Developments." *Engineering* 3 (3): 330–42. <https://doi.org/10.1016/J.ENG.2017.03.021>.

Razzak, S.A., S. Barghi, and J.-X. Zhu. 2009. "Application of Electrical Resistance Tomography on Liquid–Solid Two-Phase Flow Characterization in an LSCFB Riser." *Chemical Engineering Science* 64 (12): 2851–58. <https://doi.org/10.1016/J.CES.2009.02.049>.

Renganathan, T, and K Krishnaiah. 2005. "Voidage Characteristics and Prediction of Bed Expansion in Liquid–Solid Inverse Fluidized Bed." *Chemical Engineering Science* 60 (10): 2545–55.

Renganathan, Thiruvengadam, and Kamatam Krishnaiah. 2008. "Prediction of Minimum Fluidization Velocity in Two and Three Phase Inverse Fluidized Beds." *The Canadian Journal of Chemical Engineering* 81 (3–4): 853–60. <https://doi.org/10.1002/cjce.5450810369>.

Richardson, J.F., and W.N. Zaki. 1954. "The Sedimentation of a Suspension of Uniform Spheres under Conditions of Viscous Flow." *Chemical Engineering Science* 3 (2): 65–73.

[https://doi.org/10.1016/0009-2509\(54\)85015-9](https://doi.org/10.1016/0009-2509(54)85015-9).

Sang, Long. 2013. "Particle Fluidization in Upward and Inverse Liquid-Solid Circulating Fluidized Bed." *The University of Western Ontario, London*.

Sang, Long, and Jesse Zhu. 2012. "Experimental Investigation of the Effects of Particle Properties on Solids Holdup in an LSCFB Riser." *Chemical Engineering Journal* 197 (July): 322–29. <https://doi.org/10.1016/J.CEJ.2012.05.048>.

Trivedi, Umang, Amarjeet Bassi, and Jing-Xu (Jesse) Zhu. 2006. "Continuous Enzymatic Polymerization of Phenol in a Liquid–Solid Circulating Fluidized Bed." *Powder Technology* 169 (2): 61–70. <https://doi.org/10.1016/J.POWTEC.2006.08.001>.

Ulaganathan, N., and K. Krishnaiah. 1996. "Hydrodynamics Characteristics of Two-Phase Inverse Fluidized Bed." *Bioprocess Engineering* 15 (3): 159–64. <https://doi.org/10.1007/s004490050250>.

Wee, Eldin, and Chuan Lim. 2007. "Voidage Waves in Hydraulic Conveying through Narrow Pipes." *Chemical Engineering Science* 62: 4529–43. <https://doi.org/10.1016/j.ces.2007.05.034>.

Zheng, Ying, Jing-xu Jesse Z H U, Jianzhang Wen, Steve A Martin, and S Amarjeet. 1999. "The Axial Hydrodynamics Behavior in a LiquidSolid - Circulating Fluidized Bed" 77. <https://doi.org/10.1002/cjce.5450770213>.

Zheng, Ying, and Jing-Xu (Jesse) Zhu. 2000. "Overall Pressure Balance and System Stability in a Liquid–Solid Circulating Fluidized Bed." *Chemical Engineering Journal* 79 (2): 145–53. [https://doi.org/10.1016/S1385-8947\(00\)00168-6](https://doi.org/10.1016/S1385-8947(00)00168-6).

Zheng, Ying, Jing-Xu Zhu, Narenderpal S Marwaha, and Amarjeet S Bassi. 2002. "Radial Solids Flow Structure in a Liquid–Solids Circulating Fluidized Bed." *Chemical Engineering Journal* 88 (1–3): 141–50.

Zhu, Haiyan, and Jesse Zhu. 2008. "Gas-Solids Flow Structures in a Novel Circulating-Turbulent Fluidized Bed." *AIChE Journal* 54 (5): 1213–23. <https://doi.org/10.1002/aic.11432>.

Zhu, Jing-Xu Jesse, Dimitre G Karamanev, Amarjeet S Bassi, and Ying Zheng. 2000. "(Gas-)

Liquid-solid Circulating Fluidized Beds and Their Potential Applications to Bioreactor Engineering.” *The Canadian Journal of Chemical Engineering* 78 (1): 82–94.

Chapter 6

6 Counter-Current flow in (I)-LSCFB systems

Abstract

The characteristics of counter-current flow of liquid and solids plays an important role in the design and operation of liquid-solid circulating fluidized beds. Hydrodynamics of counter-current flow of liquid and solids were experimentally studied with two configurations using low density and high density particles. High density particles were falling in upflow liquid under various superficial liquid velocity and solids flowrate, and solids holdup was found to be decreasing from the entrance to the exist of solids. However, solids holdup of low density particles were found to be uniform when particles were rising in downflow liquid. For both counter-current flow configurations, solids holdup is increasing with solids flowrate and superficial liquid velocity. This study of counter-current flow also fills the void of liquid-solid fluidization regimes which heavily focuses on the co-current fluidization regimes.

Key words: liquid-solid fluidization, solids holdup, circulating fluidized bed, fluidization regimes, counter-current flow

6.1 Introduction

In the last a few decades (Inverse) liquid-solid circulating fluidized beds have shown great potential in chemical, biochemical and pharmaceutical processes (Epstein 2002; Zhu et al. 2000; M. Patel et al. 2008; Lan et al. 2002; A. Patel, Zhu, and Nakhla 2006; Muroyama and Fan 1985; J. Wang et al. 2019) due to their advantages over conventional liquid-solid fluidization, such as:

- 1) High liquid throughput
- 2) High contact efficiency between liquid and solid
- 3) Continuous operation of solids

Some applications such as Ion-exchange process, biological wastewater treatment and phenol polymerization have already been demonstrated with liquid – solid circulating fluidized beds in

lab or pilot scale (Nelson, Nakhla, and Zhu 2017; Trivedi, Bassi, and Zhu 2006). The performance of LSCFB reactors are highly dependent on the hydrodynamics in the fluidized beds, such as superficial liquid velocity, solids circulation rates, solids holdup, particle velocity and fluidized bed geometry all play important roles in the design and operating (I)LSCFBs. Previous studies have studied the effects of operating conditions such as superficial liquid velocity and solids circulation rate on averages solids holdup and axial/radial solids holdup distribution (Razzak, Zhu, and Barghi 2009; Razzak, Barghi, and Zhu 2010; Zheng et al. 2002, 1999). In addition, the effects of particles properties have also been investigated (Sang and Zhu 2012). Especially solids with less density than liquid, have to be fluidized with downward liquid flow, so called inverse fluidization, and has drawn some attention due to its practicality as bioreactor (Nikov and Karamanev 1991; D. Wang et al. 2010; Renganathan and Krishnaiah 2008).

The circulating fluidized beds usually have two columns operating in synchrony. Particle transporting between two columns is demonstrated with LSCFB in **Figure 6.1.1**.

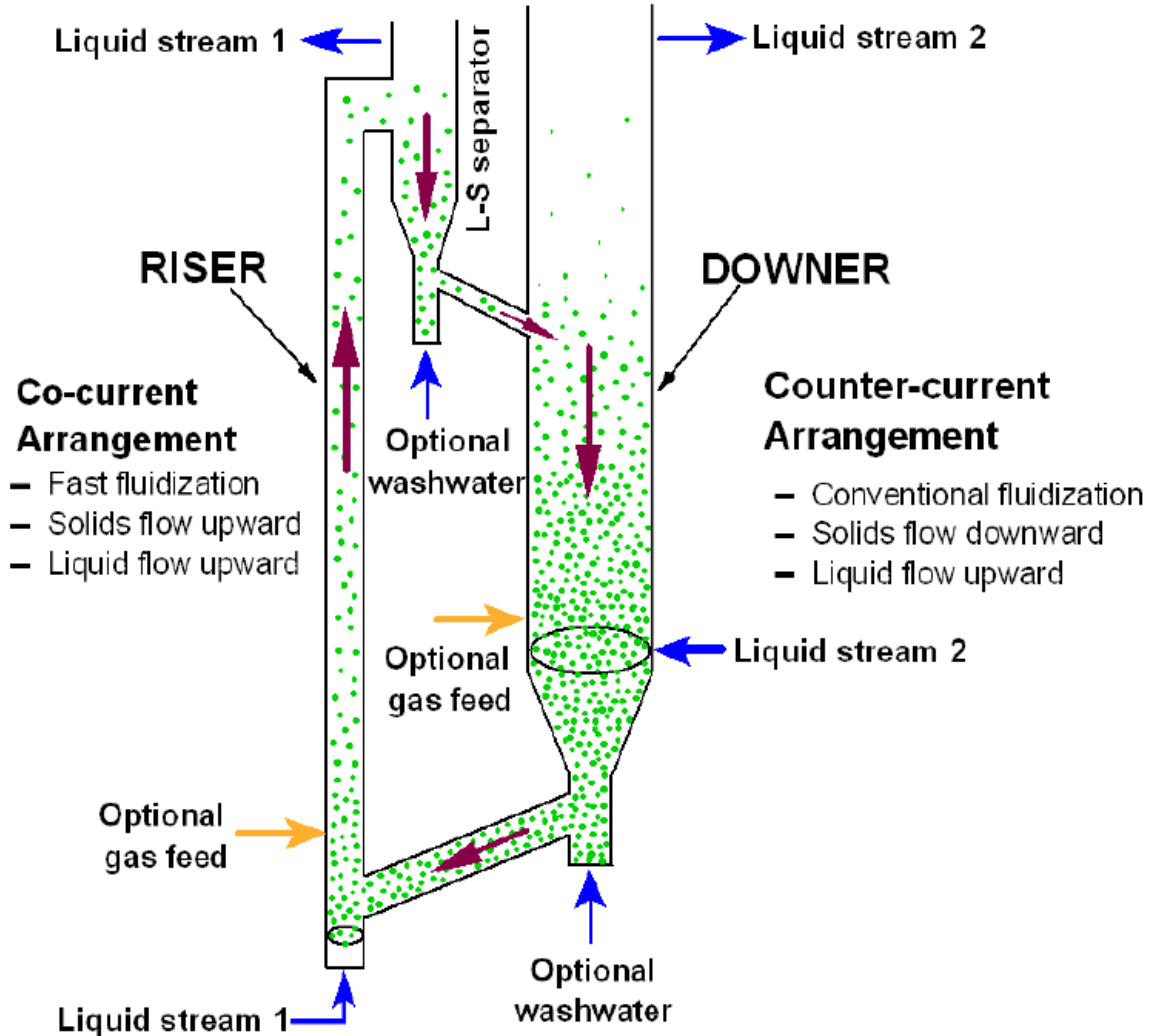


Figure 6.1.1 Schematic diagram of liquid-solid circulating fluidized bed

In one column, solids are under circulating regime where liquid velocity is beyond particle terminal velocity, the column is called riser in LSCFB and downer in (I)-LSCFB. The other column is storage column where the transported solids are stored and getting ready to be fed to the other circulating column. In a hydrodynamics perspective, the particles in storage column are often semi-fluidized with moderate liquid flow for better transporting to the other column. There are two sections in the storage column as shown in Figure 6.1.1. In the top section solids are falling down with moderate upflow liquid, and the bottom section is conventional fluidization with a net downflow of solids. In the storage column, solids and liquid are flowing counter-currently. In

conclusion, the circulation section, hindered falling section and conventional fluidization section composited the circulating fluidized bed systems.

Previous studies mainly focused on the hydrodynamics of riser in LSCFB and downer in ILSCFB, which are all circulating fluidization sections. However, the counter-current flow in the storage column is as crucial as the hydrodynamics in the circulation section, since reaction or regeneration of solids are taking place in the storage column.

In liquid-solid circulating fluidized bed bioreactor, the two columns work as a pair to optimize the reactor performance by controlling the biofilm thickness. There is an ideal biofilm thickness in fluidized bed bioreactor. The co-current column is operating with high superficial liquid velocity to provide enough shear to remove excess biomass from bio-particle.

In this study, the counter-current flow of solids has been studied experimentally with both heavy and low density particles to provide better understanding of (I)-LSCFB systems for further optimization and design.

6.2 Experiment setup

6.2.1 Operation of solids down, liquid up

The experiment is carried in a 5.4-meter tall column as shown in Figure 6.2.1. Solids are fed through a silo located at the top of the column. A short pipe is connected to the outlet of silo, and a circular plane is placed under the outlet pipe. The flowrate of solids is controlled by adjusting the distance between the plane and the pipe using the concept of angle of repose. Please see Figure 6.1.1 demonstrating the mechanism of solids flowrate control.

Angle of repose is the angle that the plane of contact between two bodies makes with the horizontal when the upper body is just on the point of sliding. The surface area of the solids in contact with the horizontal plane can be determined knowing the height of solids and angle of repose. Angle of repose is determined by the properties of solids and the horizontal plane. Thus, for a particular type of solids placed on a plane, its angle of repose is constant. Then, the contact surface area can be controlled. When the distance between of outlet pipe and circular plane is increased that the area of circular plane is less than the projected contact surface area solids begin to fall in to the

column. Further increase the distance, higher solids flowrate can be achieved due to a larger difference in area between the projected surface area and the surface plane. When solids are falling down in the column, a stream of liquid is flowing upwards, creating a counter-current flow condition. Studied particles is Plastic beads with 1457 kg/m^3 in density and 1.5 cm in diameter.

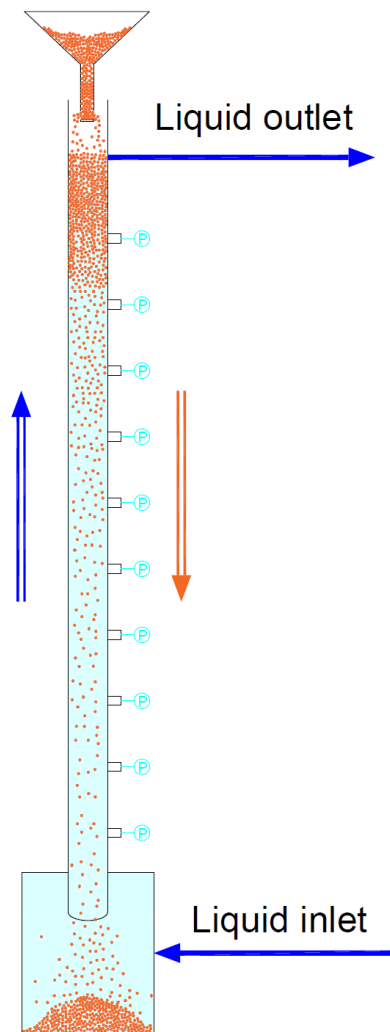


Figure 6.2.1 Schematic diagram of solids falling down in upflow liquid

6.2.2 Operation of solids up and liquid down

For the counter-current flow of low density particles rising in down flow liquid, the study was carried out in an inverse liquid-solid circulating fluidized bed as shown in Figure 6.2.2. The counter-current flow takes place bottom section in the upcomer which is 2.1 meter in height and 0.2 meter in diameter.

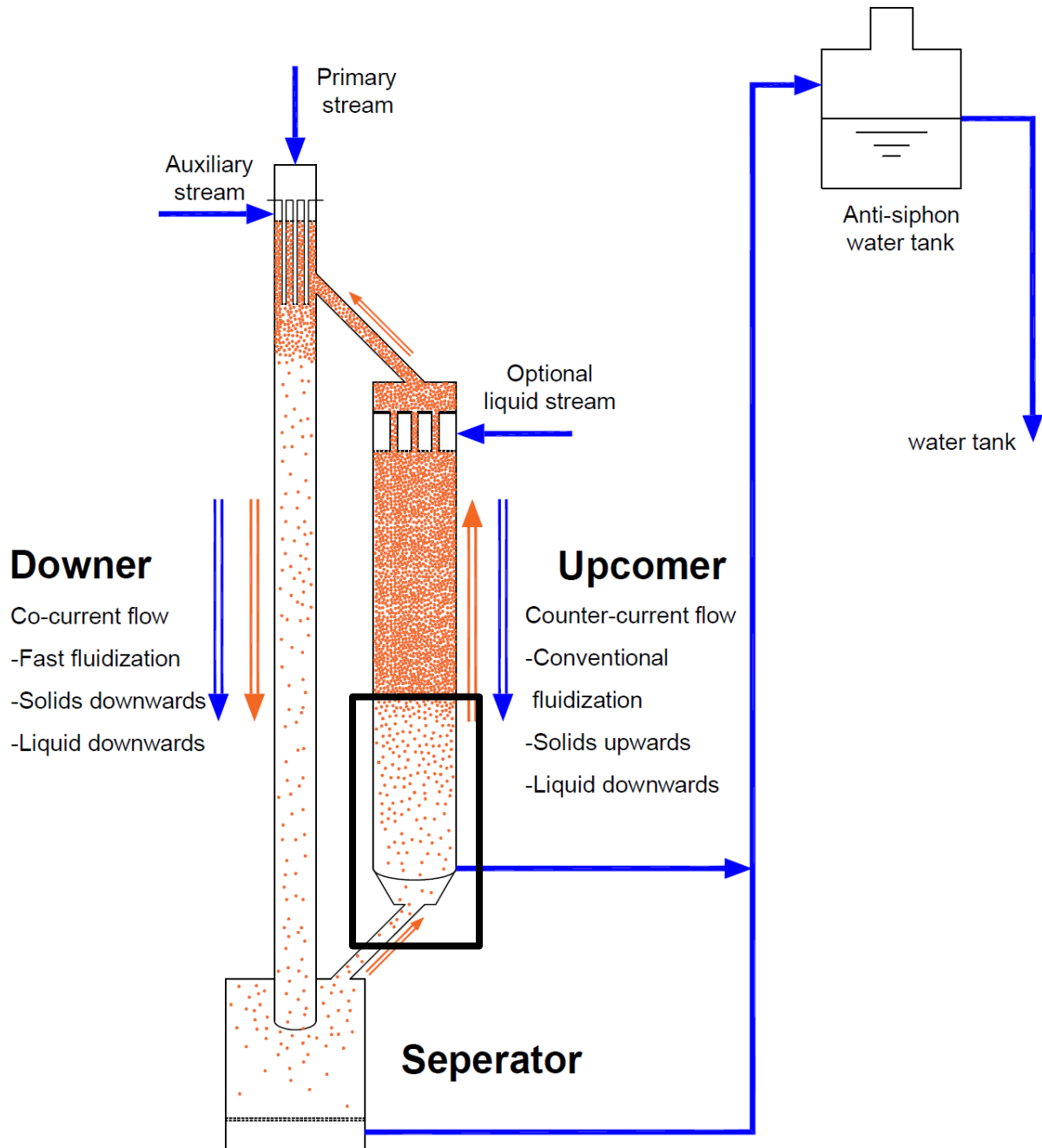


Figure 6.2.2 Schematic diagram of solids rising in downflow liquid in ILSCFB

Low density particles are transported by downward liquid flow to the bottom of the ILSCFB downer and start to rising in upcomer. A downward liquid flow is introduced from the top of the upcomer and left from the bottom of the upcomer. Upward solid flowrate in the upcomer is controlled by manipulating the pressure balance in the ILSCFB system with the help of auxiliary

flow at the top of the downer, main flow at the top of the downer, butterfly valve located in the connecting pipe between the top of the downer and upcomer and optional liquid flow in the upcomer.

The ILSCFB as a system, the downward flow of liquid in the upcomer will affect the solid circulation rate. But the bottom section of the upcomer can still be viewed as an independent unit where the hydrodynamics is solely controlled by the upward solid flow and downward liquid flow

6.3 Results and discussion

Axial solids holdup distribution in the downer with heavy particles are shown in Figure 6.3.2. The solids feed is at the top where a dense region can be seen. A sharp fall of solids holdup can be observed at the top region followed by a gradual decrease before it reaches steady concentration. This can be explained by the acceleration of solids once entering the downer. Heavy solids can be regarded have zero velocity at the top of the downer since the solids feed is very close to the surface of liquid. When solids got submerged in the water, they start to accelerate due to the net gravity. Thus, a slip velocity between liquid and solid is generated, which provide an upward drag force on the particle. Once the force balance between drag force and net gravity is reached by particle acceleration and expansion of solids mixture, a steady falling velocity is obtained.

Under the same superficial solid velocity, axial solids holdup is increasing with upward liquid velocity. Because solids falling velocity is hindered by the upward liquid flow, thus a denser solids environment is created. And the increase of superficial solid velocity will cause increase of solids holdup as well, since more solids will occupy more volume along the downer.

The exit of liquid is located at the top of the column as shown in Figure 6.2.1 where is close to the solids feed. And the exit is facing to the side, some turbulence and vortex caused by the exiting liquid flow will inhibit the solids to start falling at first place, which also contributes to the dense region at the top.

6.3.1 Force balance of particles falling

For a better understanding of axial solids holdup distribution in counter-current flow condition, a force balance is established as shown in Figure 6.3.1. Free falling particle is been used as an example.

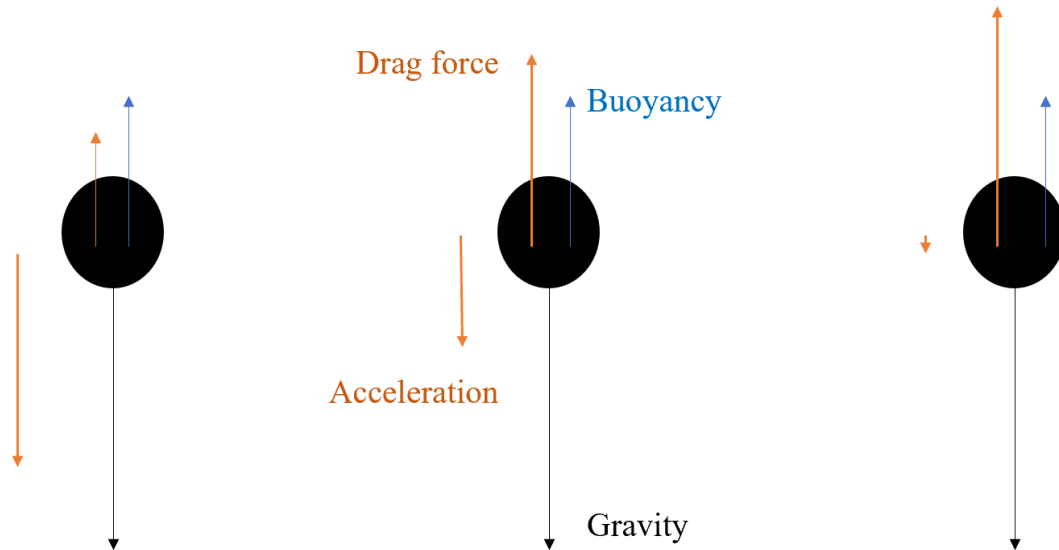


Figure 6.3.1 Force balance on heavy particles falling in upflow liquid

At steady state, net gravity of particle is countered by drag force provided by slip velocity (U_l/ϵ_l). Prior to reaching steady state, net gravity is greater than drag force due to insufficient slip velocity. And the acceleration rate is negatively related with the drag force provided by upflow liquid. The process of particles to reach steady state can be viewed as particles accelerating to achieve adequate slip velocity.

6.3.2 Effects of U_l

Effects of U_l on solids holdup axial distribution can be seen in Figure 6.3.2 under various solids superficial velocities. It is showing that a higher upward liquid velocity will lead to an increase of non-uniformity in solid holdup axial distribution. Under a constant superficial solid velocity, the sharpest change of axial solids holdup is found at highest upward liquid velocity. And U_l has more

impact on solids holdup near the feed than solids holdup in fully developed region. This is due to the hindered particle acceleration caused by upward liquid flow.

Increasing U_1 will cause the increase solids holdup at fully developed region, which can be explained by force balance as shown in Figure 6.3.1

At the top section of the column, prior to reaching a constant solids holdup, the increasing U_1 will intensified the turbulence effects on solids holdup starting from the solids feed. In addition, the increasing upward liquid velocity will provide more drag force on the particles, leading to a lessened acceleration as a result. All these above aspects contribute to the non-uniform axial profile in the counter-current flow of free-falling particles with increasing upward liquid flow U_1

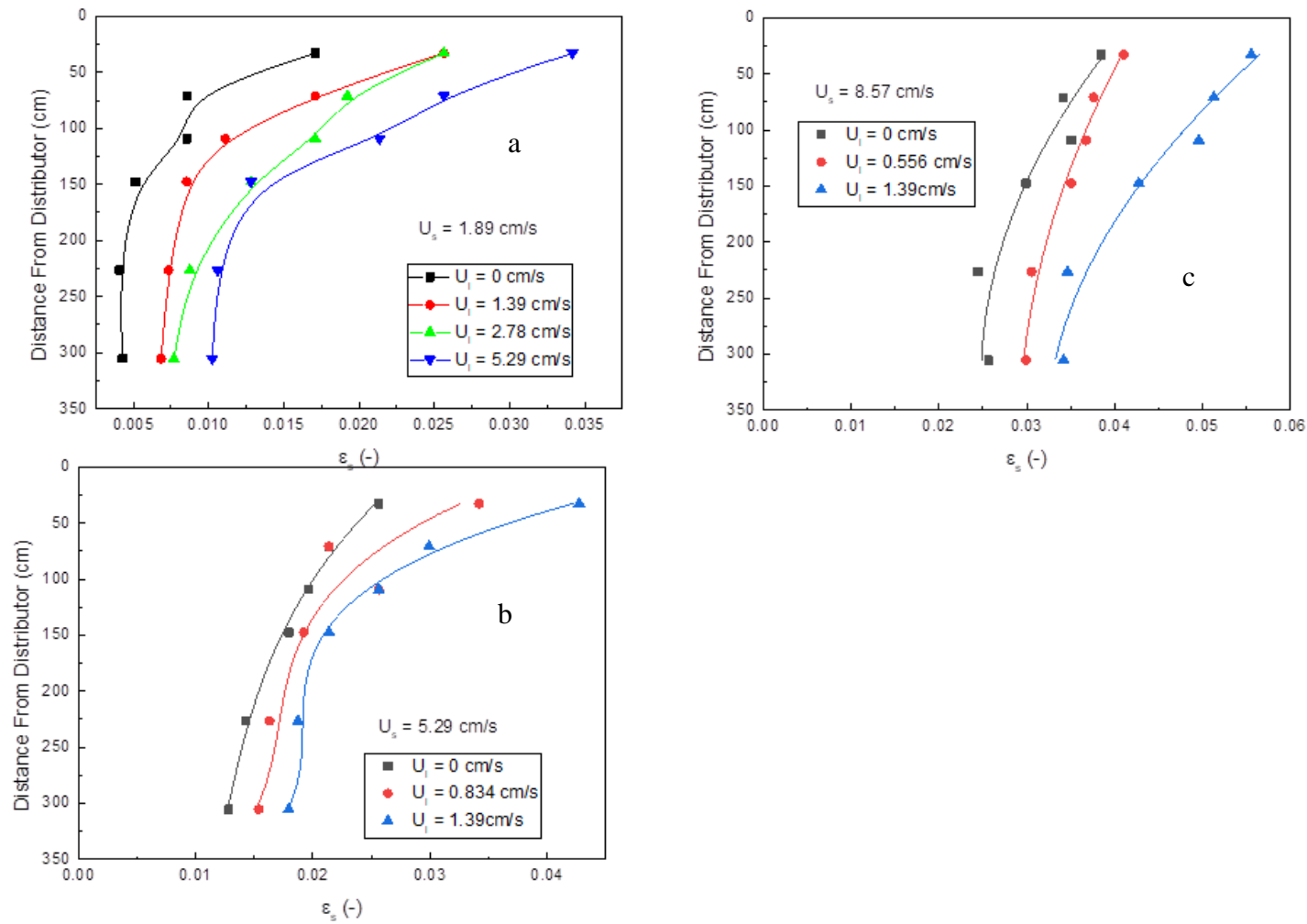


Figure 6.3.2 Axial solids holdup in counter-current flow of heavy solids at different upflow liquid and constant superficial solid velocity. (a), $U_s = 1.89$ cm/s, (b) $U_s = 5.29$ cm/s, (c) $U_s = 8.57$ cm/s

6.3.3 Effects of U_s

As shown in Figure 6.3.2, U_s has significant effect on axial solids holdup distribution. The steady-state solids holdup at fully developed region is a function of solids holdup.

Based on force balance of between particles and liquid, a steady-state solids holdup can be reached under a corresponding operating superficial liquid and solid velocities. The axial solids holdup distribution dictates the process of particle reaching steady state after being fed to the system. When particles entering the system, a dense region is created when solids are mixed with liquid. And the solids acceleration and particles expansion are happening at the same time due to the effect of net gravity. The slip velocity between liquid and particles is increasing along with particle acceleration before particles reach steady-state.

At high solids superficial solid velocity (solid feed rate), the observed dense region at the top is not that significant. And the change of average solids holdup with U_s and U_l is shown in Figure 6.3.3 and Figure 6.3.4.

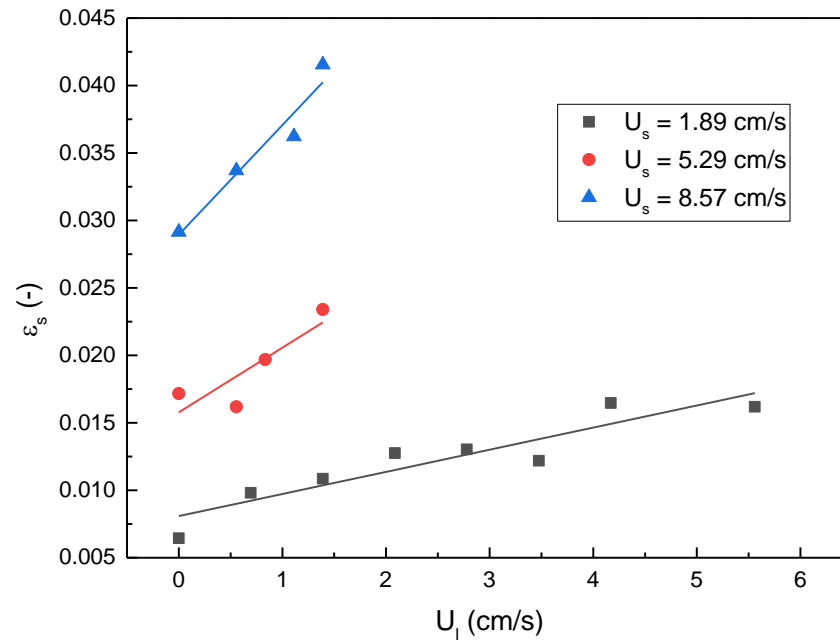


Figure 6.3.3 The change of average solids holdup with U_l at constant U_s of heavy particles

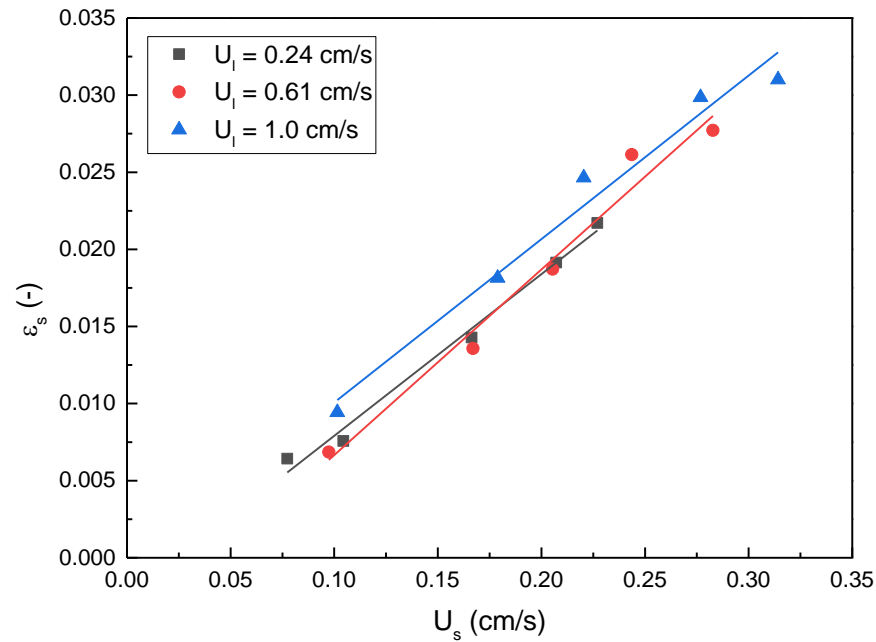


Figure 6.3.4 The change of average solids holdup with U_s at constant U_l of low density particles

6.4 Comparison between light and density particle

Axial solids holdup of rising low density particles is much more uniform than heavy particles falling in counter-current conditions as studied experimentally, shown in Figure 6.4.1. A few aspects contribute to this difference. Limited by the experiment setup, the counter-current flow of heavy particles was studied under a much higher operating U_s compared to low density particles that was studied in an inverse liquid-solid circulating fluidized bed. In the inverse liquid-solid circulating fluidized bed, the maximum U_s is dependent on many factors such as solids inventory, liquid velocities and system pressure balance, which make it difficult to reach high U_s in the large diameter storage column which the counter-current flow take place. In addition, the feed conditions were different in the studied systems. Heavy particles were fed through a hopper while low density particles were entering through a solids feed pipe as particle of I-LSCFB. Thus, low density particles were already accelerated before entering the counter-current region. Those limitations were the main reasons causing the difference of solids holdup axial distribution between the light and heavy density particles

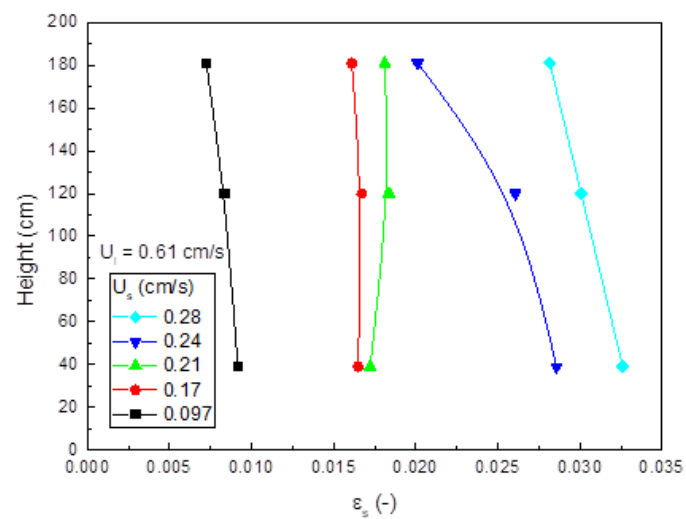
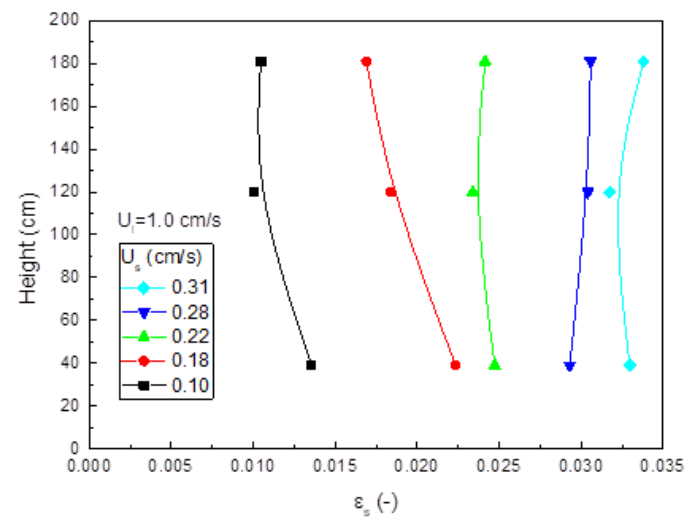
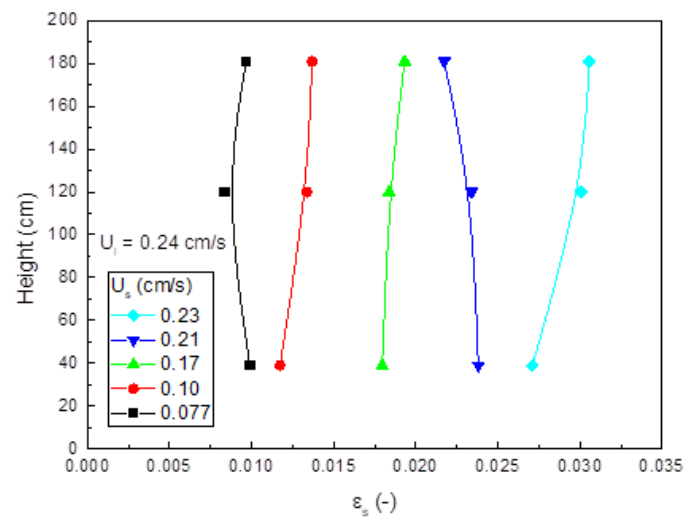


Figure 6.4.1 Axial solids holdup distribution of light particles rising

In conclusion, under similar counter liquid flow condition, the effect of solid flow is more significant affecting the solids holdup for both cases.

6.5 Conclusions and Recommendations

The hydrodynamics counter-current flow of heavy and low density particles is studied experimentally. Axial solids holdup distribution and average solids holdup were investigated and discussed based on force balance. Solids holdup distribution is not uniform due to the long acceleration path required.

The solids feeding device can be improved to increase the superficial solid flowrate to investigate the counter-current flow of solid and liquid in a wider operation window and test the limiting condition of both superficial liquid velocity and solid velocity. In addition, how the hydrodynamics of counter-current flow of solid can be compared and utilized in the commonly-used conventional liquid fluidization and liquid-solid circulating fluidization can be further studied.

The studied counter-current flow was only in dilute conditions where solids were fed into a system mainly consists of fluid. Another form of counter-current flow condition could occur in a dense condition. For example, heavy solids can be fed from the top to a conventional fluidized bed that are supported by an upward liquid, and solid should exit from the bottom of the conventional fluidized bed. Both dilute and dense counter-current flow of solids could exist due to the moderate liquid flow. In addition, the counter-current flow of low density particles mimics the flow behavior of bubbles in IGLSCFB (chapter 8) but without bubble breakage and coalesces. Which can be used to as a base case study the mechanism of bubble rising in downflow liquid.

Nomenclature

Ar	Archimedes number defined by $d_p^3 g (\rho_p - \rho_l) \rho_l / \mu_l^2$
C_D	Particle drag coefficient
d_p	Particle diameter (mm)
D	Column diameter (m)
F_b, F_d, F_g	Buoyancy, drag force and gravity
G_s	Solids circulation rate (kg/ (m ² s))
g	Gravity acceleration
Re	Reynolds number defined by $U_l d_p \rho_l / \mu_l$
Re_t	Particle terminal Reynolds number defined by $U_t d_p \rho_l / \mu_l$
U_a	Auxiliary liquid velocity (cm/s)
U_l	Superficial liquid velocity (cm/s)
U_s	Superficial solids velocity (cm/s)
U_{slip}	Slip velocity (cm/s)
U_t	Particle terminal velocity (cm/s)
U_{tr}	Transition velocity demarcate the conventional particulate regime and circulating fluidization regime (cm/s)
V_l, V_p	Local liquid velocity and local particle velocity (cm/s)
\bar{V}_p	Average particle velocity (cm/s)

Greek letters

$\bar{\varepsilon}$	Average bed voidage
$\bar{\varepsilon}_s$	Average solids holdup
μ_l	Liquid viscosity (mPa·s)
ρ_p	Particle density (kg/m ³)

Subscripts

l	Liquid
p	Particle
s	Solids

Abbreviation

LSCFB	Liquid-Solid Circulating Fluidized Bed
ILSCFB	Inverse Liquid-Solid Circulaing fluidized Bed
IGLSCFB	Inverse Gas-Liquid-Solid Circulaing fluidized Bed
CCFB	Conventional Circulating Fluidized Bed

Reference

- Epstein, Norman. 2002. "Applications of Liquid-Solid Fluidization." *International Journal of Chemical Reactor Engineering* 1 (1). <https://doi.org/10.2202/1542-6580.1010>.
- Lan, Qingdao, Amarjeet Bassi, Jing-Xu (Jesse) Zhu, and Argyrios Margaritis. 2002. "Continuous Protein Recovery from Whey Using Liquid-Solid Circulating Fluidized Bed Ion-Exchange Extraction." *Biotechnology and Bioengineering* 78 (2): 157–63. <https://doi.org/10.1002/bit.10171>.
- Muroyama, Katsuhiko, and Liang-shih (Ohio State University) Fan. 1985. "Fundamentals of Gas- Liquid -Solid Fluidization." *AIChE Journal* 31 (1): 1–34. <https://doi.org/10.1002/aic.690310102>.
- Nelson, Michael J., George Nakhla, and Jesse Zhu. 2017. "Fluidized-Bed Bioreactor Applications for Biological Wastewater Treatment: A Review of Research and Developments." *Engineering* 3 (3): 330–42. <https://doi.org/10.1016/J.ENG.2017.03.021>.
- Nikov, I., and D. Karamanev. 1991. "Liquid-Solid Mass Transfer in Inverse Fluidized Bed." *AIChE Journal* 37 (5): 781–84. <https://doi.org/10.1002/aic.690370515>.
- Patel, Ajay, Jesse Zhu, and George Nakhla. 2006. "Simultaneous Carbon, Nitrogen and Phosphorous Removal from Municipal Wastewater in a Circulating Fluidized Bed Bioreactor." *Chemosphere* 65 (7): 1103–12. <https://doi.org/10.1016/J.CHEMOSPHERE.2006.04.047>.
- Patel, Manoj, Amarjeet S. Bassi, Jesse J.-X. Zhu, and Hassan Gomaa. 2008. "Investigation of a Dual-Particle Liquid-Solid Circulating Fluidized Bed Bioreactor for Extractive Fermentation of Lactic Acid." *Biotechnology Progress* 24 (4): 821–31. <https://doi.org/10.1002/btpr.6>.
- Razzak, S. A., S. Barghi, and J.-X. Zhu. 2010. "Phase Distributions in a Gas-Liquid-Solid Circulating Fluidized Bed Riser." *The Canadian Journal of Chemical Engineering* 88 (4): n/a-n/a. <https://doi.org/10.1002/cjce.20304>.
- Razzak, S. A., J.-X. Zhu, and S. Barghi. 2009. "Particle Shape, Density, and Size Effects on the Distribution of Phase Holdups in an LSCFB Riser." *Chemical Engineering & Technology* 32 (8):

1236–44. <https://doi.org/10.1002/ceat.200900075>.

Renganathan, Thiruvengadam, and Kamatam Krishnaiah. 2008. “Prediction of Minimum Fluidization Velocity in Two and Three Phase Inverse Fluidized Beds.” *The Canadian Journal of Chemical Engineering* 81 (3–4): 853–60. <https://doi.org/10.1002/cjce.5450810369>.

Sang, Long, and Jesse Zhu. 2012. “Experimental Investigation of the Effects of Particle Properties on Solids Holdup in an LSCFB Riser.” *Chemical Engineering Journal* 197 (July): 322–29. <https://doi.org/10.1016/J.CEJ.2012.05.048>.

Trivedi, Umang, Amarjeet Bassi, and Jing-Xu (Jesse) Zhu. 2006. “Continuous Enzymatic Polymerization of Phenol in a Liquid–Solid Circulating Fluidized Bed.” *Powder Technology* 169 (2): 61–70. <https://doi.org/10.1016/J.POWTEC.2006.08.001>.

Wang, Ding, Trent Silbaugh, Robert Pfeffer, and Y.S. Lin. 2010. “Removal of Emulsified Oil from Water by Inverse Fluidization of Hydrophobic Aerogels.” *Powder Technology* 203 (2): 298–309. <https://doi.org/10.1016/J.POWTEC.2010.05.021>.

Wang, Jiaying, Yuanyuan Shao, Xilong Yan, and Jesse Zhu. 2019. “Review of (Gas)-Liquid-Solid Circulating Fluidized Beds as Biochemical and Environmental Reactors.” *Chemical Engineering Journal*, June, 121951. <https://doi.org/10.1016/J.CEJ.2019.121951>.

Zheng, Ying, Jing-Xu Zhu, Narenderpal S Marwaha, and Amarjeet S Bassi. 2002. “Radial Solids Flow Structure in a Liquid–Solids Circulating Fluidized Bed.” *Chemical Engineering Journal* 88 (1–3): 141–50. [https://doi.org/10.1016/S1385-8947\(01\)00294-7](https://doi.org/10.1016/S1385-8947(01)00294-7).

Zheng, Ying, Jing-Xu Zhu, Jianzhang Wen, Steve A. Martin, Amarjeet S. Bassi, and Argyrios Margaritis. 1999. “The Axial Hydrodynamics Behavior in a Liquid-Solid Circulating Fluidized Bed.” *The Canadian Journal of Chemical Engineering* 77 (2): 284–90. <https://doi.org/10.1002/cjce.5450770213>.

Zhu, Jing-Xu (Jesse), Dimitre G. Karamanev, Amarjeet S. Bassi, and Ying Zheng. 2000. “(Gas-)Liquid-Solid Circulating Fluidized Beds and Their Potential Applications to Bioreactor Engineering.” *The Canadian Journal of Chemical Engineering* 78 (1): 82–94. <https://doi.org/10.1002/cjce.5450780113>.

Chapter 7

7 Preliminary study of an inverse gas-liquid-solid circulating fluidized bed

Abstract

The hydrodynamics of inverse gas-liquid-solid circulating fluidized bed is first studied as a promising candidate bioreactor for wastewater treatment. The experiments is carried out in a 0.076 ID column with 5.4m height using low density particles. The operation window of upflowing gas in downflowing liquid and solids is investigated. Gas holdup is increasing with superficial gas velocity and superficial liquid velocity, but not sensitive to solids circulation rate. Solids holdup is increasing with solids circulating rate and superficial gas velocity and decreasing with superficial liquid velocity. In comparison with inverse liquid-solid circulation fluidized bed, solids holdup is found to be significantly higher, which could potentially enhance phase contact in the fluidized bed.

Key words: gas-liquid-solid fluidization, solids holdup, gas holdup, circulating fluidized bed, inverse fluidization

7.1 Introduction

Three phase fluidized bed has been widely used in chemical, biochemical, agricultural and food industries, due to its intense heat and mass transfer between different phases(Yong Jun Cho et al. 2002; Muroyama and Fan 1985). Fan has summarized different types of three phase fluidized systems based on the flow directions of each phase and the configurations of the fluidized bed, some of which have been studied extensively while the rest were rarely

With the invention of (gas)-liquid-solid circulating fluidized bed by Zhu (Zhu et al. 2000), it has drawn many attentions as bioreactor for wastewater treatment(Patel, Zhu, and Nakhla 2006; Nelson, Nakhla, and Zhu 2017b; Sang et al. 2019). The hydrodynamics of inverse three-phase fluidized bed has been studied by many researchers (Buffière and Moletta 2000; Lee, Epstein, and Grace 2000; Comte et al. 1997). And the application for wastewater treatment has already been

demonstrated in pilot scale. Although experiment setups various between different studies, all inverse three-phase fluidized share the same concept where low density particles are suspended by downward liquid, and gas bubbles are flowing upward from the bottom distributor. Thus, the liquid velocity is always limited as not to push particles to the bottom of the fluidized bed. Inheriting from gas-liquid-solid circulating fluidized bed, where particles are circulating and being stored in the upcomer, the inverse gas-liquid-solid circulating fluidized is proposed. A downcomer is added to the system collecting the low density solids from the bottom of the inverse fluidized bed. A new regime is found with downward liquid velocity beyond particle terminal velocity.

(Gas)-liquid-solid circulating fluidized bed is a potential candidate for biological waste water treatment. Biological wastewater treatment usually requires several steps of operation, aerobic and anaerobic or anoxic for removal of nutrient, the selection and sequence of each process is dependent on the wastewater properties and discharge regulations. (Gas)-liquid-solid circulating fluidized bed is a potential candidate for biological waste water treatment, since it can simulate aerobic, anaerobic and anoxic environment conditions (Heijnen et al. 1989) with the two columns in the circulating fluidized bed.

Inverse fluidized beds have shown its potential as bioreactor for waste water treatment (Chavarie and Karamanev 1986; Choi et al. 1995; Wang et al. 2010; Nikov and Karamanev 1991). Many studies have demonstrated the use of inverse fluidization for aeration, anoxic, and anaerobic digestion in lab or pilot scale. In fluidized bed bioreactor, inert particles work as biomass carrier, where microorganism are attached on the particles in the form of biofilm (Chavarie and Karamanev 1986; Nelson, Nakhla, and Zhu 2017a). Compared to conventional biological treatment method, fluidized bed bioreactor is more advanced due to its high storage of biomass because of the biofilm. The low density particles are believed to be a more suitable candidate as inert biomass carrier compared to the traditional heavy density particles in fluidized bed bioreactors. One major issue that often arise in fluidized bed bioreactor is the over growth of biofilm on the particles, which blemishes the performance of the bioreactor and often leads to clogging. The excess biofilm on particles will cause defluidization of solids due to the extra size and mass brought by the biofilm in conventional fluidized bed bioreactor where heavy solids are fluidized upward. The defluidized zone tend to take place at the bottom of the fluidized bed reactor near the distributor, as particles become hard to be fluidized. With the use of low density particles, excess biofilm will cause the

solids to be fluidized at the bottom of fluidized bed since it is heavier, which is far from the liquid distributor. Because the distributor or the liquid entrance is located at the surface of the fluidized bed.

In this study, the inverse gas-liquid-solid circulating fluidized bed is firstly studied aiming to combine the advantages of inverse fluidization and gas-liquid-solid circulating fluidization.

7.2 Experiment setup

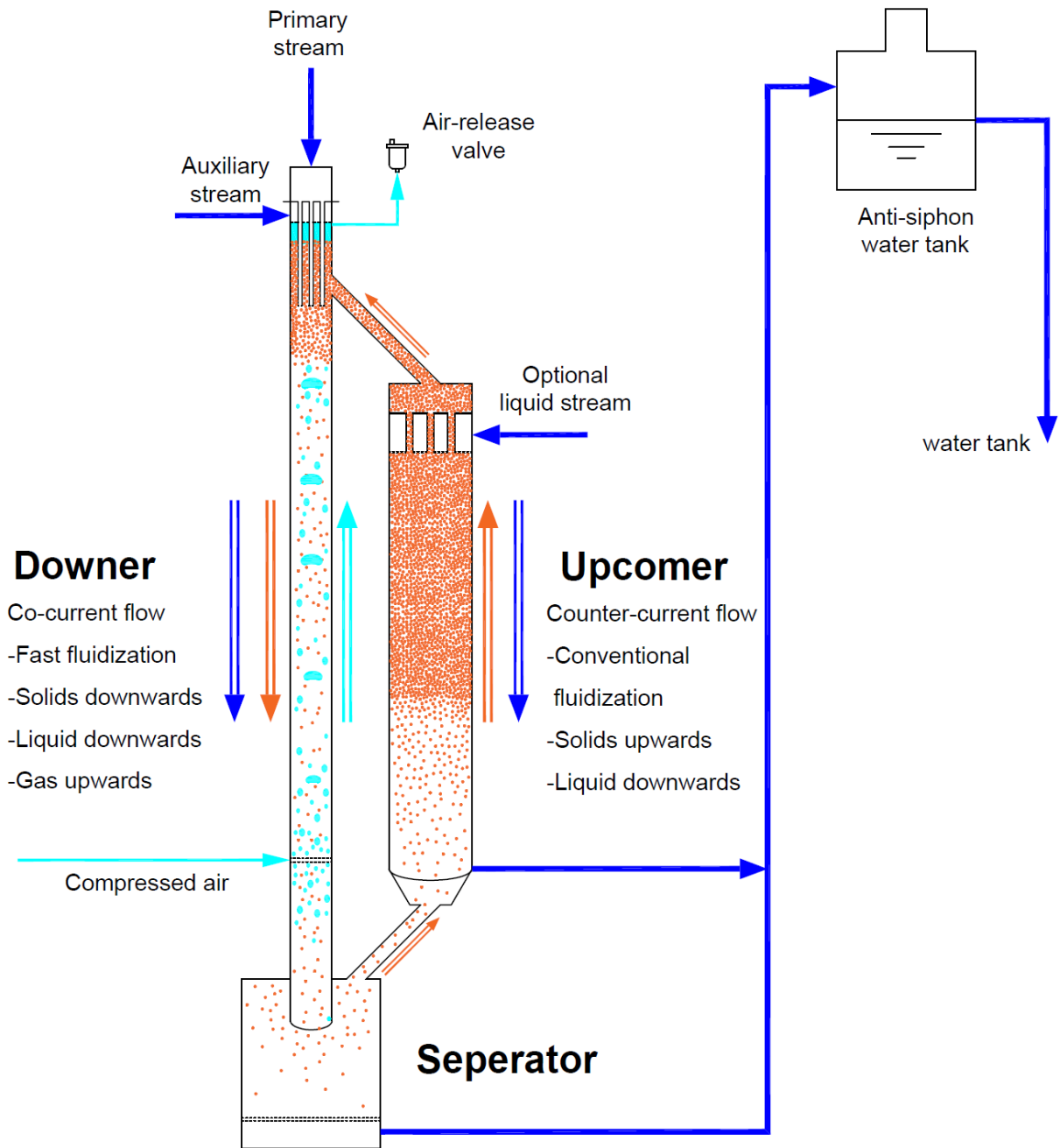


Figure 7.2.1 Schematic diagram of inverse gas-liquid-solid circulating fluidized bed

7.2.1 Operation of IGLSCFB

Since particles are carried downward by liquid flow, and gas bubbles are swarming upwards due to its low density comparing to water, a proper operation requires moderate liquid velocity, so that bubbles can still leave the column from the top while light particles maintain at circulating condition. If the velocity is too high, bubbles cannot float upward freely, causing slugging in the downer, or even accumulation of gas in the upcomer. Whereas circulation of particles can't be achieved when liquid velocity is below particle terminal velocity. Ideally, the operation liquid velocity should be controlled between particle terminal velocity and bubble terminal velocity, which is a function of particle and bubble properties. Heavy and small particles should have low particle velocity based on force balance of particles in liquid, which lead to a wide operation window. Karamanev has proposed a validated model to predict terminal velocity of low density particles with extensive experiment of particles of various sizes and densities, which is also believed can be extended for gas bubbles. However, the size of gas bubbles in liquid is subject to but not only the liquid velocity, pressure, gas velocity and gas distributor, which could vary in different condition. The error amplified when use models to estimate gas bubble diameter and then be used to predict bubble terminal velocity. It is worthwhile to study the operation window carefully for bubbles experimentally. In this study, the operation window is investigated in gas-liquid system, where manometer was used to detect when bubbles start to accumulate in the downer, assuming solid won't have a significant impact on bubble properties. And the lower end of operation window can be inherited from the starting liquid velocity of inverse liquid-solid circulating fluidized bed. It is expected to see higher gas holdup with increasing gas velocity as the residence time of gas in downer increases. For the same reason, gas holdup will increase by increase downward liquid velocity while keeping gas velocity as constant. Up to a critical liquid velocity, gas holdup reaches its maximum, when bubbles can no longer rise to the top of the downer. Experiments were carried out with constant gas velocities and adding liquid velocity until a critical velocity is found.

The bottom two manometers can be used to detect where gas start to be entrained from the bottom of the downer. The gas distributor is located between the bottom two manometers, and the manometer only measure the average gas holdup from pressure balance, thus the gas holdup obtained from the bottom two manometers should be lower than other positions, as there is no gas

between the gas distributor and the bottom manometer at low downward liquid velocity. The axial profile of gas holdup at different conditions are shown in Figure 7.3.2. At no liquid flow condition, it is obvious that the gas holdup is significant lower at the bottom position. With increasing liquid velocity, the gas holdup at the bottom increases rapidly and eventually surpass gas holdup at higher position. The result is aligned with observation, as more bubbles can be seen below the gas distributor at higher liquid velocity. When gas is introduced from the distributor, with the influence of downward liquid flow, bubbles come in various sizes. Former study has shown bubbles will grow into larger size on the way rising to the top. With downward liquid flow, small diameter bubbles may be carried downward before growing to large size, as small bubble have low terminal velocity, which explains the gas holdup at the bottom section rises and finally catches with higher position with increasing liquid velocity. Fine bubbles ($<5\text{mm}$) which have very small terminal velocity can be easily carried out of the downer. However, the gas flux from fine bubbles is so little, which can be neglected in this study.

The chosen gas distributor is different from other types of inverse three phase fluidized beds, due to the circulation of particles requires space for solids to pass through from the downer to the upcomer. A stick with 8 holes in 1mm diameter is made as gas distributor, and a uniform bubble formation can be observed with no presence of solids.

The distance between the gas distributor and the very bottom manometer is 25 cm. When the gas holdup of the bottom section matches the gas holdup in the second last section, it suggests that a significant amount of bubbles have be carried downward below the distributor. The liquid velocity at this critical condition is noted. The used particles in this study is EPS122, whose density is 122 kg/m^3 , and diameter is 1.1mm.

7.2.2 Measurement of phase holdups

Manometers can measure the mixture density along the downer based on pressure balance, which is determined by the phase holdups. In order to calculate the three phase holdups individually, a third equation has to be introduced to make the phase holdups solvable. In this experiment, solids holdup is obtained separately by measuring the accumulated bed height of solids at the top of the downer when the system is suddenly shut off at steady state for every operating condition. The accumulated height multiple solids fraction at packed condition of light particles over the height

of the downer is the average solids holdup in the downer calculated by $\epsilon_s = \epsilon_{mf} \times h/H$, and ϵ_{mf} is usually 0.58-0.6. Knowing solids holdup, the gas holdup can be calculated from average density of the mixture obtained from manometers, as $(\epsilon_g \times \rho_g + \epsilon_s \times \rho_s + \epsilon_l \times \rho_l) g = dP/dz$. In addition, phase holdups axial distribution can be further calculated assuming solids holdup to be uniform along the downer based on results from two phase inverse liquid-solid circulating fluidized bed with no presence of solids.

Gas flowrate is controlled by a rotameter and the superficial gas velocity is calibrated to atmosphere pressure for fair comparison between different operating conditions.

7.3 Gas-Liquid experiment and observation

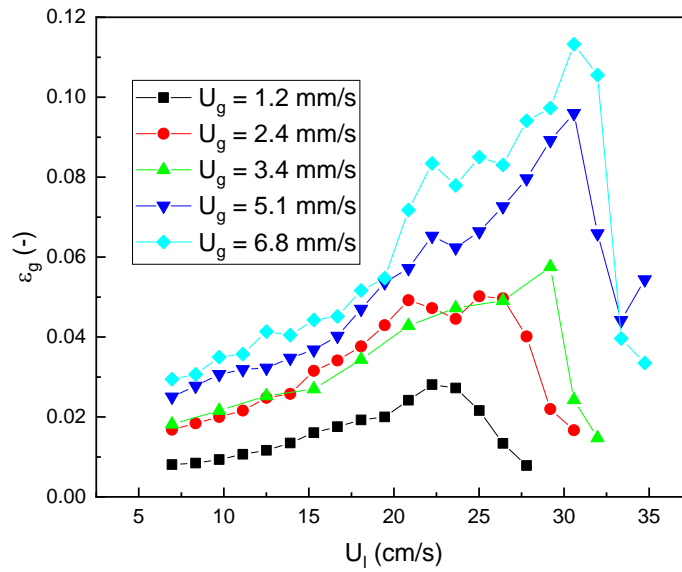


Figure 7.3.1 Gas holdup vs downflow liquid velocity at different superficial gas velocity

The operation of gas-liquid flow is first studied with upflow gas flow and downward liquid flow by gradually increase liquid velocity at constant gas velocity. The change of gas holdup is plotted in Figure 7.3.1. Higher gas velocity will lead to a higher gas holdup in the system. The gas holdup is increasing at first with upflow liquid velocity since the rising velocity of bubbles is hindered by the downward liquid. And a sharp drop of gas holdup is found after the peak of gas holdup is

reached. And the peak gas holdup is increasing with both superficial gas velocity and liquid velocity.

Drag force provided by the liquid is facing downward to counter the net buoyancy of bubbles. With increasing liquid velocity, bubble rising velocity has to be dropped assuming constant slip velocity between bubble and liquid. Thus, more gas will be contained in the system, causing the rise of gas holdup. When the liquid velocity is high enough, a switch of bubble velocity direction will take place to maintain the force balance. A downward bubble velocity is achieved, and all bubbles will be entrained out of the column, which leads to a sudden drop of gas holdup. That switch in the direction of bubble velocity is dictated by the peak of gas holdup in Figure 7.3.1. A higher gas velocity usually generates large bubble diameter in the system, based on force balance of bubbles, which requires higher liquid velocity to make the switch of bubble velocity direction to take place. As a result, peak gas holdup is reached at higher superficial liquid velocity under higher superficial gas velocity.

The maximum operating liquid velocity can be qualitatively found at the peak gas holdup condition as shown in Figure 7.3.1. However, there is a distribution of gas bubbles in the system, some entrainment of bubbles already take place before reaching peak gas holdup condition. Actual maximum superficial liquid velocity depends on the system ability in handling with gas entrainment from the bottom of the downer. In addition, since bubble size is crucial, the selection of gas distributor will be affecting the operating window as well.

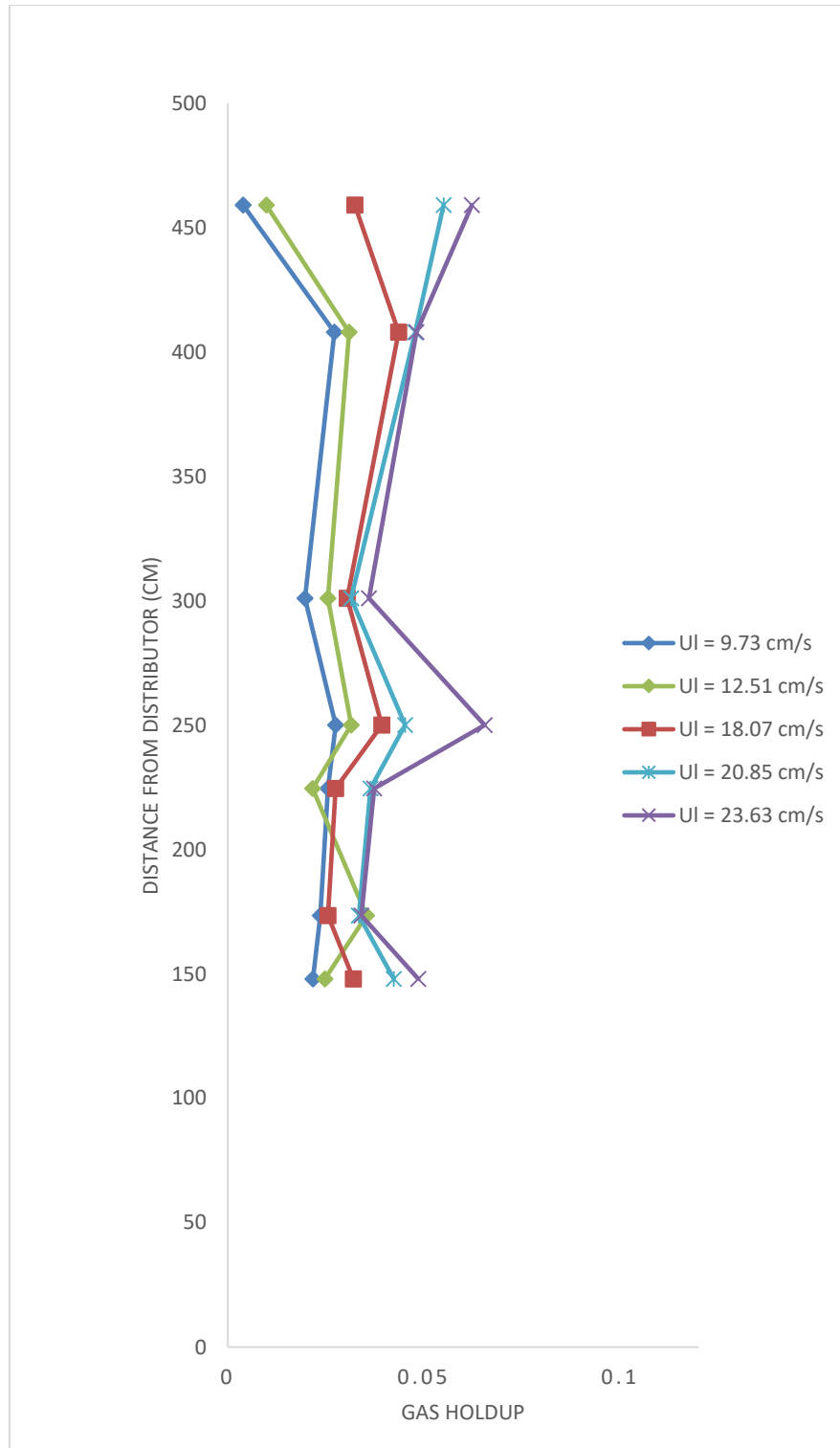


Figure 7.3.2 Gas holdup axial distribution at different downflow liquid velocity when $U_g = 4.3$ mm/s

Gas holdup axial distribution is measured in the absence of particle with different downflow liquid velocity. As shown in the Figure 7.3.2, gas holdup distribution is found to be uniform along the downer. When the distance from liquid distributor is too small, gas holdup measurement is affected by the gas outlet severely, so the results are not shown. At near the gas distributor region, which is 450 cm away from liquid distributor, there is a rapid increase of gas holdup with increasing liquid velocity. This is because high liquid velocity will inhibit the rising of small bubbles. Small bubbles will coalesce to big bubbles so buoyancy can counter the drag force provided by high velocity liquid.

7.3.1 Phase holdup distributions and mixture density

From manometers along the downer, density of the multiphase flow can be calculated based on pressure balance. Figure 7.3.3 shows mixture density axial distribution in I-GLSCFB, which is uniform along the downer. Average density of the mixture is determined by the corresponding solids holdup and gas holdup at different axial positions. Qualitatively, mixture density is a reflection of phase holdups, as uniform phase holdup distribution will lead to a uniform mixture density distribution. In addition, since air density is significantly smaller than particle and liquid density, it plays a much important role affecting the mixture density of mixture. And gas holdup distribution is measured to be uniform in two phase gas-liquid systems, which helps to explain the uniform mixture density distribution.

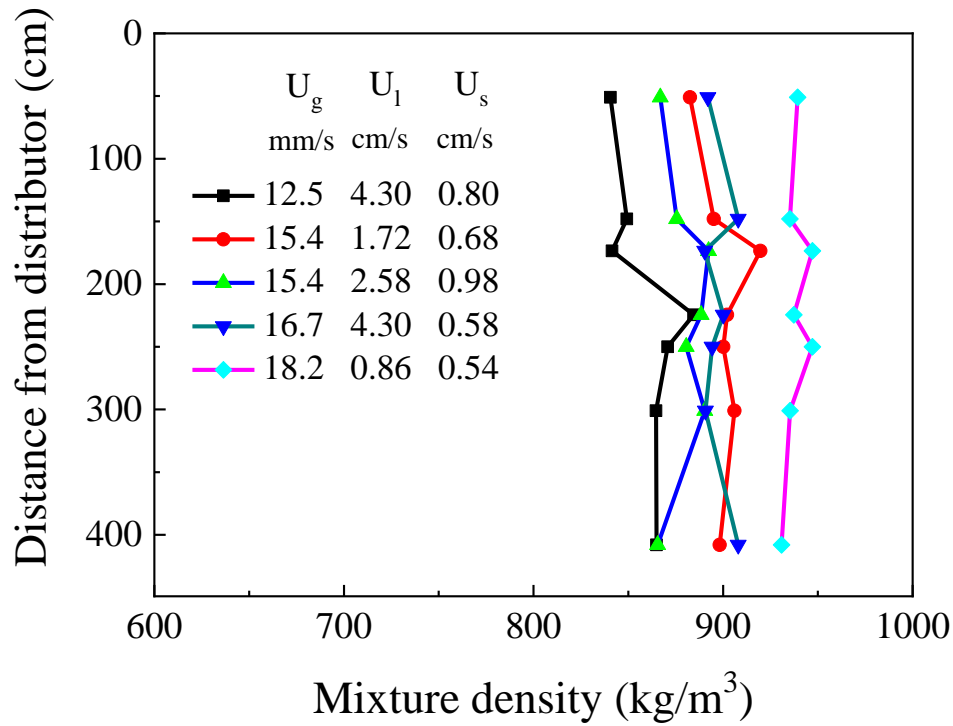


Figure 7.3.3 Mixture density of IGLSCFB

7.3.2 Average solids holdup at different operation conditions

The hydrodynamics of I-GLSCFB is determined by superficial liquid velocity (U_l), superficial gas velocity (U_g) and solid circulation rate (U_s). And solids holdup is one of the most important parameters characterizing the hydrodynamics. Figure 7.3.4 summarizes the average solids holdup and gas holdup in the downer at different operating conditions. In general, solids holdup is increasing with solid circulation rate as more solids are fed to the column. And gas holdup is increasing with superficial gas velocity. And with increasing of liquid velocity, solids holdup is decreasing as liquid to solid volume flowrate ratio is decreased as well. Within each group of constant liquid velocity, gas holdup has little effect on solid holdup, as solid and gas have no direct contact based on our observation and experience. Given both gas holdup and solids holdup are relatively small, bubbles and particles can be treated as discrete phase that travel separately in the liquid.

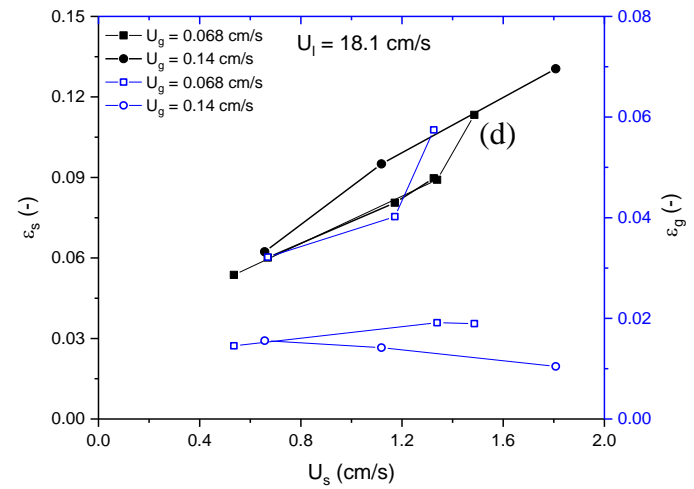
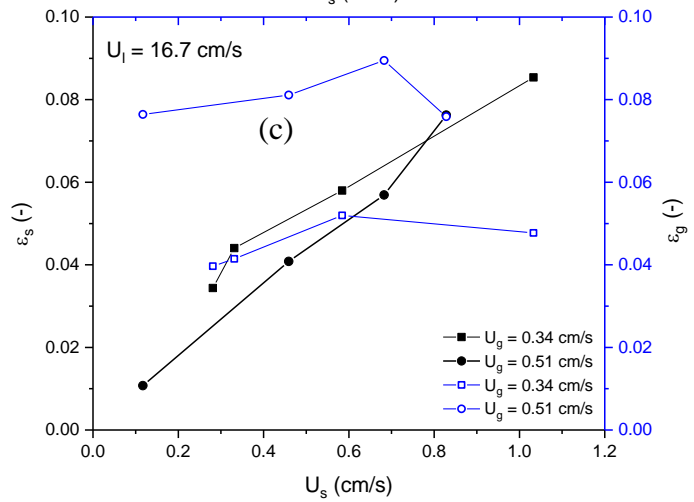
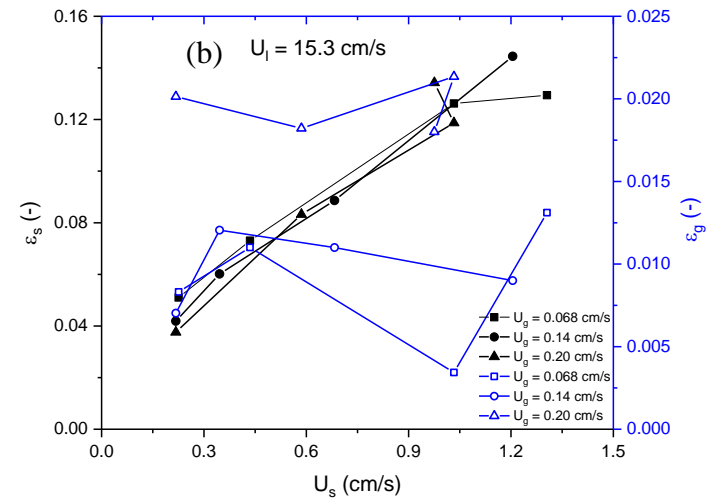
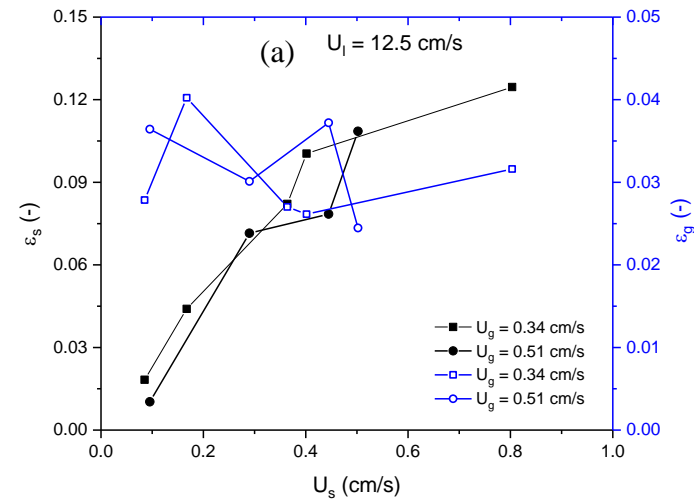


Figure 7.3.4 Solids holdup (ϵ_s) versus solids circulation (U_s) rate at constant superficial liquid velocity (U_l) and superficial gas velocity (U_g)

The relationship between ϵ_g and ϵ_s with the change of U_s are plotted in Figure 7.3.4 under constant superficial liquid velocity. The results have shown that ϵ_s is increasing linearly with U_s . And a flat response is observed between ϵ_g and U_s .

The effect of U_g on ϵ_g is very straightforward, as gas holdup is increasing with the amount of gas feeding to the system. And there seems to be no effect from U_g on ϵ_s . A detail discussion is conducted in the next section when comparing the hydrodynamics of ILSCFB and IGLSCFB, U_g as ILSCFB can be viewed as IGLSCFB when $U_g = 0$.

By comparing the ϵ_s with ϵ_g in Figure 7.3.4, the effect of U_l can be studied. Solids holdup is less when U_l is high. This can be explained as solids have to expand to accommodate the increased interstitial liquid velocity caused by the increasing liquid and the trend is consistent with LSCFB, I-LSCFB and GLSCFB. (Razzak, Zhu, and Barghi 2009; Zhu et al. 2000; Sang et al. 2019; Zheng et al. 1999)

The effect of U_g on ϵ_g is very straightforward, as gas holdup is increasing with the amount of gas feeding to the system. And there seems to be no effect from U_g on ϵ_s . A detail discussion is conducted in the next section when comparing the hydrodynamics of ILSCFB and IGLSCFB, U_g as ILSCFB can be viewed as IGLSCFB when $U_g = 0$.

7.4 Comparison between the behavior of gas and solid in IGLSCFB

As the result from Figure 7.3.4, solids holdup is decreasing with U_l while gas holdup is increasing with U_l . But for both bubbles and solids, they share the same force balance as downward drag is required from downflow liquid to counter the net buoyancy. The different trend observed with solids holdup and gas holdup is because the composition of slip velocities is different even the direction of drag force is the same. Since bubbles are lighter than the solids, a larger slip velocity is needed to reach force balance. In IGLSCFB, the slip velocity of rising bubbles in downflow liquid is calculated as $U_{slip} = U_l + U_b$. On the other hand, the slip velocity of particles is relatively small, so the slip velocity is

obtained from $U_{\text{slip}} = U_l - U_p$. In this case, U_b is bubble rising velocity, U_l is liquid velocity around bubble or particle and U_p is particle velocity. Thus, the change of superficial liquid velocity will have different impact on slip velocity of particles and bubbles, which lead to a contrast trend of change in phase holdups to accommodate the change of drag force to maintain force balance.

7.5 Comparison between IGLSCFB and ILSCFB

The comparison of solids holdup between ILSCFB and IGLSCFB are shown in Figure 7.5.1. The configurations of ILSCFB are mentioned in Chapter 3 and 4. Same particle were selected for the comparison under similar superficial liquid and solid velocities.

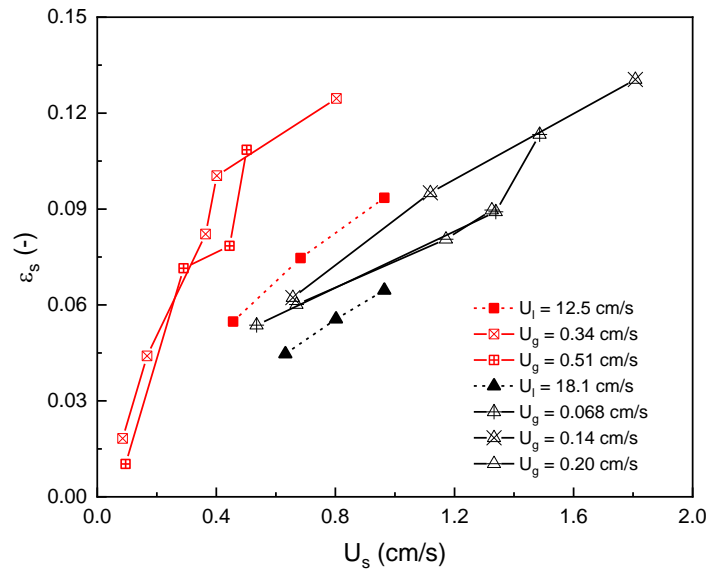


Figure 7.5.1 Comparison between ILSCFB and IGLSCFB

In ILSCFB (Chapter 4), solids holdup is more sensitive to U_s compared with U_l , and the same trend is found in IGLSCFB. For both circulating fluidized bed, a linear relationship is found between U_s and ϵ_s . But under the same solid circulation rate and superficial liquid velocity, higher solids holdup is observed in IGLSCFB compared with ILSCFB. This can be explained by the effects of U_g . The rising gas bubbles. Due to the counter-current flow conditions of bubble and liquid, the flow of liquid is largely interfered. The rising bubbles

will cause change of the field of downflow liquid, especially with large bubbles that is occupying large volume. In addition, some liquid is trapped in the bubble that will be carried upward. The effects of bubbles will cause turbulence and vortex, thus hindering the solids from exiting the column. As a result, the solids holdup is found to be always higher in the IGLSCFB.

However, solids holdup is almost constant with increasing U_g in IGLSCFB. Which means the change of U_g on solids holdup is not significant when U_g is relatively low. In addition, the increased interstitial liquid velocity with U_g will also lead to decrease of solids holdup, thus balancing some of the effects by U_g . The same explanation also applies to accounts for the relationship between average solids holdup ϵ_s and operating conditions, U_l , U_s , and U_g .

In the regards of operation window, the onset velocity of superficial liquid velocity in ILSCFB is found to be a fixed value, usually particle terminal velocity (Zheng et al. 2001). However, in IGLSCFB the onset velocity of liquid to achieve solid circulation will be affected by the flow of gas. This is because of the upward gas flow will increase the net flow of liquid downward and thus increase interstitial liquid velocity. And it is believed that a higher gas flow will lead to a decrease in onset velocity of liquid.

7.6 Conclusions and recommendations

Inverse three-phase circulating fluidized bed is firstly studied experimentally with low density particles in at 5.4 m tall inverse circulating fluidized bed. The operation window is examined, which is closely related to superficial gas and liquid velocity. And the feasible operation range depends on the allowance of gas entrainment from the top of the downer. A wide range of superficial liquid and gas velocity and solid circulation rate is investigated. Axial mixture density is shown to be uniform in most conditions. Solids holdup is increasing with U_s , decreasing with U_l and not sensitive to U_g . Some similarities are found between ILSCFB and IGLSCFB.

In the future, the bubble properties such as diameter, shape and rising velocities could be further investigated. In addition, the gas distributor could be modified to have a better control of initial bubble size. Experiments have found slugging of bubble in rare occasions, it would be beneficial to study the hydrodynamics of IGLSCFB in a column with larger diameter. In addition, the gas release system on the top of IGLSCFB downer could be improved for a smooth feed of solids without intervening with gas release.

More comparison can be made between IGLSCFB and traditional gas-liquid-solid circulating fluidized or inverse gas-liquid solid fluidized bed, to further distinguish the characteristics of IGLSCFB.

In experiment, it is observed that some fine bubbles will be trapped between particles and act as a glue that bond particles together. The phenomenon is believed to be caused by the surface tension between liquid, particle and gas. The surface properties of particles could be quantified and modified, and the surfactant effect from liquid could also be studied in the future.

Nomenclature

Ar	Archimedes number defined by $d_p^3 g (\rho_p - \rho_l) \rho_l / \mu_l^2$
C_D	Particle drag coefficient
d_p	Particle diameter (mm)
D	Column diameter (m)
F_b, F_d, F_g	Buoyancy, drag force and gravity
G_s	Solids circulation rate (kg/ (m ² s))
g	Gravity acceleration
Re	Reynolds number defined by $U_l d_p \rho_l / \mu_l$
Re_t	Particle terminal Reynolds number defined by $U_t d_p \rho_l / \mu_l$
U_a	Auxiliary liquid velocity (cm/s)
U_l	Superficial liquid velocity (cm/s)
U_s	Superficial solids velocity (cm/s)
U_{slip}	Slip velocity (cm/s)
U_t	Particle terminal velocity (cm/s)
U_{tr}	Transition velocity demarcate the conventional particulate regime and circulating fluidization regime (cm/s)
V_l, V_p	Local liquid velocity and local particle velocity (cm/s)
\bar{V}_p	Average particle velocity (cm/s)

Greek letters

$\bar{\varepsilon}$	Average bed voidage
$\bar{\varepsilon}_s$	Average solids holdup
μ_l	Liquid viscosity (mPa·s)
ρ_p	Particle density (kg/m ³)

Subscripts

l	Liquid
p	Particle
s	Solids
b	Bubble
g	gas

Abbreviation

LSCFB	Liquid-Solid Circulating Fluidized Bed
ILSCFB	Inverse Liquid-Solid Circulaing fluidized Bed
IGLSCFB	Inverse Gas-Liquid-Solid Circulaing fluidized Bed
CCFB	Conventional Circulating Fluidized Bed

Reference

- Buffière, Pierre, and René Moletta. 2000. "Collision Frequency and Collisional Particle Pressure in Three-Phase Fluidized Beds." *Chemical Engineering Science* 55 (22): 5555–63. [https://doi.org/10.1016/S0009-2509\(00\)00186-X](https://doi.org/10.1016/S0009-2509(00)00186-X).
- Chavarie, C, and D Karamanev. 1986. "Use of Inverse Fluidization in Biofilm Reactors." In *Proc. Int. Conf. on Bioreactor Fluid Dynamics, Cambridge (15-17 April)*, 181–90.
- Choi, Yoon Chan, Dong Seog Kim, Tae Joo Park, Kyung Kee Park, and Seung Koo Song. 1995. "Wastewater Treatment in a Pilot Scale Inverse Fluidized-Bed Biofilm Reactor." *Biotechnology Techniques* 9 (1): 35–40. <https://doi.org/10.1007/BF00152997>.
- Comte, M.P., D. Bastoul, G. Hebrard, M. Roustan, and V. Lazarova. 1997. "Hydrodynamics of a Three-Phase Fluidized Bed—the Inverse Turbulent Bed." *Chemical Engineering Science* 52 (21–22): 3971–77. [https://doi.org/10.1016/S0009-2509\(97\)00240-6](https://doi.org/10.1016/S0009-2509(97)00240-6).
- Heijnen, J.J., A. Mulder, W. Enger, and F. Hoeks. 1989. "Review on the Application of Anaerobic Fluidized Bed Reactors in Waste-Water Treatment." *The Chemical Engineering Journal* 41 (3): B37–50. [https://doi.org/10.1016/0300-9467\(89\)80029-2](https://doi.org/10.1016/0300-9467(89)80029-2).
- Lee, Dong-Hyun, Norman Epstein, and John R. Grace. 2000. "Hydrodynamics Transition from Fixed to Fully Fluidized Beds for Three-Phase Inverse Fluidization." *Korean Journal of Chemical Engineering* 17 (6): 684–90. <https://doi.org/10.1007/BF02699118>.
- Muroyama, Katsuhiko, and Liang-shih (Ohio State University) Fan. 1985. "Fundamentals of Gas- Liquid -Solid Fluidization." *AIChE Journal* 31 (1): 1–34. <https://doi.org/10.1002/aic.690310102>.
- Nelson, Michael J., George Nakhla, and Jesse Zhu. 2017a. "Fluidized-Bed Bioreactor Applications for Biological Wastewater Treatment: A Review of Research and Developments." *Engineering* 3 (3): 330–42. <https://doi.org/10.1016/J.ENG.2017.03.021>.
- Nikov, I., and D. Karamanev. 1991. "Liquid-Solid Mass Transfer in Inverse Fluidized

Bed.” *AIChE Journal* 37 (5): 781–84. <https://doi.org/10.1002/aic.690370515>.

Patel, Ajay, Jesse Zhu, and George Nakhla. 2006. “Simultaneous Carbon, Nitrogen and Phosphorous Removal from Municipal Wastewater in a Circulating Fluidized Bed Bioreactor.” *Chemosphere* 65 (7): 1103–12. <https://doi.org/10.1016/J.CHEMOSPHERE.2006.04.047>.

Razzak, S. A., J.-X. Zhu, and S. Barghi. 2009. “Particle Shape, Density, and Size Effects on the Distribution of Phase Holdups in an LSCFB Riser.” *Chemical Engineering & Technology* 32 (8): 1236–44. <https://doi.org/10.1002/ceat.200900075>.

Sang, Long, Tian Nan, Amin Jaber, and Jesse Zhu. 2019. “On the Basic Hydrodynamics of Inverse Liquid-Solid Circulating Fluidized Bed Downer.” *Powder Technology*, April. <https://doi.org/10.1016/j.powtec.2019.04.021>.

Wang, Ding, Trent Silbaugh, Robert Pfeffer, and Y.S. Lin. 2010. “Removal of Emulsified Oil from Water by Inverse Fluidization of Hydrophobic Aerogels.” *Powder Technology* 203 (2): 298–309. <https://doi.org/10.1016/J.POWTEC.2010.05.021>.

Yong Jun Cho, Hee Young Park, And Sang Woo Kim, Yong Kang*, and Sang Done Kim. 2002. “Heat Transfer and Hydrodynamics in Two- and Three-Phase Inverse Fluidized Beds.” *Industrial and Engineering Chemistry Research*. <https://doi.org/10.1021/IE0108393>.

Zheng, Ying, Jing-Xu Jesse Zhu, W-g Liang, S-l Zhang, J-x Zhu, Y Jin, Z-q Yu, Cr Ž Z-W Wang, and Flow Characteristics. 2001. “The Onset Velocity of a Liquid-Solid Circulating Fluidized Bed.” *Powder Technology*. Vol. 114. www.elsevier.com/locate/powtec.

Zheng, Ying, Jing-Xu Zhu, Jianzhang Wen, Steve A. Martin, Amarjeet S. Bassi, and Argyrios Margaritis. 1999. “The Axial Hydrodynamics Behavior in a Liquid-Solid Circulating Fluidized Bed.” *The Canadian Journal of Chemical Engineering* 77 (2): 284–90. <https://doi.org/10.1002/cjce.5450770213>.

Zhu, Jing-Xu Jesse, Dimitre G Karamanev, Amarjeet S Bassi, and Ying Zheng. 2000.

“(Gas-) Liquid-solid Circulating Fluidized Beds and Their Potential Applications to Bioreactor Engineering.” *The Canadian Journal of Chemical Engineering* 78 (1): 82–94.

Chapter 8

8 General Discussion

8.1 Development of Four-Quadrant Fluidization Regime map

Many researches have been carried out to study the flow regimes map of liquid-solid fluidization, result in multiple critical liquid velocities to set apart different flow regimes. With the develop of circulating liquid-solid fluidized bed, experiments have found that the hydrodynamics is dependent not only on liquid velocity but also on solid flowrates. Thus, solid flowrate in conjunction with liquid velocity were used as two axes to diagram the flow regimes. Since both solid and liquid could have two flowing directions, a four-quadrant flow regimes map proposed by Zhu is established, with superficial liquid velocity as horizontal axis and solid flowrate as vertical axis

X axis

X axis represent superficial liquid velocity, and upflow liquid velocity occupies the positive side of the axis, and downflow liquid velocity is on the opposite. On the $x+$ axis, the solids are suspended with upflow liquid with no net solids flowrate, dictated as conventional fluidized bed with heavy particles. On the contrary, at $x-$ axis it is inverse conventional fluidized bed with low density particle by reversing liquid flow direction. For both conventional fluidized beds, their corresponding regime starts with minimum fluidization velocity and ends at particle terminal velocity, as all solids will be entrained from the fluidized bed beyond terminal velocity.

Y axis

On the y axis, solids flowrate exists with zero liquid flowrate. The free rising of low density particles in stagnant liquid occupies the entire $y+$ axis. And the free falling of heavy particle is going to take the entire $y-$ axis.

In this study, multiple liquid-solid circulating fluidized bed systems from the proposed Four-Quadrant Fluidization Regime Map have been studied experimentally. The

hydrodynamics of Inverse Liquid-Solid Circulating Fluidized Bed (ILSCFB) is firstly studied with low density particles flowing downward. Followed by the study of ILSCFB, a comparative study with upward Liquid-Solid Circulating Fluidized Bed is conducted. Which tried to cover the first and third Quadrant in the Four-Quadrant Fluidization Regime Map where co-current of solid and liquid flow take place as shown in Figure 8.1.1. Many similarities have been found between ILSCFB and LSCFB since both flow structure is uniform.

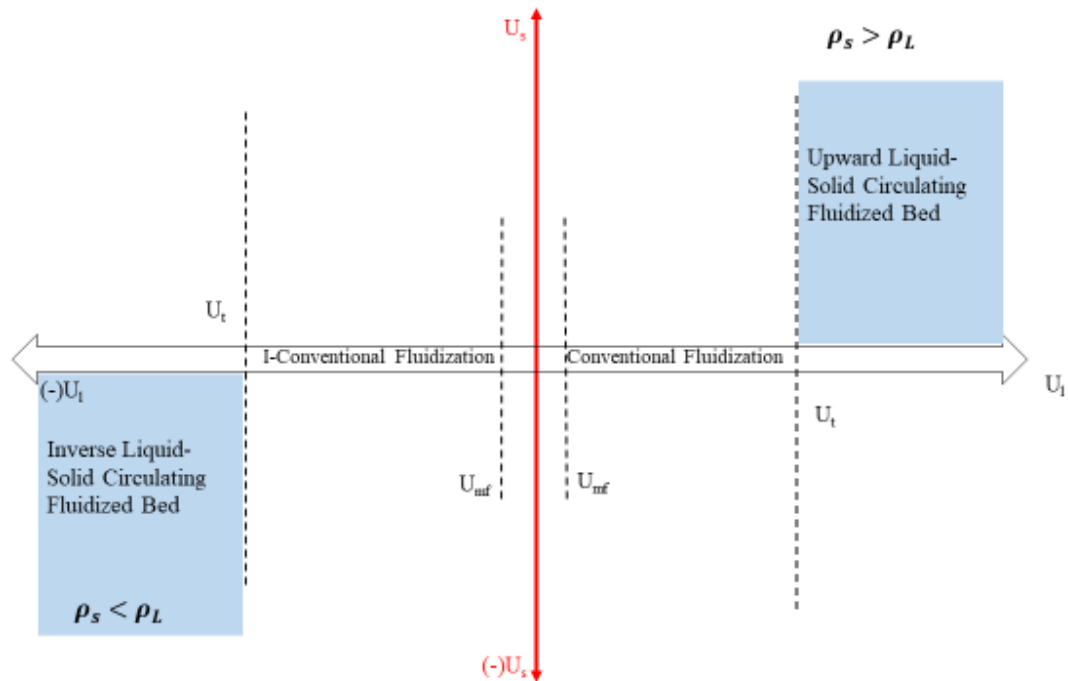


Figure 8.1.1 Four-Quadrant Fluidization Regimes Map with operating liquid velocity beyond particle terminal velocity.

After the study of LSCFB and ILSCFB where operating superficial liquid velocity is beyond particle terminal velocity, the concept of Conventional Circulating Fluidized Bed is proposed by forcing solid circulation in conventional fluidized bed that is operating below particle terminal velocity. The exploration of CCFB greatly enriches the Four-Quadrant Fluidization Regime Map as shown in Figure 8.1.2. CCFB adds solids circulation

to the convention fluidized bed, which helps the control of solids holdup. In addition, solids holdup is significantly increased compared with both conventional fluidization and circulating fluidization. Then, to fill the blank area in the second and fourth Quadrant, counter-current flow of light and heavy particles was studied. Thus, an up-to-date Four-Quadrant Fluidization Regime Map is concluded in Figure 8.1.3.

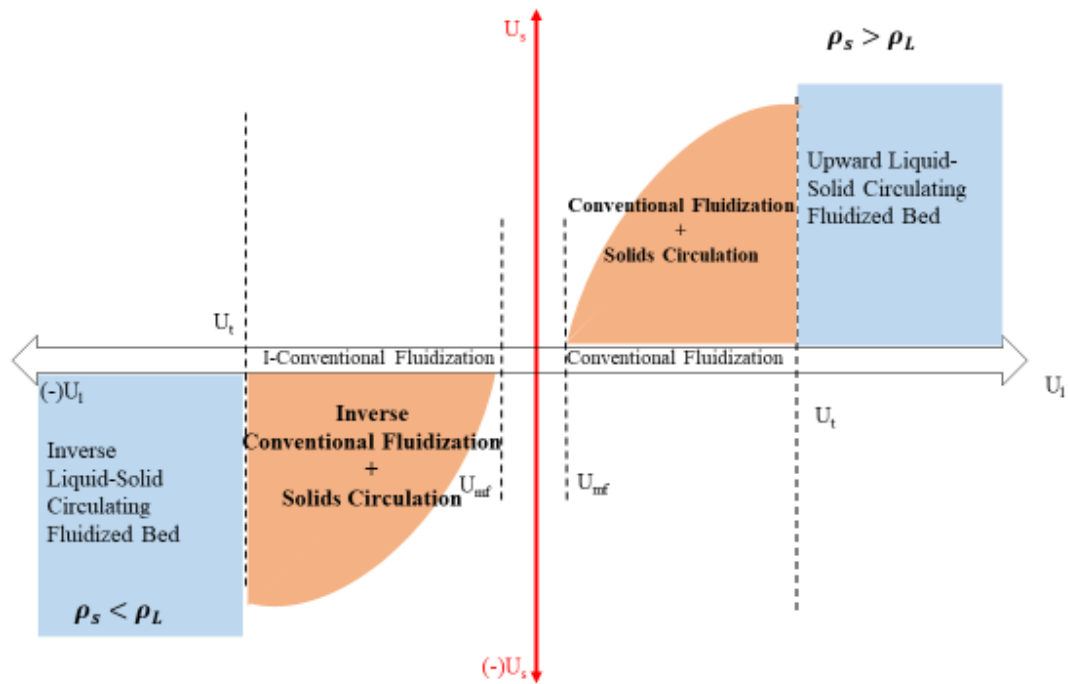


Figure 8.1.2 Four-Quadrant Fluidization Regimes Map with conventional circulating fluidized bed.

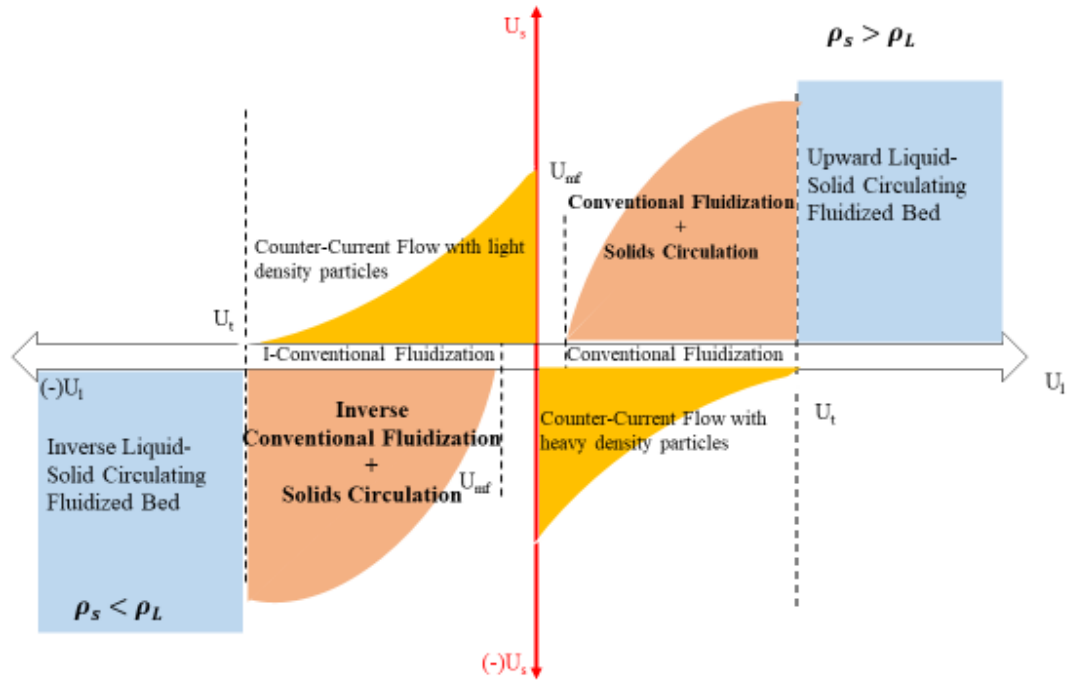


Figure 8.1.3 Four-Quadrant Fluidization Regimes Map

8.2 Description of each Quadrant

Quadrant-I

In Quadrant-I, both liquid and solids are flowing upwards, which is the most common liquid-solid fluidized bed with high density particles. Traditionally, fluidization only occurs after minimum fluidization. Starting from minimum fluidization velocity it is the well-studied conventional fluidization, which lies on the horizontal axis since there is no solid flowrate. Many correlations have been established for minimum fluidization velocity for the prediction of the start of conventional fluidization. After minimum fluidization the solids holdup or voidage is determined by superficial liquid velocity as expressed by Richardson-Zaki equation. If an upward solids flowrate is introduced in conventional fluidized bed, a new flow regime (CCFB) is created above the horizontal axis. In CCFB, experiments have found the solids holdup to be higher than conventional fluidized bed with the help of solid circulation rate. Moving right on the liquid velocity axis, when upward liquid velocity is beyond particle terminal velocity, it enters circulating regime with the addition of upward solid flowrate, so called liquid-solid circulating fluidized bed (LSCFB).

In general, solids holdup increases with solid flowrate and decreases with superficial liquid velocity.

Quadrant-II

In the Quadrant-II, particles are moving upward while liquid is moving downward. Experiments were carried out as counter-current flow of solids and liquid, where low density particles rising from the bottom of the liquid fluidized bed, and downward liquid stream is added from the top. Two zones were observed based on solids holdup a dense region and a dilute region. The theoretical upper limit of downward liquid velocity is particle terminal velocity.

Quadrant-III

In the third quadrant, both solids and liquid are flowing downward. A lot of similarities exist between Quadrant-I and Quadrant-III since the solid and liquid are flowing in the same direction. The major difference is low density particles are used in the experiment study in Quadrant-III. Inverse conventional fluidization lies on the negative direction of the liquid velocity axis since solid flowrate is zero. Inverse liquid-solid circulating fluidized bed is operating beyond particle terminal velocity. Solids flowrate can be introduced under inverse conventional fluidized bed, result in a new flow regime.

Quadrant-IV

In the last quadrant, another configuration of counter-current flow is present with heavy solids falling in upflowing liquid. The configuration is similar to Quadrant-II by flipping the flow directions of solid and particles, while heavy particles are used instead.

The direction of flow of solids and liquid is summarized in **Table 8.2-1**. In the first and fourth quadrant, heavy particles were used experimentally, as the downward net gravity of particles would need upward liquid flow to provide sufficient drag force for fluidization. On the contrary, low density particles were used in the second and third quadrant, since downward drag is needed to counter buoyance. Comparison of the hydrodynamics of different flow regimes are made based on the experiment results of solids holdup under

different superficial liquid velocity and solid flowrate. In all four quadrants, solids holdup is increasing with solids flowrate and decreasing with superficial liquid velocity. When superficial liquid velocity is high, solids holdup is more sensitive to solids flowrate. And the impact of superficial liquid velocity is more significant than solids flowrate when the liquid velocity is relatively low.

Empty area of in the flow regimes map represent operating conditions that haven't been studied yet. The empty area in the flow regimes map can be fulfilled with the assistance of CFD modelling if no experiment data is available or challenging to obtain. For example, the upflow of low density solids with upflowing liquid, and down flow heavy density particles with downflow of liquid

Table 8.2-1 Flow directions of solids and liquid in four-quadrant flow regimes map

Quadrant	Flow Direction of Solids	Flow Direction of Liquid	Solid-liquid Relative Density
I	Up	Up	Heavy
II	Up	Down	Light
III	Down	Down	Light
IV	Down	Up	Heavy

The proposed four-quadrant flow regimes map has the following characteristics:

1. All the combinations of flow directions of solids and liquid are presented in one graph, which provide a guidance for future flow regimes investigation.
2. The flow regime map is presented as a contour, with solid circulation rate and superficial liquid velocity as axes and solids holdup as indicating level. The four-

quadrant map allows detail flow regimes demographic based on solids holdup for specific need in the future.

3. Fluidization of low density particles and heavy density particles were analyzed separately in different quadrant as they behave differently.
4. Counter-current flows of liquid and solids which occurred very often in fluidized systems were first to be summarized as individual flow regimes
5. It provides guidance for developing new flow regimes in the empty area of the flow regimes map

8.3 Projection of solids holdup in different modes of operation

In homogeneous fluidization, the expression U_{slip} is similar for different modes of operation. It is believed that Richardson-Zaki equation could be suitable for the prediction of solids holdup, which has already been proved in chapter 4 and 6 and other literatures. Some modification might be made for each case, but the form of equation remains the same. So, Richardson-Zaki equation is used to describe the effects of operating conditions on the change of solids holdup, and also demonstrate the relationship and difference between different regimes in Four-Quadrant Fluidization Regime Map.

Richardson-Zaki equation is widely used in the prediction of solids holdup in conventional fluidization. The interstitial liquid velocity provides the drag force to balance the net weight of particles. For a single particle, in Stokes region, the slip velocity is particle terminal velocity and the relationship between solids holdup and superficial liquid velocity can be expressed as $U_l/(1-\epsilon_s) = U_t$. In the presence of multiple particles, particle-particle interaction come into play. Thus, exponent n is used as a factor to adjust the slip velocity, $U_l/(1-\epsilon_s) = U_t^n$. As a result, the slip velocity is a function of solids holdup.

Assuming $n = 4$, solids holdup can be predicted in full range of operating conditions as shown in Figure 8.3.1 and Figure 8.3.2. For simplicity, particles whose density are higher

than the fluid is chosen. Solids holdup is determined by superficial liquid velocity and solids flowrate. The change of solids holdup with U_s under difference dimensionless U_l/U_t is shown in Figure 8.3.1. When solid flowrate is zero, it is conventional fluidization, represented by a vertical dash line when $U_s = 0$. By adding solids flowrate in the same direction as liquid, it enters Quadrant_I, the regime of circulating fluidized beds that contains liquid-solid circulating fluidized bed (LSCFB) and conventional circulating fluidized bed (CCFB). The theoretical boundary between the two circulating fluidized beds is $U_l = U_t$. In LSCFB, U_l/U_t is greater than 1, and in CCFB, U_l/U_t is less than 1. And LSCFB always start when $\epsilon_s = 0$, while CCFB starts when $\epsilon_s > 0$. Then change of ϵ_s with U_l and U_s is similar. Solids flowrate can also be added in the opposite direction of liquid flow, which is the counter-current flow condition in Quadrant_IV, and it only happens when $U_l/U_t < 1$. If the liquid velocity is flipped downward, a new operation mode with is found with both solids and liquid flowing downward in Quadrant_III. And there is no limit of operating downward liquid velocity since particle is heavy than the liquid, particle velocity (U_s/ϵ_s) is higher than the liquid velocity ($U_l/(1-\epsilon_s)$).

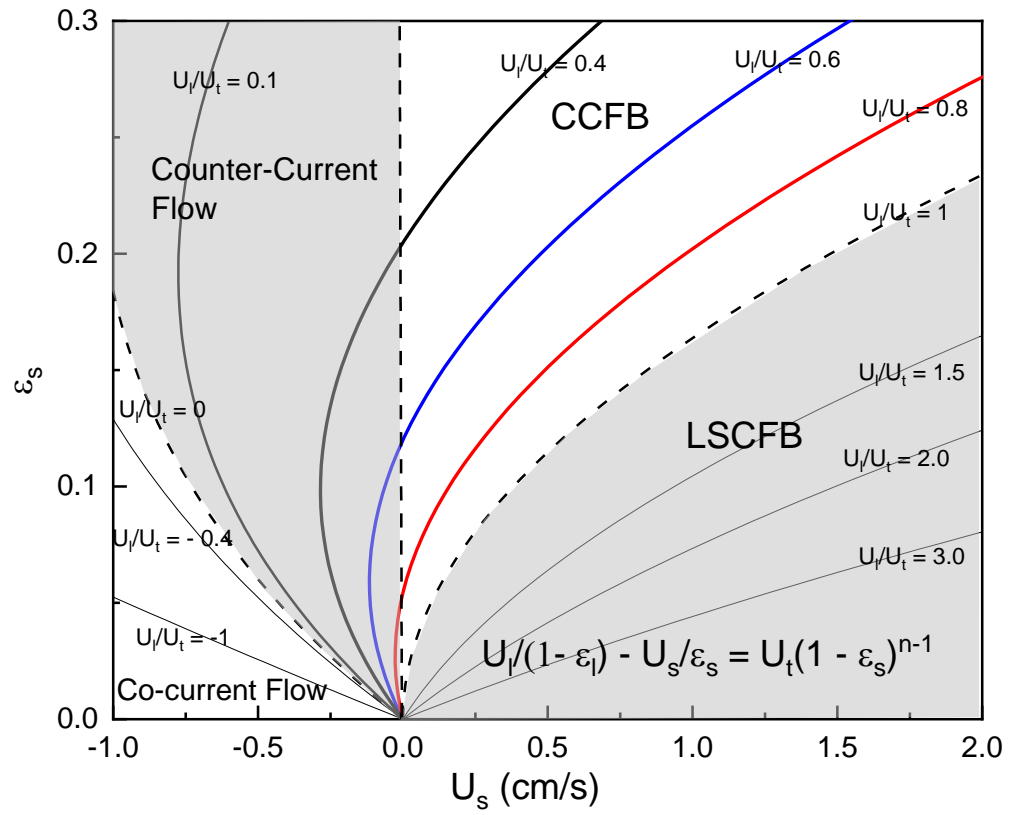


Figure 8.3.1 Projection of ε_s versus U_s based on Richardson-Zaki equation ($n = 4$)

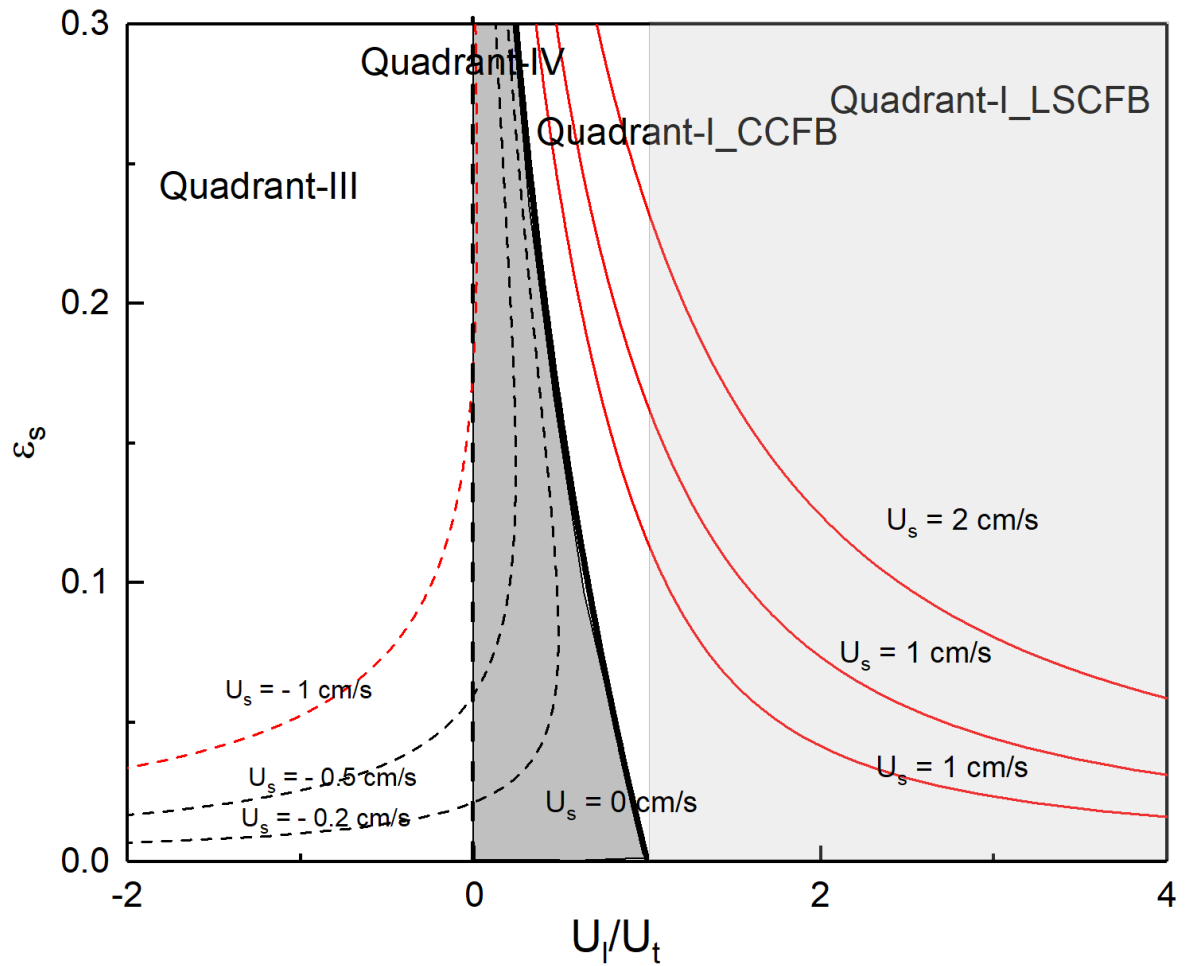


Figure 8.3.2 Projection of ϵ_s versus U_l/U_t based on Richardson-Zaki equation ($n = 4$)

The change of solids holdup with U_l/U_t under difference U_s is shown in Figure 8.3.2. Similarly, conventional fluidization take place when $U_s = 0$, represented by a bold line. And conventional fluidization also separates Quadrant_IV and Quadrant_I, which can also be referred to Figure 8.1.3. When U_l/U_t is less than 0, only downward solids flow is feasible, and when U_l/U_t is greater than 1, only upward circulating fluidized bed is the only mode of operation. When U_l/U_t is between 0 and 1, It could be in counter-current flow or CCFB, depending on the direction of solids flowrate.

In LSCFB, where superficial liquid velocity is beyond particle terminal velocity, solids holdup is increasing with solids flowrate and decreasing with superficial liquid velocity, starting from zero solids holdup condition. Similar trend is observed in CCFB, but the solids holdup starts at a value higher than zero.

So far, the counter-current flow in Quadrant_IV and LSCFB and CCFB in Quadrant_I have been studied experimentally with high density particles fluidized with upflow liquid. The fluidization of high-density particles can also take place with downflow liquid, which belongs in the third quadrant. Heavy particles will fall in the downflow liquid. Thus, both U_l and U_s will be negative in the Richardson-Zaki equation. The projected solids holdup under different operating conditions are shown in Figure 8.3.1. Based on the same force balance, solids holdup will be increasing with U_s and decreasing with U_l .

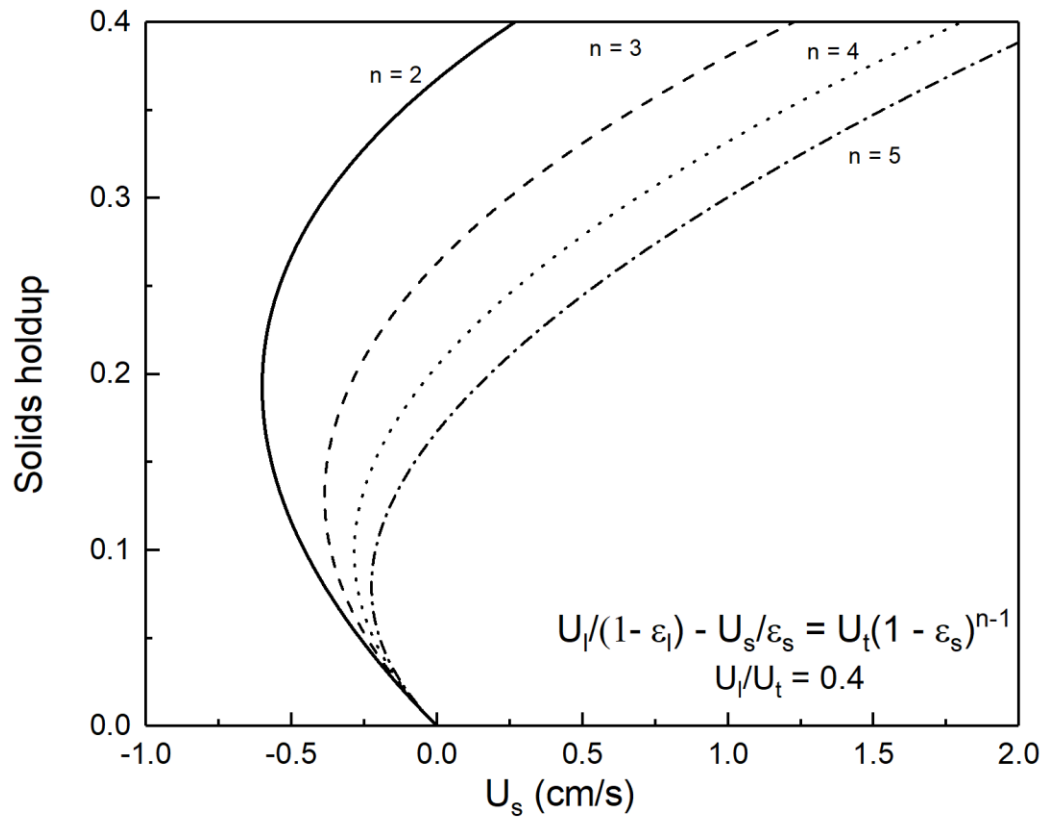


Figure 8.3.3 Effects of n on the change of ε_s with U_s in circulating fluidized bed below U_t

Effects of exponent n can also be estimated. Under the same U_l and U_s , solids holdup is decreasing with exponent n . In addition, the effects of exponent n on solids holdup is more significant when superficial liquid velocity is low in CCFB as shown in Figure 8.3.3. In LSCFB, the effects of n is not that significant as solids holdup is already very low, the effects of particle-particle interaction is not severe. And the effects of exponent n is more sensitive when n is relatively low. As the projected trends of solids holdup get closer with increasing n .

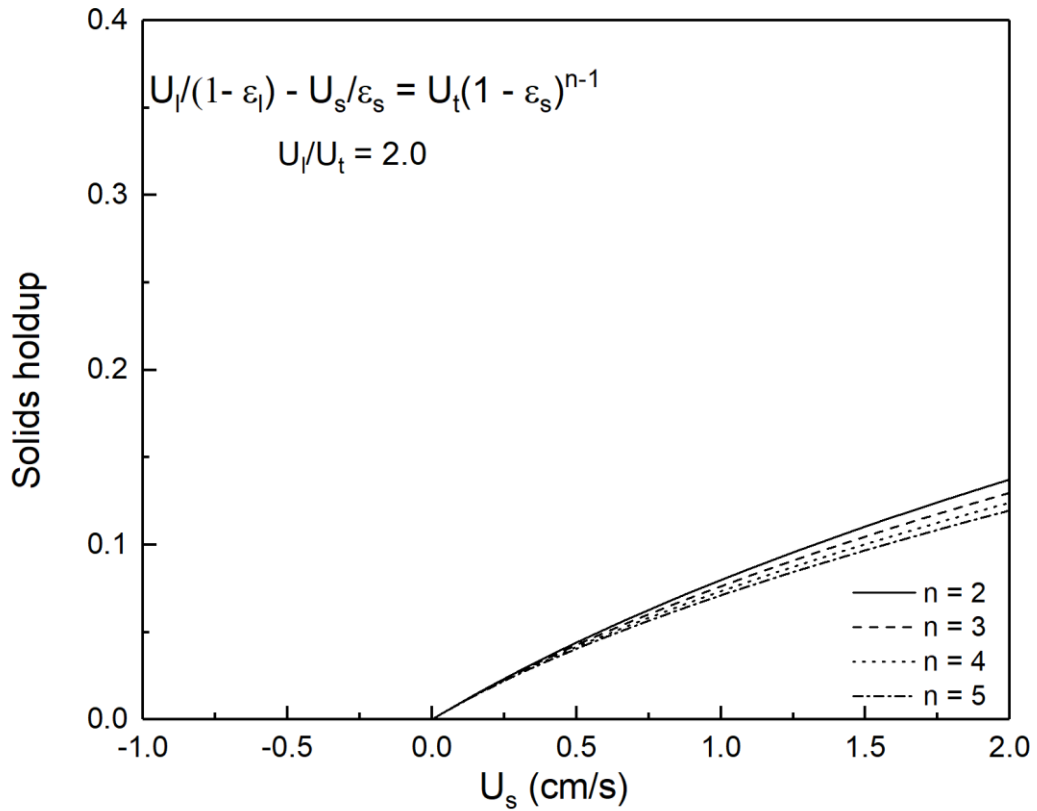


Figure 8.3.4 Effects of n on the change of ϵ_s with U_s in LSCFB

Effects of U_l and U_s on regime transition

By changing the liquid and solid flowrates and flow directions the same type of solids could be operated in different regimes from the Four-Quadrant Fluidization Regime Map. If superficial liquid velocity is beyond particle terminal velocity, the flow direction of solids can only be aligned with the flow direction of liquid, as governed by the force balance. And the fluidized bed can only be operating at circulating regime, where solids are constantly being transported in the column with sufficient solids feed. When superficial liquid velocity is below particle terminal velocity, there is no change on the upward solid flow. But now downward solids flow can be achieved. And there is a maximum downward solids flowrate for each upflow condition. When $0 < U_l < U_t$, the fluidized bed can be operated in circulating regime (CCFB), conventional fluidization regime and countercurrent regime by changing the solids flowrates. When $U_l < 0$, downward liquid flow condition, the feasible solids flow direction is only downward which is aligned with

the liquid. And there is no maximum solids flowrate until the fluidized bed reaches its highest solids holdup condition ($\varepsilon_s = 0.55-0.60$). As a result, only U_l determines the regime when $U_l > U_t$ or $U_l < 0$. Both U_l and U_s determine the regime when $0 < U_l < U_t$.

Discussion on exponent n

Exponent n and particle terminal velocity can be measured from hindered settling experiments. In hindered settling experiment, the settling velocity of a suspension of solids is found to be decreasing with solids holdup. The settling velocity is measured from a series of solids holdup condition to obtain the exponent n , which dictate the relationship between solids holdup and slip velocity. In the four-quadrant fluidization regime map, hindered settling belongs to the y axis, where solids are falling down in the absence of liquid flow. And conventional fluidization is on the x -axis, where upward liquid flow is supporting the solids. Richardson-Zaki equation has been proved to be valid in both x -axis and y -axis, and in these cases exponent n is only a function of particle and fluid properties. Although some trend between slip velocity and solids holdup have been found in different regimes, no universal relationship has been established to quantify the relationship for a wide range of operation conditions and particle properties. In particular, exponent n in Richardson-Zaki equation is hard to be determined as it might be related operating conditions which has not been carefully studied before. Exponent n represents particle-particle interaction in the fluidized bed. Particle properties, particle alignment and liquid property will cause the change of the velocity gradient around the particles, which is reflected by exponent n , as derived by JF. Richardson. This study (Chapter 4 and 6) has discovered the difference of exponent n

8.4 Critical solids flowrates and liquid velocities

In all feasible operating zones from the four-quadrant flow regimes map, solids flow is either assisted or hindered by liquid flow. If solids flow needs the help from liquid flow to initiate, there is a lower limit of liquid flowrate which is the minimum fluidization velocity (U_{mf}). If the solids flow is hindered by the liquid flow, an upper boundary of superficial liquid velocity exists.

The onset velocity of heavy particles from conventional to circulation is measured by Ying and has found the value to be very close to particle terminal velocity. Tian and Saleh also found the same phenomena with low density particles. It is commonly believed that if superficial liquid velocity is beyond particle terminal velocity, particles need a net velocity according to force balance, thus a net solids flowrate must exist. So particle terminal velocity (U_t) is used as a critical velocity where particle transportation take place.

The initial state of particles in the liquid is also another criterion to demarcate different regimes. Two types of initial states could be found in the four-quadrant map.

I. Stagnant state

II. Dynamic state

In stagnant state, solids and liquid are both in stagnant condition. For example, heavy particles packed at the bottom of the liquid and light particles floating at the top of the liquid. Whereas, in dynamic state, solids are forces at an unsteady position with external help, and the fluidization take place instantaneously once solids are released.

In stagnant state, solids flow must be assisted by liquid flow. ($V_l > V_p$). And in dynamic state, liquid could either assisting ($V_p > V_l$) or hindering solids flow (V_p and V_l in different direction).

Because of the interchangeable flow direction of solids and liquid, the relationship between solids and liquid could vary at different conditions. For example, when free setting particles are falling in stagnant liquid with downflow of liquid, as dictated in Quadrant-III, the liquid is assisting the particles to fall at a faster speed. Moving right on the U_l axis, the liquid maintain to the same function until the liquid flow direction is switched to upward, entering in Quadrant-IV. In this Zone, the liquid flow is hindering the solids flow, and solids flow will be stopped when the liquid flow reaches a critical value, usually that critical value is near particle terminal velocity. By further increasing superficial liquid velocity, the free-falling solids will be carried upwards by high velocity liquid in Quadrant-I. The liquid is supporting the heavy solids not to fall. Thus, three types of liquid flow can be categorized. The assisting flow, hindering flow and supporting flow.

8.4.1 Stagnant liquid flow

In stagnant liquid, heavy particles are free falling or low density particles are free rising. The liquid environment is viewed with infinite volume. Particles will accelerate when entering the liquid and reach steady state when the net-gravity is balanced by drag force due to slip velocity between liquid and solid. And at steady state, particles are travelling at particle terminal velocity if particle-particle interaction is not significant. The direction of drag force provided by liquid is opposite to the direction of solid flow as dictated

8.4.2 Assisting flow

If the liquid is assisting flow, the flow direction of liquid follows the flow direction of solids in stagnant liquid, which is downward for free-setting solids and upward for free-rising particles. No studies have been focused with assisting flow in liquid-solid fluidized bed. Analogy from gas-solid fluidized bed downer can be used. The co-current flow of liquid will only make the solids flowing faster.

8.4.3 Hindering flow

If the flow is hindering flow, solids and liquid are flowing counter-currently. The flow direction of liquid is opposite to the flow direction of solids in stagnant liquid, so is the drag force provided by the liquid. The resistance from hindering flow will slow down the speed of each particle in the slows flow by providing, thus a denser environment is created. Both solids holdup is increasing the liquid velocity.

8.4.4 Supporting flow

When hindering flow velocity is greater than certain threshold value, the solids flow direction is reversed by liquid flow. The solid flow is supported by the sufficient drag force provided the liquid, thus making the liquid as supporting flow. The lower threshold of supporting flow velocity is the minimum fluidization velocity, where the net weight of particles was all being supported by the liquid flow. In supporting flow, the movement of solids differs the most from natural state, free falling or free rising, which makes the hydrodynamics very sensitive to liquid flow. In Supporting flow, solids holdup is decreasing with increasing superficial liquid velocity.

Table 8.4-1 Summary on different types of flow

Types of flow	Expression of U_{slip}	Position in Regime Map	
Stagnant liquid flow	$U_l/(1-\epsilon_s)$	X axis	Chapter 8
Assisting Flow	$U_s/\epsilon_s - U_l/(1-\epsilon_s)$	Quadrant_III	Yet to be done
Hindering flow	$U_s/\epsilon_s + U_l/(1-\epsilon_s)$	Quadrant_IV	Chapter 8
Supporting flow	$U_l/(1-\epsilon_s) - U_s/\epsilon_s$	Quadrant_I	Chapter 4&6

8.5 Transition between regimes

The mentioned many regimes are somewhat connected in the Four-Quadrant Fluidization Regime Map. The transition between the connected regimes is different. Understanding the transition could be important to study the critical operating conditions that demarcate each regime.

8.5.1 Connection between CCFB and LSCFB

By experiment, the transition from CCFB to LSCFB is smooth, and not significant change in hydrodynamics has been observed during the transition. And as shown in Figure 8.3.1, the effects of U_l and U_s are the same on CCFB and LSCFB. In the four-quadrant flow regime map, conventional fluidized bed with solids circulation and liquid-solid circulating fluidized bed are two distinctive flow regimes, demarcated by particle terminal velocity. Before the idea of CCFB, it is regarded that solid circulation start at particle terminal velocity. But CCFB approves that solid circulation could already take place below reaching particle terminal velocity. In conventional fluidization, solid circulation is achieved by forcing excess solid into moderate liquid flow. While in liquid-solid circulating fluidized bed, it is believed that the excess liquid velocity is the cause to transport solid to the exit. It is not possible that only one mechanism of for solid circulation could exist in each circulating fluidized bed. Excess solids could be fed to the fluidized bed when superficial

liquid velocity is beyond particle terminal velocity. And in CCFB the observed increased solids holdup will lead to increasing slip velocity that will induce the net flow of solids. In addition, there is a smooth transition from CCFB to LSCFB for both light and heavy density particles in experiment. Axial solids holdup profiles are uniform, and no distinct difference in hydrodynamics behavior is observed, especially when superficial liquid velocity is not too far from particle terminal velocity. There is a possibility that at relative low superficial liquid velocity ($U_1 < 1.5 \sim 2 U_t$), the mechanism of solids transportation in CCFB is still dominating in LSCFB. A dilute transport regime could exist where the solids are not excessively occupying the space, and solid movement are only caused by the high liquid velocity. A detailed flow regimes map could be further proposed based on hydrodynamics and mechanism of solid transport.

8.5.2 Connection between counter-current flow and circulating fluidized bed

The transition from LSCFB to counter-current flow is almost impossible since the operating conditions are so different. However, a smooth transition is possible between CCFB and counter-current flow by flipping the solids flow direction as shown in Figure 8.3.1.

The boundary of counter-current of solid and liquid flow is particle terminal velocity which is based on single particle force balance. Similarly, particle terminal velocity is also regarded as the starting superficial liquid velocity for circulating fluidized bed. However, due to particle-particle interaction, the slip velocity differs from particle terminal velocity under different solids holdup condition. It is useful to know the relationship between slip velocity and solids holdup in both counter-current and co-current flow conditions with net solid flowrate.

The well-established Richardson-Zaki equation was aimed to serve the purpose, by applying the hindered settling results to bed expansion, but it has been approved that it may not be satisfying to account for all conditions with the existence of net solids flow. It is possible that the study in counter-current flow could give a better understanding for co-current circulating fluidized bed.

8.6 Feasible operating conditions of heavy density particles

From the above analysis, the feasible operating regimes can be derived. Feasible operating regimes refers to states where solids and liquid flow can form a steady state solids suspension for liquid and solids interaction to take place.

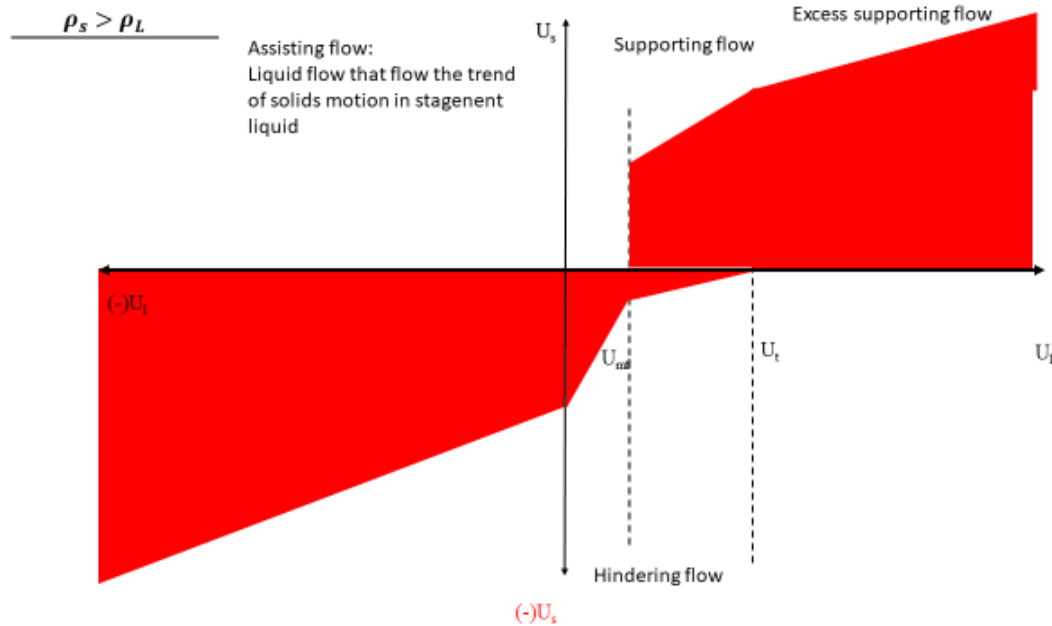


Figure 8.6.1 Feasible operating condition of heavy density particles

By combining the feasible operating regions of both heavy and low density particles, the blue region represents the regimes that can only be operated with low density particles, and the red region represents the regimes that can only be operated with heavy density particles and the region in purple stands for regimes that can be operated by either heavy or low density particles or both.

In principle, the fluidization of binary particles can only take place in the purple region. Which must be co-current flow of solids and liquid in Q_I and Q_III. And the liquid velocity must be about U_{mf} .

8.7 Feasible operating conditions of low density particles

Low density particles will rise in stagnant liquid. When low density particles are submerged under liquid, they will float at the top of the liquid because of their buoyance is greater than gravity. All the boundary of each regime was speculated based on experience and common sense.

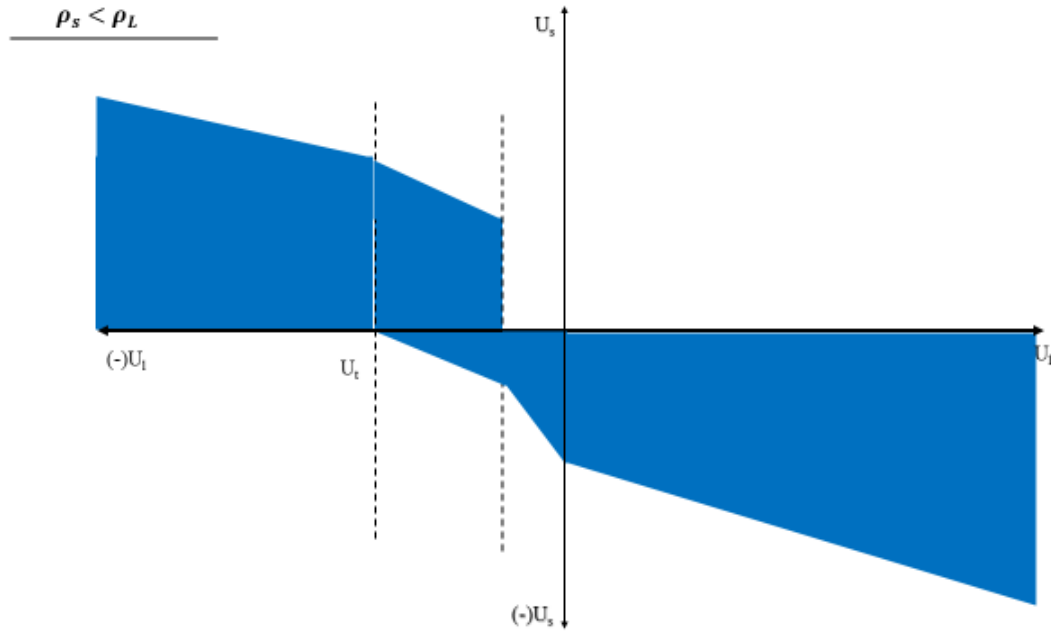


Figure 8.7.1 Feasible operating condition of low density particles

Nomenclature

Ar	Archimedes number defined by $d_p^3 g (\rho_p - \rho_l) \rho_l / \mu_l^2$
C_D	Particle drag coefficient
d_p	Particle diameter (mm)
D	Column diameter (m)
F_b, F_d, F_g	Buoyancy, drag force and gravity
G_s	Solids circulation rate (kg/ (m ² s))
g	Gravity acceleration
Re	Reynolds number defined by $U_l d_p \rho_l / \mu_l$
Re_t	Particle terminal Reynolds number defined by $U_t d_p \rho_l / \mu_l$
U_a	Auxiliary liquid velocity (cm/s)
U_l	Superficial liquid velocity (cm/s)
U_s	Superficial solids velocity (cm/s)
U_{slip}	Slip velocity (cm/s)
U_t	Particle terminal velocity (cm/s)
U_{tr}	Transition velocity demarcate the conventional particulate regime and circulating fluidization regime (cm/s)
V_l, V_p	Local liquid velocity and local particle velocity (cm/s)
\bar{V}_p	Average particle velocity (cm/s)

Greek letters

$\bar{\varepsilon}$	Average bed voidage
$\bar{\varepsilon}_s$	Average solids holdup
μ_l	Liquid viscosity (mPa·s)
ρ_p	Particle density (kg/m ³)

Subscripts

l	Liquid
p	Particle
s	Solids
b	Bubble
g	gas

Abbreviation

LSCFB	Liquid-Solid Circulating Fluidized Bed
ILSCFB	Inverse Liquid-Solid Circulaing fluidized Bed
IGLSCFB	Inverse Gas-Liquid-Solid Circulaing fluidized Bed
CCFB	Conventional Circulating Fluidized Bed

Chapter 9

9 Conclusions and Recommendations

9.1 Conclusions

In this study, a comprehensive investigation is carried out to study the hydrodynamics of four modes of liquid-solid fluidization, Inverse Liquid-Solid Circulating Fluidized Bed (ILSCFB), Inverse Conventional Circulating Fluidized Bed (ICCFB), Inverse Gas-Liquid-Solid Circulating Fluidized bed (IGLSCFB) and Counter-Current flow of solids and liquid. The flow behavior of low density particles is mainly focused, and compared with well-studied the behavior of heavy particles.

The hydrodynamics of Inverse Liquid-Solid Circulating Fluidized Bed (ILSCFB) have been studied extensively. Both axial and radial flow structure have been and investigated with particle density ranging from 28kg/m^3 to 1020kg/m^3 . It is found that the flow structure is very uniform in ILSCFB, and particle property effects is significant in affecting the slip velocity. A modified Richardson-Zaki equation is proposed for the prediction of solids holdup. Followed by the study of ILSCFB, a comparative study with upward Liquid-Solid Circulating Fluidized Bed is conducted based on residence time of liquid and solid. Many similarities have been found between ILSCFB and LSCFB since both flow structure is uniform. Some degree of cluster phenomenon is believed to be existing, and it is related to particle Reynolds number at particle terminal velocity.

Experiments also found that net solids flow can also be added to a conventional fluidized bed. So, the idea of Conventional Circulating Fluidized Bed (CCFB) is proposed. The hydrodynamics of inverse CCFB is studied with low density particles but the idea of CCFB is nor restricted to particle density. Limited by the operating range of this particular experiment, solids circulation was achieved relatively high superficial liquid velocity, but lower than particle terminal velocity. Solids holdup is significantly increased compared with both conventional fluidization and circulating fluidization. And the relationship between U_{slip} with ϵ_l is similar to conventional fluidization that can be described with Richardson-Zaki equation.

Following the study of co-current flow of circulating fluidized bed with low density particles, counter-current flow of light and heavy particles was studied. The axial hydrodynamics is found to be not uniform due to the slow acceleration of particles in liquid.

Preliminary study on Inverse Gas-Liquid-Solid Circulating Fluidized Bed is carried out as a complimentary to ILSCFB. They operation window to achieve solids downflow and gas upflow is discussed. It has also found that the change of solids holdup with operating conditions is very similar to ILSCFB. The effects of gas on solids holdup is observed, but not very significant.

9.2 Recommendations

Through the study of liquid-solid circulating fluidized bed, mainly with low density particles. Many insight and experience have driven me to propose the following recommendation in the field of fluidization.

Study on counter-current flow under dense condition. The studied counter-current flow was only in dilute conditions where solids were fed into a system mainly consists of fluid. Another form of counter-current flow condition could occur in a dense condition. For example, heavy solids can be fed from the top to a conventional fluidized bed that are supported by an upward liquid, and solid should exit from the bottom of the conventional fluidized bed. Both dilute and dense counter-current flow of solids could exist due to the moderate liquid flow.

The new regimes where free-rising particles are fluidized with upward liquid flow and free-falling particles are fluidized by downward liquid is wait to be investigated. Based on analysis on the feasible operation of low density fluidized bed that is an empty region that lack of study, as it is believed to be too easy to fluidize the particles. But it could be used as a tool to understand other more common fluidization regimes.

The relationship between counter-current flow and co-current flow could be further investigated. The main difference between counter-current flow and co-current flow is the formation of slip velocity, but the force balance is the same. The similarities of underlying mechanism between counter-current and co-current flow could be investigated.

Clustering phenomenon should be further investigated in liquid fluidized which is greatly overlooked in the past. It is believed that liquid-solid cluster might come in a much large scale compared with gas-solid clusters in circulating fluidized bed. The study of liquid-solid cluster should be carried out in a column with large dimension. And it could benefit the scale up of liquid-solid fluidized bed. And it can also serve as a base case to study the more complicated gas-solid clusters.

More detailed study on the micro and meso scale of particle behavior should be taken more attention. The study of particle collision should be taken in to consideration in liquid-solid circulating fluidized bed system. It is believed that particle collision should be distinctively different between conventional fluidization and circulating fluidization, both in frequency and intensity. Furthermore, it should also be different between low density particles and heavy density particles. Simple analysis on drag force or slip velocity can't be sufficient to explain the change of solids holdup in the circulating fluidized bed system, for both inverse and upward circulating fluidized bed. Furthermore, particle collision may also be a bench mark to study the difference between gas-solid and liquid-solid fluidization.

More comparison could be conducted between gas and liquid fluidization. The four-quadrant flow regime map can be easily extended to the gas-solid systems, and some researchers have already done some comparative study in similar categorization method based on operation conditions of gas and solid.

In chemical and biochemical processes, gas-solid fluidization has way more applications that have been commercialized. And no application of liquid-solid fluidized bed has reach the scale and productivity of gas-solid fluidized bed reactors exemplified by fluid catalytic crack (FCC) process. The hydrodynamics of liquid-solid and gas-solid fluidized bed are distinctively different. The most common saying is that the varsity difference of density ratio between fluids and solid is the cause to the different characteristics between gas-solid and liquid-solid fluidized bed. Some resemblance have also been found between gas and liquid systems, such as particle clustering. Liquid fluidization can be used a tool to study the essence in the complicated gas-solid system.

The use of the multiple liquid fluidization regimes could be extended to the study of gas-solid systems. Drastic hydrodynamics difference always exists between gas-solid and liquid-solid circulating fluidized beds, such as solids holdup axial and radial distribution, onset velocity of circulation, macro and micro flow structure of liquid and solid, etc. And those were mainly attributed to the change of fluidization medium. A fluidization medium, or a combination of solids and fluid under certain physical conditions could link the fluidization with gas and liquid. Which could help us understand the underlying mechanism between liquid and gas fluidization system. The common explanation for the difference in hydrodynamics between gas and liquid system is the huge difference in fluid/solid ratio, which is far from enough. Dimensionless analysis should be conducted to represent the operating conditions.

The study of light particles rising could be further investigated in a microscopic view. Clusters could exist during the rising process, and the formation and disintegration could be capture. In addition, the study might be helpful to understand the behavior of bubble coalesce and breakage in bubble column. Similarities exists in the formation of clusters and coalesce of bubbles when bubble and low density particles share similar density.

Appendices

A. Materials and Method

Solids preparation

Low density particle is selected for inverse downflow fluidization. One objective of the study is to investigate the particle property effects on hydrodynamics of inverse circulating fluidized bed. Thus, various types of particles with a wide span of densities is preferred. Unfortunately, not many low density particles are available at an affordable price. Some porous particles have been tried experimentally, and most of them fail due to the adsorption water which makes increases particle density to be higher than water over time. After some trials, expanded polystyrene particles are selected due to its closed pore structure.

The density of expanded polystyrene particles is usually below 100kg/m^3 . Unexpanded polystyrene particles weigh around $1020 - 1100\text{ kg/m}^3$. In order to obtain particle's density between 100 and 1000kg/m^3 , polystyrene particles have to undergo a non-fully expansion process.

Expansion solvent agent is used in the formation of polystyrene particles. Once the particle is heated, the solving agent will be released forming closed pores inside the particles, which will cause particle expansion at the same time, thus the density can be reduced. The expansion process can be controlled by the modifying the amount of solvent agent that are added in the formation of particles or exposure time to heating. In this study, one type of particles is made in the lab with water bath for heating, two types of particles are custom made from a polystyrene factory in China. And one ready-to-use PS is purchased in Canada that has a density of 28kg/m^3 , and the last set of particles has a density of 1020 kg/m^3 , and experiment was carried out in salted water with 1080kg/m^3 density.

PS particle expansion process has been adopted by Karamanev when studying the free rising behavior of neutral buoyant particles. Considering the amount of PS particles is needed for the inverse liquid-solid circulating fluidized bed, the expansion process has been modified. The challenge is how to achieve uniform expansion, which lead to a uniform particle property for experiment. Due to size of the water bath available in the lab, the

expansion process has to be finished in many batches. The temperature of the water bath is controlled at 92° C to prevent over expansion of particles. Each batch, 500ml of unexpanded particles are put in a mesh bag which will be submerged in the hot water bath for 5 minutes. A stick was used to stir the bag while ensure it maintain submerged in the water to increase heat transfer. Once it was taken out of the water bath the bag was cooled down in sink of cold tap water to ensure the expansion stops immediately. Particles are sieved after the expansion step to achieve a narrow size and density distribution. Eventually, unexpanded heavy and small particles are separated from the bottom of an inverse fluidized bed under conventional fluidization regime. And a clear boundary can be observed between the fluidized bed and the free board, which is an indication of narrow particle size and density distribution. The custom-made particles from China undergo the same separation process in the fluidized be to ensure uniform particle property. And particle size and density were measure after they were taken out of the fluidized bed.

Particle Properties

Particle terminal velocity will be used as variable to represent particle properties including particle density, diameter and shape. Particle terminal velocity is property of single particle. Due to the size distribution and density distribution in this case, particle terminal velocity of each particle may vary. Thus, in this case, the particle terminal velocity is extrapolated from bed expansion data based on Richardson-Zaki equation (KHAN and RICHARDSON 1989). The particle terminal velocity can be found from the intercept in $\ln(\epsilon_s)$ - $\ln(U_i)$ plot as seen in fig. And particle properties are summarized in

Table A-1 Particle properties

Table A-1 Particle properties

***Experiment carried out in salt water with 1080 kg/m³ density EPS stands for expanded polystyrene, and PS stands for polystyrene**

Particles	Density (kg/m³)	Diameter (mm)	U_t (cm/s)
EPS	28	0.8	13.4
EPS	122	1.1	16.0
EPS	303	1.2	7.37
EPS	637	1.1	4.86
PS*	1020	0.9	0.53*

Operation of Inverse Liquid-Solid Circulating Fluidized Bed

Operation of Inverse Liquid-Solid Circulating Fluidized Bed

The schematic diagram of ILSCFB is shown in Figure A.1. The inverse liquid-solid circulating fluidized bed contains a 5.4-meter downer (0.076m ID) and a 4-meter upcomer (0.203m ID), which are connected by connecting pipes from the top and the bottom. Liquid

flow enters from the top of the downer, through main flow distributor and auxiliary flow distributor. Solids are stored at the top of the upcomer and fed to the top of the downer by controlling the auxiliary flow rate. Detailed experiment apparatus descriptions can be found from Long and Zhu (Sang et al. 2019).

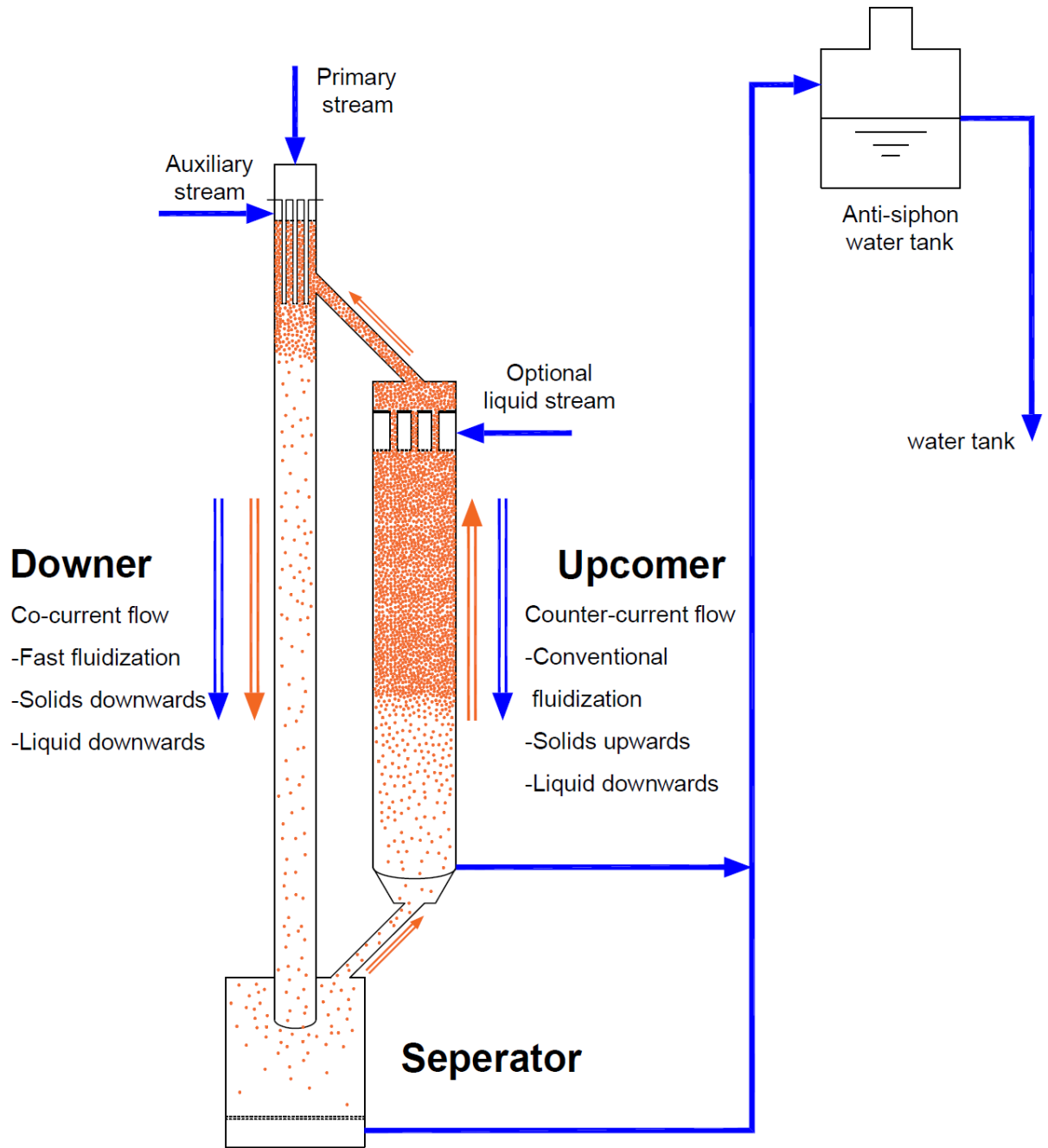


Figure A.1 Schematic diagram of inverse liquid-solid circulating fluidized bed

Effects of optional stream in the upcomer on solids circulation rate

Various methods have been adopted to increase solids circulation rate in liquid-solid circulating fluidized beds. In this study an optional stream in the upcomer was used to help increase the solids circulation rate. A significant increase of solids circulation rate has been observed, so as solids holdup in the downer, with little addition of optional flow. The impact of optional stream on solids holdup is similar to the effects of bed inventory and auxiliary flow as reported.

Pressure balance of the inlet region can be used to explain the effect of optional stream. Solids circulating rate is determined by the pressure difference between the upcomer and downer at the top. High pressure difference from the upcomer to the downer will lead to more solids been transported. Total pressure from the upcomer comes from the free rising particles that were stored in a packing condition. Auxiliary flow works as a non-mechanic valve that control the release of particles to the dower. Optional stream that flows through the packed bed will generate more pressure as part of the solids' buoyance is transferred to the mixture of solids and liquid, which can be predicted using Ergun equation. As indicated from Ergun equation, the pressure at the top of the upcomer is dependent of bed height.

Solids holdup is directly related to solid circulation rate in the downer. Previous studies have found the relationship between solid circulation rate and auxiliary flow, bed inventory, which further lead to their effects on solids holdup in the circulating fluidized bed. Auxiliary flow and bed inventory have similar effects on solids holdup. The increase of auxiliary flow or bed inventory will induce a higher pressure for solids to be returned to the inlet. Thus, more solids will be fed to the circulating fluidized bed, generating a denser solids environment.

Operation of Circulating Conventional Fluidized Bed

The circulating fluidized is comprised of a 5.4 m downer (0.076 m ID) and a 4 m upcomer (0.20 m ID). Primary and auxiliary flow distributors are located at the top of the downer; additional distributor is at the top of the upcomer.

Main flow distributor is located below the particle feeding pipe, thus cannot control solids feed. However, auxiliary flow distributor is located above the feeding pipe, which can push particles downward to converge with main flow, as seen in Figure A.2. Although main flow distributor is where fluidization started, it is auxiliary flow that serve as non-mechanical valve to travel the particles to the fluidized bed(Zheng and Zhu 2000). In addition to auxiliary flow, additional stream is introduced from the top of the upcomer to fluidize the inventory particles so that light particles have more pressure to travel to the downer. Solids feed rate, so called solids circulating rate can be controlled by adjusting the auxiliary flow and the additional flow stream in the upcomer. Increasing auxiliary flow or addition flow in the upcomer and improve solids circulating rate. Solids circulation rate is monitored using two butterfly valves located at the bottom of the upcomer, which collects the of solids leaving the downer. As at steady state, the volume flowrate of solids leaving the downer equals solids circulation rate.

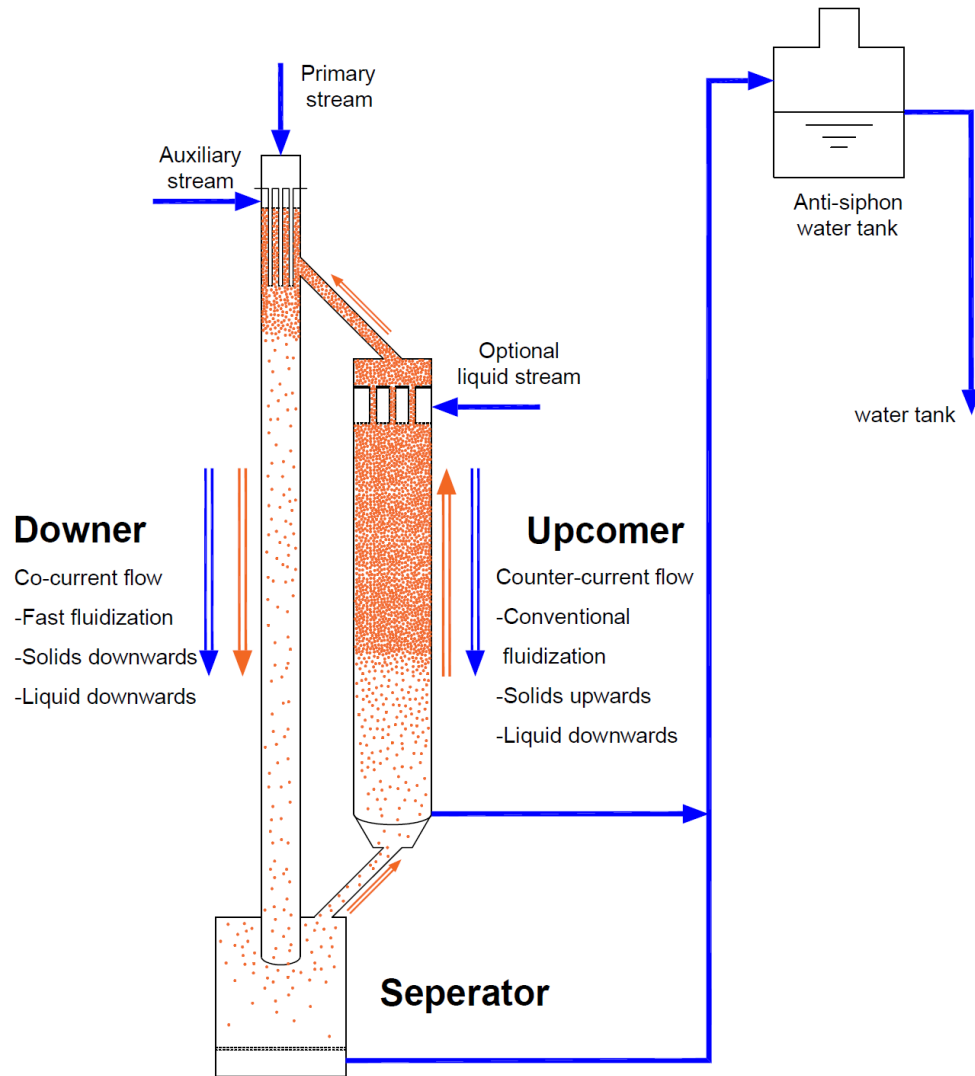


Figure A.2 Schematic diagram of CCFB

Measurement techniques

Measurement of superficial solids velocity

Superficial solids velocity is the velocity of solids in the absence of water. Normally superficial solids velocity is used to describe the solid circulation rate.

In the inverse liquid solid circulating fluidized bed, two half butterfly valves are mounted in the storage column with a height difference of 40 cm. By properly flipping the two valves a certain amount of particles can be accumulated between the two butterfly valves when

the inverse circulating fluidized bed is running. The particles occupy half of the cross-sectional area and the height of the particles can be measured and by knowing the amount of particles accumulated and the time required solid circulation rate can be measured.

Superficial solid velocity can be obtained from the following equation **Error! Reference source not found.:**

$$U_s = \frac{\text{Solid volume flow rate}}{\text{Cross - section area of the downer}} = \frac{\frac{1}{2} h A_r \varepsilon_p \frac{1}{2} h A_r \varepsilon_p / t}{A_d A_d} \quad \text{A-1}$$

where A_s and A_d are the cross-section area of the storage column and downer respectively.

After the particles are collected by the butterfly valves, they are in packed bed form, ε_p is the solids holdup of packed bed.

Average solids holdup

Manometers can be used to measure the average solids holdup. Six ports at different heights were placed along the downer. These ports were connected by tubes to a series of manometers. Manometers measure the pressure drop between these ports, from which average solids holdup in each section can be calculated.

Since the hydrostatic pressure at different heights of both columns was high, open-end manometers were not used in this experiment to prevent the overflowing of water in manometers. In this case, the ends of the manometers were connected to a tank filled with air and the pressure of air inside the tank was controlled.

The pressure balance between two manometers is shown in the following equation A-2:

$$P_g + \rho_L g \cdot (\Delta h + X_1) = P_g + \rho_L g \cdot h_m + [\rho_L (1 - \varepsilon_s) + \rho_s \cdot \varepsilon_s] g \cdot \Delta h \quad \text{A-2}$$

where h_m the height difference between manometers, P_g is the pressure above the water in the manometers, ρ_L and ρ_s are the density of water and particles respectively.

The solids holdup can be calculated from the height difference, knowing the density of particles:

$$\varepsilon_s = \frac{\rho_L \cdot h_m}{(\rho_L - \rho_s) \Delta h} \quad \text{A-3}$$

Measurement of local solids holdup with optical fiber probe

Optical fiber probe has been used widely to measure local solids holdup in circulating fluidized bed. By emitting light to the multiphase system, the reflection of light dictates the solids holdup at the tip of probe, which is transferred to voltage as output signal. Calibration between voltage and solids holdup must be performed prior to the measurement. Detailed calibration method has been proposed by Zhang and Zhu in 1999. A black box is used to set the range of voltage, which is usually from 0-4.5. The calibration take place in a downer where particles are fed from the top, and the voltage from OFP is correlated with solids holdup measured by two clips. The calibration curve can be affected by the setup of black box and ‘offset’ and ‘gain’ setting when transfer light intensity to voltage. Offset determines the base line while gain determines the amplitude of the signal. The original signal is shown in fig. 2. One drawback of the popular calibration method is that the voltage signal could easily exceed the higher and lower limit as only the average voltage is considered in calibration process. The large peaks in the original signal contribute the most to the average voltage. When the actual high voltage signals should be above the higher limit 5, it is only captured as the maximum 5 as can be seen from the original data. So the change of solids holdup didn’t account for the portion of signal above the maximum, which reduces the resolution of the measurement, also lead to a skewed calibration curve.

It is not a serious issue when the local solids holdup varies in a wide range, as the case of gas-solid circulating fluidized bed, where a core-annulus region exist. In liquid-solid system, the degree of non-uniformity of solids holdup distribution is not as severe in gas solid system. Copying the same calibration method in gas-solid system, the resolution of optical fiber probe in measuring solids holdup is not high enough to detect the subtle non-uniformity. Which explains the perfect uniform radial solids holdup distribution found in Inverse liquid-solid circulating fluidized bed. In order to increase the accuracy a better

resolution of local solids holdup measurement, a modified calibration method is proposed. The calibration is done on site in the downer of the inverse liquid-solid circulating fluidized bed. The probe is placed at the center of the downer. The first step is adjusting the ‘offset’ and ‘gain’ setting on OFP to make all the voltage signals within the boundary at the most dilute and dense conditions in the downer by manipulating the solids circulating rate and liquid velocity. The next step is to measure the 7 voltage signals from center to the wall and solids holdup from manometers at a series of solids holdup conditions. The voltage signals at different radial positions are averaged. Calibration curve can be made between average voltage and solids holdup.

Local particle velocity

The optical fiber probe is a type of probe, which can be used to measure solids concentration and particle velocity simultaneously. The particles in the downer move downward to reflect the light emitted by the probe back to channel B and channel A respectively, which are two bundles of receiving fibers, as shown in Figure A.3 The particle velocity can be determined by

$$V_p = L_e / T_{AB} \quad (\text{A-4})$$

Where L_e is the effective distance between channel A and B, which is calibrated by the manufacturer (1.59 mm in this study). T_{AB} is the time lag between the signal of one particle detected by channel B and channel A, which is obtained from cross-correlation, as shown in equation A-5.

$$\phi_{AB}(\tau) = \lim_{T \rightarrow \infty} \frac{1}{T} \int_0^T A(t)B(t + \tau)dt \quad (\text{A-5})$$

The corresponding τ to the maximum ϕ_{AB} is the time lag T_{AB} between two impulse signals.

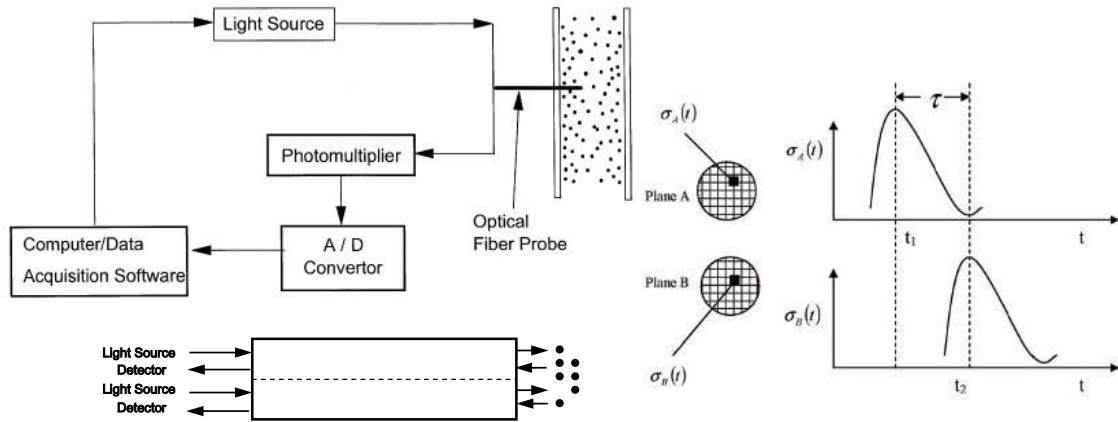


Figure A.3 Measurement of local particle velocity with OFP

And the threshold of cross-correlation coefficient is set to be 0.6 to determine the similarity between times series data. It is assumed that if the cross-correlation is lower than 0.6, it is not the same group of particles passing along the tip of the probe.

B. Average solids holdup of each particle

Appendix B-1 Average solids holdup data of EPS122

EPS122					
U₁(cm/s)	U_s (cm/s)	ε_s	U_l(cm/s)	U_s (cm/s)	ε_s
15.3	0.54	0.047	20.3	0.67	0.051
15.3	0.50	0.049	20.3	0.83	0.066
15.3	0.58	0.051	20.3	1.35	0.092
15.3	0.63	0.053	20.9	0.68	0.041
15.3	0.71	0.055	20.9	0.84	0.049
15.3	0.76	0.061	20.9	1.00	0.055
15.3	0.88	0.075	23.6	0.88	0.042
15.3	1.02	0.075	23.6	1.18	0.053
15.3	0.94	0.079	23.7	0.71	0.046
15.3	0.99	0.079	23.7	0.96	0.062
15.3	1.10	0.093	23.7	1.35	0.088
16.9	0.56	0.054	26.4	0.82	0.037
16.9	0.73	0.081	26.4	0.99	0.041
16.9	1.06	0.100	27.0	1.13	0.061
18.1	0.63	0.045	27.0	1.28	0.077
18.1	0.80	0.056	27.0	1.77	0.087
18.1	0.96	0.065	32.0	0.98	0.034
19.5	0.63	0.044			
19.5	0.73	0.046			
19.5	0.77	0.055			
19.5	0.88	0.059			
19.5	1.17	0.060			
19.5	0.88	0.062			
19.5	1.48	0.086			

Appendix B-2 Average solids holdup data of EPS638

EPS638		
$U_i(\text{cm/s})$	$U_s (\text{cm/s})$	ϵ_s
12.5	0.38	0.123
13.9	0.19	0.068
13.9	0.83	0.129
15.3	0.73	0.104
16.7	0.42	0.058
16.7	0.51	0.075
16.7	1.13	0.117
16.7	1.62	0.154
18.1	1.54	0.065
18.1	2.83	0.180
19.5	0.48	0.054
19.5	0.67	0.070
19.5	1.35	0.112
22.2	0.46	0.044
22.2	0.90	0.067
22.2	1.71	0.111
22.2	2.76	0.149
25.0	0.64	0.047
25.0	1.01	0.061
27.8	1.14	0.059
27.8	1.87	0.091
27.8	1.60	0.073
30.6	1.37	0.057
30.6	0.48	0.028
30.6	1.54	0.069
30.6	2.69	0.101
36.1	1.62	0.056
36.1	2.76	0.091
41.7	2.69	0.080

Appendix B-3 Average solids holdup data of EPS303

EPS303		
U_1 (cm/s)	U_s (cm/s)	ϵ_s
12.5	0.15	0.069
12.5	0.42	0.088
12.5	0.55	0.114
12.5	0.76	0.123
12.5	0.92	0.139
15.3	0.33	0.060
15.3	0.44	0.076
15.3	0.67	0.093
15.3	0.86	0.108
15.3	1.08	0.123
18.1	0.35	0.054
18.1	0.64	0.071
18.1	0.85	0.085
18.1	0.98	0.096
18.1	1.46	0.117
20.9	0.45	0.048
20.9	0.67	0.060
20.9	0.84	0.071
20.9	1.18	0.088
20.9	1.57	0.106
26.4	0.70	0.045
26.4	0.88	0.053
26.4	1.33	0.072
26.4	1.57	0.081
26.4	1.90	0.101
26.4	2.02	0.095
32.0	0.57	0.031
32.0	0.87	0.042
32.0	1.15	0.059
32.0	1.62	0.089

Appendix B-4 Average solids holdup data of EPS28

EPS28					
U_1 (cm/s)	U_s (cm/s)	ϵ_s	U_1 (cm/s)	U_s (cm/s)	ϵ_s
15.3	0.30	0.058	26.4	0.70	0.046
15.3	0.62	0.091	26.4	1.25	0.071
16.7	0.24	0.041	26.4	1.92	0.100
16.7	0.35	0.055	27.8	0.48	0.036
16.7	0.55	0.077	27.8	1.00	0.066
16.7	0.69	0.086	27.8	0.64	0.043
18.1	0.49	0.057	27.8	0.93	0.054
18.1	0.83	0.087	29.2	0.75	0.044
18.1	1.37	0.117	29.2	1.95	0.091
19.5	0.31	0.039	30.6	0.56	0.033
19.5	0.75	0.073	30.6	0.66	0.038
19.5	0.84	0.084	30.6	0.95	0.052
19.5	0.46	0.057	30.6	1.11	0.063
20.9	0.66	0.067	33.4	0.85	0.042
20.9	0.54	0.052	33.4	0.64	0.034
20.9	1.08	0.083	33.4	1.07	0.049
20.9	1.48	0.110	33.4	1.22	0.058
22.3	0.36	0.041	34.8	0.78	0.042
22.3	0.45	0.047	36.2	0.70	0.034
22.3	0.73	0.065	36.2	0.89	0.041
22.3	0.89	0.076	36.2	1.04	0.047
23.7	0.64	0.050	36.2	1.28	0.057
23.7	1.10	0.077	39.0	0.75	0.033
23.7	1.74	0.111	39.0	0.86	0.040
25.0	0.97	0.069	39.0	1.12	0.047
25.0	0.42	0.036			
25.0	0.48	0.043			
25.0	0.83	0.060			


Appendix B-5 Average solids holdup data of PS1020

PS1020		
$U_1(\text{cm/s})$	$U_s (\text{cm/s})$	ϵ_s
5.6	0.15	0.096
7.0	0.22	0.087
8.3	0.25	0.089
9.7	0.26	0.077
11.1	0.30	0.117
13.9	0.40	0.093
16.7	0.51	0.099
22.2	1.41	0.147
16.7	1.66	0.170
16.7	0.34	0.065
11.1	0.16	0.049
12.5	0.81	0.146

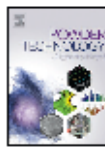
C. Published article

Appendix C-1 Published article in ILSCFB with previous student

ARTICLE IN PRESS
PTEC-14253; No of Pages 9
Powder Technology xxx (2019) xxx

**ELSEVIER**

Contents lists available at ScienceDirect
Powder Technology
journal homepage: www.elsevier.com/locate/powtec



On the basic hydrodynamics of inverse liquid-solid circulating fluidized bed downer

Long Sang, Tian Nan, Amin Jaber, Jesse Zhu*

Department of Chemical and Biochemical Engineering, The University of Western Ontario, London, Ontario N6A 3K7, Canada

ARTICLE INFO

Article history:
Received 6 July 2018
Received in revised form 22 December 2018
Accepted 8 April 2019
Available online xxxxx

Keywords:
Inverse liquid-solid circulating fluidized bed (ILSCFB)
Liquid-solid circulating fluidized bed (LSCFB)
Solids holdup
Liquid velocity
Particle terminal velocity

ABSTRACT

A new type of fluidized bed called Inverse Liquid-Solid Circulating Fluidized Bed (ILSCFB) has been developed. The circulating fluidized bed consists of the downer with an inner diameter of 7.6 cm and the height of 5.4 m, upcomer with an inner diameter of 20 cm, separator, and connecting pipes between the downer to the storage column. The operation window has been demonstrated at different solids circulation rate and liquid velocity. The hydrodynamic characteristics in the downer of ILSCFB are investigated experimentally by fluidization of the styrofoam and Hollow Glassbeads whose densities are smaller than that of the fluidization media. Average solids holdup in the downer is measured where different liquid velocity and different solids circulation rate in terms of superficial solids velocity. For both types of particles, axial solids holdup distribution is quite uniform under various operating conditions, while radial solids holdup distributions are slightly non-uniform with a minor increase in solids holdup adjacent to the wall under various operating conditions, but no obvious "core-annulus" structure is observed. The comparisons of the hydrodynamics in the ILSCFB and Liquid-Solid Circulating Fluidized Bed (LSCFB) are also made based on the single particle force balance discussion, enabling the generalization of inverse and upwards circulating fluidization of particles.

© 2019 Elsevier B.V. All rights reserved.

1. Introduction

Generally, the solids are fluidized upwards in the fluidized bed where the density of the particles is higher than that of the surrounding liquid, such as in the Liquid-Solid Fluidized Bed (LSFB) and the Liquid-Solid Circulating Fluidized Bed (LSCFB). Whereas, when the density of the solids is lower than that of the surrounding liquid, the downwards fluidization is necessary, and referred to as the inverse fluidization [12]. A good understanding of hydrodynamics in the inverse conventional fluidization system is crucial to the design operation, mathematical modeling and optimizing of the inverse fluidized bed reactors such as bioreactors [3]. Some limited previous experimental and modeling research has been done to investigate the hydrodynamics in the conventional Inverse Liquid-Solid Fluidized Bed (ILSFB). For example, the bed voidage, the minimum fluidization velocity [2,4,5], the drag coefficient and the particle terminal velocity in Newtonian fluids [6] and non-Newtonian fluids [7] flow regimes and pressure drops across the bed [8], voidage waves [9], and layer inversion of binary particle system [10], were all studied experimentally or modeled mathematically. Some other related characteristics such as heat transfer [11,12] and mass transfer [13,14] were also studied. The application of ILSFB mostly focused in wastewater treatment as bioreactor, where microorganism attached on the surface of inert particles as biofilm. [3,15]

However, all the above-mentioned studies focused only on the conventional fluidization regime under which the superficial liquid velocity is lower than that of the particle terminal velocity. When the superficial liquid velocity is higher than the particle terminal velocity, the particles will be fluidized under the circulating fluidization regime, which has unfortunately not been reported by any research work.

In this paper, a new type of fluidized bed called Inverse Liquid-Solid Circulating Fluidized Bed (ILSCFB) has been developed to investigate the hydrodynamics in the inverse circulating fluidization regime by fluidizing two different types of particles whose densities are lower than that of the fluidization media. The axial and radial solids holdup distributions are studied under various operating conditions. Comparisons of ILSCFB and LSCFB are also made based on single particle force balance analysis.

2. Materials and methods

2.1. The ILSCFB configuration

The set-up of ILSCFB system is shown schematically in Fig. 1a. The system mainly consists of a 0.076 m ID Plexiglas downer column where the inverse fluidization takes place, a liquid-solid separator, an upcomer, and a device for measuring the solids circulation rate at the

Abbreviations: ILSFB, Inverse Liquid-Solid Circulating Fluidized Bed.
* Corresponding author at: Department of Chemical and Biochemical Engineering, University of Western Ontario, 1151 Richmond St., London ON N6A 3K7, Canada.
E-mail address: jzhu@uwo.ca (J. Zhu).

<https://doi.org/10.1016/j.powtec.2019.04.021>
0032-5910/© 2019 Elsevier B.V. All rights reserved.

Please cite this article as: L. Sang, T. Nan, A. Jaber, et al., On the basic hydrodynamics of inverse liquid-solid circulating fluidized bed downer, Powder Technol., <https://doi.org/10.1016/j.powtec.2019.04.021>

Curriculum Vitae

Name: Tian Nan

Post-secondary Education and Degrees: Zhejiang University
Hangzhou, Zhejiang, China
2010-2014 B.Eng.

The University of Western Ontario
London, Ontario, Canada
2014-2019 Ph.D.

Honors and Awards: China Scholarship Council (CSC)
Doctoral Fellowship
2014-2018

Related Work Experience Teaching Assistant
The University of Western Ontario
2015-2019

Instructor
The University of Western Ontario
2017

Publications:

Sang, L., Nan, T., Jaber, A., & Zhu, J. (2019). On the basic hydrodynamics of inverse liquid-solid circulating fluidized bed downer. *Powder Technology*.